Max-Planck-Institut
für Kohlenforschung

Max-Planck-Institut für Kohlenforschung

Report for the Period of

January 2011 – December 2013

confidential

Printed January 2014

Max-Planck-Institut
für Kohlenforschung

Max-Planck-Institut für Kohlenforschung

Kaiser-Wilhelm-Platz 1
45470 Mülheim an der Ruhr, Germany
Tel. +49 208 3 06 1
Fax +49 208 3 06 29 80
http://www.kofo.mpg.de

Managing Director Professor Dr. Benjamin List

Director of the *Department of Homogeneous Catalysis*
Professor Dr. Benjamin List
Tel. +49 208 3 06 24 10
Fax +49 208 3 06 29 99
E-mail: list@mpi-muelheim.mpg.de

Director of the *Department of Heterogeneous Catalysis*
Professor Dr. Ferdi Schüth
Tel. +49 208 3 06 23 73
Fax +49 208 3 06 29 95
E-mail: schueth@mpi-muelheim.mpg.de

Director of the *Department of Organometallic Chemistry*
Professor Dr. Alois Fürstner
Tel. +49 208 3 06 23 42
Fax +49 208 3 06 29 94
E-mail: fuerstner@mpi-muelheim.mpg.de

Director of the *Department of Theory*
Professor Dr. Walter Thiel
Tel. +49 208 3 06 21 50
Fax +49 208 3 06 29 96
E-mail: thiel@mpi-muelheim.mpg.de

Director of the *Department of Organic Synthesis*
Professor Dr. Manfred Reetz (until 2011)
Tel. +49 6421 28 25 500
Fax +49 6421 28 25 620
E-mail: reetz@mpi-muelheim.mpg.de

Emeritus Scientific Members of the Max-Planck-Institut für Kohlenforschung

Professor Dr. Günther Wilke
Professor Dr. Roland Köster (deceased, June 2009)
Professor Dr. Manfred Reetz (since 2011)

External Scientific Members of the Max-Planck-Institut für Kohlenforschung

Professor Dr. Alois Haas
Medonstraße 17
14532 Kleinmachnow
Germany

Professor Dr. Jack Halpern
University of Chicago
Department of Chemistry
5735 South Ellis Avenue
Chicago, Illinois 60637
USA

Professor Dr. Walter Leitner
Lehrstuhl für Technische Chemie und Petrolchemie
Institut für Technische und Makromolekulare Chemie
Rheinisch-Westfälische Technische Hochschule Aachen
Worringer Weg 1
52074 Aachen
Germany

Members of the Scientific Council of the Max Planck Society,
Section of Chemistry, Physics and Technology

Dr. Claudia Weidenthaler (July 2009 – July 2012)
Dr. Christian Lehmann (since July 2012)

Table of Contents

CHAPTER 1

The Max-Planck-Institut für Kohlenforschung

1.1 History

The decision to found a Kaiser-Wilhelm-Institut für Kohlenforschung (coal research) in Mülheim/Ruhr was taken in 1912 by the Kaiser Wilhelm Society, representatives of the coal industry and the town of Mülheim/Ruhr. In 1913 Franz Fischer (1877-1947), who in 1911 had been appointed professor for electrochemistry at the Technical University in Berlin-Charlottenburg, was chosen as the first Director.

Franz Fischer and his co-workers carried out basic research in a number of areas concerning the formation and chemical composition of coal as well as on its conversion into solid, liquid and gaseous products. The most important contribution culminated in the so-called Fischer-Tropsch process for coal liquefaction. In 1925, Franz Fischer and the group leader Hans Tropsch reported that liquid hydrocarbons (alkanes) can be produced from carbon monoxide and hydrogen in the presence of solid metal catalysts. The mixture of the two gases (synthesis gas) necessary for this new process was prepared by the "gasification" of coal with steam and oxygen at 900°C. In 1925 the "Studien- und Verwertungsgesellschaft mbH" was founded for the purpose of exploiting the patents. By the early 1940s nine industrial plants were operating in Germany producing ca. 600 000 tons of liquid hydrocarbons per year. Today there is a renewed interest in Fischer-Tropsch technology with plants in Sasolburg/South Africa, Malaysia, and Qatar (using natural gas instead of coal). In 1939 Franz Fischer instigated a change in the status of the Institute; it became a foundation of private law with the objective of supporting the scientific investigation of coal for the public benefit.

Following Fischer's retirement in 1943 Karl Ziegler (1898-1973) was appointed Director of the Institute. After the founding of the Max Planck Society as the successor of the Kaiser Wilhelm Society in 1948, the Institute obtained its present name in 1949. As a consequence of Ziegler's appointment, the main research efforts shifted to organometallic chemistry. Based upon his earlier experience with the organic compounds of the alkali metals, Ziegler and his co-workers turned their attention to aluminum. In 1949 they reported the multiple addition of ethylene to aluminum alkyls which became known as the "Aufbau reaction". The product of this oligomerization was a mixture of aluminum alkyls having long, linear alkyl chains attached to the metal; these compounds could be converted into α-olefins or primary alcohols, the latter being important for the production of biodegradable detergents. An unexpected observation during the systematic investigation of this reaction led to the discovery that transition metals have a dramatic effect on the "Aufbau" reaction; in particular, the addition of

compounds of titanium or zirconium led to the coupling of up to 100 000 ethylene molecules at normal pressure and temperature. The optimized process employed the so-called organometallic “Mischkatalysatoren” consisting of an aluminum alkyl and a transition metal salt. It was patented in 1953 and led to a dramatic development of the industrial production of polyethylene and polypropylene as cheap and versatile polymers. The licensing of the patents enabled the Institute to be operated on an independent financial basis for nearly 40 years. As a result the Institute expanded and a number of new buildings such as the library, the main research laboratory, pilot plant facilities, high pressure workshops and an instrumental analysis building were constructed. Karl Ziegler was awarded the Nobel Prize for Chemistry in 1963 (together with Guilio Natta who analyzed the stereochemistry of polypropylene). Ziegler subsequently created the Ziegler-Fund (in 1968) and the Ziegler-Foundation (in 1970), which still play an important role in financing the Institute.

In recognition of the fundamental importance of Karl Ziegler’s discoveries and their tremendous implications for industry, the German Chemical Society (GDCh) bestowed the title “Historische Stätte der Chemie” (Historical Landmarks of Chemistry) on the Institute in 2008. A bronze plaque on the historic building commemorates this event. On this occasion, a brochure was published, which reviews the Ziegler era in some detail. This information is also available via the Internet at http://www.mpi-muelheim.mpg.de/kofo/english/institut/geschichte_e.html.

Günther Wilke followed Karl Ziegler as Director in 1969. His research concentrated on the organometallic chemistry of the transition metals (especially nickel) and its application in homogeneous catalysis. For example, the developed cyclodimerization and the cyclotrimerization of butadiene using homogeneous nickel catalysts were exploited industrially. Ligand-control led to the development of highly selective homogeneous catalysts, including catalysts bearing chiral enantiopure ligands. The Institute also pursued research in electrochemistry, contributing an efficient electrochemical synthesis of iron(II) ethanolate which became industrially important for the production of ferrocene. Investigations on the use of supercritical gases for purification purposes, which was first described by Kurt Zosel at the institute in 1963, led to a large-scale industrial process for the decaffeination of green coffee beans using supercritical carbon dioxide. Roland Köster, a Scientific Member of the Max Planck Society since 1969, headed his own group during these years, which was primarily concerned with organoboron chemistry.

In 1993 Manfred T. Reetz was appointed Director of the Institute. As an organic chemist he initiated projects in his own group pertaining to catalysis, transition metal colloids and directed evolution of enzymes. He also re-defined the scientific activities of the Institute as a whole, a development which resulted in the establishment of five Departments comprising Synthetic Organic Chemistry, Homogeneous Catalysis, Heterogeneous Catalysis, Organometallic Chemistry and Theory. This plan foresaw the appointment of Scientific Members as Directors of these Departments. In 1995 Andreas Pfaltz joined the Institute as the Director of the Department of Homogeneous Catalysis, while Manfred T. Reetz headed the Department of Synthetic Organic Chemistry. Thereafter the appointments of Ferdi Schüth (Heterogeneous Catalysis), Alois Fürstner (Organometallic Chemistry) and Walter Thiel (Theory) followed. Thus, the scientific activities of the Institute were put on a broad and interdisciplinary basis.

Following Andreas Pfaltz' move back to Basel, the position of the Director of the Department of Homogeneous Catalysis remained vacant for some time. Benjamin List from the Scripps Research Institute, La Jolla, was identified as a pioneer in the then emerging field of organocatalysis. He was hired on a C3-position (associate professor) in 2003, and promoted to become the Director of the Department in 2005.

The Directors of the Departments form a Board which is responsible for all decisions. The affairs of the Institute are taken care of by a Managing Director elected from this Board. As successor to Manfred Reetz, Ferdi Schüth served as Managing Director from 2003-2005, followed by Walter Thiel (2006-2008), Alois Fürstner (2009-2011) and Benjamin List (2012-2014).

In September 2011 Manfred Reetz became an Emeritus. He now works at the Philipps-Universität Marburg as Hans Meerwein Research Professor and External Group Leader of our Institute.

1.2 Current Research Areas

The research areas of the Max-Planck-Institut für Kohlenforschung are defined by the five Departments comprising Synthetic Organic Chemistry, Homogeneous Catalysis, Heterogeneous Catalysis, Organometallic Chemistry and Theory. The central theme pervading all Departments is basic research in the catalytic transformation of compounds and materials with the highest degree of chemo-, regio- and stereoselectivity under conditions which maximize efficient use of natural resources.

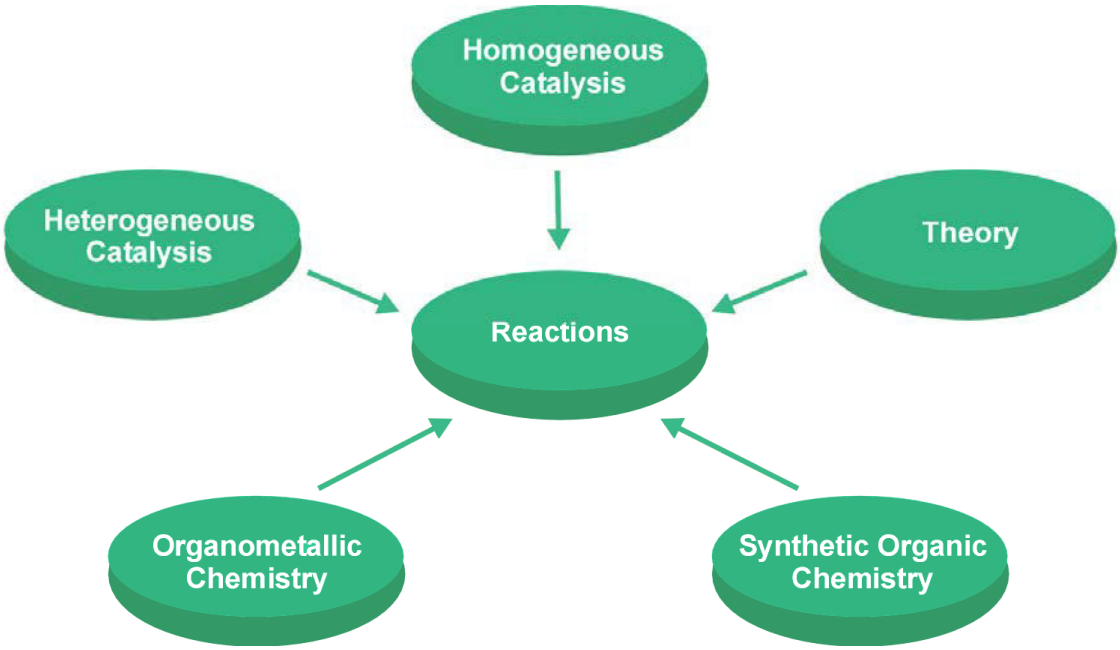

Catalysis is viewed world-wide as the key technology in the establishment of economically viable and ecologically benign chemical processes of the future. However, the efficiency of numerous catalytic systems is far from ideal and for many important chemical transformations appropriate catalysts have not even been found. Moreover, many fundamental aspects of catalysis are still poorly understood. Research in catalysis from a fundamental point of view calls for a high degree of interdisciplinarity. For a truly integrated approach, expertise is needed in homogeneous and heterogeneous catalysis, organocatalysis, biocatalysis, organometallic chemistry, organic as well as inorganic synthesis, and theory. By necessity, this requires the appropriate laboratories, equipment and instrumentation all in one unit. The idea of assembling five research Departments encompassing all major branches of catalysis under one roof therefore ensures the “critical mass” and the diversity necessary for meeting the scientific

challenges in this field. It is this factor which distinguishes research in Mülheim/Ruhr from related activities at universities. Indeed, the organizational concept of the Institute fosters an atmosphere conducive to scientific cross-fertilization and various kinds of synergisms. Traditional “gaps” between homogeneous and heterogeneous catalysis as well as biocatalysis are losing significance, and specific links between the Departments have developed. Moreover, a number of collaborations between the Institute and university groups are in operation, leading to significant scientific output as well as efficient use of the available instrumentation. Finally, a four-semester cycle of lectures, which covers homogeneous and heterogeneous catalysis, organocatalysis, biocatalysis, theory, and aspects of chemical engineering, provides special training for the doctoral students and post-docs of the Institute and contributes to the unique nature of the Institute.

Specific projects in the experimentally oriented Departments include the design and evolution of unusual kinds of achiral and chiral ligands, novel solid materials displaying specific functional properties, catalytic reactions using small organic molecules as catalysts, new transformations catalyzed by noble and non-noble metals, and directed evolution of selective enzymes for use in organic chemistry. Much emphasis is also placed on the development of atom-economical strategies for catalysis-based syntheses of complex natural products and biologically interesting compounds, the implementation of environmentally benign one- and two-phase solvent systems for catalytic reactions, the creation of combinatorial techniques in catalysis, and the study of how solid materials nucleate from solutions of relevant precursors. The results of many of these studies are expected to stimulate further research in actual catalyst design. The development of theoretical methods in quantum mechanics and molecular modeling in the Theory Department is also of prime importance, not only for extending the scope of computational methodology, but also for specific applications in homogeneous transition metal catalysis and biocatalysis.

In summary, the Institute has been organized to meet the needs for concerted interdisciplinary catalysis research from a fundamental point of view. Its objective is to carry out basic research to the point where industry and/or institutions dedicated to applied science can take over.

1.3 Organigram 2013

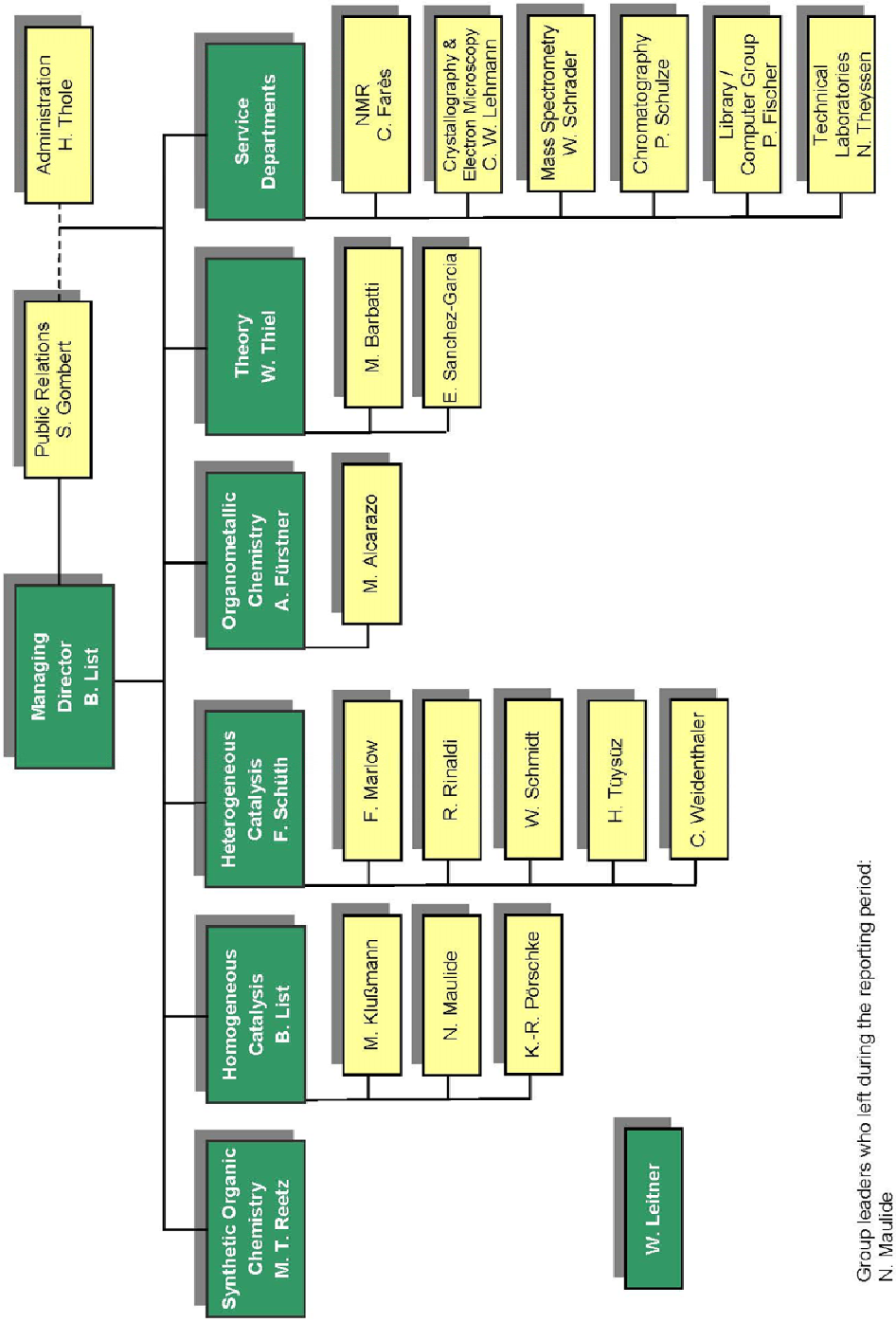

Group leaders who left during the reporting period:
N. Maulide

1.4 Members of the Scientific Advisory Board

(a) For the period until the end of 2005:

Professor Dr. Avelino Corma	Universidad Politécnica de Valencia Instituto de Tecnologia Quimica Avenida de los Naranjos s/n. 46022 Valencia, Spain
Professor Dr. Pierre Henri Dixneuf	Université de Rennes 1 UMR 6509 CNRS Campus de Beaulieu 35042 Rennes Cedex, France
Professor Dr. Dieter Enders	Institut für Organische Chemie der RWTH Aachen Professor-Pirlet-Straße 1 52074 Aachen, Germany
Professor Dr. Ben L. Feringa	University of Groningen Faculty of Mathematics and Natural Sciences Organic and Molecular Inorganic Chemistry Nijenborgh 4 9747 AG Groningen, The Netherlands
Professor Dr. John A. Gladysz	Institut für Organische Chemie der Universität Erlangen-Nürnberg Henkestraße 42 91054 Erlangen, Germany
Professor Dr. Henri Kagan	Université de Paris Sud Institut de Chimie Moléculaire d'Orsay CNRS Upresa 8075 91405 Orsay Cedex, France
Professor Dr. Joachim Sauer	Humboldt-Universität zu Berlin Institut für Chemie Unter den Linden 6 10099 Berlin, Germany
Professor Dr.-Ing. Jens Weitkamp	Universität Stuttgart Institut für Technische Chemie I Pfaffenwaldring 55 70569 Stuttgart, Germany

(b) For the period 2006-2011:

Professor Dr. Pierre Henri Dixneuf	Université de Rennes 1 UMR 6509 CNRS Campus de Beaulieu 35042 Rennes Cedex, France
Professor Dr. Dieter Enders	Institut für Organische Chemie der RWTH Aachen Professor-Pirlet-Straße 1 52074 Aachen, Germany
Professor Dr. Peter Hofmann	Organisch-Chemisches Institut der Universität Heidelberg Lehrstuhl für Organische Chemie III Im Neuenheimer Feld 270 69120 Heidelberg, Germany
Professor Dr. Eric N. Jacobsen	Harvard University Department of Chemistry 12 Oxford Street Cambridge, MA 02138, USA
Professor Dr. Joachim Sauer	Humboldt-Universität zu Berlin Institut für Chemie Unter den Linden 6 10099 Berlin, Germany
Professor Dr. Richard R. Schrock	Massachusetts Institute of Technology Department of Chemistry 77 Massachusetts Ave. Cambridge, MA 02139, USA
Professor Dr. Rutger A. van Santen	Eindhoven University of Technology Chemical Engineering and Chemistry PO Box 513, Helix STW 3.35 5600 MB Eindhoven, The Netherlands
Professor Dr.-Ing. Jens Weitkamp	Universität Stuttgart Institut für Technische Chemie I Pfaffenwaldring 55 70569 Stuttgart, Germany

(c) For the period 2012-2014/2017:

Professor Dr. Janine Cossy	Laboratoire de Chimie Organique ESPCI 10, rue Vauquelin 75231 Paris Cedex 05, France
Professor Dr. Jeremy Harvey	School of Chemistry University of Bristol Cantock's Close Bristol BS8 1TS, UK
Professor Dr. Peter Hoffmann	Organisch-Chemisches Institut der Universität Heidelberg Lehrstuhl für Organische Chemie III Im Neuenheimer Feld 270 69120 Heidelberg, Germany
Professor Dr. Eric N. Jacobsen	Harvard University Department of Chemistry 12 Oxford Street Cambridge, MA 02138, USA
Professor Dr. Graham Hutchings	School of Chemistry Cardiff University Park Place Cardiff CF10 3 AT, UK
Professor Dr. Paul Knochel	Fakultät Chemie und Pharmazie LMU München Butenandtstraße 13 81377 München, Germany
Professor Dr. Rutger A. van Santen	Eindhoven University of Technology Chemical Engineering and Chemistry PO Box 513, Helix STW 3.35 5600 MB Eindhoven, The Netherlands
Professor Dr. Helma Wennemers	Laboratory of Organic Chemistry ETH Zürich, HCI H313 Wolfgang-Pauli-Straße 10 8093 Zürich, Switzerland

1.5 Members of the Board of Governors ("Verwaltungsrat") 2012-2016

Representative of the Ministerium für Innovation, Wissenschaft und Forschung des Landes Nordrhein-Westfalen

Helmut Dockter

Representative of the Municipality of Mülheim an der Ruhr

Dagmar Mühlenfeld, Mayor of the City of Mülheim an der Ruhr

Representatives of the Max Planck Society

Dr. Ludwig Kronthaler, Secretary General of the Max Planck Society

Prof. Dr. Klaus Müllen

Dr. Jörn Rüter (Chairman)

Representatives of the Studiengesellschaft Kohle mbH

Prof. Dr. Michael Dröscher

Dr. Peter Nagler

Prof. Dr. Dieter Jahn (until 2013)

Dr. Peter Schuhmacher (since 2013)

Dr. Werner Schwilling, Honorary Member

Prof. Dr. Günther Wilke, Honorary Member

CHAPTER 2

Research Programs

2.1 Department of Synthetic Organic Chemistry

Director / External Group Leader

Manfred T. Reetz (born 1943)

Further group leaders:

Walter Leitner (born 1963)
external scientific member of the Institute

Curriculum Vitae: Manfred T. Reetz

1943	Born in Hirschberg (Germany) on August 13, 1943
1965	Bachelor degree, Washington University, St. Louis, USA
1967	Master degree, University of Michigan, Ann Arbor, USA
1969	Doctoral degree, Universität Göttingen with U. Schöllkopf
1971-72	Post-doc with R.W. Hoffmann at Universität Marburg
1973-1978	Assistant Professor at Universität Marburg (including Habilitation)
1978	Guest Professor at University of Wisconsin, USA
1978-1980	Associate Professor at Universität Bonn
1980-1991	Full Professor at Universität Marburg
1989-1990	Guest Professor at Florida State University, Tallahassee/USA
1991-2011	Director at the Max-Planck-Institut für Kohlenforschung, Mülheim/Ruhr
1993-2002	Managing Director of the Max-Planck-Institut für Kohlenforschung
1992-2011	Honorary Professor at Ruhr-Universität Bochum
1993-2011	Chairman of Studiengesellschaft Kohle mbH (SGK)

Awards and Honors

1976	Chemical Industries Prize (Dozentenstipendium des Fonds der Chemischen Industrie)
1977	Jacobus van't Hoff Prize (The Netherlands)
1978	Chemistry Prize of the Academy of Sciences Göttingen
1986	Otto-Bayer-Prize (Germany)
1989	Leibniz Award of the Deutsche Forschungsgemeinschaft
1997-	Member of German National Academy of Sciences Leopoldina
1997	Fluka-Prize "Reagent of the Year 1997"
2000	Nagoya Gold Medal of Organic Chemistry
2001-	Member of Nordrhein-Westfälische Akademie der Wissenschaften
2003	Hans Herloff Inhoffen Medal
2005-	Foreign Member of the Royal Netherlands Academy of Arts and Sciences
2005	Karl-Ziegler-Prize (Germany)
2005	Cliff S. Hamilton Award in Organic Chemistry (USA)
2006	Ernst Hellmut Vits-Prize (Germany)
2006	Prelog Medal (Switzerland)
2007	Honorary Professor at Shanghai Institute of Organic Chemistry (China)
2007	Ruhr-Prize for Arts and Science (Germany)

2009	Lilly Distinguished Lectureship Award (Czech Republic)
2009	Arthur C. Cope Award, ACS (USA)
2009	Yamada-Koga Prize (Japan)
2011	Honorary doctoral degree of Johann Wolfgang Goethe-Universität, Frankfurt (Germany)
2011	Tetrahedron Prize for Creativity in Organic Chemistry
2011	Otto-Hahn-Prize (Germany)
2012	IKCOC-Prize (Japan)

1980-2010 > 155 Plenary Lectures and Name Lectureships

Other Activities / Committees

1987-1988	Chairman of Chemistry Department, Universität Marburg
1989-1992	Committee Member of Fonds der Chemischen Industrie (Engeres Kuratorium)
1990-1995	Member of the Board, German Chemical Society (GDCh)
1992-1996	Chairman of Selection Committee, August-Wilhelm-von-Hofmann-Prize (Denkmünze, GDCh)
1993-2004	Member of the Scientific Advisory Board, Institut für Katalyseforschung Rostock
1994-1998	Member of Selection Committee, Carl-Duisberg-Prize (GDCh)
1994-1999	Member of Advisory Board, *Nachrichten aus Chemie, Technik und Laboratorium*
1994-2001	Member of Selection Committee, Karl Heinz Beckurts-Prize
1995	Vice-President of German Chemical Society (GDCh)
1997	President of Bürgenstock-Conference
1997-2001	Member of Board, Katalyseverbund NRW
1997-2012	Member of Advisory Board, *Topics in Organometallic Chemistry*
1998-2005	Member of Selection Committee, Emil-Fischer-Medaille (GDCh)
1999-2007	Member of Advisory Board, Catalysis NRSC (The Netherlands)
1999-2005	Chairman of Selection Committee, Adolf-von-Baeyer-Prize (Denkmünze, GDCh)
1999-	Member of Selection Committee, Alfried Krupp-Prize
1999-2011	Member of Selection Committee, Otto Bayer-Prize (Bayer AG)
2000-	Member of Advisory Board, *Russian Journal of Organic Chemistry*
2000-2005	Member of Advisory Board, *Advanced Synthesis & Catalysis*

2001-2005	Member of Scientific Advisory Board for the School of Engineering and Science, International University Bremen
2002-2010	Member of Editorial Board, *Angewandte Chemie*
2003-2017	Member of the Kuratorium der Alfried Krupp von Bohlen und Halbach-Stiftung
2003-	Member of the International Advisory Board, *QSAR & Combinatorial Science*
2005-2013	Member of the Editorial Advisory Board, *Bulletin of the Chemical Society of Japan*
2006-2011	Member of the Advisory Board, *Topics in Stereochemistry*
2006/2007	Member of the International Advisory Board of the Chemistry Department of Nagoya University (Japan)
2007-2015	Senator of the Chemistry Section, German National Academy of Sciences Leopoldina
2008-2010	Member of Advisory Board of the Karl Ziegler-Foundation (German Chemical Society)
2008-	Member of Ethics Committee of the Max Planck Society
2009-	Associate Editor of Chemistry and Biology
2009-2010	President of BOSS XII
2009-2010	Coordinator of ORCHEM 2010
2011-2013	Speaker of Class I of the German National Academy of Sciences Leopoldina
Since 1980	Member of Advisory Committees of numerous scientific conferences

Research in the Department of Synthetic Organic Chemistry

During the last three years the primary focus of research in the Reetz group was on methodology development in directed evolution of selective enzymes as catalysts in synthetic organic chemistry. The purpose was to make this Darwinian approach to asymmetric catalysis more efficient and therefore faster than in the past. Advanced gene mutagenesis methods and strategies were developed for the evolution of enhanced stereoselectivity, broader substrate scope (rate), higher thermostability and increased resistance to denaturing organic solvents. This involved the development of gene mutagenesis strategies characterized by high efficacy, improved molecular biological protocols, new approaches to high-throughput screening and selection as well as the design of bioinformatics-based and machine-learning techniques. Emphasis was also placed on 1) uncovering the reasons for increased efficacy, and 2) unveiling the source of enhanced stereoselectivity on a molecular level by means of mechanistic and theoretical studies.

Matthias Haenel, the only coal researcher in the Institute, retired in 2009. The External Member of the Institute, Walter Leitner (chair at TU Aachen), continued to run a small 2-3 person group here in Mülheim in the "Versuchsanlage", studying catalytic reactions in non-conventional solvents such as ionic liquids and supercritical CO_2. During the last three year evaluation period, research by the local Leitner group led to 24 publications.

The Director of the Department, Manfred T. Reetz, was originally scheduled to retire in 2008 at the age of 65, but received special permission from the President of the Max Planck Society to continue until 68 (extension of contract until 31 August 2011). Due to the Institute's plans regarding the successor and the concomitant extensive renovation of the respective floors in the high-rise laboratory building, the Reetz labs were closed in October 2010. Parallel to this development, Manfred Reetz accepted an offer from the University of Marburg to become the first Hans-Meerwein-Research-Professor starting 2011. The Marburg Chemistry Department will provide gene labs for about five coworkers as well as the general infrastructure, while the Max Planck Society has agreed to finance the research for five years following the formal termination of the Reetz-Directorship in August 2011. Thus, Manfred Reetz will head an external research group of the Max-Planck-Institut für Kohlenforschung, while also being a member of the Marburg faculty.

Due to the retirement of Manfred Reetz, new group leaders (assistant professors for Habilitation) were not recruited for the Department.

2.1.1 Research Area "Methodology Development in Directed Evolution" (M. T. Reetz)

Involved: C. G. Acevedo-Rocha, J. P. Acevedo, R. Agudo, Y. Gumulya, S. Kille, L. P. Parra, S. Prasad, J. Sanchis, E. Siirola, P. Soni, P. Torres Salas, Z.-G. Zhang, H. Zheng, F. E. Zilly

Objective: The goal was methodology development in the quest to make directed evolution more efficient than what it is was in 2010 with formation of higher-quality mutant libraries.

Results: Directed evolution involves repeating rounds of gene mutagenesis, expression and screening (or selection) of improved enzyme mutants. In the case of stereoselectivity, a fundamentally new approach to asymmetric catalysis has emerged (Scheme 1),[5,17,19] first demonstrated by our group in 1997 using a lipase as a catalyst in kinetic resolution.

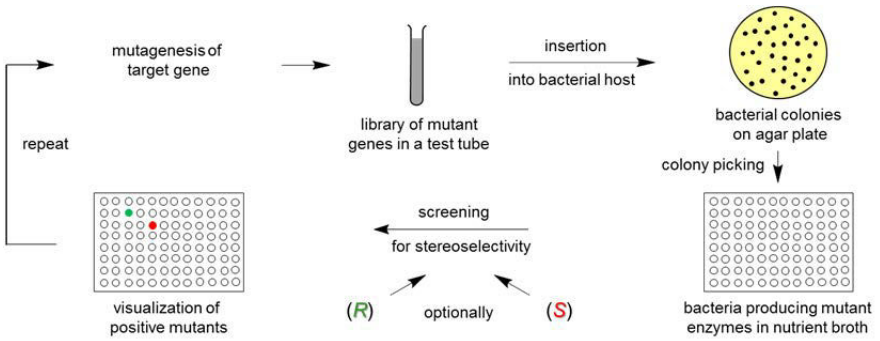

Scheme 1. Steps in the concept of directed evolution of stereoselective enzymes.[5,17,19]

During the last three years we have not just continued to apply this concept using various types of enzymes for practical purposes (Report 2.1.2), but have also *focused on methodology development in the quest to make directed evolution more efficient and reliable.* In the previous Report (2008-2010), we suggested that *I*terative *S*aturation *M*utagenesis (ISM) may be the best way to generate highest-quality mutant libraries requiring less screening effort. Thanks to the advanced techniques and strategies that we recently introduced, notable progress has been made. *ISM is now a knowledge-driven approach to directed evolution which requires only small libraries and thus a minimum of screening, the latter now being performed by standard automated GC or HPLC.*[5] Sites labeled A, B, C, D, etc. in an enzyme comprising one or more amino acid

positions are subjected to saturation mutagenesis (introduction of all 20 natural amino acids), and the genes of the hits are then used as templates for randomization at the other sites (Scheme 2). When targeting stereoselectivity and/or substrate acceptance (rate), sites around the binding pocket are chosen on the basis of our previously developed *C*ombinatorial *A*ctive-Site *S*aturation *T*est (CAST) (Scheme 2).

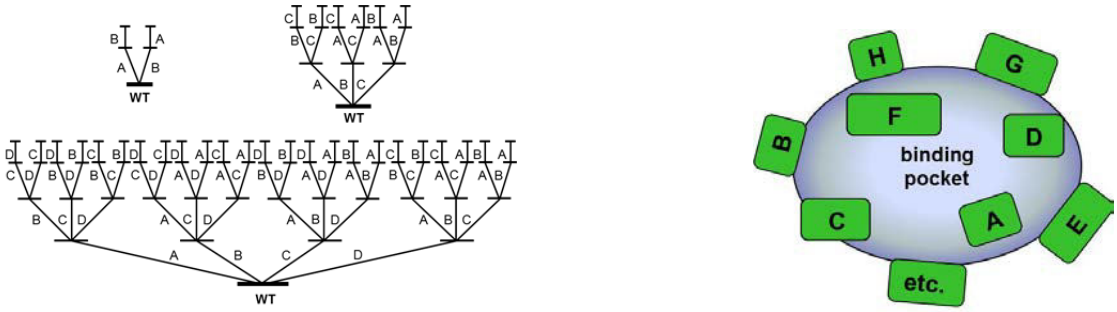

Scheme 2. Left: 2-, 3- and 4-site ISM systems; right: CAST sites for saturation mutagenesis.[5,17,19]

When applying saturation mutagenesis, it is necessary to consider statistical factors relating to the degree of oversampling necessary for covering a certain percentage of the library (number of transformants/mutants to be screened). Using the Patrick/Firth algorithms, we have devised a computer aid (CASTER) for designing mutant libraries and for calculating the respective oversampling number, e.g., for 95% library coverage.[5] The computed oversampling depends upon the number of amino acid positions at a given site and on the number of amino acids used as building blocks as set down by the codon degeneracy. The larger the randomization site and the larger the amino acid alphabet, the greater the screening effort. For example, instead of using the normal NNK codon degeneracy encoding all 20 canonical amino acids, we have shown by statistical analysis that NDT codon degeneracy encoding only 12 amino acids (Phe, Leu, Ile, Val, Tyr, His, Asn, Asp, Cys, Arg, Ser and Gly) requires in the case of a 2-residue site the screening of only 430 transformants, while classically NNK calls for 3,000. In the case of a 3-residue site the respective numbers are ≈5,000 (NDT) versus ≈ 100,000 (NNK). In the lab we have performed several studies using different enzymes and model reactions during the last three years comparing the classical NNK with NDT and with codon degeneracies encoding even smaller amino acid alphabets,[2,3,4,11,22,25,27,30,32,34,36] resulting in the conclusion that the *use of properly chosen amino acid alphabets constitutes one of the most proficient tools in present-day directed evolution.* Smaller amino acid alphabets reduce the structural diversity of the enzyme mutants in a given library, but the benefits in terms of dramatically reduced screening effort are enormous. *It is also useful to consider structural and mechanistic data as a*

guide in a bioinformatics approach. Application of the Nov-algorithms in our work has shown that screening can be reduced even more when targeting not the best mutant, but the second or nth best variant in a given library, while still leading to excellent mutants.[32]

Usually we considered only 1-, 2- and 3-residue sites due to statistical considerations. However, recently we devised a project in which two "mega-sites" A and B were chosen, each consisting of five amino acid positions (residues). For 95% library coverage, one would have to screen the astronomical number of 10^8 transformants if all 20 canonical amino acids were to be used as building blocks (NNK codon degeneracy). Therefore we tested *the idea of using extremely reduced amino acid alphabets*, and screened only a few thousand mutants, the model system being a stereoselective Baeyer Villiger reaction catalyzed by a Baeyer-Villiger monooxygenase. Both pathways A → B and B → A were experimentally explored requiring only four mutant libraries, and both pathways proved to be successful.[32] Notably improved mutants were evolved, yet only 8-9% of the theoretical protein sequence space was covered. We suggest that the Nov-algorithm focusing not on the best, but on the nth best mutant in a given library is a better way to assess the statistics. *We also conclude that grouping single residues into "mega-sites" is currently the best way to perform ISM*. This reduces the number of possible evolutionary pathways (Scheme 2) and cuts the screening effort drastically.[32]

The phenomenon of amino acid bias due to the (natural) degeneracy of the genetic code constitutes a different problem which diminishes library quality when using all 20 canonical amino acids as building blocks. Our "trick" is simple and efficient: *Use of a designed mixture of three primers which create a degeneracy of 22 unique codons encoding all 20 canonical amino acid*s.[23] NDT, VHG and TGG codon degeneracies are chosen, which reduces the screening effort as shown by P450 experiments. Nature utilizes 64 codons (NNN); until recently we and others employed 32 codons (NNK) which is better, but now we are down to 22 codons for 20 amino acids which reduces amino acid bias considerably (Scheme 3).[32]

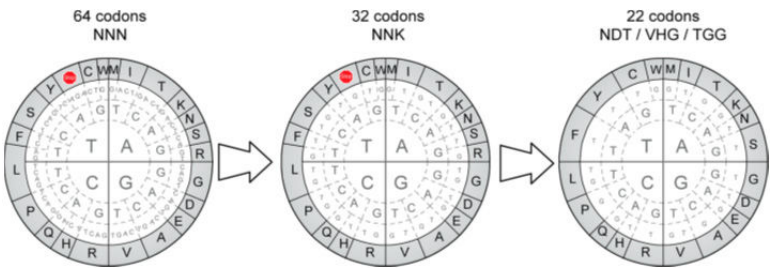

Scheme 3. Stepwise reduction of amino acid bias when using all 20 canonical amino acids.[32]

Another advancement during the 3-year assessment period is the systematic development of the Quick Quality control (QQC) of mutant libraries: *A pool of plasmid DNA belonging to all clones of a library is sequenced in a single run and analyzed to determine whether the designed degeneracy has been introduced and whether removal of the WT-sequence has been achieved.*[3,8,11,23,32,34,36] Low quality libraries should not be screened, e.g., those that contain a lot of WT enzymes or do not harbor many of the designed mutants. Should poor quality be indicated in a given case, such parameters as annealing temperature, primer length, and GC content as well as position and sequence of the target codon in the gene should be re-considered. In a chapter for *Methods in Molecular Biology* based on new and older experimental data, tips on how to apply ISM optimally while avoiding potential pitfalls are summarized as a guide for the experimenter. *In another contribution we focused on our previous method called Assembly of Designed Oligonucleotides (ADO), which is a type of synthetic DNA shuffling, but which can now be applied to saturation mutagenesis and thus to ISM.*[33]

A traditional problem in directed evolution arises when a newly created designed mutant library fails to contain any improved variant. *We have discovered a simple way to escape from such local minima in the fitness landscape*: *Simply use a non-improved or even an inferior mutant as a template for saturation mutagenesis in the following ISM cycle at a different randomization site.*[15] This seemingly "contra-intuitive" approach was illustrated using the epoxide hydrolase from *Aspergillus niger* (ANEH) All 24 evolutionary pathways of a 4-site ISM system (Scheme 2) were explored using the kinetic resolution featured in Scheme 4:

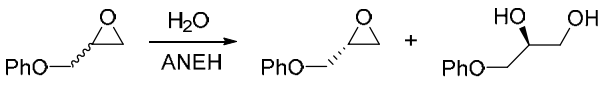

Scheme 4. Kinetic resolution of glycidyl phenyl ether as the model reaction.

Out of the 24 pathways, 8 exhibited local minima. In these cases an inferior mutant in a library lacking any hits was nevertheless used in the subsequent ISM round of saturation mutagenesis. Improved enantioselectivity of at least E = 30 was achieved in all such cases, which demonstrates that this approach constitutes a simple way to escape from local minima.[15] The 12 best pathways leading to selectivity factors of E > 88 are shown in Scheme 5 (the other 12 pathways provide mutants showing E = ≈ 30-70, not included here for clarity).

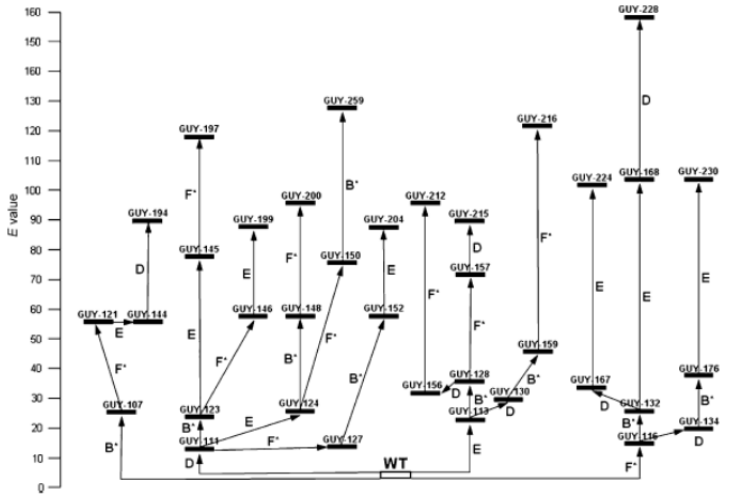

Scheme 5. Best 12 of the 24 pathways describing the fitness landscape.[15]

A fitness-pathway landscape was generated by systematic deconvolution of all sets of mutations that accumulated in every one of the 24 pathways (Scheme 6).[15] A typical pathway devoid of a local minimum is marked in green and one containing a local minimum is featured in red as part of the whole fitness landscape. There are 16 green and 8 red pathways.

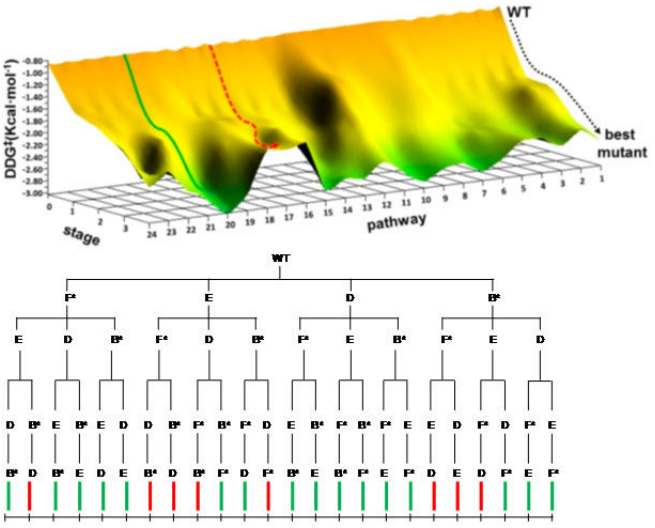

Scheme 6. Left: Fitness landscape (see text); right: scheme of all 24 evolutionary ISM pathways.[15]

In collaboration with H. Rabitz (Princeton/USA), *an approach to in silico directed evolution was developed based on the adaptive substituent reordering algorithm (ASRA)* (Scheme 7).[14] Increased efficiency at every evolutionary stage was achieved. Potential enzyme mutants with desired properties from minimal sampling of focused libraries can be identified, which reduces the screening effort. This was demonstrated

using an epoxide hydrolase in the hydrolytic kinetic resolution of the chiral epoxide glycidyl phenyl ether (see above).

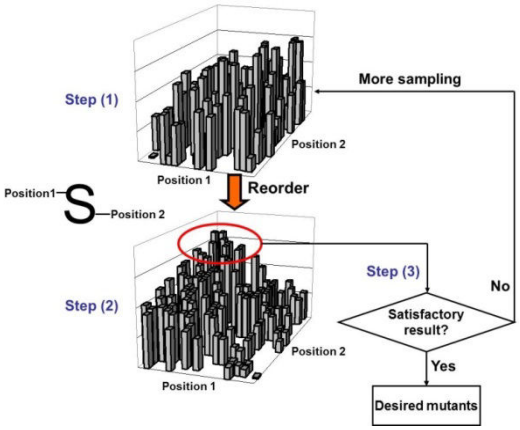

Scheme 7. Representation of steps involved in an ASRA operation as applied to ISM.[15]

Finally, the overall experimental process based on ISM can be improved even more by optimizing the screening step. In collaboration with O. Trapp (Heidelberg), application of his multiplexing chromatography algorithm to the HPLC analysis of a 3,000-membered library of ANEH mutants was successful, requiring less than a few hours (to be published in 2014).

Future directions: In order to increase the efficacy of ISM further, novel concepts will be tested: The use of super large randomization sites of ≥ 10 single positions aligning the binding pocket using the smallest amino acid alphabets possible, in the extreme case only one amino acid as building block. A second amino acid will then be used in ISM, both choices depending on structural and mechanistic data. Testing ADO in these cases is also planned.

Publications resulting from this research area: 2, 3, 4, 5, 8, 14, 15, 23, 24, 32, 33, 34

External funding: Arthur C. Cope foundation (USA)

Cooperations: H. Rabitz (Princeton/USA), O. Trapp (Heidelberg)

2.1.2 Research Area "Applications of Advanced Directed Evolution Methods" (M. T. Reetz)

Involved: C. G. Acevedo-Rocha, J. P. Acevedo, R. Agudo, W. Augustyniak, M. Bocola, Y. Gumulya, A. Ilie, S. Kille, L. P. Parra, S. Prasad, G.-D. Roiban, F. Schulz, E. Siirola, P. Soni, P. Torres Salas, Q. Wu, Z.-G. Zhang, H. Zheng, F. E. Zilly

Objective: The goal was to apply the newly developed directed evolution methods to selected regio- and stereoselective transformations in synthetic organic chemistry not readily possible by state of the art transition metal catalysis or organocatalysis.

Results: One of several projects concerned enantioselective ketone reductions. Prochiral ketones $R^1R^2C{=}O$ can be reduced with high enantioselectivity to the respective alcohols using Noyori-type Ru-catalysts, provided the groups R^1 and R^2 are sterically sufficiently different. Alcohol dehydrogenases (ADHs) constitute an alternative. However, substrate scope and/or stereoselectivity are often limited, which calls for directed evolution. An example that we worked on in our group is the reduction of the ketone shown below, which leads to an axially chiral alcohol.[22] The robust ADH from *Thermoethanolicus brockii* (TbSADH), which had been characterized by X-ray crystallography, is only moderately *R*-selective (66% *ee*). As expected, chiral Ru-complexes as catalysts fail completely (< 5% *ee*). Upon applying ISM (see Report 2.1.1), *R*-selectivity was boosted to 97% *ee*, and reversal of enantioselectivity was likewise achieved with *S*-selectivity amounting to 98% *ee*. Other substrates were also tested successfully. T*he bromide is a key compound because transition Pd-catalyzed carbonylation and Suzuki coupling provided a number of derivatives, showing that the combination of biocatalysis and transition metal catalysis constitutes an attractive synthetic strategy.*[22]

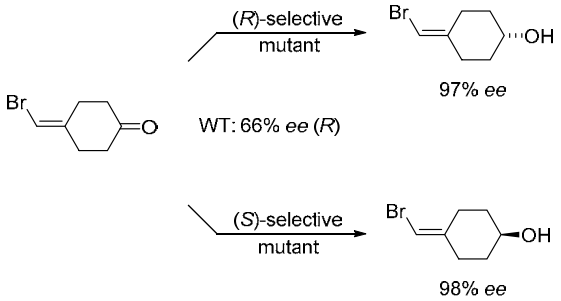

Scheme 1. Induced axial chirality using evolved ADH mutants.[22]

Another synthetically rewarding focus was on selective C-H activating oxidative hydroxylation catalyzed by P450 monooxygenases, especially in those cases in which synthetic reagents or catalysts fail. *Although in this area dozens of directed evolution studies had already appeared, up to 2010 no protein engineering method existed allowing the control of regio-* ***and*** *stereoselectivity.* The mechanism involves a high energy radical abstraction of an H-atom by the high-spin heme-Fe=O followed by rapid C-O bond formation of the intermediate radical. With ISM in hand,[5] we turned to this challenge by initially considering the hydroxylation of testosterone as the model reaction (Scheme 2).[3] Whereas the starting enzyme P450-BM3-F87A is not regioselective (1 : 1 mixture of alcohols at the 2- and 15-positions, plus small amounts of other alcohols, we succeeded in evolving 2ß- and 15ß-selective mutants, each showing > 99% diastereoselectivity (no trace of α-alcohols). A molecular dynamics (MD) investigation revealed for the 2ß-selective mutant a 2ß-pose directly above the catalytically active heme-Fe=O, and for the 15ß-selective mutant the respective 15ß-pose (see Report 2.1.3). Other steroids such as progesterone were also studied.[3]

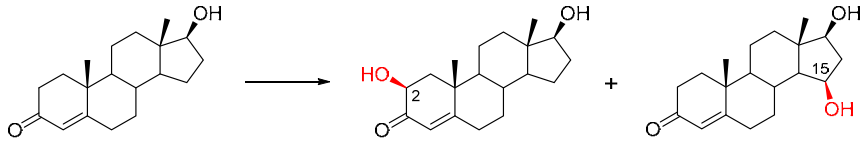

Testosterone	2β-Hydroxytestosterone		15β-Hydroxytestosterone
P450-BM3(F87A)	50	:	50
2β-selective mutant	97	:	3
15β-selective mutant	4	:	96

Scheme 2. Regio- and stereoselective oxidative hydroxylation of testosterone using P450-BM3 mutants.[3]

Other steroids such as progesterone were also tested, generally with mutants already evolved for testosterone, i.e., without performing additional mutagenesis experiments.[3] A few of the results are shown in Scheme 3.

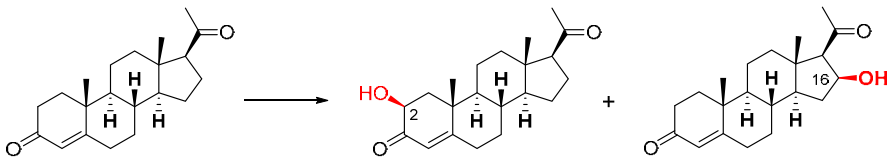

Progesterone			
P450-BM3(F87A)	18	:	82
2β-selective mutant	>99	:	<1
16β-selective mutant	9	:	91

Scheme 3. Regio- and stereoselective oxidative hydroxylation of progesterone using P450-BM3 mutants.[3]

Most recently we have used testosterone as the model compound in order to target other positions and also to reverse diastereoselectivity (α-attack). For example, only two rounds of ISM led to 16α- and 16ß-selective mutants, respectively, showing 83-85% selectivity (which still needs to be improved by further mutagenesis experiments).

We originally surmised that in the binding pocket of P450 enzymes, known to be geometrically large, the selectivities of bulky compounds such as steroids are easier to control than of smaller substrates. In order to check this uncertainty, cyclohexene-1-carboxylic acid ester was tested (Scheme 4).[11] Gratifyingly, it was indeed possible to evolve regio- and enantioselective P450-BM3 mutants. Following the initial steroid examples, *this is the first case of directed evolution of a P450 enzyme in which regio- and enantioselectivity* (*in favor of either enantiomer) of a "small" substrate was shown to be possible.*[11] Here again subsequent transition metal catalyzed reactions were performed, in this case with formation of novel GABA-analogs.[11] However, upon testing 1-methylcyclohexene (which lacks a functional group helpful in ensuring a specific pose in the binding pocket), directed evolution was less successful (mixtures of products).[30] This shows that state the art directed evolution needs further improvement, at least in the case of P450-catalyzed oxidative hydroxylation of such non-functionalized substrates.

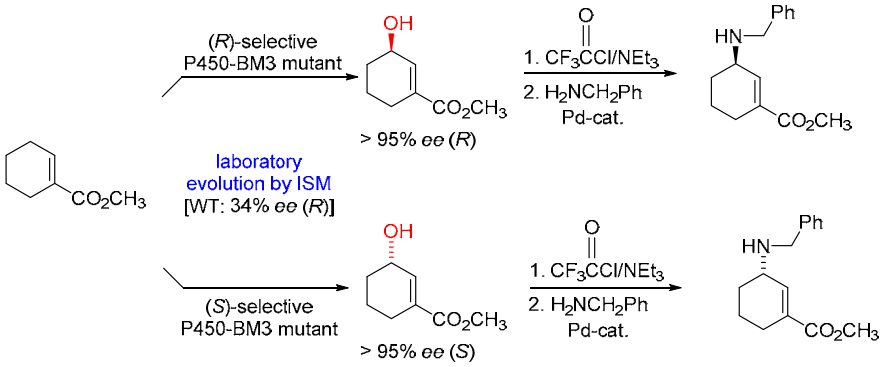

Scheme 4. Selective oxidative hydroxylation of a small molecule catalysed by P450-BM3 mutants.[11]

Although it can be argued that the above chiral alcohols can be obtained by other routes, this does not apply to the structurally more complex *S*-alcohol shown in Scheme 5. It was previously prepared by Berchtold et al. in 1987 in 11 steps and subsequently used in several natural products syntheses. Without performing additional mutagenesis experiments, the previously obtained *S*-selective mutant was tested in this reaction, leading to 93% *ee* (89% conversion)[11]:

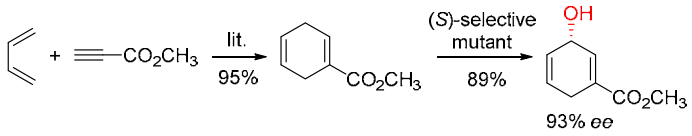

Scheme 5. Hydroxylation catalyzed by a P450-BM3 mutant evolved for the substrate shown in Scheme 4.[11]

Yet another difficult synthetic transformation, not at all possible by standard synthetic organic reagents or catalysts, concerns the diastereoselective Baeyer-Villiger reaction of compounds of the type represented by 4-bromomethylene-cyclohexanone (Scheme 6). *This type of transformation has not been considered previously in organic chemistry nor in biocatalysis.* Whereas control experiments using such reagents as MCPBA led to 1 : 1 mixtures of *E*- and *Z*-products, as expected, we discovered that wild-type (WT) Baeyer-Villiger monooxygenase CHMO accepts the compound with 99% *E*-selectivity.[27] Application of ISM provided a mutant showing reversed diastereoselectivity (82% *Z*-selective). *Subsequent Pd-catalyzed carbonylation and Suzuki coupling reactions were performed, demonstrating once more the power of combining biocatalysis with transition metal catalysis.* The approach constitutes a novel way to selectively prepare *E*- and *Z*-olefins.[27] Further examples of directed evolution of stereoselective Baeyer-Villiger monooxygenases were also reported.[20,32]

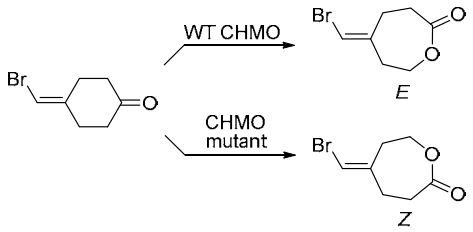

Scheme 6. Diastereoselective Baeyer-Villiger reactions catalysed by CHMO.[27]

Hydrolytic enzymes such as lipases have been used successfully for decades in organic chemistry and biotechnology, kinetic resolution of chiral alcohols or desymmetrization of meso-diols being typical examples (which can also be performed to some extent by applying chiral organocatalysts). In contrast, chiral acids or esters are often more difficult to handle, e.g., the robust and industrially viable lipase *Candida antarctica* B (CALB) cannot be used for this type of substrates (slow reactions with poor stereoselectivity), and organocatalysts show only moderate stereoselectivity as recently shown by the groups of I. Shiina and V. B. Birman. Therefore, we initiated a project directed toward evolving CALB mutants with broad substrate scope.[25] ISM was first

applied to the model transformation involving the ibuprofen-type of substrate shown in Scheme 7, then other substrates were likewise tested.

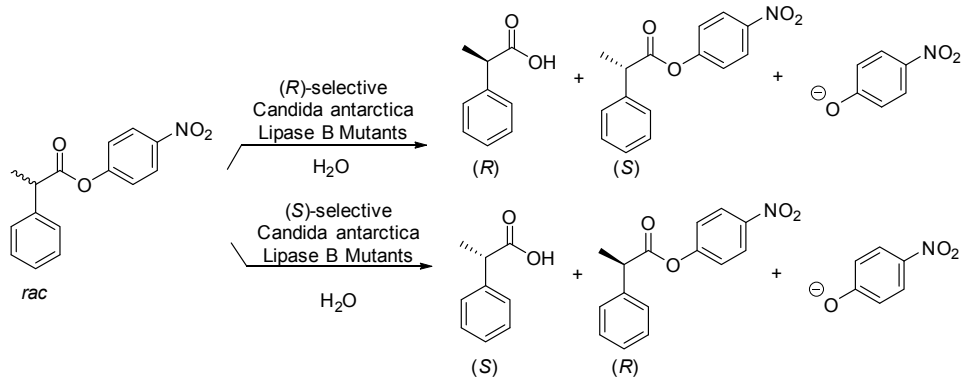

Scheme 7. Hydrolytic kinetic resolution catalyzed by CALB mutants.[25]

Five CAST sites A, B, C, D and E around the binding pocket were chosen for saturation mutagenesis. Exploration of a select few upward/downward pathways provided *S*- and *R*-selective mutants, respectively (Figure 1).[25] The results were explained on a molecular level by extensive MD simulations and docking experiments. Enzyme kinetics were also performed, demonstrating notably enhanced catalytic activity in the reaction of this particular compound, but also when subjecting structurally related substrates to this kind of hydrolytic kinetic resolution.[25] The superiority of ISM was also demonstrated using other lipases.[4,13]

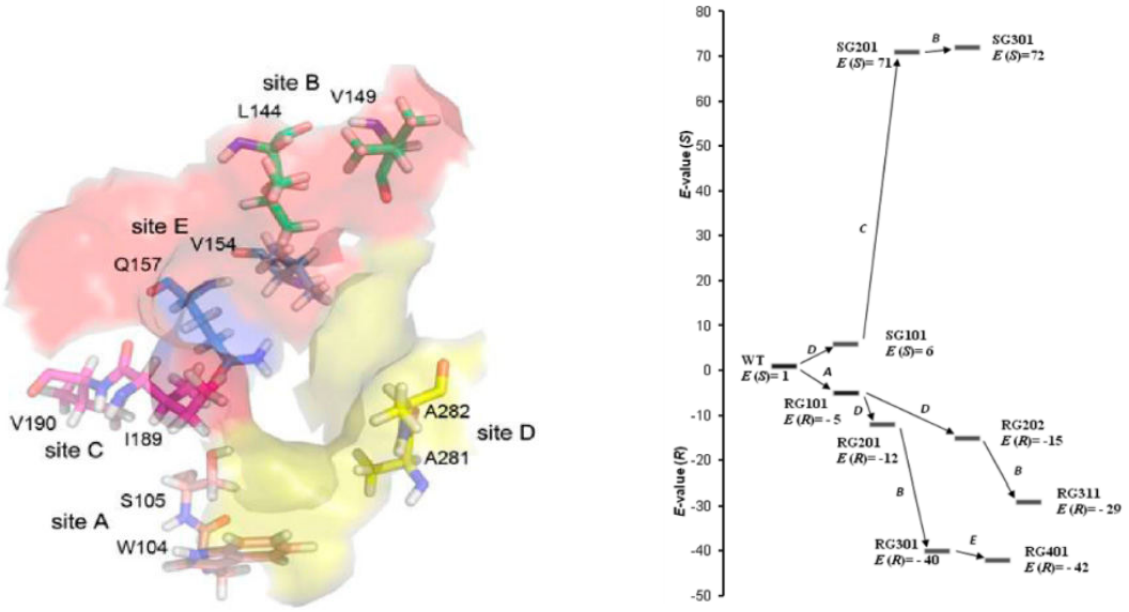

Figure 1. Left: CAST sites A-E in CALB; right: ISM results of the model reaction.[25]

In research regarding biocatalysis not related to directed evolution, we discovered that the activity and selectivity of P450-BM3 can be notably enhanced by the use of chemically inert additives of the type per-fluoro fatty acids $CF_3(CF_2)_nCO_2H$, which presumably enter the large binding pocket with concomitant reduction of its size, while also switching the low-spin form of heme-Fe to the catalytically active high-spin state.[9] A number of small alkanes not accepted by WT P450-BM3 such as propane are oxidatively hydroxylated regioselectively (only isopropanol) with high TON values (≈ 3000), which may have practical ramifications.[9] Methane as originally reported does not undergo oxidation to such an extent, if at all, which has been corrected. Nevertheless, the notion that an additive of this kind acts as a molecular switch, turning on the catalytically active state of the enzyme while effectively reducing the volume of the large binding pocket, constitutes a practical approach. It can be combined with directed evolution: We have shown that the selectivity of P450-BM3 mutants evolved by ISM as catalysts in steroid hydroxylation can be influenced by treatment with such additives (S. Kille, M.T. Reetz, unpublished results). Lipases also respond to such additives as recently demonstrated by our group, but the phenomenon behind such effects is a different one.[10]

Other work concerns thermostabilization of selected enzymes and higher expression rates using directed evolution and rational design as well as enzyme immobilization.[8,12,21] In collaboration with E. Meggers (Marburg), *we have also evolved the first P450-BM3 mutants for selective bioorthogonal deprotection reactions occurring in cells* (unpublished). Finally, *a synthetically intriguing goal is the question of stereoconvergent transformation of racemic compounds allowing for 100% conversion instead of the usual kinetic resolution*. This was tested using an epoxide hydrolase (EH), although epoxides cannot be racemized. While some examples of stereoconvergency are known in the literature using certain WT EHs and we had previously performed directed evolution of the EH from *Aspergillus niger* (ANEH) for this purpose in one case, we recently turned to the limonene epoxide hydrolase (LEH) due to its higher intrinsic activity towards bulky substrates. An example is shown in Scheme 8. Initial results appear promising, setting the stage for further ISM-based optimization. Currently we record an *ee*-value of 70% at 95% conversion in favor of the (1*S*, 2*S*)-diol (E. Siirola, M.T. Reetz, unpublished). It means that one enantiomeric form of the epoxide reacts with water regioselectively at one C-atom, while the enantiomer reacts at the other C-atom, both with inversion of configuration leading to the same enantiomeric product! *One and the same mutant induces two different reactions of*

opposite regioselectivity by enforcing two different poses of the two enantiomers in the enzyme's binding pocket.

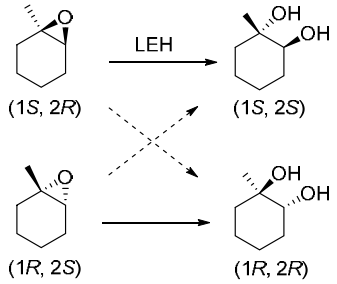

Scheme 8. Stereoconvergent process catalyzed by an evolved LEH mutant (E. Siirola, M.T. Reetz, unpublished).

Future direction: Further research is planned in the area of P450-catalyzed regio, stereo- and chemoselective oxidative hydroxylation of steroids, especially in the quest to reverse diastereoselectivity from ß- to α-attack, while also targeting different C-atoms. A new concept for creating two (or three!) new stereocenters (rather than just one as done thus far) in a single hydroxylation step will also be tested, as in the P450-catalyzed hydroxylation of methylcyclohexane which when reacting at the two methylene units flanking the methyl-bearing C-atom may lead to four different stereoisomers. The challenge will be to control the stereoselectivity in the reaction of such a simple substrate, which however lacks a functional group for possible specific binding. Fully bioorthogonal P450-catalyzed deprotection systems occurring in cells (e.g., *E. coli*), based on evolved P450-mutants, will be developed (hopefully!). Another project will attempt the deracemization of chiral alcohols by directed evolution. Finally, promiscuous enzyme-catalyzed processes will be attempted by de novo design coupled with directed evolution based on ISM.

Publications resulting from this research area: 3, 4, 5, 6, 7, 9, 10, 11, 13, 17, 18, 19, 20, 22, 25, 26, 27, 28, 30, 31, 36

External funding: Arthur C. Cope foundation (USA)

Cooperations: P. Diaz (University of Barcelona/Spain); Q. Wu (Zhejiang University/China); L. P. Parra (Santiago/Chile); J. P. Acevedo (Santiago/Chile); E. Meggers (Marburg)

2.1.3 Research Area "Learning from Directed Evolution" (M. T. Reetz)

Involved: J. P. Acevedo, C. G. Acevedo-Rocha, A. Augustyniak, W. Augustyniak, M. Bocola, Y. Gumulya, S. Kille, L. P. Parra, S. Prasad, J. Sanchis, F. Schulz, P. Soni, P. Torres Salas, Z.-G. Zhang, H. Zheng, F. E. Zilly

Objective: Two goals were defined: a) to unveil the reasons for increased selectivity and enhanced thermal robustness of mutant enzymes evolved in the laboratory, and b) to understand on a molecular level the efficacy of iterative saturation mutagenesis (ISM).

Results: Two fundamentally different lessons were learned from directed evolution, specifically because additional research efforts were invested following the actual directed evolution studies:

a) Upon performing biophysical characterization of the mutants including enzyme kinetics flanked by MD and QM investigations, the factors leading to improved catalyst improvement can be revealed, which also deepens our understanding of how enzymes function in general.
b) Upon deconvoluting the point mutations or sets of mutations that accumulate along an evolutionary ISM pathway, knowledge is generated which reveals whether additive or non-additive interactions (cooperative, deleterious or none) occur between the individual components (mutations) in the experimentally generated fitness landscape.

In a collaborative effort with the group of Walter Thiel regarding the origin of enantioselectivity in the oxidative desymmetrization of 4-methyl- and 4-hydroxycyclohexanone catalyzed by the Baeyer-Villiger monooxygenase CHMO, a QM/MM molecular dynamics study was performed.[16] Although the gross mechanism had been established decades earlier as involving a flavin-hydroperoxide anion ($FADHOO^-$) attacking the carbonyl function with formation of a Criegee-intermediate followed by fragmentation and migration of a σ-bond, details crucial for a true understanding were lacking. The computations showed that the Criegee-intermediate is stabilized by a strong H-bond due to Arg-329. It was also shown that the traditional stereoelectronic requirement for low-energy σ-bond migration in the Criegee intermediate of synthetic reactions, namely an anti-periplanar arrangement of the C-C-O-O moiety, is decisive for fast and stereoselective CHMO-catalyzed reactions. The

energy difference between the chair conformer of 4-methylcyclohexanone with equatorial methyl and the chair conformer with methyl in the axial position (≈ 2.3 kcal/mol) determines the outcome of the desymmetrization reaction! *Insight into the mechanism of CHMO as a typical Baeyer-Villiger monooxygenase was thereby generated, increasing our knowledge of how this class of enzyme functions.*[16] In the case of desymmetrization of 4-hydroxy-cyclohexanone catalyzed by a CHMO mutant, H-bonds to the hydroxyl group was found to play a major role.[29]

Another theoretical problem relates to the question *why certain P450-BM3 mutants obtained by ISM show pronounced regio- and stereoselectivity when used as catalysts in the oxidative hydroxylation of such substrates as steroids,* whereas the starting enzyme is unselective (Report 2.1.2). Since a high-energy radical process is involved, it is unlikely that the transition state is stabilized by the protein environment as it is in most other enzyme-catalyzed transformations (Pauling hypothesis of why enzymes are so active). Rather, any regio- and stereoselective P450-catalyzed reaction must involve a protein environment which simply holds the substrate in a certain pose with the respective C-H moiety pointing directly at the catalytically active high-spin heme-Fe=O. Therefore, the 2ß- and 15ß-selective P450-BM3 mutants as catalysts in the oxidation of testosterone were subjected to extensive MD simulations and docking experiments.[3] It turned out that in the case of the 2ß-selective mutant the energetically most favorable pose is indeed the one in which the 2ß-hydrogen atom points directly at heme-Fe=O, ready to be attacked via H-abstraction followed by rapid C-O bond formation of the short-lived radical. In the case of the 15ß-selective mutant, only one active pose is revealed in which the 15ß-hydrogen atom is poised for oxidative attack (Figure 1).

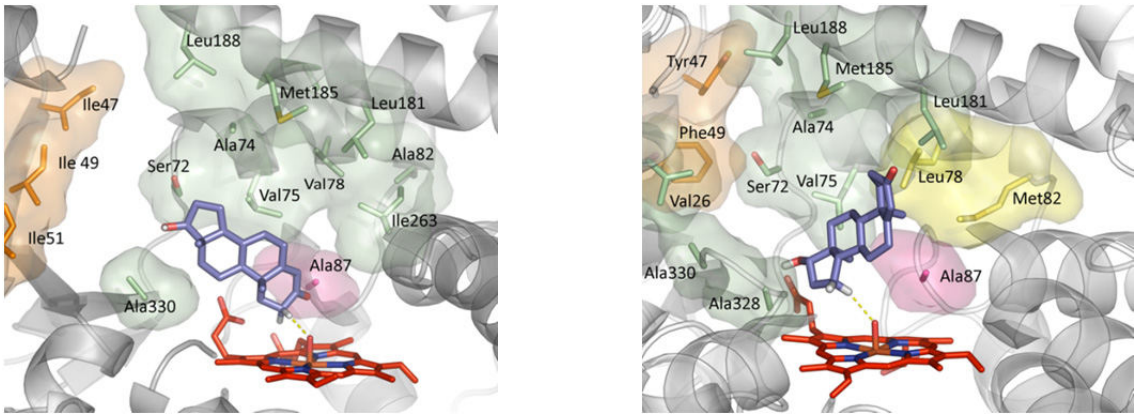

Figure 1. Left: Lowest energy pose of testosterone above catalytically active heme-Fe=O in 2ß-selective mutant; right: respective pose in 15ß-selective mutant.[3]

In contrast to P450 catalyzed reactions, those mediated by hydrolases such as lipases or epoxide hydrolases involve transition states in which the protein environment exerts a stabilizing effect due to many different interactions between the substrate and the binding pocket wall. Quite often these can be identified by MD simulations and docking experiments without the need to perform QM calculations. *We have utilized this option in our own group routinely, thereby enabling the identification of factors responsible for the observed mutational effects on catalysis, insights which deepen our understanding of how these enzymes function in detail.* One of several examples during the last three years concerns the study of (*R*)- and (*S*)-selective mutants of the lipase CALB as catalysts in the kinetic resolution of α-phenyl propionic acid ester (Report 2.1.2). Additional stabilizing H-bonds of the oxy-anion intermediate were identified in each case, thereby explaining the role of mutants.[25] Similar effects were uncovered in the directed evolution of *Ps. aeruginosa* lipase.[4]

A very different goal is to gain an understanding as to why ISM is so effective. *For this purpose we have performed extensive deconvolution studies with concomitant construction of fitness landscapes reflecting the energies of complete ISM pathways as determined by experimental* $\Delta\Delta G^{\neq}$ *values* (Report 2.1.2). In order to analyze the vast data more carefully, the question of additivity versus non-additivity of mutational interactions needs to be posed and answered at every step of an evolutionary pathway.[15,24,25,32,34] Consider a 4-step pathway in a 4-site ISM scheme (Report 2.1.1). The influence of the first set of mutations (or possibly single point mutation) in library A is known experimentally, and when visiting site B the effect of the sum of the first mutational set (A) and the second mutational set (B) is also accessible by measuring the catalytic property of interest (e.g., enantioselectivity). However, the effect of mutational set B alone is not known. Therefore, in a deconvolution step the mutational set B is introduced by site-specific mutagenesis of the original WT enzyme with formation of a new mutant.

In traditional protein engineering, scientists expected mathematical additivity of the two sets of mutations (or two different single point mutations). *What we find in our work is the "surprising" fact that most often (mathematical) additivity does not pertain.*[24] Rather, non-additivity is observed in terms of pronounced cooperative effects, i.e., more than additivity. For example, the effect at mutational set B alone can be very small, but in concert with the mutational set A as observed in the ISM step an enormous increase in desired catalytic property results at stage A-B of the evolutionary pathway. Sometimes this type of deconvolution leads to an even more surprising effect, namely that A increases for example (*R*)-selectivity as does the accumulation of the mutational

set B in the subsequent ISM step, but deconvolution of A-B reveals that the mutational set B alone is actually (*S*)-selective. Mutational set B alone can formally be considered to be deleterious, but in concert with mutational set A, strong communication on a molecular level leads to enhanced (*R*)-selectivity (Scheme 1).[15,25,32]

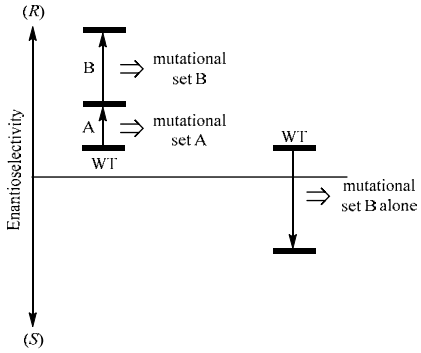

Scheme 1. Example of strong non-additivity characterized by a pronounced cooperative effect.[15, 25,32]

Data of this kind also throws light on the efficacy of ISM and is relevant to protein engineering in general. We routinely encountered even more surprising results. For example, upon deconvoluting an evolved (*S*,*S*)-enantioselective double mutant (95% *ee*) of an epoxide hydrolase as a catalyst in the desymmetrization of cyclopentane oxide (Scheme 2), "strange" observations were made (E. Siirola, M. T. Reetz, unpublished): Each of the two single point mutations alone induce (*R,R)*-selectivity, i.e., opposite enantioselectivity! MD studies directed toward understanding these cooperative effects on a molecular level are underway.

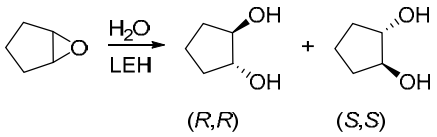

Scheme 2. Hydrolytic desymmetrization catalyzed by LEH mutants (E. Siirola, M.T. Reetz, unpublished).

More data emerging from deconvolution studies is being collected in our group.[24] Today we believe that such phenomena occur more often than previously thought (also in Nature?). *The amino acids in any given protein interact with one another (unpredictably? in a non-linear manner*. We have performed an analysis of our extensive laboratory data accumulated thus far and of rare results of other groups, which has opened a new research area.[24]

Finally, *in order to uncover the reasons for enhanced thermal robustness of a Bacillus subtilis lipase mutant on a molecular level, protein NMR studies and other biophysical investigations were performed in collaboration with R. Boelens and B. Dijkstra*

(Groningen/Netherlands).[12,21] The effect of the mutations was traced to a notably reduced deleterious protein/protein interaction which in the WT lipase leads to aggregation and undesired precipitation upon heat treatment. Such behavior in the WT lipase shuts down catalytic performance, but in the mutant it is sharply reduced! We have learned a lot from this unusual phenomenon.[12,21]

Future directions: Research in the intriguing area of non-additive (cooperative or deleterious) mutational effects as uncovered by deconvolution experiments of evolved mutants will be extended, flanked by theoretical studies in hope of explaining such unusual effects on a molecular level. With the help of a new postdoc in Marburg, QM/MM studies of P450 mutants are also planned (dynamic effects of these mechanistically complex enzymes!). The recently initiated collaboration with Walter Thiel concerning stereoselective sulfoxidation of prochiral thio-ethers catalyzed by Baeyer-Villiger monooxygenases will be intensified.

Publications resulting from this research area: 2, 3, 4, 12, 14, 15, 16, 20, 21, 24, 29, 32

External funding: Arthur C. Cope Foundation (USA)

Cooperations: H. Rabitz (Princeton, USA); R. Boelens (Groningen/Netherlands); B. Dijkstra (Groningen/Netherlands)

2.1.4 Research Area "Constructing Designer Cells for Enzymatic Cascade Reactions Based on Directed Evolution" (M. T. Reetz)

Involved: R. Agudo

Objective: The goal was to construct designer cells for stereocomplementary *de novo* enzymatic cascade reactions based on directed evolution.

Results: The benefits of exploiting sequential organic transformations in a single reaction vessel using synthetic reagents, catalysts or enzymes without isolating intermediate products have been documented in many studies. Nature orchestrates the buildup of structural complexity by enabling such reaction sequences *in vivo* in the cytosol of cells in which a multitude of enzymes function as selective catalysts. In the quest to produce complex natural products or biofuels, researchers have used whole cells, state of the art metabolic engineering offering many opportunities. These systems are considerably more complex than ordinary so-called designer cells such as engineered *E. coli* cells harboring, for example, an alcohol dehydrogenase (ADH) and the necessary NAD(P)H regeneration enzyme as a platform for asymmetric reduction of non-natural prochiral ketones. Industry often prefers whole cell catalysis relative to the *in vitro* use of isolated enzymes.
The de novo construction of designer cells with the aim of realizing any given reaction sequence that an organic chemist might envision is a different type of problem not covered by metabolic engineering, and indeed few examples have been reported to date and none utilizing directed evolution. Particularly challenging are those cases of cascade reactions in designer cells that involve several sequential redox steps, especially when the control of regio-, chemo- and stereoselectivity is required.

Along these lines we have conceived, as a proof-of-principle, the following redox reaction sequence to be performed in a one-pot manner in stereocomplementary designer cells.[35] Starting from a simple compound **1** a value-added structurally more complex product **4** was envisioned to be formed in either of the two enantiomeric forms on an optional basis. One whole cell system was designed to provide the (*R*)-configurated final product (*R*)-**4**, while the other cell system was supposed to lead to the enantiomeric (*S*)-**4** (Scheme 1).

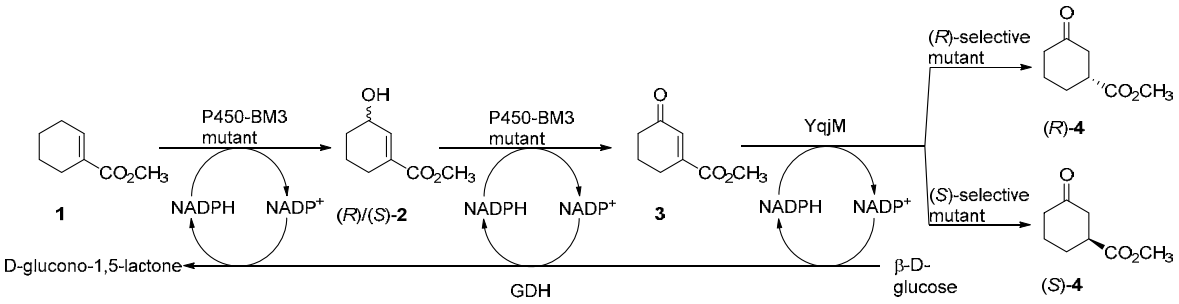

Scheme 1. Stereodivergent designer *E. coli* cells for converting starting compound **1** into either (*R*)-**4** or (*S*)-**4** in one-pot processes, respectively.[35]

The genes of three different enzymes were considered in this plan, namely a P450 monooxygenase for regio- and chemoselective *oxidation*, an enoate reductase for chemo- and stereoselective *reduction* and glucose dehydrogenase (GDH) for *cofactor regeneration*. In traditional synthetic organic chemistry the simultaneous use of oxidizing and reducing agents is generally problematic, but in biocatalysis it is more likely to succeed.[28] The major challenge in the present system is, *inter alia*, the two-step chemo- and regioselective C-H activating oxidative hydroxylation of compound **1** with formation of ketone **3** in the absence of alternative oxidation products resulting from **1** or **2** as well as the absence of likewise undesired oxidation events possibly occurring with **3** or **4**. We used P450-BM3 as the monooxygenase for the first two steps in *E. coli* cells, and therefore first carried out a study aimed at creating a mutant that catalyzes the **1** → **2** → **3** conversion with maximum efficiency. Since WT P450-BM3 fails (mixture of many oxidation products), we screened several mutant libraries obtained by saturation mutagenesis (CAST), the best mutant being Val28Leu/Ala82Phe/Phe87Ala. The gene of this mutant was then incorporated in *E. coli* designer cells (BOU730) harboring glucose dehydrogenase (GDH) necessary for NADPH regeneration. We had previously engineered the *E. coli* BOU730 cells in a study concerning stereoselective enoate reductases, and indeed this cell strain can be used conveniently in any enzymatic redox reaction that requires NADPH (or NADH) regeneration. For the last reduction step we envisioned the use of the enoate reductase YqjM from the Old Yellow Enzyme family. In our laboratory we had already applied ISM for evolving (*R*)- and (*S*)-selective mutants, respectively.[36] In control experiments it was ensured that these mutants are also chemoselective in that they do not catalyze the reduction of the starting material **1** which is not accepted by the enzymes.

In this proof-of-principle study we wanted to gain as much experience as possible regarding the choice of the molecular biological setup in relation to the final synthetic outcome, and therefore designed three different experimental platforms[35]:

(1) Use of two different engineered *E. coli* cells in a one-pot process, i.e., BOU730 cells containing an appropriate P450-BM3 mutant gene and BOU730 cells containing the respective YqjM mutant genes. This enables a convenient control element over the multistep process, because the ratio of the two cells can be appropriately adjusted, and after an appropriate time-lag the second cells can be added strategically once the first cell strain has performed its function as revealed by the reaction progress.

(2) Use of a one-pot two plasmid system based on BOU730 cells transformed with two different plasmids that encode for P450-BM3 and YqjM mutants, all in *E. coli* cells. This may lead to a metabolic burden influencing bacterial growth rate and/or protein expression rates.

(3) Use of engineered *E. coli* strains that harbor one of the YqjM genes inserted into the genome with P450-BM3 remaining in a plasmid. Problems similar to approach (2) may occur.

Approach (1): Upon adding in separate experiments *R*- or *S*-selective YqjM strains, respectively, to the reaction vessels in which the P450-BM3-catalyzed reaction had occurred for about one hour, both enantiomeric products were readily obtained after an additional 15 minutes as shown by GC analysis: ≈ 85% overall conversion to (*R*)-**4** (99% *ee*) and (*S*)-**4** (99% *ee*). Upon upscaling the reaction to 7.3 mM of starting compound **1**, the two-cell systems led to 72% of (*R*)-**4** and 75% of (*S*)-**4**, each enantiomerically pure. Control experiments testing the use of a mixture of isolated enzymes *in vitro* resulted in poor conversion to the desired products (< 24 %), which clearly demonstrates the superiority of using whole cells as nanoreactors.[35]

Approach (2): When applying the two-plasmid system, BOU730 cells transformed with two different plasmids, pRSF-P450BM3 and pACYC-YqjM, were used. These encode the P450-BM3 and YqjM mutants, respectively, under regulation of the bacteriophage T7 promoter. Upon adding IPTG to the medium, both proteins were successfully expressed as shown by control experiments. Although optimization was not strived for, the results proved to be reasonable: ≈ 50% regioselectivity and 99% enantioselectivity. The undesired side-products are due to overoxidation of the intermediate compounds and partially of **4**.[35]

Approach (3): This is the most challenging option in terms of controlling all necessary parameters, in which a one-plasmid system encoding the P450-BM3 mutant necessary in the first two steps is utilized while the YqjM coding sequences of the *R*-selective mutant (or *S*-selective mutant) are likewise inserted into the *E. coli* chromosome using BOU730 cells. Nevertheless, surprisingly good results were observed, although here again full optimization was not strived for: 50-52% conversion to the desired final products **4** in enantiomerically pure form.[35]

The limiting factor with regard to the formation of (*R*)-**4** or (*S*)-**4**, respectively, is the obvious possibility of indiscriminate oxidation of four different compounds, namely **1**, **2**, **3** and **4**, which complicates matters in the present system. Since the oxidation steps are rate-limiting as shown by control experiments, the use of two designer cells according to approach (1) with an optimal time-lag between their uses constitutes a useful tool. Nevertheless, all three approaches deserve attention in future studies using structurally more demanding substrates. Other types of enzymes also need to be studied in such an approach which minimize the possibility of conflicting side-reactions as in our first attempt to enter this challenging new field. *Finally, we conclude that the approach described herein nicely complements present day metabolic engineering.*

Future directions: Due to the molecular biological challenges, this research area is far from trivial, but we shall nevertheless attempt the de novo design and experimental realization of a new one-pot cascade reaction sequence constructed in *E. coli* cells.

Publications resulting from this research area: 35

External funding: Arthur C. Cope Foundation (USA)

Cooperations: none

2.1.5 Research Area "Development of Novel Catalyst Systems for Epoxidation Reactions" (W. Leitner, N. Theyssen)

Involved: Y. Qiao

Objective:
The development of efficient catalytic epoxidation protocols for olefins remains an attractive target. Especially, if environmentally benign oxygen sources like hydrogen peroxide are used and catalyst systems with good recyclability are realized.

Results: (Figure 1).
We have synthesized a variety of heterogeneous epoxidation catalysts with a ferromagnetic core in nanoscale allowing a most easy catalyst recovery in a multi-batch procedure by a permanent magnet. Each ferrit core is covered by a dense SiO_2 layer to prevent unproductive iron ion-initiated decomposition of hydrogen peroxide.

In a first project, the catalytically active peroxotungstate anion, $[W_2O_{11}]^{2-}$, was immobilised via ionic forces to positively charged imidazolium containing entities (Figure 1). In accordance with results from diffuse reflectance IR-spectroscopy (DRIFTS) and ^{29}Si cross polarization magic angle spinning NMR-spectroscopy (CP/MAS), the imidazolium motives seem to be bounded in the envisaged manners to the coated ferrit core: either by hydrogen bonds (catalyst **1**) or covalent linkages (catalyst **2**).

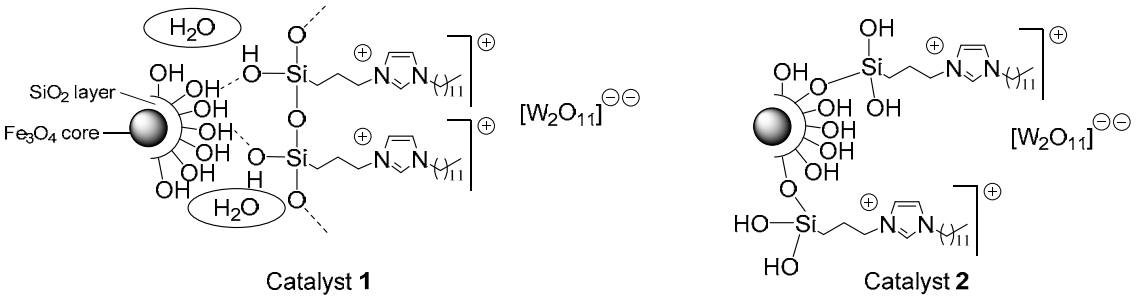

Figure 1: Magnetically recoverable catalysts for epoxidation based on peroxotungstate anions.

The epoxidation of cyclooctene was chosen as a benchmark reaction for both catalytic systems. A summary of the obtained results is given in the following:

- A methanol/water mixture (volume ratio 10:1) was found to be most suited in terms of catalyst activity, selectivity and stability. The small water fraction was shown to be crucial for long life stability of both systems.

- Surprisingly, the hydrogen bonded catalyst **1** turned out to be more stable in comparison with **2**, which immobilisation is reached by covalent bonds: under optimised conditions, 10 respective 7 consecutive runs could be performed using catalysts **1** and **2** without any performance loss. Complete conversion and perfect selectivity was detected in every cycle.
- Hot filtration experiments support the presence of heterogeneous catalysis. However, it cannot be excluded that the solid catalyst fraction might function as a reservoir for dissolvable active species. If this is the case, a quite fast deactivation of dissolved species would happen.
- Derived catalyst of simpler structures shows much weaker performances. For example, an impregnation of the shielded ferrit cores with $K_2W_2O_{11}$ resulted in a conversion of only 9%. Likewise, a physical mixture of the ionic components $[DMIm]_2$ (D = dodecyl) and $[W_2O_{11}]$ with the shielded ferrit cores gave only 34% conversion.

A substrate screening identifies cycloheptene and allylic alcohols as additional suitable substrates. 3-methyl-2-buten-1-ol, geraniol and cinnamyl alcohol were converted completely with good to perfect selectivities. Cyclohexene and styrene gave product mixtures, whereas 1-decene gave poor conversions but perfect selectivity.

In a follow-up project we have tried to enhance both the catalytic activity and immobilisation stability via the hydrogen bond mode. Therefore a catalyst was designed in which a heteropoly anion, $[PW_{11}O_{39}]^{7-}$ (a lacanury-type polyoxometalate), was used as the catalytically active moiety (Figure 2).

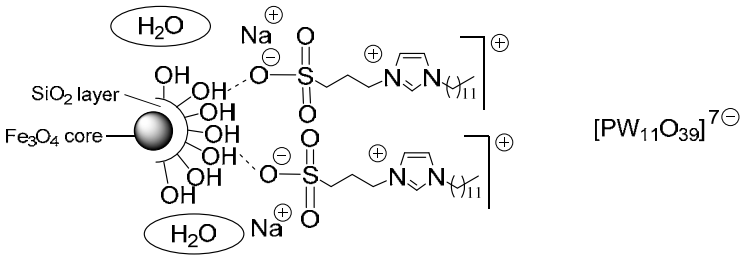

Catalyst **3**

Figure 2: Magnetically recoverable catalyst based on a lacunary-type polyoxometalate

Further differences were implemented in the imidazolium cation structure which now contains sulfonate groups in order to increase the bond strength of the hydrogen bonds to the silanol groups of the covered ferrit nanoparticles (Figure 2). Catalyst **3** works best under solvent-free conditions. 10 recycles without any activity loss in the epoxidation of

cyclooctene were monitored. Noteworthy, the leaching rate was reduced from 870 ppm in methanol to 3 ppm under solvent-free conditions which is so far the lowest value detected in our studies. Hot filtration experiments argue for heterogeneous catalysis only in the latter case.

During the reaction, **3** is present in an emulsion between aqueous H_2O_2 and cyclooctene. The addition of ethyl acetate after reaction breaks the emulsion and the catalyst can be separated easily by a magnetic field. In comparison to catalyst **1**, the substrate scope with **3** under solvent-free conditions is more limited. In addition to cyclooctene, allylic alcohols like 3-methyl-2-buten-1-ol, geraniol and crotyl alcohol were converted to more than 85% with over 93% selectivity.

Finally, a quasi-homogeneous catalyst **4** was developed on the made experiences. Here, the same imidazolium cation as in catalyst **1**, **2** and **3** was combined with the lacunary-type polyoxometalate of **3**. The study revealed that the optimal ratio of the two components is 7:1 which reflects the charge ratio of these ions. Moreover, a variation in the alkyl chain length of the imidazolium cation showed that the dodecyl group is crucial. Its substitution by a methyl or hexyl group resulted in a very low cyclooctene conversion of only 1% and 2% respectively.

4 builds a fully homogeneous phase with aqueous hydrogen peroxide. The addition of cyclooctene results again in the formation of a stable emulsion, which makes an additional solvent unnecessary. Under such conditions this catalyst is extremely active allowing an epoxidation of cyclooctene already at 0 °C. Quantitative yield was obtained after 3 h reaction time. The activation energy was determined to be 34 kJ/mol. This is unprecedented low in comparison to values reported in the literature for epoxidation of cyclooctene (49-86 kJ/mol). Recycling of **4** is of course not as easy and elegant as in case of catalysts **1**-**3**, but possible via extraction with cyclohexane. This procedure allows at least three runs without activity loss.

External Funding: Chinese Scholarship Council (CSC)

Cooperations: Z. Hou (Research Institute of Industrial Catalysis, East China University of Science and Technology, Shanghai, P.R. China)

2.1.6 Publications 2011-2013 from the Department of Synthetic Organic Chemistry

Reetz Group

(1) Braunstein, P.; Reetz, M. T.; Sun, W.-H. *C. R. Chimie* **2011**, *14*, 787-788.

(2) Gumulya, Y.; Reetz, M. T. *ChemBioChem* **2011**, *12*, 2502-2510.

(3) Kille, S.; Zilly, F. E.; Acevedo, J. P.; Reetz, M. T. *Nat. Chem.* **2011**, *3*, 738-743.

(4) Prasad, S.; Bocola, M.; Reetz, M. T. *ChemPhysChem* **2011**, *12*, 1550-1557.

(5) Reetz, M. T. *Angew. Chem., Int. Ed.* **2011**, *50*, 138-174.

(6) Reetz, M. T. Die Evolutionsmaschine als Quelle für selektive Biokatalysatoren. In *Molekule aus dem All*; Al-Shamery, K., Ed.; Wiley-VCH, Weinheim, 2011, pp. 243-273.

(7) Reetz, M. T.; Krebs G. P. L. *C. R. Chimie* **2011**, *14*, 811-818.

(8) Reetz, M. T.; Zheng, H. *ChemBioChem* **2011**, *12*, 1529-1535.

(9) Zilly, F. E.; Acevedo, J. P.; Augustyniak, W.; Deege, A.; Häusig, U. W.; Reetz, M. T. *Angew. Chem., Int. Ed.* **2011**, *50*, 2720-2724; Corrigendum: *Angew. Chem. Int. Ed*. **2013**, *52*, 13503.

(10) Acevedo-Rocha, C. G.; Reetz, M. T. *Catal. Sci. Technol.* **2012**, *2*, 1553-1555.

(11) Agudo, R.; Roiban, G.-D.; Reetz, M. T. *ChemBioChem* **2012**, *13*, 1465-1473.

(12) Augustyniak, W.; Brzezinska, A. A.; Pijning, T.; Wienk, H.; Boelens, R.; Dijkstra, B. W.; Reetz, M. T. *Protein Sci.* **2012**, *21*, 487-497.

(13) Cesarini, S.; Bofill, C.; Pastor, F. I. J.; Reetz, M. T.; Diaz, P. *Process Biochem.* **2012**, *47*, 2064-2071.

(14) Feng, X.; Sanchis, J.; Reetz, M. T.; Rabitz, H. *Chem.-Eur. J.* **2012**, *18*, 5646-5654.

(15) Gumulya, Y.; Sanchis, J.; Reetz, M. T. *ChemBioChem* **2012**, *13*, 1060-1066.

(16) Polyak, I.; Reetz, M. T.; Thiel, W. *J. Am. Chem. Soc.* **2012**, *134*, 2732-2741.

(17) Reetz, M. T. Directed Evolution of Enzymes. In *Enzyme Catalysis in Organic Synthesis*; Drauz, K., Gröger, H., May, O., Eds.; 3rd Edition, Vol. 1-3, Wiley-VCH, Weinheim, 2012, Vol. 1, pp.119-190.

(18) Reetz, M. T. *Chem. Rec.* **2012**, *12*, 391-406.

(19) Reetz, M. T. *Tetrahedron* **2012**, *68*, 7530-7548.

(20) Zhang, Z.-G.; Parra L. P.; Reetz, M. T. *Chem. Eur. J.* **2012**, *18*, 10160-10172.

(21) Augustyniak, W.; Wienk, H.; Boelens, R.; Reetz, M. T. *Biomol. NMR Assign.* **2013**, *7*, 249-252.

(22) Agudo, R.; Roiban, G.-D.; Reetz, M. T. *J. Am. Chem. Soc.* **2013**, *135*, 1665-1668.

(23) Kille, S.; Acevedo-Rocha, C. G.; Parra, L. P.; Zhang, Z.-G.; Opperman, J. J.; Reetz, M. T.; Acevedo J. P. *ACS Synth. Biol*. **2013**, *2*, 83-92.
(24) Reetz, M. T. *Angew. Chem., Int. Ed*. **2013**, *52*, 2658-2666.
(25) Wu, Q.; Soni, P.; Reetz, M. T. *J. Am. Chem. Soc.* **2013**, *135*, 1872-1881.
(26) Roiban G.-D.; Reetz, M. T. *Angew*. *Chem., Int. Ed*. **2013**, *52*, 5439-5440.
(27) Zhang, Z.-G.; Roiban, G.-D.; Acevedo, J. P.; Polyak, I.; Reetz, M. T. *Adv. Synth. Catal.* **2013**, *355*, 99-106.
(28) Reetz, M. T. *J. Am. Chem. Soc*. **2013**, *135*, 12480-12496.
(29) Polyak, I.; Reetz, M. T.; Thiel. W. *J. Phys. Chem. B*, **2013**, *117*, 4993-5001.
(30) Roiban, G.-D.; Agudo, R.; Reetz, M. T. *Tetrahedron*, **2013**, *69*, 5306-5311.
(31) Reetz, M. T. Practical Protocols for Lipase Immobilization Via Sol-Gel Techiques. In *Methods in Biotechnology*; Guisan, J. M., Ed.; 2nd Edition, Humana Press, Totowa, 2013, Vol. 241, pp. 241-254.
(32) Parra, L. P.; Agudo, R.; Reetz, M. T. *ChemBioChem* **2013**, *14*, 2301-2309.
(33) Acevedo-Rocha, C. G.; Reetz, M. T. Assembly of Designed Oligonucleotides: A Useful Tool in Synthetic Biology for Creating High Quality Combinatorial DNA Libraries. In *Directed Evolution Library Creation: Methods and Protocols*; *Methods in Molecular Biology*; Ackerley, D., Copp, J., Gillam, E., Eds.; 2nd Edition, Humana Press, Totowa, 2013.
(34) Acevedo-Rocha, C. G.; Kille, S.; Reetz, M. T. Iterative Saturation Mutagenesis: A Powerful Approach to Engineer Proteins by Simulating Darwinian Evolution. In *Directed Evolution Library Creation: Methods and Protocols; Methods in Molecular Biology;* Ackerley, D., Copp, J., Gillam, E., Eds.; 2nd Edition, Humana Press, Totowa, **2013**.
(35) Agudo, R.; Reetz, M. T. *Chem. Comm.* **2013**, *49*, 10914-10916.
(36) Kille, S., Reetz, M. T. Protein Engineering: Development of Novel Enzymes for the Improved Reduction of C=C Double Bonds. In *Synthetic Methods for Biologically Active Molecules-Exploiting the Potential of Bioreductions*; Brenna, E., Ed.; Wiley-VCH, Weinheim, **2013**.

Leitner / Theyssen group

(37) Qiao, Y.; Li, H.; Hua, L.; Orzechowski, L.; Yan, K.; Feng, B.; Pan, Z.; Theyssen, N.; Leitner, W.; Hou, Z. *ChemPlusChem* **2012**, **77**, 1128-1138.
(38) Qiao, Y., Hua, L.; Chen, J.; Theyssen, N.; Leitner, W.; Hou, Z. *J. Mol. Catal. A: Chem.* **2013**, 380, 43-48.
Further papers of W. Leitner regarding other topics see publication list in the appendices.

2.2. Department of Homogeneous Catalysis

Director:

Benjamin List (born 1968)

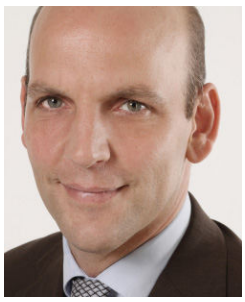

Further group leaders:

Martin Klußmann (born 1974)

Nuno Maulide (born 1979)
left the Institute in September 2013

Klaus-Richard Pörschke (born 1949)

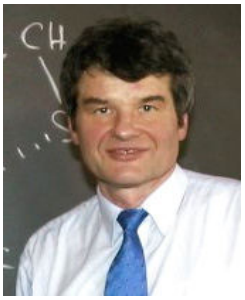

Curriculum Vitae: Benjamin List

1968	Born in Frankfurt/Main, Germany
1993	Chemistry Diploma, Freie Universität Berlin
1997	Ph.D., Johann Wolfgang Goethe-Universität Frankfurt, with Prof. J. Mulzer
1997-1998	Postdoc, Scripps Research Institute, La Jolla, USA, with Prof. R. Lerner
1999-2003	Assistant Professor (Tenure Track), Scripps Research Institute, La Jolla, USA
2003-2005	Group Leader at the Max-Planck-Institut für Kohlenforschung
2004-	Honorary Professor at the Universität zu Köln
2005-	Director at the Max-Planck-Institut für Kohlenforschung
2012-	Managing Director of the Max-Planck-Institut für Kohlenforschung

Awards and Honors

1997-1998	Feodor-Lynen Fellowship of the Alexander von Humboldt Foundation
1994-1995	NaFoeG-Graduate Fellowship of the Senate of Berlin
2000	Synthesis-Synlett Journal Award
2003	Carl-Duisberg-Memorial Award
2004	Degussa Prize for Chiral Chemistry
2004	Lieseberg Prize
2004	Lecturer Award of the German Chemical Industry Fund
2005	Visiting Professorship, Gakushuin University, Tokyo, Japan
2005	Society of Synthetic Chemistry, Japan: 2005 Lectureship Award
2005	AstraZeneca European Lecturer
2005	Novartis Young Investigator Award
2006	JSPS Fellowship, Japan
2006	100 Masterminds of Tomorrow, Germany
2006	Wiechert Lectureship, FU Berlin, Germany
2007	Fonds der Chemischen Industrie Award, Germany
2007	OBC Lecture Award
2007	AstraZeneca Research Award in Organic Chemistry
2008	Visiting Professorship, Sungkyunkwan University, Korea
2009	Organic Reactions Lectureship, USA
2009	Boehringer-Ingelheim Lectureship, Canada
2009	Thomson Reuters Citation Laureate

2010	High Levels Lectureship for Graduate Students, University of Science and Technology of China, Hefei
2010	New Honors Program Lectureship, National University of Singapore
2011	Boehringer-Ingelheim Lectureship, Harvard University, USA
2011	ERC-Advanced Grant
2012	Novartis Chemistry Lectureship Award 2012-2013
2012	Otto-Bayer-Prize, Germany
2013	Musher Memorial Lecture, Jerusalem, Israel
2013	Novartis Lectureship, UC Berkeley, USA
2013	Horst-Pracejus-Prize, Germany
2013	Mukaiyama Award, Japan
2013	Ruhrpreis, Mülheim, Germany
1999-2013	ca. 180 Plenary and Name Lectureships

Other Activities / Committees

2004	Co-Editor (with C. Bolm), Special Edition: "Organocatalysis", *Advanced Synthesis & Catalysis*
2004	Co-Editor (with K. N. Houk), Special Edition: "Enantioselective Organocatalysis", *Accounts on Chemical Research*
2005-	Co-Editor, *Synfacts* (Thieme)
2005-2011	Coordination of the DFG Priority Program (SPP1179) "Organocatalysis"
2006	Editor "Organocatalysis", *Chemical Reviews*
2006-	Member of the Selection Committee for Max Planck Group leaders
2008-	Editorial Advisory Board, *Beilstein Journal of Organic Chemistry*
2008-2009	Editor "Asymmetric Organocatalysis", *Topics in Current Chemistry*
2009-2010	Co-Editor (with K. Maruoka) "Asymmetric Organocatalysis", *Science of Synthesis Reference Library*
2010-	Editorial advisory panel, *Nature Communications*
2011-	Regional Editor of *Synlett* (Thieme)
2011-	Academic Advisory Board *Advanced Synthesis and Catalysis*
2011	Co-Editor (with K. Maruoka) "Asymmetric Organocatalysis", *Science of Synthesis* (Thieme)
2011	Editor "Asymmetric Organocatalysis", *Beilstein Journal of Organic Chemistry*

Research in the Department of Homogeneous Catalysis

Researchers in our Department continue focusing on the development of new catalysis concepts within the areas of organocatalysis and transition metal catalysis. We explore new catalysts, expand the substrate scope of certain catalytic reactions, apply asymmetric catalysis in natural product and pharmaceutical synthesis, study mechanisms of homogeneous catalytic reactions, and explore catalysis with textile-supported catalysts (B. List, K.-R. Pörschke, M. Klußmann, N. Maulide).

During the last three years, the Department grew again significantly, mainly due to the expansion of the group of Nuno Maulide to about twenty co-workers. During the evaluation period between 2011 and 2013, the Department consisted altogether of four groups, in addition to that of the head of the Department, Professor Benjamin List, those led by Professor K.-R. Pörschke, who has been a group leader at the institute since over twenty years, by Dr. M. Klußmann, who has been a group leader here since 2007, and of Dr. N. Maulide, who has joined the Department in 2009 and left in the fall of 2013 to take a chair at the University of Vienna.

The group of **Professor List** primarily advances enantioselective organocatalysis as a fundamental approach complementing the already more advanced fields of biocatalysis and transition metal catalysis. The List group has a profound interest in developing "new reactions", designs and identifies new principles for the development of organocatalysts, expands the scope of already developed catalysts such as proline, uses organocatalysis in the synthesis of natural products and pharmaceuticals, and also investigates the mechanisms by which organocatalysts activate their substrates.

Since 2005, the group has first conceptualized and then significantly advanced another approach to asymmetric catalysis, asymmetric counteranion directed catalysis (ACDC). Initially, merely an idea, this approach has progressed within the Department but now also at other institutions around the globe, into a truly general strategy for asymmetric synthesis and has found utility in organocatalysis but also in transition metal catalysis and Lewis acid catalysis. This area is now the main research field in the List group. More recently, a new approach to heterogeneous catalysis was developed, in which organic catalysts are immobilized on inexpensive textile materials and used as efficient and recyclable catalysts.

Research in the laboratory of **Professor Pörschke** continues to center on transition metal complexes. The group conducts fundamental research in the areas of coordination chemistry, organometallic chemistry, homogeneous catalysis, and solid state phase properties (organometallic plastic crystals). Transition metals under focus are Ni, Pd, and Pt, which are often used in combination with main group metal compounds (Li, Mg, Al, Ge, Sn). As a new line of research, the group now also investigates cisplatin-related metal complexes as potential cytostatic compounds.

The group of **Dr. Klußmann** has focused on mechanistic and synthetic studies in the area of oxidative cross-coupling catalysis. They investigate reactions that allow the coupling of two C–H-fragments, establishing a C–C-unit. The substrates are activated under oxidative conditions, ideally resulting in water as the only byproduct.

The group of **Dr. Maulide** was established in 2009 after its leader had obtained a prestigious and highly competitive Max-Planck Research Group Leader position, which is fully supported from central MPG funds. The group has diverse activities in the area of organic synthesis and catalysis and published extensively within the last four years. As a result many awards have been secured and calls to different universities were obtained by Nuno Maulide. In the meantime, the group has left to the University of Vienna.

2.2.1 Research Area "Catalysis with chiral imidodiphosphates" (B. List)

Involved: J. H. Kim, I. Čorić, S. Liao, S. Vellalath, Q. Wang

Objective: The field of Brønsted acid catalysis has acquired wide popularity and importance in recent years. However, reactions of small aliphatic substrates that do not possess sterically demanding protecting groups, large aromatic or planar surfaces, or bulky substituents are still rare. This might be due to the inability of current synthetic Brønsted acid catalysts to provide a truly compact chiral microenvironment. We therefore propose the development of "confined acid catalysts" (Figure 1). The aim of this project was to design and synthesize novel confined Brønsted acid catalysts based on a C_2-symmetric imidodiphosphoric acid, possessing an extremely sterically demanding chiral microenvironment.

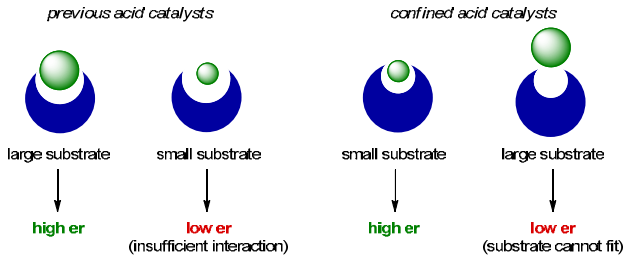

Figure 1. Schematic comparison of the expected performance of chiral confined acids and phosphoric acid type catalysts with large and small substrates.

Results: C_2-Symmetric imidodiphosphoric acids, based on the interlocking of two identical BINOL subunits, were designed and prepared (Scheme 1).

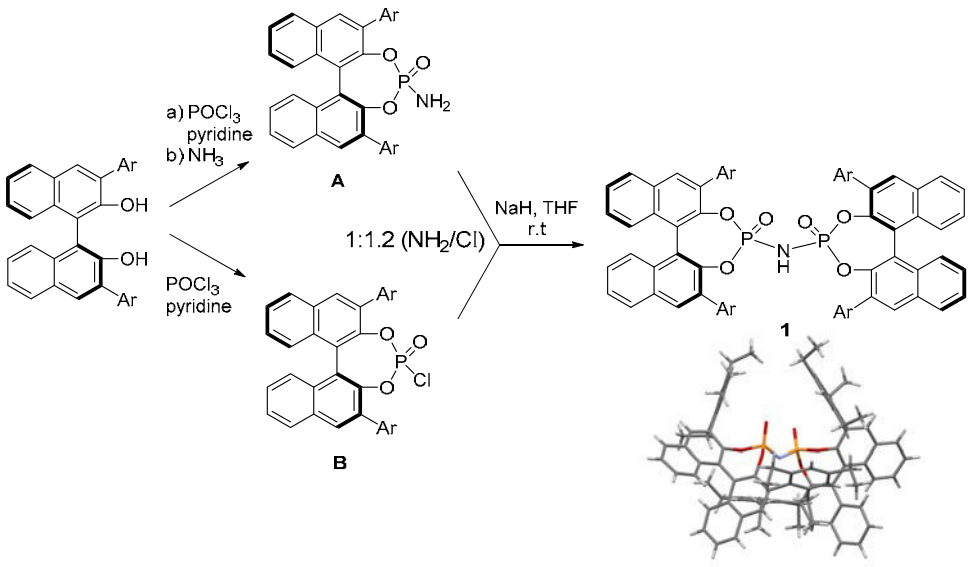

Scheme 1. Synthetic strategy for C_2-symmetric imidodiphosphoric acids.

Starting from readily available 3,3'-substituted BINOL-derivatives, synthetic intermediates **A** and **B** are obtained in a single step. Their coupling under basic conditions directly affords the desired C_2-symmetric imidodiphosphoric acid **1**.

A) *O,O*-acetals

As part of our interest in asymmetric acetalization reactions, we have developed direct enantioselective syntheses of spiroacetals and cyclic *O,O*-acetals from aldehydes. Although *O,O*-acetals are among the most common stereocenters in organic molecules, their catalytic asymmetric syntheses have only been achieved recently due to problems associated with asymmetric additions to oxocarbenium ions using chiral Brønsted acid catalysts.

Spiroacetalization

Spiroacetal natural products are widely found in insects, plants, and bacterial and marine sources, and display a diverse set of biological activities. Their spiroacetal subunit is not only essential for the bioactivity but is also a privileged pharmacophore in drug discovery. An extensive screening of a wide range of known chiral Brønsted acids gave only disappointing results in the generation of both the 5,5- and the 6,6-spiroacetal. Extremely sterically demanding Brønsted acid catalyst **1a** efficiently catalyzed the asymmetric conversion of small and further unfunctionalized hydroxy enolether substrates (Scheme 2).

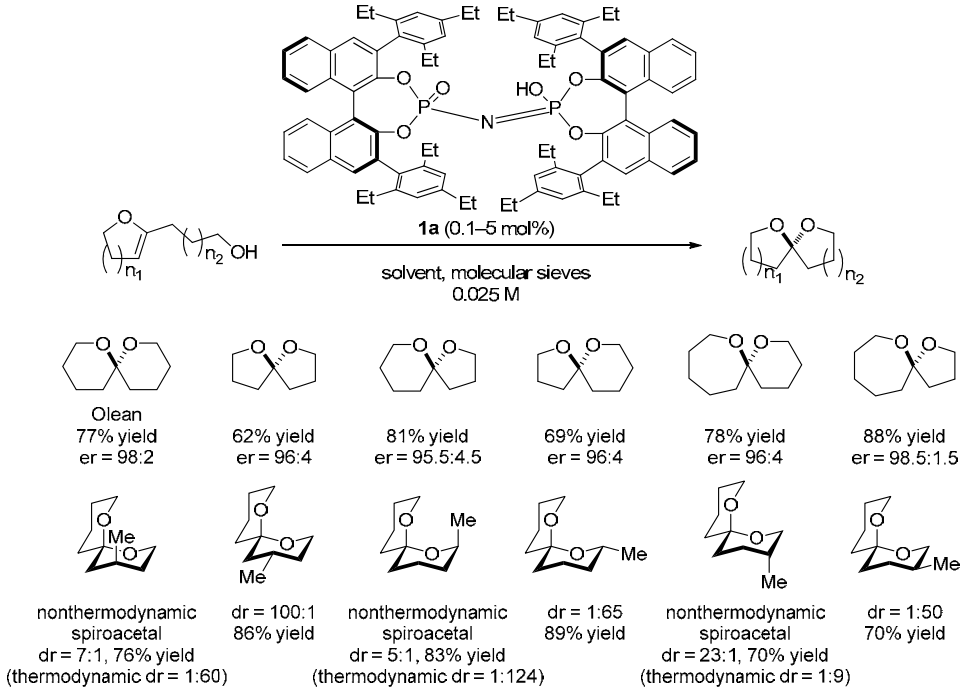

Scheme 2. Catalytic asymmetric spiroacetalization.

Various spiroacetals were obtained with high enantioselectivity by the formation of either 6- or 5-membered rings. Catalyst **1a** also enabled the first catalytic asymmetric synthesis of the natural product olean. A variety of non-thermodynamic spiroacetals could be formed with diastereomeric ratios ranging from 5:1 to 23:1, against a strong thermodynamic preference of up to 1:124.

Asymmetric acetalization

Although our laboratory has pursued the direct asymmetric acetalization of aldehydes with alcohols for many years now, and has investigated numerous chiral Brønsted acid catalysts, unfortunately, very little success towards this goal has been encountered. Here the newly developed class of chiral confined Brønsted acids finally enables this elusive transformation with excellent selectivity and scope. In a condensation reaction of diols and aldehydes imidodiphosphoric acid **1b** delivered chiral *O,O*-acetals in high yield and with high enantioselectivity (Scheme 3).

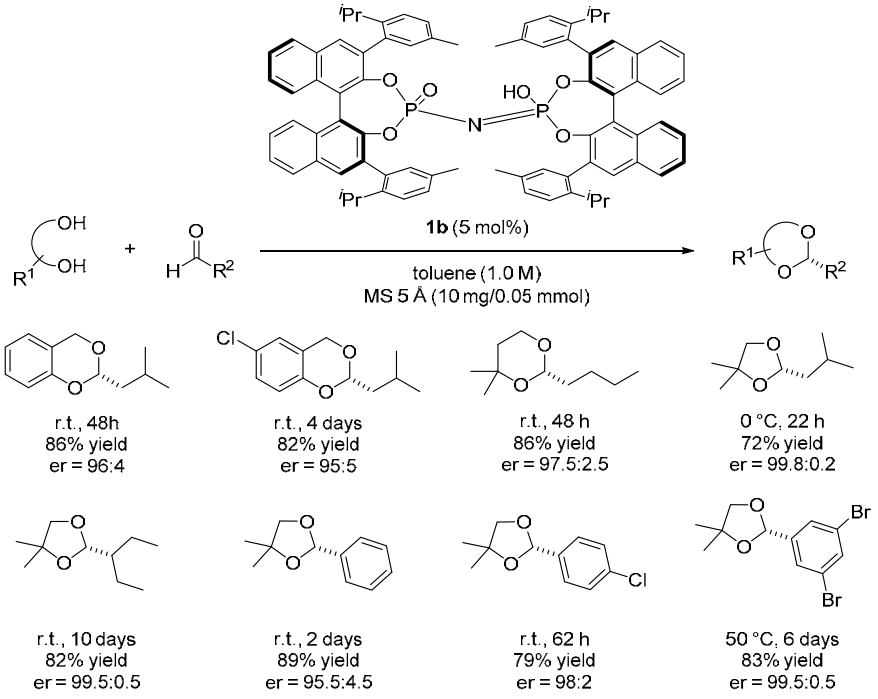

Scheme 3. Catalytic asymmetric acetalization.

1,2-Diols are versatile intermediates in organic synthesis. Our asymmetric acetalization can be conveniently applied to the kinetic resolution of diols, giving enantio-enriched diols and acetal products with selectivity factors up to 400 (Scheme 4).

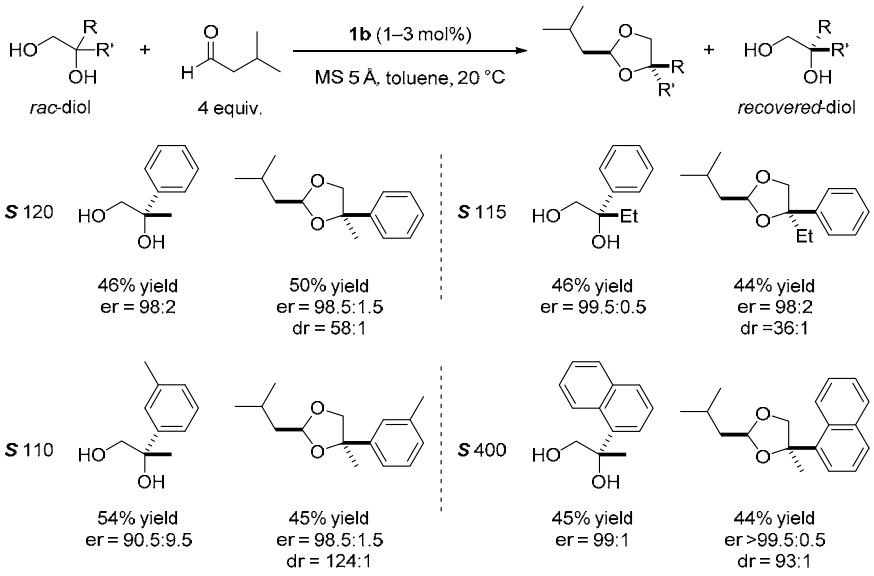

Scheme 4. Kinetic resolution of diol *via* asymmetric acetalization.

B) Sulfoxidation

Despite significant efforts to utilize H_2O_2 in asymmetric oxidation catalysis, only few general systems work well with this abundant, environmentally benign, atom economic, and relatively safe oxidant. In asymmetric organocatalysis, H_2O_2 has been employed in the epoxidation of α,β-unsaturated carbonyl compounds, Baeyer-Villiger reactions, and in oxidations catalyzed by ketones, iminium salts, or carboxylic acids. All of these reactions rely on the nucleophilic properties of H_2O_2, to form covalent adducts with electrophilic substrates or catalysts. We envisioned an alternative scenario, in which H_2O_2 could be electrophilically activated towards nucleophilic substrates with a chiral Brønsted acid catalyst (Scheme 5).

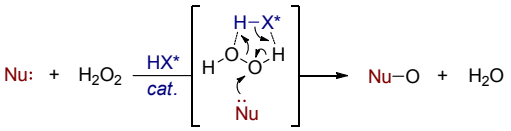

Scheme 5. Activation of H_2O_2 with a chiral Brønsted acid catalyst.

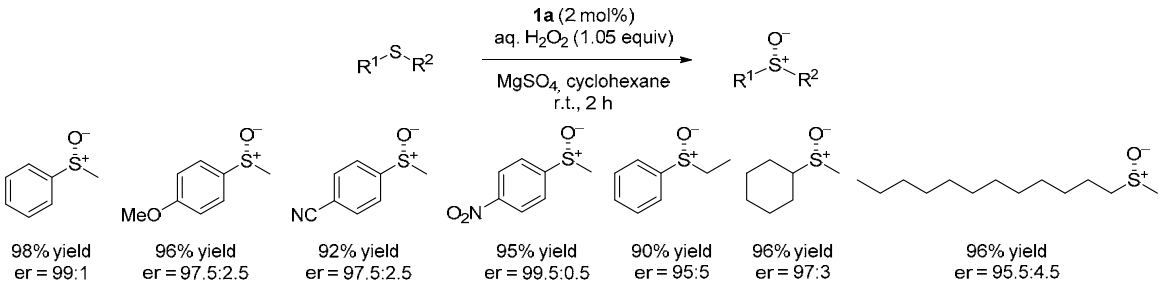

Scheme 6. Catalytic asymmetric sulfoxidation.

Imidodiphosphoric acid catalyst **1a**, which presumably binds hydrogen peroxide inside its chiral cavity, was found to catalyze an efficient sulfoxidation reaction of sulfides (Scheme 6). Other known common Brønsted acids gave much lower enantioselectivity.

The methodology has been applied to the enantioselective synthesis of the non-steroidal anti-inflammatory drug Sulindac, which has recently found additional utility in cancer treatment (Scheme 7).

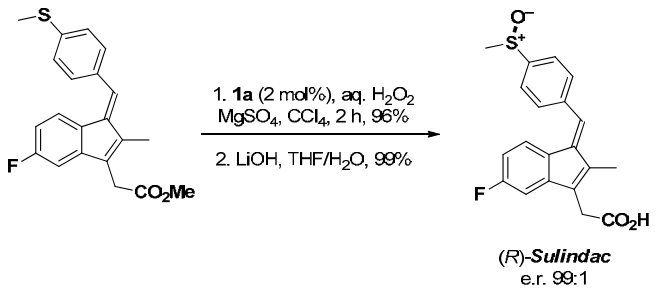

Scheme 7. Enantioselective synthesis of Sulindac.

In summary, we have developed chiral imidodiphosphates to be of use in tackling current challenges with reactions that include small volume and/or loosely organized transitions states. With our new catalysts, we have developed the first catalytic asymmetric spiroacetalization, direct acetalization of aldehydes with diols, and asymmetric sulfoxidation with hydrogen peroxide.

Publications resulting from this research area: 11, 13, 29

External funding: European Research Council Advanced Grant (HIPOCAT)

Cooperations: none

2.2.2 Research Area "Organotextile Catalysis" (B. List)

Involved: J.-W. Lee, T. James

Objective: Homogeneous catalysis plays a central role in modern chemistry at both research and production scales, facilitating the synthesis of molecules which were once considered an insurmountable challenge. However, in contrast to heterogeneous catalysis, many homogeneous processes require significant effort to recover catalytic components from reaction media. Approaches which utilize the exquisite control of homogeneous catalysts with the practicality and recyclability of heterogeneous systems are highly sought after. To date there is no general approach to provide inexpensive and accessible solid materials on which a desired organic molecule can be mounted. To address this challenge we developed a facile immobilization of various functionalized organocatalysts onto textile material by irradiation with ultra violet light (UV) (Figure 1). This process allows immobilization of a desired molecule on the solid support, by covalent C–C bond formation, to generate organotextile catalysts, which can be used for various transformations with unprecedented numbers of cycles.

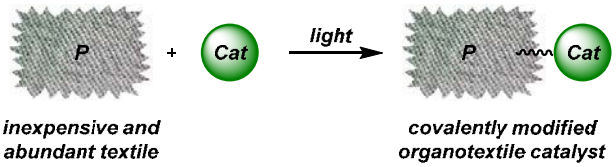

Figure 1. Schematic representation of approach taken towards the functionalization of textile surfaces with organic catalysts.

Results: To show the generality of our methodology, the immobilization of different organocatalysts was investigated; a Lewis base catalyst **1**, a Brønsted acid catalyst **2** and bifunctional chiral catalyst **3** (Figure 2). The immobilization process was conducted by UV irradiation of a solution of an organic catalyst in the presence of a textile material (Nylon 6,6), which facilitated covalent bond formation between the textile surface and unsaturated sites present within the catalyst structure (Scheme 1). The inclusion of a cross-linker (pentaerythritol tetraacrylate, PETA) allowed control of catalyst loading on the solid surface. The variation of the

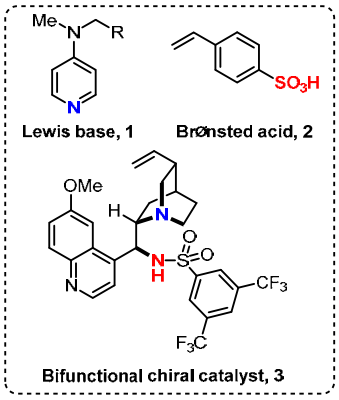

Figure 2. Examples of organocatalysts investigated in these studies.

amount of PETA could affect the immobilization pathway by changing the degree of branching points. Further optimization of catalyst loading and catalytic activity was simply conducted by changing UV irradiation time. Lewis basic catalyst **1a**, Brønsted acid catalyst **2** and bifunctional organocatalyst **3a** were equally well tolerated under the photochemical reaction conditions, yielding textile catalysts. DMAP derivative **1a** was successfully immobilized on the textile support to generate catalyst **OrganoTexCat-1a**. The SEM image of the obtained catalyst showed irreversible polymerization of organic substances on the surface, again without significant physical damage to the textile material. Catalyst loading was determined by acid/base titration.

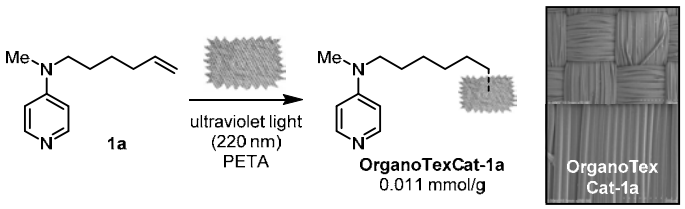

Scheme 1. Immobilization of DMAP derivative **1a** on textile.

The catalytic activity of **OrganoTexCat-1a** was evaluated in the acylation of sterically demanding phenol **4** with anhydride **5** (Scheme 2). In the absence of **OrganoTexCat-1a**, or in the presence of blank polyamide, almost no conversion was observed under otherwise identical reaction conditions. However, the employment of **OrganoTexCat-1a** in this transformation led to the formation of the ester **5** in near quantitative yields. After full conversion of phenol **4**, the catalyst was simply recovered by decanting the liquid phase, washing with dichloromethane and drying. Several recycling experiments showed the robustness of **OrganoTexCat-1a**; for more than 10 cycles no significant erosion of the catalytic activity was observed. It is noteworthy that the catalyst could be deactivated by forming an acid-base complex with the carboxylic acid by-product. However, the catalytic activity could simply be recovered by washing the catalyst with NEt_3 to regenerate it with good activity (recycle 4 to 5).

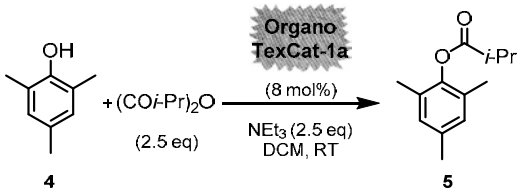

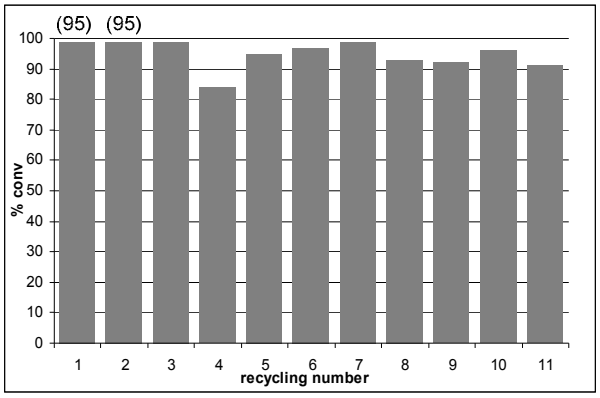

Scheme 2. Acylation of phenol **4** to ester **5** and demonstration of catalyst recycling.

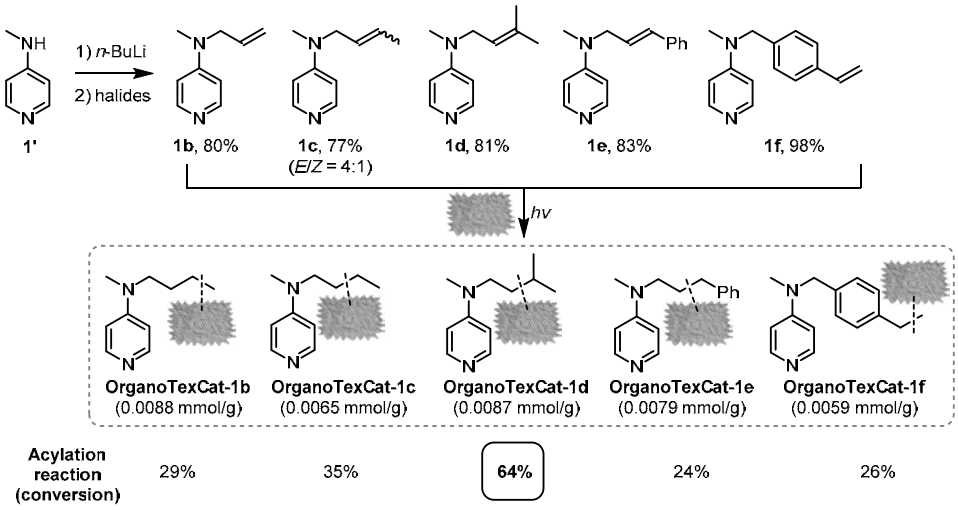

Scheme 3. Evaluation of formation and catalytic ability of various immobilized DMAP derivatives.

To investigate the effect of the olefin-containing side chain, we screened various DMAP derivatives (**1b-1f**) which were immobilized onto the textile material under identical immobilization conditions; a direct comparison of the relative catalyst activity is presented (Scheme 3). A longer side chain and higher substitution on the olefin are beneficial in terms of catalytic activity as observed in the case of **OrganoTexCat-1d**. This effect is quite general in heterogeneous catalysis due to a more efficient mass transfer and higher flexibility of the catalytically active site. Olefins with higher substitution can, in principle, provide a more stable radical intermediate, which facilitates selective immobilization without any side reaction. However, inferior catalytic activity was observed with **OrganoTexCat-1e**, although the catalyst immobilization was efficient.

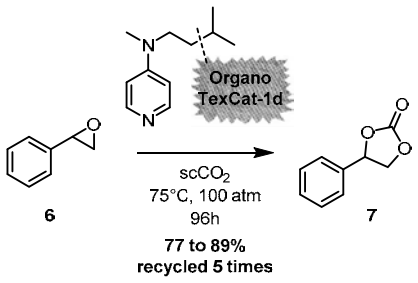

Scheme 4. Organotextile catalyzed cyclic carbonate formation.

Catalyst **OrganoTexCat-1d** also showed good activity and recyclability in cyclic carbonate formation (Scheme 4). The treatment of styrene oxide **6** with supercritical carbon dioxide in the presence of **OrganoTexCat-1d** led to the formation of carbonate **7** in good yield. This result highlights the high stability of catalyst **OrganoTexCat-1d** under high pressures (100 atm) and temperatures (up to 75 °C).

A facile immobilization of a commercially available Brønsted acid, the sulfonic acid **2**, was achieved giving **OrganoTexCat-2** with good catalyst loadings (Scheme 5). **OrganoTexCat-2** showed good activity in the intramolecular hydroetherification, affording the corresponding tetrahydrofuran **9**, from the alcohol **8**, in excellent yield.

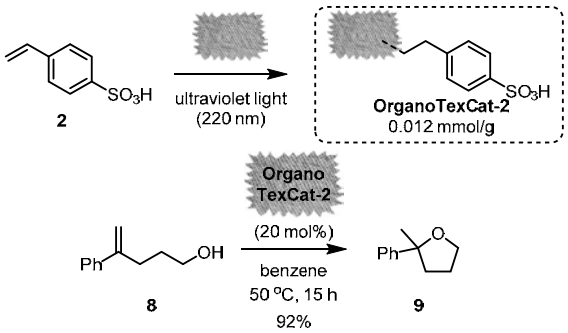

Scheme 5. Intramolecular hydroetherification of alcohol **8** catalyzed by **OrganoTexCat-2**.

No background reaction was observed in the absence of the catalyst under reaction conditions. It is noteworthy that the immobilized catalyst is easy to handle and displays robust stability for the transformation, the primary advantages of solid-supported catalysts.

Finally, we aimed to develop a textile material furnished with a chiral organocatalyst. Cinchona alkaloids have been widely used in the area of asymmetric organocatalysis and naturally bear an olefin group appended to the molecular scaffold. It was postulated that this alkene could be utilized as a handle to allow immobilization onto the textile support. As shown, the quinine-derived sulfonamide **3** was successfully immobilized under UV irradiation, giving **OrganoTexCat-3** (Scheme 6). The obtained catalyst showed comparable enantioselectivity to the homogeneous unsupported system in the desymmetrization of the anhydride **10a** to the hemiester **11a**, although a longer reaction time was required. The robustness of this approach was investigated by the recycling of **OrganoTexCat-3** through numerous iterative cycles of catalytic desymmetrization of **10a** to **11a** (Scheme 7). The asymmetric methanolysis could be repeated more than 300 times without significant erosion of catalytic activity and enantioselectivity. These recycling experiments

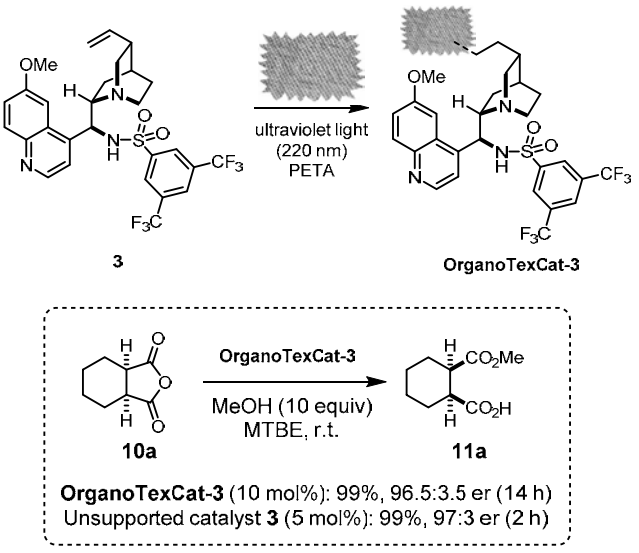

Scheme 6. Immobilization of bifunctional catalyst **3** and demonstration of catalytic ability in the desymmetrization of *meso*-anhydride **10a**.

illustrate the robustness of the textile supported catalyst and clearly demonstrate the power of heterogeneous organocatalysis.

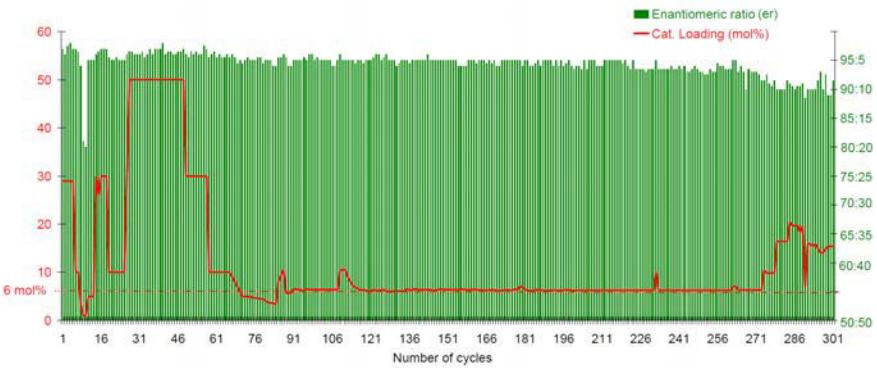

Scheme 7. Recycling of **OrganoTexCat-3** in the desymmetrization of **10a** for over 300 cycles.

Further application of the chiral textile catalyst was conducted by investigating the substrate scope (Scheme 8). Various *meso*-anhydrides were smoothly transformed into enantio-enriched hemiesters with excellent yields (up to 99%) and enantioselectivities (er up to 97:3). Bi- and tri-cyclic compounds could also be used to afford the expected products with high enantioselectivities, showing a comparable selectivity to the homogeneous catalytic systems. Due to the flexibility, compatibility and robustness of textile catalysts, we envisioned a continuous reactor system with our catalyst material. Enantio-enriched product **11h** was obtained in excellent yield (>99%) and enantioselectivity (up to 97:3 er) by using an iterative continuous fixed-batch approach. The textile-filled column was reused for more than 10 cycles, on multiple gram scales, showing identical activity and enantioselectivity.

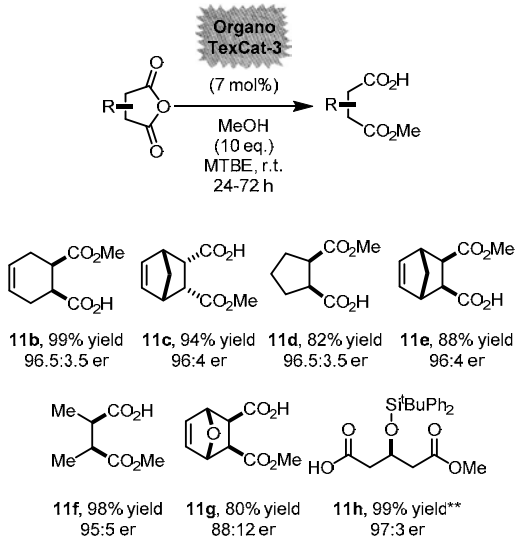

Scheme 8. Scope of desymmetrization of *meso*-anhydrides catalyzed by **OrganoTexCat-3**.

Publications resulting from this research area: 33

External Funding: Gesellschaft für Chemische Technik und Biotechnologie (DECHEMA)

Cooperations: Deutsches Textilforschungszentrum Nord-West gGmbH (Krefeld, D), C. E. Song (Suwon, South Korea), J. S. Gutmann (Essen, D)

2.2.3 Research Area "Activation of Carboxylic Acids in Organocatalysis" (B. List)

Involved: M. R. Monaco, S. Prévost, B. Poladura, M. Diaz de los Bernardos, M. Leutzsch, R. Goddard

Objective: During the last years, organocatalysis has become a general approach to asymmetric synthesis. Its success is arguably due to the detailed codification of general activation modes for some classes of substrates. Enamine and iminium ion catalysis, hydrogen bonding catalysis and Brønsted acid or base catalysis represent powerful tools for the transformations of certain imine, carbonyl or closely related substrates. Interestingly however, a well-defined and general activation mode for carboxylic acids, a useful and abundant chemical class, has not yet been established. The aim of this project is to identify a novel, simple and efficient system for the enhancement of their reactivity and for the control of their asymmetric reactions.

Results: Carboxylic acids, as well as phosphoric acid diesters, feature both a hydrogen-bond acceptor and a hydrogen-bond donor. Since intramolecular stabilization in apolar media is structurally not possible, they reach mutual stabilization by "self-association" in an apolar environment. This dimerization was first observed at the beginning of the 20th century and is nowadays accepted as a general phenomenon. This self-assembly is presumably sterically hampered for bulky binaphtol derived phosphoric acid diesters, which have recently raised the attention of the scientific community due to their role as privileged organocatalysts in the field of asymmetric Brønsted acid catalysis.

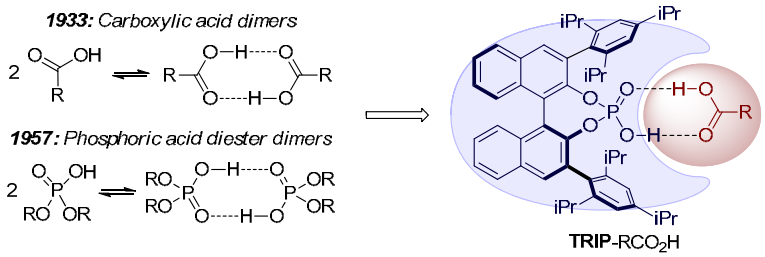

Scheme 1. Heterodimeric self-assembly for the activation of carboxylic acids in organocatalysis.

On this basis, we hypothesized that a small carboxylic acid molecule could enter the catalytic pocket in the absence of repulsive forces and a heterodimeric species may be established. This interaction may additionally influence the electronic structure of carboxylic acids, thus representing a strategy for their activation.

The formation of the heterodimer was investigated by NMR analysis. The ^{1}H NMR spectrum reveals that the addition of carboxylic acid in apolar media reduces the rotational freedom of the 3,3′-substituents of **TRIP** phosphoric acid, suggesting its presence in the catalytic pocket. Diffusion-Ordered Spectroscopy (DOSY) measurements showed the change of the translational diffusion coefficients of both species upon self-assembly, thus confirming the variation of the hydrodynamic volumes.

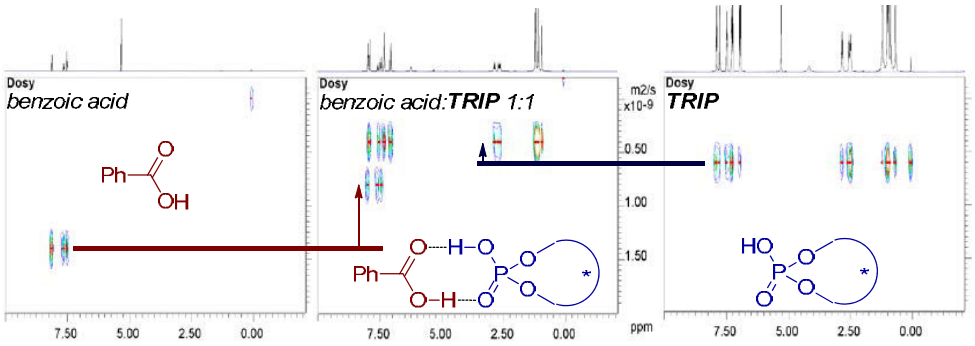

Figure 1. DOSY measurements of benzoic acid and **TRIP** phosphoric acid mixtures.

The strength of the association could be evaluated. As for 1:1 host-guest complexes, the binding isotherms of **TRIP** with benzoic acid and acetic acid were plotted following the shift of the phosphorous signal in the ^{31}P NMR spectrum and the association constants, $K_{a,}$ were determined *via* a non-linear regression approach (**TRIP**·BzOH *Ka* = (3981 ± 98) M^{-1}, **TRIP**·AcOH *Ka* = (1948 ± 26) M^{-1}).

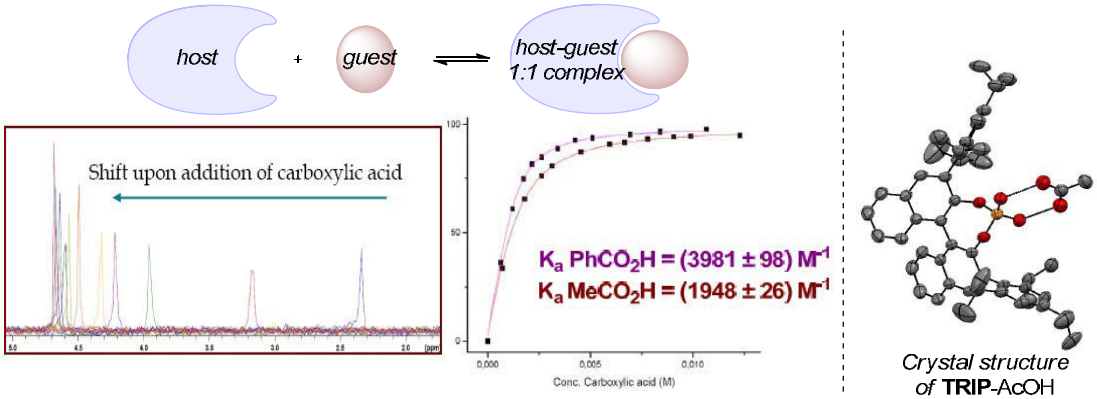

Figure 2. Determination of binding constants *via* ^{31}P NMR titration and crystal structure of **TRIP**-AcOH.

Final confirmation of the heterodimer formation was then obtained by cocrystallizing acetic acid and **TRIP**, which gave a crystal suitable for X-ray analysis.

The upfield shift of the proton signals of carboxylic acid in the NMR spectrum fascinatingly suggested that the self-assembly with phosphoric acid raises the energy of its HOMO orbital. This leads to the somewhat counterintuitive possibility that, despite being a stronger acid, the phosphoric acid is formally behaving like a base within the dimer due to the strong effect of the P=O bond. Therefore we started to investigate the role of the heterodimeric system as a source of nucleophilic carboxylic acids. The ring opening of aziridines has been chosen as ideal testing ground for our concept since an asymmetric catalytic conversion leading to amino alcohols has not yet been reported.

The novel system turned out to be effective in the desymmetrization of *meso*-aziridines with benzoic acid. The scope of the reaction confirms generality of the approach. Indeed, several different cyclic and acyclic substrates successfully reacted affording the expected products **2a-k**. The reactions with acetic acid gave comparably high yields and enantioselectivities albeit with the need of longer reaction time and higher nucleophile concentration, which confirms the importance of the affinity between **TRIP** and the carboxylic acid for the reacting system.

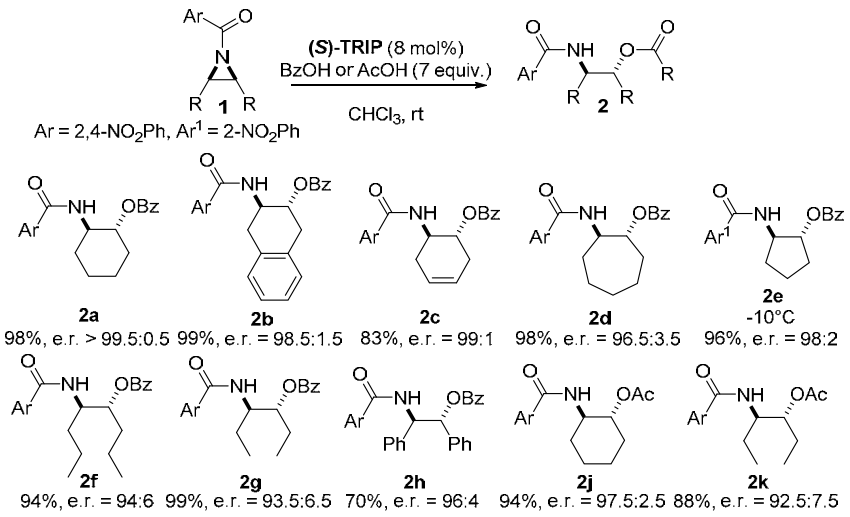

Scheme 2. Scope of the ring opening desymmetrization of *meso*-aziridines with carboxylic acids.

Next we turned our attention to the kinetic resolution of terminal aziridines. Lowering the temperature to -30 °C, high selectivity factors could be reached both for linear substrates as well as for branched ones (*S* from 37 to 51). The high regioselectivity of the reaction is remarkable and probably due to a partial positive charge on the aziridine fragment in the reaction transition state.

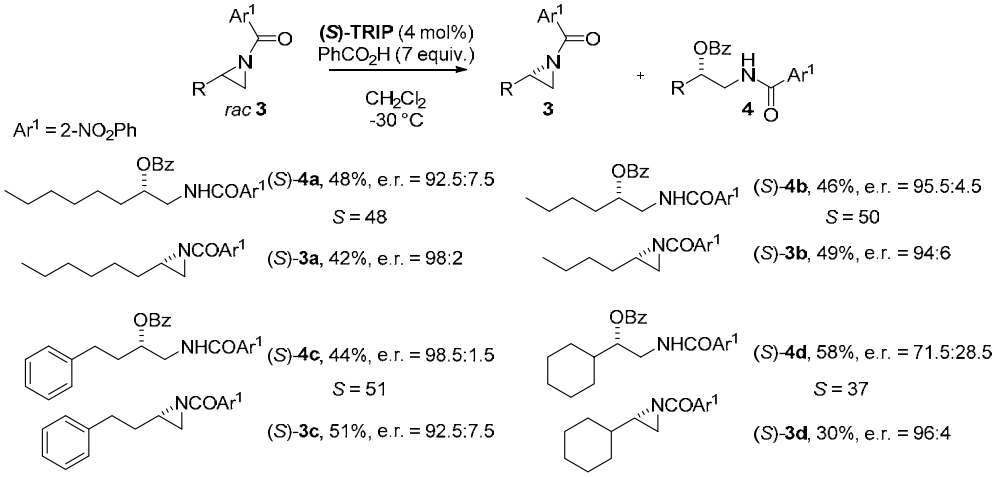

Scheme 3. Scope of the ring opening kinetic resolution of terminal aziridines with carboxylic acids.

A catalytic cycle can be proposed. The chiral nucleophile is first generated by self-assembly and then the aziridine is engaged in the nucleophilic attack, which possibly occurs through a concerted transition state in which the electrophile benefits from an additional Brønsted acid activation. A highly asynchronous S_N2 pathway is suggested by the exclusivity of *trans*-products in the desymmetrization strategy and by the perfect regioselectivity of the kinetic resolution, which reveals a strong localized δ^+ charge at the reacting centre.

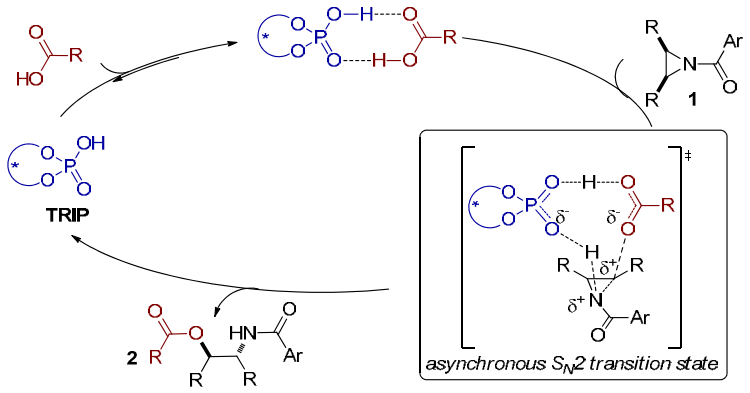

Scheme 4. Proposed mechanism for the activation of carboxylic acids in organocatalysis.

Encouraged by the results achieved in the ring opening of aziridines, we turned our attention to the reaction of carboxylic acids with epoxides. Our system indeed proved to be suitable. However, the enantioselectivity achieved with **TRIP** phosphoric acid was only modest. A novel binaphtol derived phosphoric acid catalyst **5**, in which the 3,3′-substituents are fused polycyclic moieties, gave

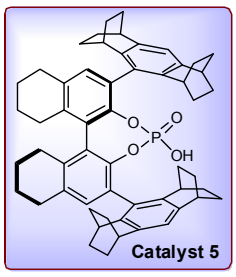

significantly improved results, delivering monoprotected glycols **7** from the corresponding *meso*-epoxides **6** in good yields and enantioselectivities.

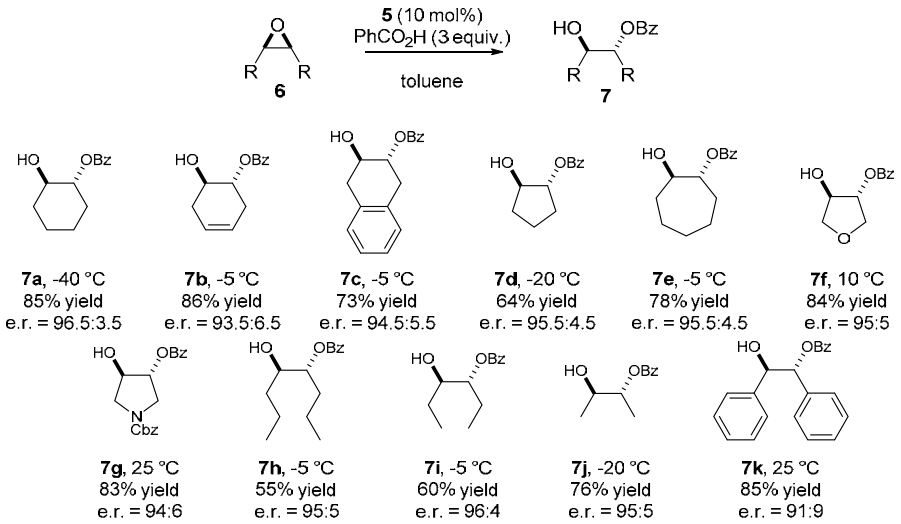

Scheme 5. Scope of the ring opening desymmetrization of *meso*-epoxides with carboxylic acids.

In summary, the first approach to the activation of carboxylic acids in organocatalysis has been developed. The self-assembly between chiral phosphoric acids and carboxylic acids has been observed by analytical methods and has been applied to interesting methodologies, such as the asymmetric ring opening of aziridines and epoxides. A cooperative mechanism has been suggested: the carboxylic acid prevents the catalyst degradation by limiting the direct interaction with the electrophile, while the phosphoric acid activates and directs the nucleophilic attack of the carboxylic acid partner.

Publications resulting from this research area: none

External funding: European Research Council Advanced Grant (HIPOCAT)

Cooperations: none

2.2.4 Research Area "Lewis Acid Organocatalysis" (B. List)

Involved: S. Gandhi, P. García-García, J. Guin, M. Leutzsch, C. Rabalakos, M. van Gemmeren (né Mahlau), Q. Wang

Objective: Organocatalysts function by donating or removing electrons or protons, defining four distinct activation modes: Brønsted base catalysis, Brønsted acid catalysis, Lewis base catalysis, and Lewis acid catalysis. While the areas of Lewis base, Brønsted acid and base organocatalysis are relatively well developed, organic Lewis acid catalysis was until recently almost unexplored. Our group has developed chiral analogs of triflimide (Tf_2NH), which is a powerful achiral Mukaiyama aldol pre-catalyst that generates the highly reactive Lewis acid Tf_2NTMS as the actual catalyst. These catalysts exploit the concept of asymmetric counteranion-directed catalysis (*ACDC*) developed by our group, by pairing the catalytically active silylium ion equivalent with a chiral disulfonimide anion, which is responsible for the stereoinduction. Based on these results we were interested in the application of this type of catalysts to further reactions known to be challenging for metal-based Lewis acid catalysts. Additionally, the very low catalyst loadings achieved in our work on the Mukaiyama aldol reaction spurred our interest in developing new, even more active variants of our disulfonimide catalysts, in order to equal the extremely low catalyst loadings sometimes achieved in transition metal or biocatalysis.

Results: In spite of some progress in the development of catalytic systems for hetero-Diels-Alder reactions (HDA) these reactions are still very limited in their scope of dienes, and both substituted and functionalized dienes have proven to be highly challenging substrates. In particular, substituted 1,3-bis(silyloxy)-1,3-dienes **2**, which are readily synthesized in one step from commercially available and inexpensive 1,3-diketones, had not been reported in asymmetric catalysis prior to our studies, conceivably due to a competing achiral silylium catalyzed background reaction. This rendered them ideal model substrates to expand the applicability of our catalytic system. In order to achieve high enantioselection in these reactions, we developed the perfluoroisopropyl version **3a** of the initially introduced disulfonimide. This catalyst promoted the highly enantioselective HDA of aldehydes **1** and dienes **2** to give a variety of products in good to excellent enantioselectivities. The disulfonimide system was found to be suitable for tetrasubstituted diene substrates, thus giving access to 2,5,6-trisubstituted dihydropyridines **4a-e** in high yields and excellent enantioselectivities. On the aldehyde side, electronrich or electronically unbiased aromatic aldehydes, as well as

cinnamaldehyde derivatives were suitable electrophiles, giving for example **4f-h** in excellent yields and enantioselectivities. The utility of our methodology was further demonstrated by the first asymmetric synthesis of a potent aromatase inhibitor, which was achieved by oxidation of **4e** to the aromatic product **5** and subsequent removal of the benzyl group to give the desired pharmacologically active compound **6** without loss of enantiopurity (Scheme 1).

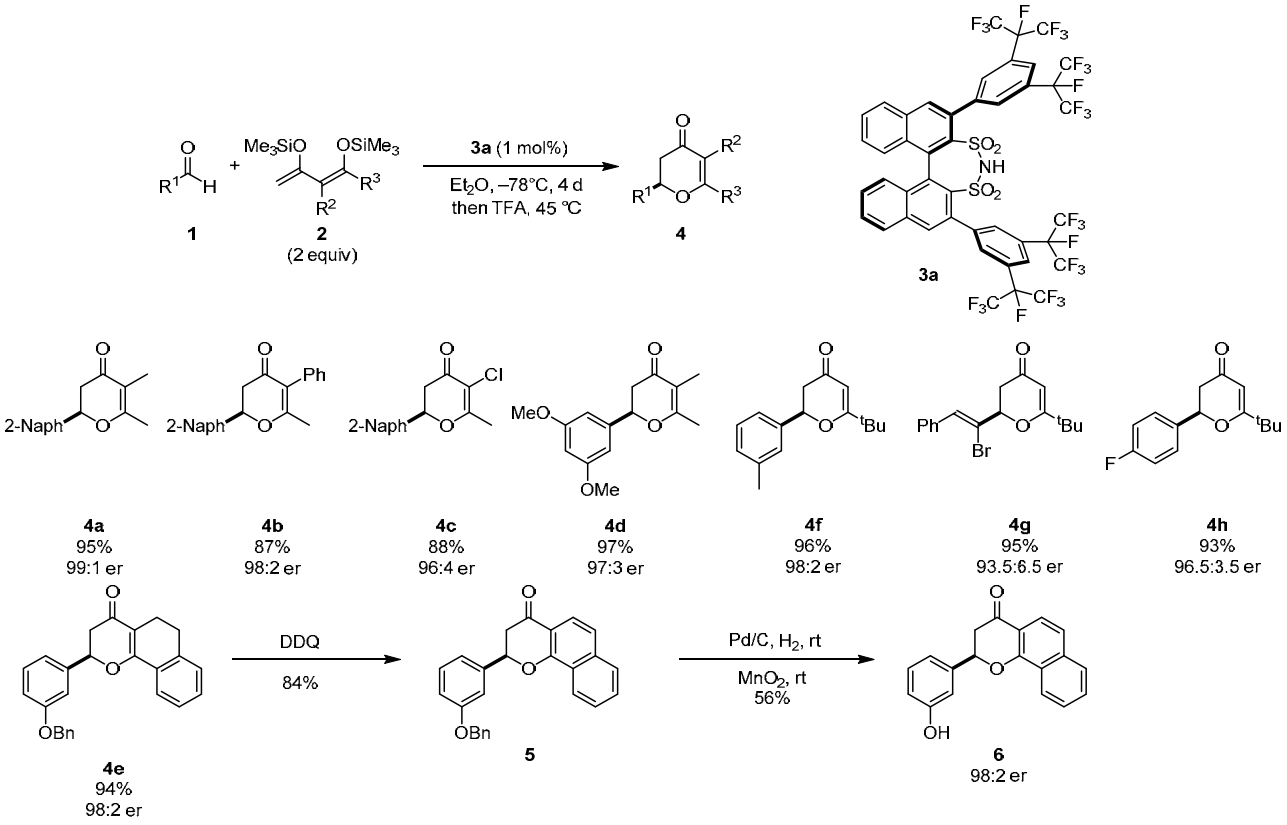

Scheme 1. Disulfonimide catalyzed asymmetric hetero-Diels–Alder reactions.

Another reaction, which has traditionally posed great difficulties to enantioselective Lewis acid catalysis is the Hosomi-Sakurai reaction, which shares a number of mechanistic features with the Mukaiyama-aldol reaction. Thus, prior to our studies, only a limited number of enantioselective methodologies were known for this reaction and we reasoned that our ACDC approach using disulfonimides as catalysts should allow for the enantioselective catalysis of this reaction. Indeed we realized the catalytic asymmetric methallylation of aldehydes utilizing the nitro-substituted catalyst **3b**.

A variety of aldehydes **1** and allylsilane nucleophiles **7**, bearing both aliphatic and aromatic substituents, could be employed and the allylation products **9** were

obtained in high yields and enantioselectivities (Scheme 2). As in many metal-based systems, simple allyltrimethyl silane could not be employed, due to its dramatically lower reactivity. The optimized conditions for this reaction involved the use of silyl ketene acetal **8a** in catalytic amounts, which accelerated the initial silylation of the precatalyst.

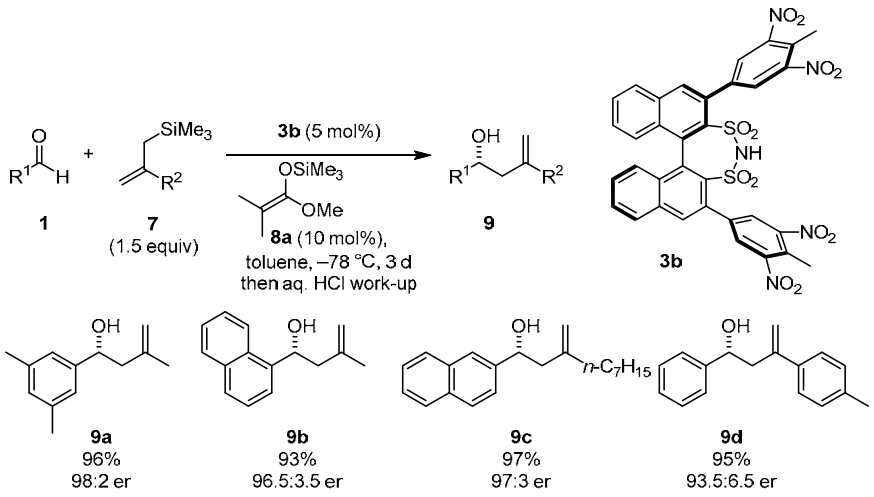

Scheme 2. The asymmetric counteranion-directed catalytic Hosomi-Sakurai reaction.

Just as chiral enantiopure homoallylic alcohols, the corresponding homoallylic amines are valuable intermediates in the synthesis of natural products and pharmaceutically active compounds. Despite the elegance of this strategy, direct asymmetric reactions between aldehydes, carbamates or amines and allyltrimethyl silane were unknown prior to our studies. Instead, the corresponding homoallylic amines were accessed by stereoselective allylations of preformed imines or other, indirect methods.

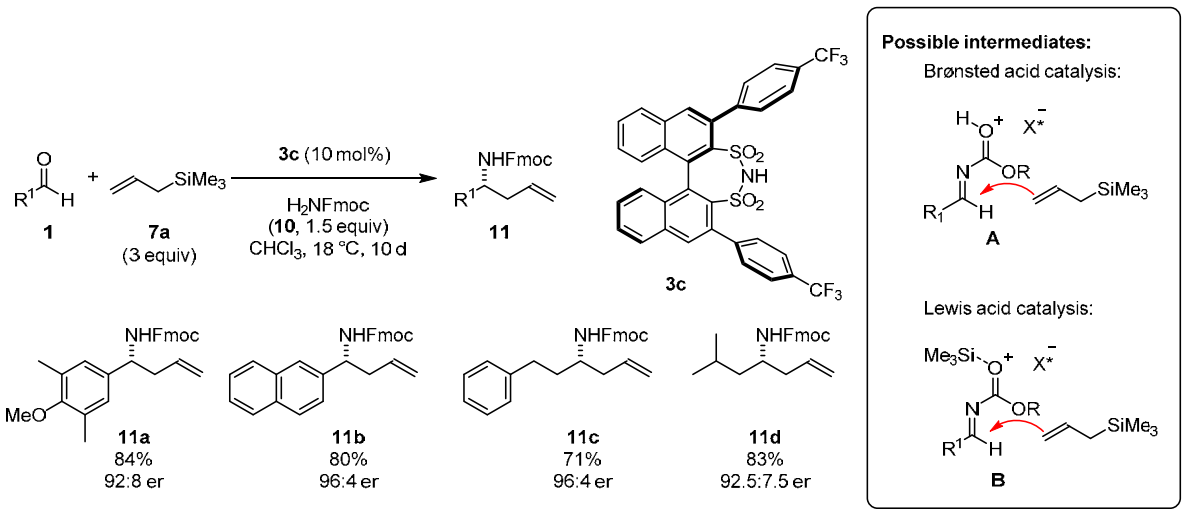

Scheme 3. Disulfonimide catalyzed enantioselective three-component aminoallylations.

The development of *para*-substituted catalyst **3c** and the optimization of nitrogen-source and reaction conditions allowed us to develop a highly enantioselective direct aminoallylation of aldehydes (Scheme 3).

The reaction between aldehydes **1**, allyltrimethyl silane (**7a**) and 9-fluorenylmethyl carbamate (H_2NFmoc, **10**) gave both aromatic (**11a** and **11b**) and aliphatic (**11c** and **11d**) products with high yield and enantioselectivity. As one equivalent of water is released in the catalytic cycle of this three-component reaction, we were interested whether this reaction proceeds through Brønsted acid catalysis (intermediate **A**) or Lewis acid catalysis (intermediate **B**). As silylium ion equivalents are highly water sensitive, the reaction mixture would have to be completely dry, in order for intermediate **B** to be involved. Considering the self-healing capability of our disulfonimide catalysts (using up two equivalents of nucleophile per molecule of water) and the observed necessity for three equivalents of nucleophile in our reaction, we assume that this reaction is in fact Lewis acid catalyzed. This interpretation is further corroborated by the fact that identical enantioselection was obtained, when presilylated catalyst and preformed imine were reacted with trimethylallyl silane **7a**.

Having discovered the ability of the disulfonimide catalysts to activate (*in situ* generated) imines, we became interested in the generation of the β^3-amino ester scaffold, which is present in a large number of synthetically valuable intermediates, and can be generated by the enantioselective Mannich reaction between an ester enolate equivalent and an imine. However, methods known for this transformation often suffer from the instability of the imine substrates. As these imines are in many cases prepared by elimination from amino sulfones, we reasoned that it should be possible to combine the Mannich reaction and the *in situ* generation of the imine using Lewis acid organocatalysis. Indeed, using the sterically demanding catalyst **3d**, the reaction of *N*-Boc-amino sulfones **12** with commercially available silyl ketene acetal **8b** could be catalyzed to give β^3-amino esters **13**.

Aromatic substrates with different substitution patterns were found to give excellent yields and enantioselectivities under the optimized reaction conditions (**13a-c**, Scheme 4). Although currently achieved stereoselections are modest, the methodology was shown to be applicable to aliphatic *N*-Boc-amino sulfones, giving for example **13d**. These products are usually difficult to access, as their imine precursors are even less stable than their aromatic counterparts.

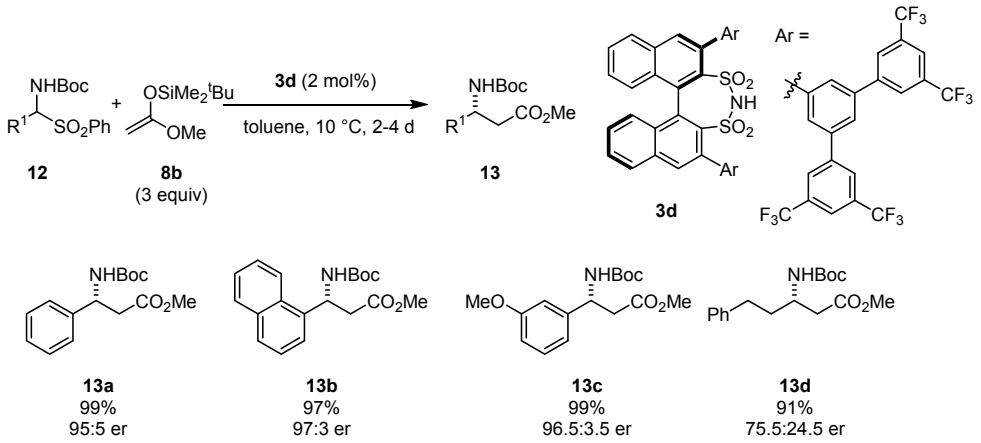

Scheme 4. Enantioselective Mukaiyama-Mannich reactions starting directly from *N*-Boc-amino sulfones.

We proceeded to investigate the mechanism of this two-step process and found that the elimination from the *N*-Boc-amino sulfone to give the proposed imine substrate is rate limiting, as the reaction of a preformed imine under identical conditions was significantly faster giving nearly identical selectivity. The rate limiting step was also determined from NMR measurements.

Publications resulting from this research area: 14, 23, 26, 34

External funding: European Research Council Advanced Grant (HIPOCAT), Alexander von Humboldt Foundation (S. Gandhi, J. Guin), Fonds der Chemischen Industrie (M. van Gemmeren), Spanish Ministerio de Educación y Ciencia (Fellowship to P. García-García)

Cooperations: none

2.2.5 Research Area "Secondary Amine Catalysis" (B. List)

Involved: I. Corić, P. S. J. Kaib, A. Lee, M. Leutzsch, S. C. Pan, M. van Gemmeren (né Mahlau)

Objective: Asymmetric S_N2-α-alkylations of carbonyl compounds with alkyl halides are powerful transformations that commonly involve chiral auxiliaries or phase transfer catalysts. Despite some progress towards organocatalytic variants, such as an intramolecular proline catalyzed reaction of halo-aldehydes developed by our group, and several studies combining enamine catalysis with radical or S_N1-pathways, the intermolecular S_N2-reaction of aldehydes and alkyl halides has remained elusive and has been termed a "holy grail" of organocatalysis. The goal of this research project was to develop a system capable of catalyzing this reaction.

Results: When developing such a catalytic system, the plethora of undesired side reactions has to be considered. Amongst them, avoiding self-aldolization of the substrate, racemization of the product, and catalyst alkylation are considered to be crucial. To achieve this goal we chose to study α-branched aldehydes, thus generating α-quaternary products and avoiding the issue of product racemization. We further designed our catalytic system based on the following considerations: Using a buffer of acid and base additives might be able to retain the potential advantages of adding base, while eliminating some of the undesired side effects. More specifically, this system should accelerate enamine formation and prevent very acidic or basic conditions throughout the course of the reaction, thus reducing catalyst alkylation to a minimum.

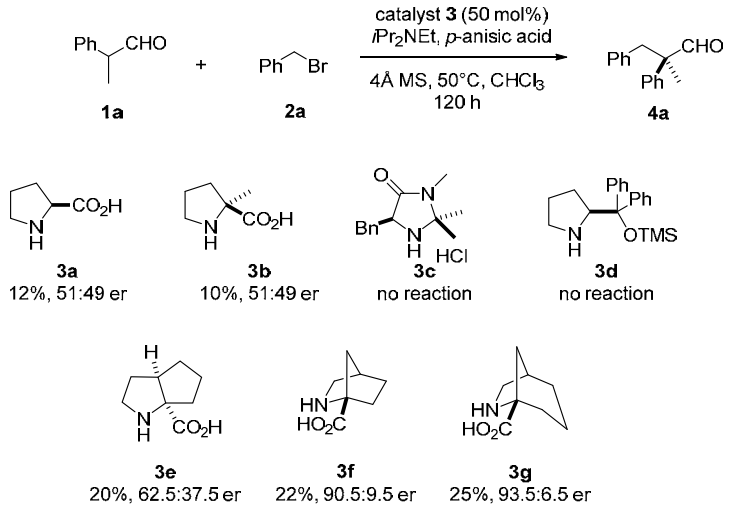

Scheme 1. Catalyst evaluation.

We commenced our study by screening various potential catalysts, including several newly developed, sterically hindered proline analogs (Scheme 1).

A preliminary screening of catalysts revealed these new catalysts to be highly promising and a screening of reaction conditions was undertaken in order to achieve catalyst turnover. As the base additive was considered to be crucial, due to the predicted ion pairing between the protonated base and the carboxylate moiety of the catalyst, we screened various bases and identified tetramethylguanidine as the base of choice, which enabled both catalyst turnover and optimal enantioselectivity (Table 1).

Table 1. Influence of the base[a].

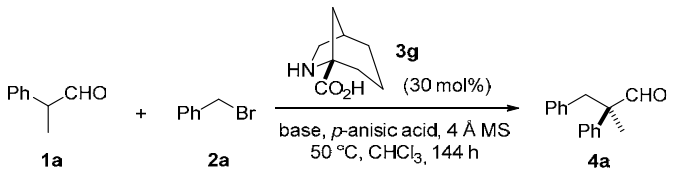

Entry	Base	Yield [%][b]	e.r.[c]
1	DMAP	30	65:35
2	imidazole	33	61:39
3	DBU	20	79:21
4	1,3-diphenylguanidine	60	88:12
5	1,3-di-(*o*-tolyl)-guanidine	63	90:10
6	1,1,3,3-tetramethylguanidine	80	95.5:4.5
7	2',2'-(naphthalene-1,8-diyl)-bis(1,1,3,3-tetramethylguanidine)	80	53:47

[a] Conditions: aldehyde **1a** (0.1 mmol) and benzyl bromide **2a** (0.5 mmol), catalyst **3l** (0.03 mmol), *p*-anisic acid (0.5 mmol), base (0.5 mmol), 4 Å MS (80 mg) in chloroform (0.5 mL) at 50 °C for 144 h. [b] Determined by GC-MS using *n*-dodecane as internal standard. [c] Determined by GC analysis on a chiral stationary phase.

We also studied the reaction stoichiometry with regard to acid, base and alkylating agent and found that molecular sieves have a beneficial effect on the reaction. The reaction is best conducted using five equivalents of buffer and alkylating agent in chloroform at 50 °C in the presence of molecular sieves.

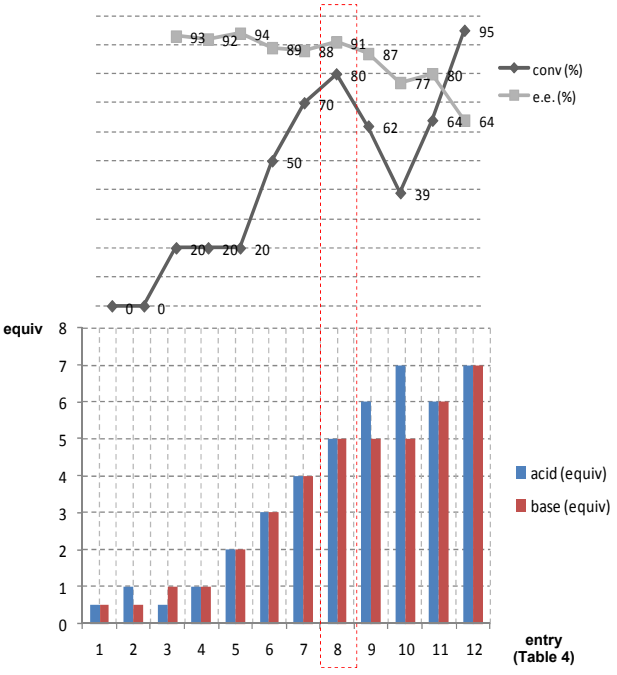

Figure 1. Evaluation of the amount of acid and base.

Using our optimized reaction conditions we explored the scope of our newly developed S_N2-α-alkylation of α-branched aldehydes and found that a number of substrates reacted smoothly giving moderate to good yields and

enantioselectivities (Scheme 2). The use of substituted benzyl bromide derivatives was also confirmed to be possible. As expected, α-unbranched aldehydes turned out to be unsuitable as substrates, giving predominantly double alkylated products and self-aldolization products.

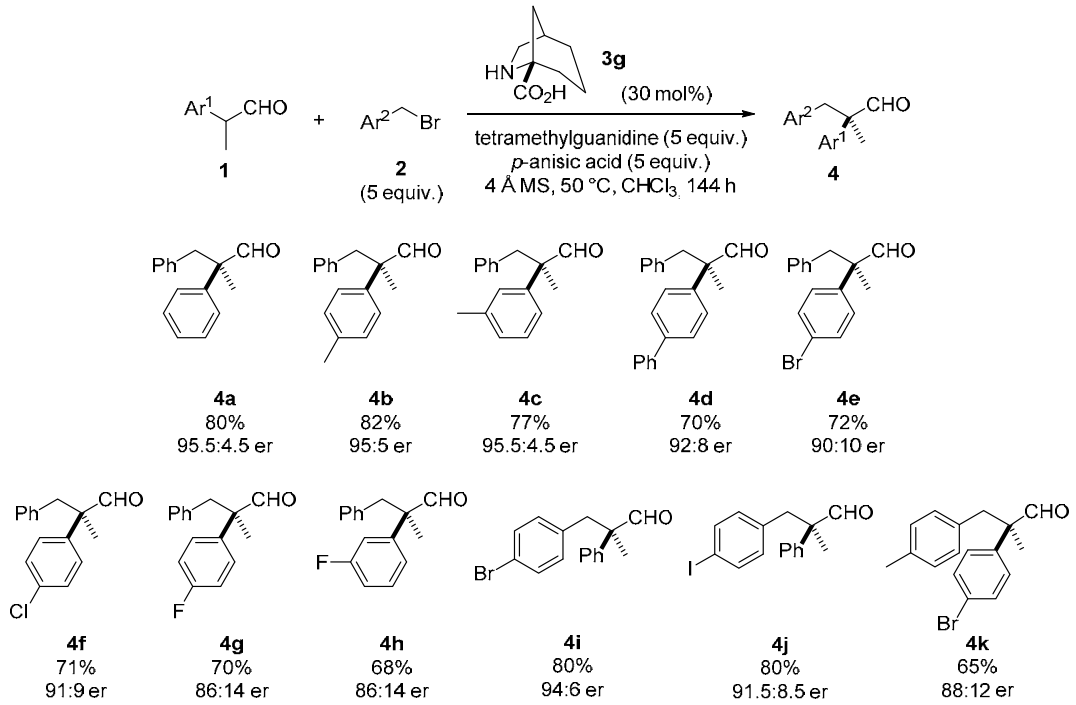

Scheme 2. Substrate scope.

The absolute configuration of our model product **4a** was determined to be (*R*) and we could rationalize this by analogy to our previous intramolecular reaction, for which transition state **B** was computationally determined. Thus we suggested a transition state **A** for our current catalytic system (Figure 2).

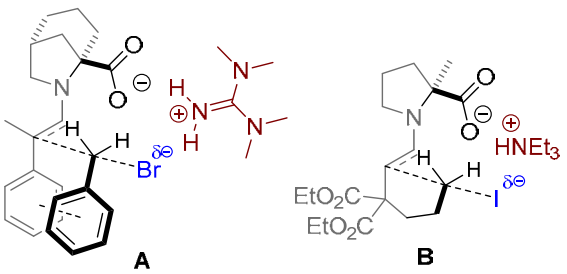

Figure 2. Proposed transition state of the intermolecular α-alkylation (**A**). Calculated transition state of the intramolecular α-alkylation (**B**).

In order to confirm the suggested roles of acid and base in the reaction, we conducted NMR experiments using different ratios of acid and base with proline (**4a**) and our optimal catalyst **3g**. These experiments confirmed that the reaction between catalyst and substrate is greatly enhanced by the addition of acid and/or base and that the base additionally shifts the equilibrium between enamine and oxazolidinone towards the enamine intermediate.

Thus, we concluded that the buffer utilized in this reaction works in the following way: The role of the base is to solubilize the catalyst and to increase the ratio, in which the enamine intermediate is formed.

Table 2. Equilibrium between catalysts and aldehyde in $CDCl_3$ with various equivalents of additives.

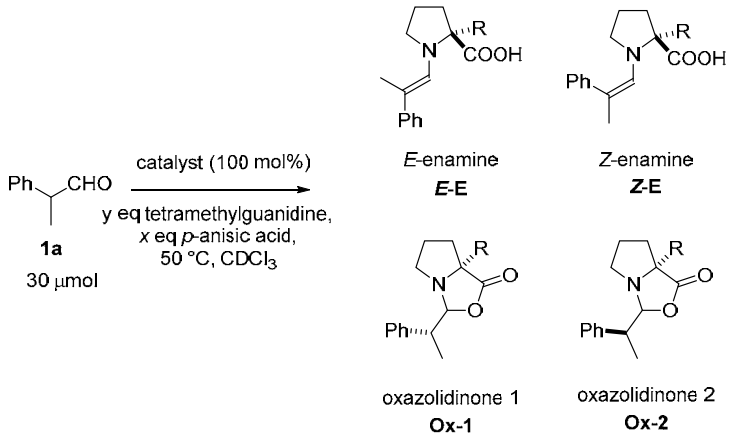

Entry	x	y	Catalyst	Ratio aldehyde : intermediates	Ratio Intermediates *E*-E : *Z*-E : Ox-1 : Ox-2
1	0	0	**3a**	> 99 : 1	-
2	0	1	**3a**	74 : 26	46 : 5 : 0 : 0
3	1	0	**3a**	71 : 29	0 : 0 : 5 : 4
4	1	1	**3a**	87 : 13	4 : 1 : 4 : 4
5	2	2	**3a**	89 : 11	5 : 1 : 6 : 5
6	5	5	**3a**	84 : 16	9 : 2 : 2 : 2
7	0	0	**3g**	98 : 2	0 : 0 : 1 : 2
8	1	0	**3g**	96 : 4	0 : 0 : 1 : 1
9	0	1	**3g**	84 : 16	19 : 6 : 21 : 28
10	1	1	**3g**	93 : 7	0 : 0 : 3 : 4
11	2	2	**3g**	89 : 11	3 : 1 : 7 : 8
12	5	5	**3g**	88 : 12	12 : 1 : 14.5 : 17

The role of the acid is to prevent undesired side effects of the base. As tetramethyl guanidine is a strong base and stabilizes the more nucleophilic anionic form of the catalyst, alkylation could potentially deactivate the catalyst. The alkylated catalyst was in fact observed by GC-MS even under optimal conditions. The alkylation could be prevented by the acid, which can reduce the catalyst's nucleophilicity. Additionally, strong bases such as guanidines are known to promote enolate alkylations. Thus the acid may also act by preventing a competing non-enantioselective reaction.

In summary, we developed the first catalytic asymmetric α-alkylation of α-branched aldehydes utilizing a buffer system and a bulky proline analog as catalyst. Although this

catalytic system is rather complicated and not applicable to linear aldehydes at the current state, we believe that our discovery represents progress towards the development of universally applicable S_N2-α-alkylations of carbonyl compounds with alkyl halides.

Publications resulting from this research area: 37

External Funding: European Research Council Advanced Grant (HIPOCAT), Fonds der Chemischen Industrie (M. van Gemmeren)

Cooperations: Oleksandr O. Grygorenko, Igor Komarov, Andrey V. Tymtsuniknone (Kyiv, Ukraine)

2.2.6 Research Area "The [3,3]-Diaza Cope Rearrangement in Asymmetric Catalysis" (B. List)

Involved: S. Müller, M. J. Webber, A. Martínez, L. Kötzner, F. Pesciaioli, C. K. De

Objective: The [3,3]-sigmatropic rearrangement is a well-established versatile pericyclic reaction, which has been successfully utilized in organic synthesis. Interestingly, the utility of the [3,3]-diaza Cope rearrangement remained limited. This rearrangement is a powerful synthetic principle utilized to generate a C–C bond at the expense of an N–N bond. It forms the basis of important and fundamental acid-catalyzed transformations such as the Fischer indolization, its associated reactions and the benzidine rearrangement, of which asymmetric versions despite their synthetic and scientific relevance have remained elusive to date. Chiral Brønsted acids, which have been established as a powerful tool in organocatalysis, may be capable of catalyzing these [3,3]-diaza Cope rearrangements leading to enantio-enriched indole derivatives and aromatic diamines.

Results: Although numerous methods are known for the construction of indoles, one of the most abundant heterocyclic compounds in nature, the acid-mediated Fischer indolization remains one of the most widely used procedures. Nevertheless, catalytic asymmetric Fischer indolizations have remained difficult to implement so far. Our strategy relies on the indolization of 4-substituted cyclohexanone-derived phenylhydrazones to give chiral tetrahydrocarbazoles *via* a [3,3]-diaza Cope rearrangement. However, to enable the use of a chiral Brønsted acid at substoichiometric loadings catalyst poisoning due to ammonia formation during the course of the reaction had to be addressed. As expected, the use of *N*-benzyl-protected hydrazone **1a** with a catalytic amount (5 mol%) of phosphoric acid led to a dramatic decrease in the reaction rate. Unfortunately, reaction condition screenings did not give any improvement. When testing different additives, the addition of Amberlite® CG50, a weakly acidic cation exchange resin, was found to have a beneficial effect on the catalyst reactivity and increased the yield. We thus investigated the scope of our reaction under the optimized conditions. The *N*-benzyl-protected hydrazone **1a** and the iodinated analogue **1b** both gave the corresponding products in 94% and 99% yield and enantiomeric ratios of 94:6 and 95:5, respectively. Despite the different electronic properties of their protecting group, both hydrazones gave 6-substituted tetrahydrocarbazoles in good yields and high enantioselectivities (**2c**–**2e**). Phenylhydrazones with substituents at different ring positions were also found to be suitable substrates (**2f**–**2h**). Hydrazones in which R^3 consists of a substituted aromatic ring (**2i**–**2o**) or an aliphatic group (**2p**–**2r**) gave the desired products in typically good yields and with high levels of enantioselectivity. Heteroatom-substituted

substrates were also well suited and gave the desired products in 99% yields (**2s**–**2t**) and with high levels of enantioselectivity. Tetrahydrocarbazole **2u** bearing a quaternary stereogenic center proved to be a challenging substrate. Interestingly, the hydrazone derived from cyclopentanone gave the desired product **2v** in 62% yield and 90.5:9.5 er at elevated temperatures and after a prolonged reaction time.

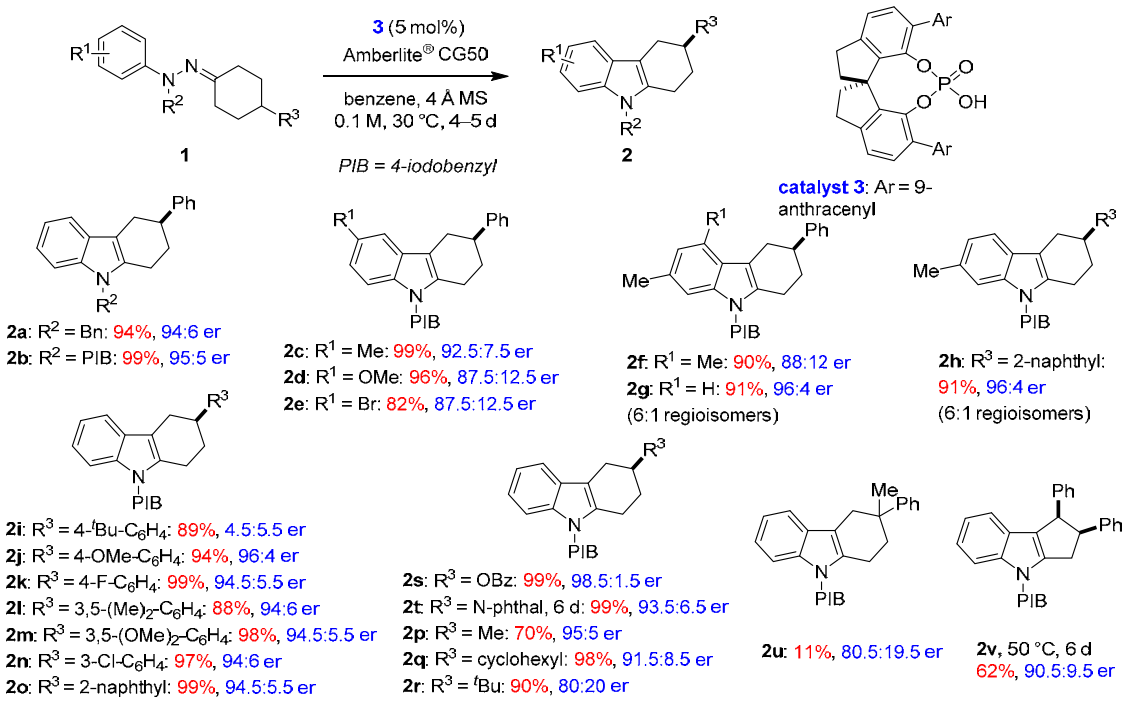

Scheme 1. Catalytic asymmetric Fischer indolization.

As application of the developed method, a formal synthesis of the thromboxane receptor antagonist Ramatroban (**6**) was targeted. Indolization of hydrazone **1t** on a 2.0 mmol scale proceeded without compromising the yield or enantioselectivity. In this process 55% of catalyst **3** were recovered. Starting from tetrahydrocarbazole **2t**, a three-step sequence of deprotection of the phthalimide, debenzylation under Birch conditions and subsequent sulfonylation gave the literature-known intermediate **7** in good overall yield without diminishing the initial optical purity.

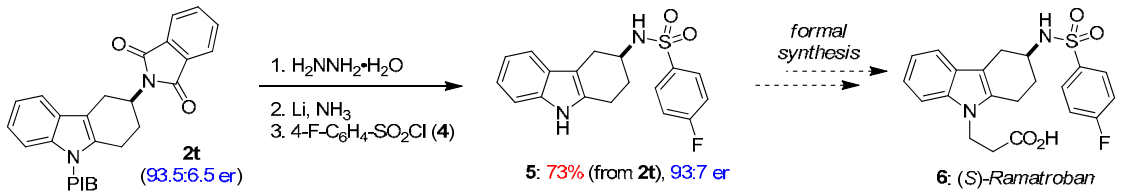

Scheme 2. Application of the catalytic asymmetric Fischer indolization.

3,3-Disubstituted fused indolines are privileged substructures of diverse natural products and biologically active molecules for which the [3,3]-diaza Cope rearrangement could be a complementary synthesis strategy based on the Fischer indolization. Starting from *N*-

benzyl-*N*-phenylhydrazine (**7a**) and 2-phenylcyclohexanone (**8b**) in the presence of a variety of chiral phosphoric acids and the weakly acidic Amberlite® CG50 as additive, indoline-enamine **9a** was obtained in promising yields and enantioselectivities. Further tuning of the reaction conditions revealed that the hindered SPINOL phosphoric acid STRIP (**10**) is the best catalyst for this transformation. The scope of the reaction was evaluated under the optimized conditions. Indolines **9** could be obtained typically in quantitative yields and with high levels of enantioselectivity irrespective of the aryl substituent at R^3 (**9a**, **9c**–**9e**).

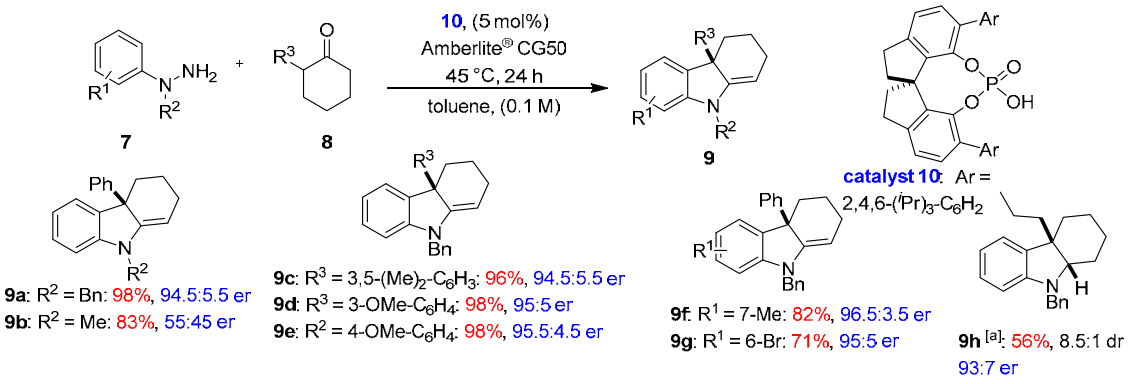

[a] After in situ reduction of the unstable enamine with $NaBH_3CN$.

Scheme 3a. Interrupted asymmetric Fischer indolization with α-substituted cyclohexanone.

Remarkably lower er was obtained when the protecting group on the hydrazine was modified from Bn to Me (**9b**). Irrespective of the electronic and steric nature of the substituents R^1 the desired products **9f**–**9g** could be isolated in good yields and with high level of enantioselectivity. 2-Alkylcyclohexanones were found to be less reactive, thus the reaction was performed at elevated temperature, and product **9h** was obtained after *in situ* reduction of the corresponding unstable enamine with $NaBH_3CN$ in moderate yield and good enantioselectivity and diastereoselectivity (8.5:1 dr). The major diastereoisomer was found to be the *cis*-fused system with an er of 93:7.

Inspired by these findings, a similar transformation with 2-substituted cyclopentanones was pursued which were beforehand found to be challenging for the Fischer indolization. Interestingly, the reaction yielded 2-hydroxyindolines **13**, rather than the corresponding indoline-enamines. Both alkyl and benzyl substituents were well-tolerated (**13a**–**13c**). By incorporating a reductive step we could achieve a more stable product and increase the yield. Once the indolization was judged to be completed, addition of $NaBH_3CN$ gave an improved yield of the reduced indoline **14a**. Following

this reaction sequence, reduced indoline products (**14b**–**14d**) were obtained in good yields and high enantioselectivities.

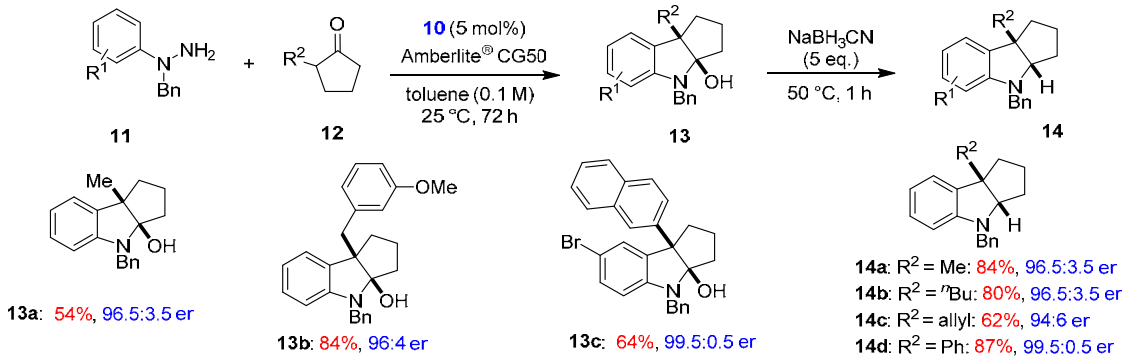

Scheme 3b. Interrupted asymmetric Fischer indolization with α-substituted cyclopentanone.

Encouraged by these results, this method was applied for the synthesis of more complex molecules using a suitable design of the starting ketone with an appropriate tethered nucleophile or pro-nucleophile. The Fischer indolization pathway could be interrupted by the attack of a nucleophile on the iminium functionality, which is formed upon loss of NH_3.

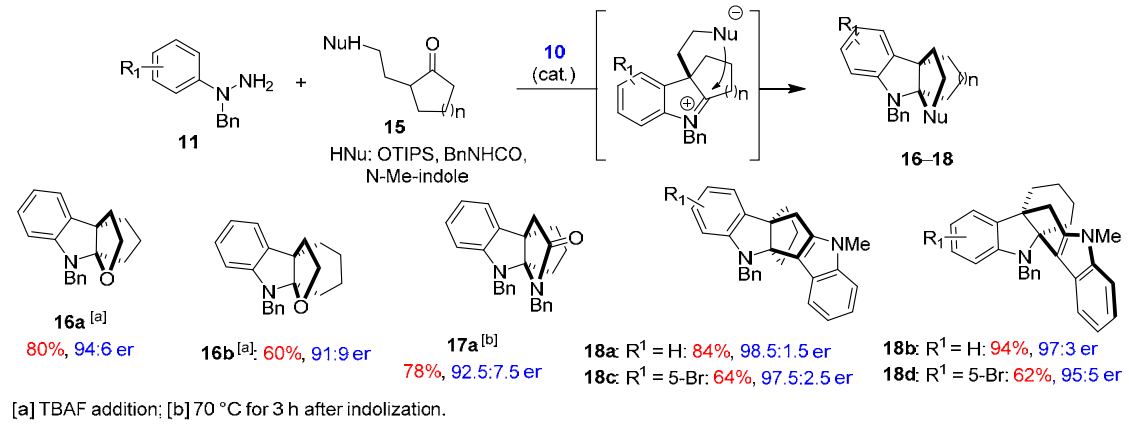

[a] TBAF addition; [b] 70 °C for 3 h after indolization.

Scheme 3c. Synthesis of the polycyclic indolines *via* interrupted asymmetric Fischer indolization.

Ketones containing a γ-silyl ether on the side chain were reacted with hydrazine **11a** and, after *in situ* treatment with TBAF, led to the corresponding [3.3.3]- and [3.3.4]-oxapropellane furoindolines **16a** and **16b** in good yields and enantioselectivities. For amide-containing ketones, an elevated reaction temperature was required upon completion of the indolization to accelerate the ring closure by nucleophilic attack of the amide N-atom. Following this reaction sequence indoline **17a** was obtained in moderate yield and with good enantioselectivity. Finally, incorporation of an electronrich *N*-methylindole moiety into the side chain gave the polycyclic indolines (**18a**–**18d**) bearing two vicinal quaternary

stereocenters in good yields and enantioselectivities. To the best of our knowledge, interrupted Fischer indolization featuring a carbon-based nucleophile was unprecedented.

Molecules exhibiting helical chirality have recently attracted enormous attention, in fields as diverse as catalysis, materials science, molecular self-assembly and biology. Our interest in the field was stimulated by our recent progress in the above-mentioned development of a catalytic asymmetric variant of the Fischer indole synthesis. We hoped that in accordance with the established mechanism of the Fischer indolization, a chiral Brønsted acid might promote an enantioselective [3,3]-sigmatropic rearrangement upon condensation of a phenyl hydrazine **19** with an appropriate polyaromatic ketone **20** and furnish enantio-enriched azahelicenes of type **22**.

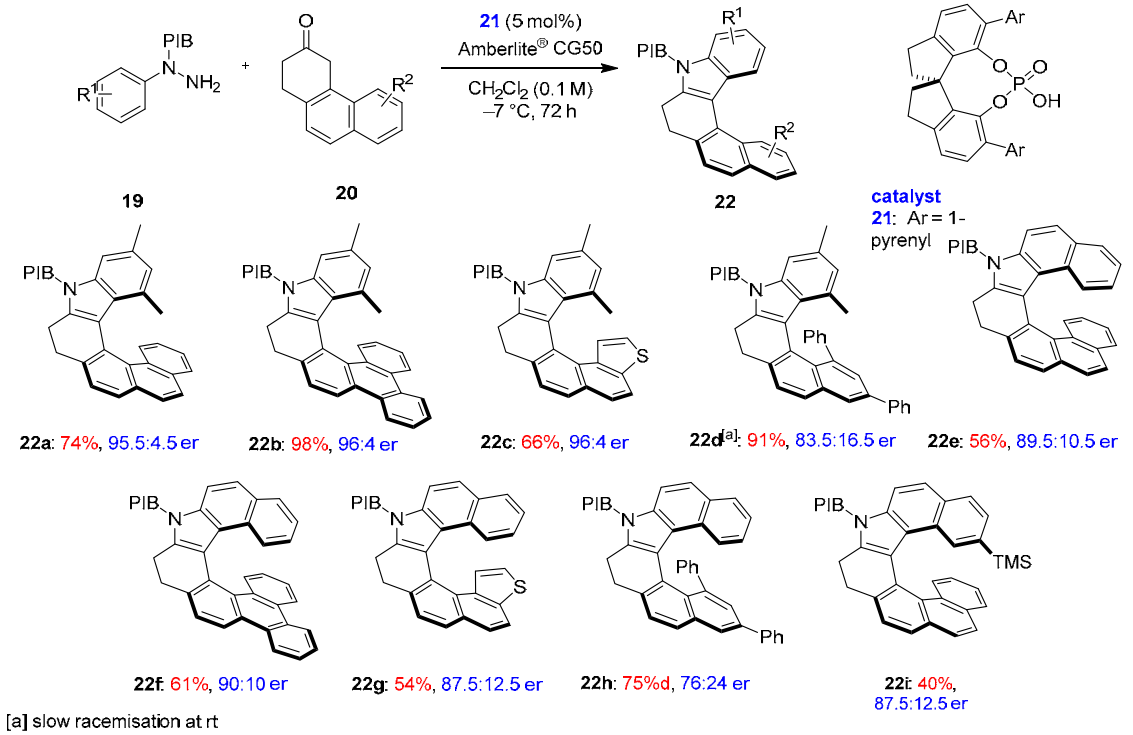

Scheme 4. Synthesis of enantio-enriched azahelicenes *via* asymmetric Fischer indolization.

By evaluating various chiral phosphoric acids as catalysts, it was found that the increase of the π-surface of the 3,3'-substituents led to higher enantioselectivity. Optimizing the reaction conditions, it was found that catalyst **21** in CH_2Cl_2 at –7 °C gave the highest enantioselectivity in our reaction. We started to study the substrate scope under the optimized conditions, combining different hydrazines and ketones. Hydrazine **19a** reacted smoothly with different polycyclic ketones, giving the corresponding [6]-azahelicenes **22a–c** in good yields and enantioselectivities. When hydrazine **19b** was reacted with the same ketones lower enantioselectivities were obtained for compounds **22e–h**. Most synthesized compounds were sensitive to oxidation after prolonged storage under

air. Since fully oxidized helicenes show interesting properties, compound **22a** was oxidized to the corresponding azahelicene **23a**. After some reaction screening we could get helicene **23a** in the presence of tetrachlorobenzoquinone (chloranil) and diphenylphosphate (DPP) in $CHCl_3$ at 50 °C in good yields.

In light of the mechanistic similarities between Fischer indole synthesis and benzidine rearrangement, we envisioned that a catalytic enantioselective benzidine rearrangement of N,N'-dinaphthylhydrazines could potentially be a powerful and general approach towards BINAM derivatives catalyzed by a chiral phosphoric acid *via* [3,3]-diaza Cope rearrangement. We started our studies by reacting hydrazine **24a** with different chiral Brønsted acid catalysts. Spirocyclic phosphoric acid catalysts, which provided excellent results in all three previous projects, gave inferior results in terms of both yield and er. Evaluation of binaphthyl-based phosphoric acids gave only moderate results except for catalyst **25**, which gave product **26a** in promising yield and enantioselectivity. Screening of standard reaction parameters showed that product **26a** could be obtained in good yield and with high level of enantioselectivity at 0.025 M and –50 °C.

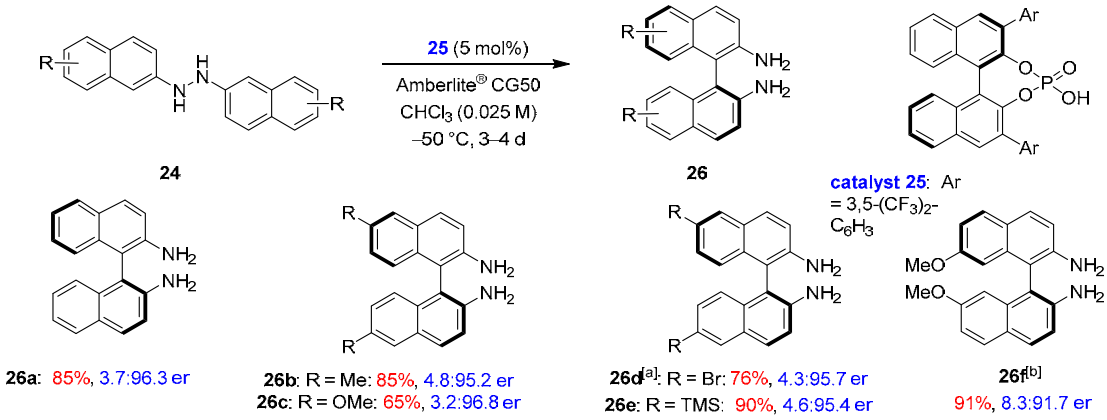

[a] Reaction was run at –30 °C with 10 mol% catalyst loading. [b] Reaction was run at –45 °C with 10 mol% catalyst loading.

Scheme 5. Catalytic asymmetric benzidine rearrangement.

The scope of the reaction was explored under the optimized conditions. The reaction showed good generality towards different hydrazines allowing the synthesis of various BINAM derivatives with electronically diverse substituents at different ring positions. Hydrazines with substituents at the 6- or 7-position gave the corresponding BINAM derivatives (**26a**–**26f**) irrespective of their electronic nature with good yields and with high level of enantioselectivity.

Publications resulting from this research area: 9, 31, 32

External funding: European Research Council Advanced Grant (HIPOCAT), Deutsche Forschungsgemeinschaft (S. Müller), Alexander von Humboldt Foundation (C. K. De)

Cooperations: none

2.2.7 Research Area "Oxidative Coupling Reactions – Methods and Mechanisms" (M. Klußmann)

Involved: E. Böß, P. Karier, K. M. Jones, T. Hillringhaus, C. Schmitz, J. Demaerel, B. Schweitzer-Chaput, N. Gulzar, N. Uemiya

Objective: The transformation of two C–H bonds into a new C–C bond can be achieved by oxidative coupling, e.g. by using a catalyst together with a terminal oxidant.[38] We aim to develop sustainable oxidative coupling reactions, using simple and cheap catalysts and low molecular weight oxidants. Additionally, we investigate the mechanisms of these reactions to gain inspirations for the development of new and improved methods:

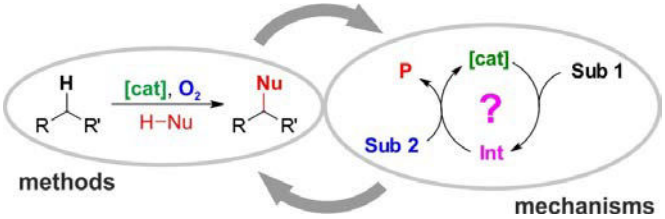

Scheme 1. Research interests of the Klußmann group.

Results: One area which has enjoyed rapid growth is the coupling α to nitrogen in tertiary amines, the most successful and widely studied being *N*-aryl tetrahydroisoquinolines (THIQ) **1**.[42] The mechanism of these reactions including the nature of intermediates and the role of catalyst and oxygen, however, remained essentially unknown.

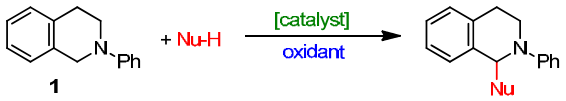

Scheme 2. Oxidative coupling reactions with *N*-phenyltetrahydroisoquinoline.

We have provided the first dedicated mechanistic studies in this field for two copper-catalyzed methods.[40,45] The first, using $CuCl_2$*$2H_2O$ as catalyst and oxygen as oxidant, was developed in our own group and still represents one of the simplest and most sustainable methods for this type of reaction which additionally has the broadest reported nucleophile scope. We could observe an iminium cuprate salt **2** as key intermediate, which is formed by oxidation of **1** with Cu(II).[40] In the presence of water

or methanol (a preferred solvent), this species is in equilibrium with a hemiaminal **3** or a hemiaminal ether **4** which provide a reservoir for the reactive iminium ion **2**. Addition of nucleophiles to the iminium provides the desired, thermodynamically preferred, coupling products **5**. Reoxidation of Cu(I) to Cu(II) by oxygen regenerates the catalyst.

The second method, using CuBr as catalyst and *tert*-butylhydroperoxide as oxidant, was reported by the group of C.-J. Li and has been most influential by inspiring many other research groups worldwide. We could establish a mechanism based on our studies which clarified the role of catalyst, oxidant and key intermediate **6**, a peroxide formed through a radical pathway initiated by CuBr and *tert*-butylhydroperoxide.[45]

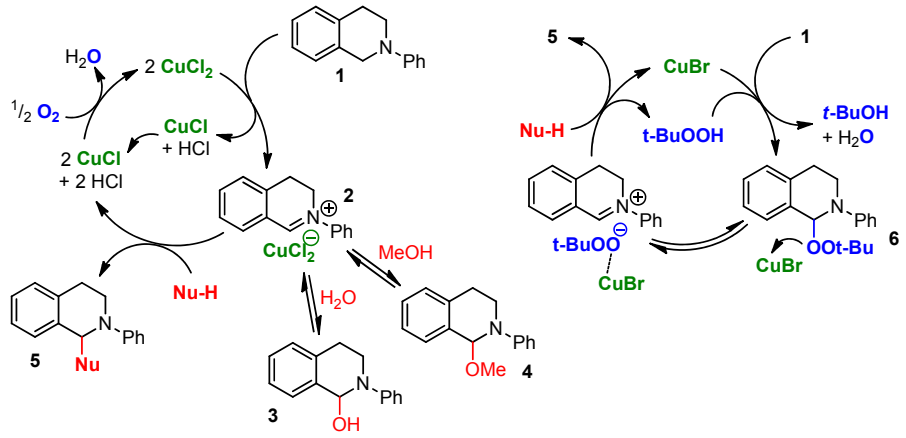

Scheme 3. Proposed reaction mechanisms of Cu-catalyzed oxidative coupling reactions with *N*-phenyltetrahydroisoquinolines.

The discovery that peroxide **6** converts to the reactive iminium ion intermediate by Lewis acid catalysis inspired us to develop an oxidative coupling of *N*-carbamate-protected THIQ's by Brønsted acid catalysis.[46] These compounds can be conveniently deprotected in contrast to *N*-aryl-THIQ's.

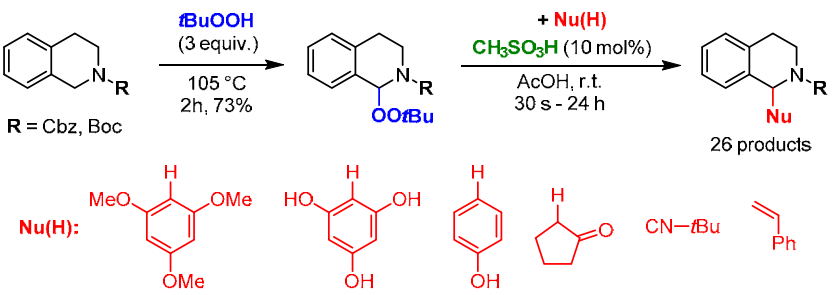

Scheme 4. Oxidative coupling with *N*-carbamoyltetrahydroisoquinolines *via* intermediate peroxides.

Recently, we had discovered a surprising oxidative coupling that proceeds without any redox-active catalyst. For example, xanthene is coupled with ketones by simply stirring the substrates under oxygen at ambient temperature and pressure in the presence of catalytic amounts of a strong Brønsted acid like methanesulfonic acid. The reaction is mostly limited to xanthene and ketones, but at high partial pressure of oxygen, the scope can be extended.[44]

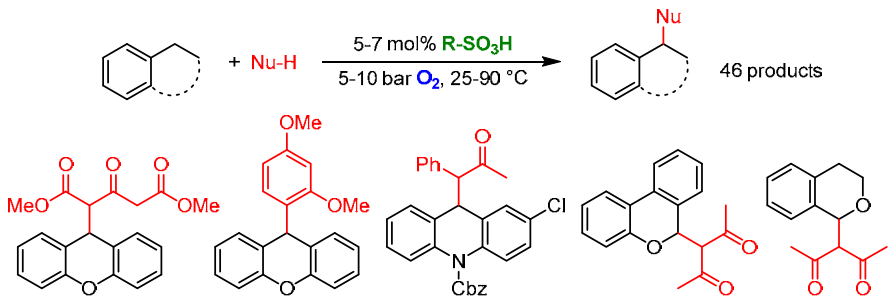

Scheme 5. Autoxidative coupling at elevated partial pressure of oxygen.

A mechanistic study of this reaction, with the coupling of xanthene **7** with cyclopentanone as model reaction, revealed the autoxidation of xanthene to hydroperoxide **8** as the key step.[49] In the presence of a strong Brønsted acid, the hydroperoxide group is substituted by the ketone nucleophile, probably *via* xanthylium ion **9**. Interestingly, the reaction proceeds faster than the rate limiting autoxidation. The waste product hydrogen peroxide accelerates the reaction by a synergistic action of Brønsted acid and ketones that generates radicals (path **A**, mechanism not yet fully understood).

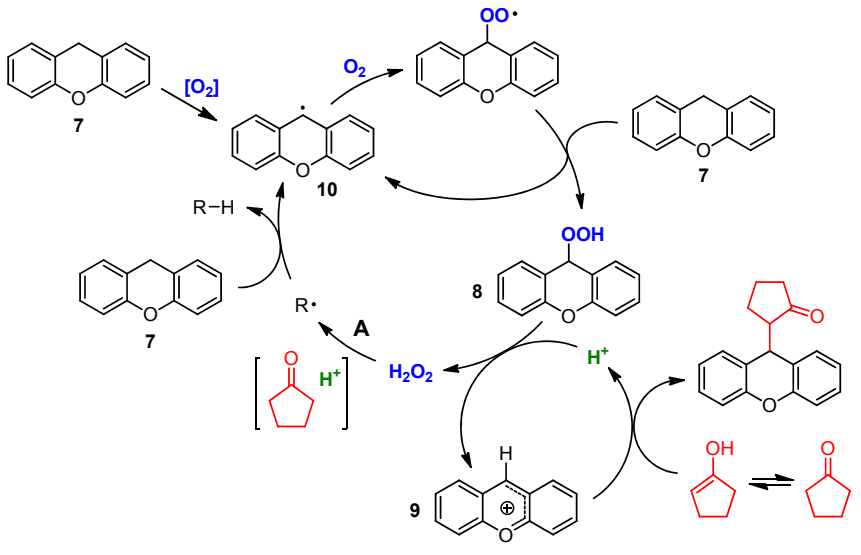

Scheme 6. Proposed mechanism of the autoxidative coupling of xanthene with cyclopentanone.

We assume that under these conditions, perketals or related structures are formed that decompose into radicals, which in turn abstract a hydrogen atom from xanthene. The resulting xanthenyl radicals **10** are quickly trapped by oxygen, thereby accelerating the autoxidation to form more of the key intermediate **8**.

This discovery has inspired several still ongoing research projects. For example, we have developed a programme of C–H functionalization *via* Intermediate PeroxideS, termed CHIPS, which will provide means to derive valuable products from C–H bonds in a sustainable manner, only requiring catalysis and oxygen as the only stoichiometric reagent. As a proof-of-principle, we have developed a photochemical and Brønsted acid catalyzed two-step method to functionalize tetrahydrocarbazole derivatives *via* hydroperoxides **11**, which enables the synthesis of potent antiviral compounds like **12**- and **13**.[48]

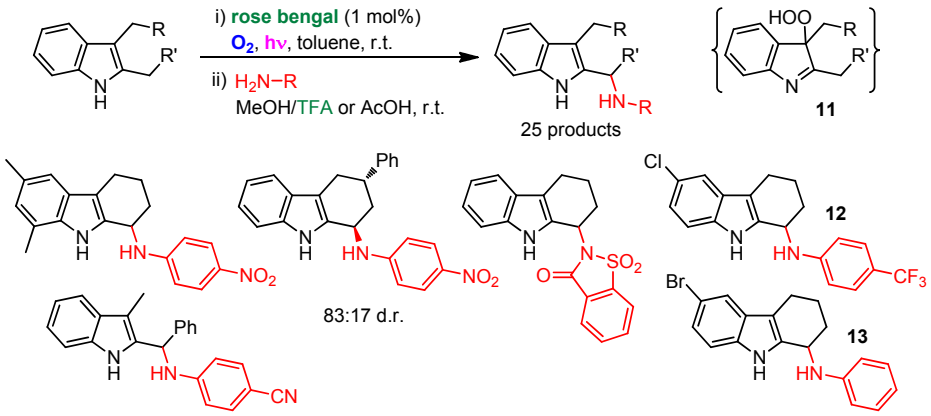

Scheme 7. C–H amination of indole-derivatives *via* intermediate hydroperoxides.

In a related project, we have used hydroperoxides derived from the reaction of phenols with singlet oxygen to synthesize spirolactones.[47] And by applying the discovery of the synergistic effect of hydro(gen)-peroxide, ketones and Brønsted acid catalysis, we have developed novel ways of performing oxidative coupling reactions without involvement of redox-active catalysts.[49]

These studies are expected to have broader implications for the understanding of radical and autoxidation chemistry.

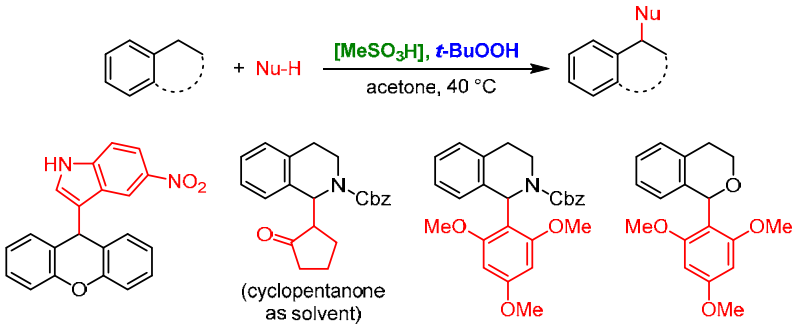

Scheme 8. Oxidative coupling reactions by the synergistic action of a Brønsted acid catalyst, hydroperoxide and ketone solvents.

Future directions

Our group will continue with a combination of mechanistic studies and method development, with the goal of developing novel sustainable methods for the C–H functionalization of various organic compounds and gaining an improved understanding of the underlying reaction mechanisms. In particular, we will focus on the principle of CHIPS (C–H functionalization *via* Intermediate PeroxideS) and on the newly gained mechanistic insight into the synergistic action of acid, hydroperoxide and ketone solvents.

Using the principle of CHIPS, we want to develop one-pot methods to functionalize C–H bonds by visible light and simple acid catalysts, for C–H bonds in allylic or heterocyclic compounds (along the lines of Scheme 7).

The mechanistic insight from the autoxidative coupling reaction (Scheme 6) has already allowed us to develop oxidative coupling reactions without the use of redox-active catalysts (Scheme 8). We have found indications that the intermediate radicals ("R·" in Scheme 6) are ketone-derived, this knowledge will be used to develop novel radical reactions to functionalize ketones. We have already achieved a hydrofunctionalization and a 1,2-difunctionalization of olefins with ketones, depending on reaction conditions. The reactions are reminiscent of the so-called SOMO-catalysis. Further studies towards the extension of these methods as well as an elucidation of their mechanisms are expected to be a major focus of our group's future research activities.

Publications resulting from this research area: 38-49

External funding: Deutsche Forschungsgemeinschaft (Sachbeihilfe, Heisenberg Scholarship), Alexander von Humboldt Foundation (scholarship to K. M. Jones), Japan Society for the Promotion of Science (scholarship to N. Uemiya), Fonds der Chemischen Industrie

Cooperation: Zeev Gross (Technion, Haifa, Israel)

2.2.8 Research Area "Electrophilic Domino Rearrangements of Keteniminium Derivatives" (N. Maulide)

Involved: L. Carvalho, I. Jurberg, C. Madelaine, D. O'Donovan, B. Peng, D. Petkova, V. Valerio, M. Winzen

Objective: The selective activation of amides with suitable electrophilic reagents allows access to novel reactivity manifolds and opens up intriguing perspectives in synthesis. We have previously reported on the discovery of new pericyclic domino transformations of keteniminium salts generated *via* electrophilic activation of amides. Herein we report progress made since the original observations of 2009 and 2010.

Results: This area of research is predicated on our original observation that electrophilic activation of the γ-alkoxyamide **1** under the typical conditions for generation of an intermediate keteniminium salt (triflic anhydride and a base) did not lead to the anticipated [2+2] cycloadduct. Instead, we were surprised to observe the <u>*exclusive*</u> formation of α-allyl butyrolactone **2** (Scheme 1).

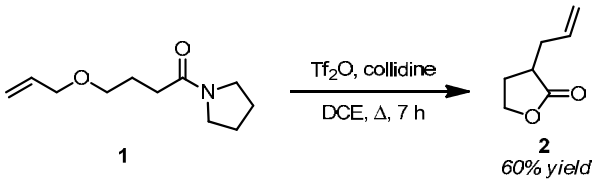

Scheme 1

Mechanistically (Scheme 2), we believe that after initial activation of the amide carbonyl by the electrophilic reagent, elimination to form keteniminium **3** probably takes place. The enhanced electrophilicity of this intermediate then triggers an unusual nucleophilic addition step. This generates a vinyl-allyl-oxonium **4** poised to undergo a [3,3]-sigmatropic rearrangement. Such a reorganization should lead to the stabilized carbenium ion **5**, hydrolysis of which then accounts for the formation of lactone **2**.

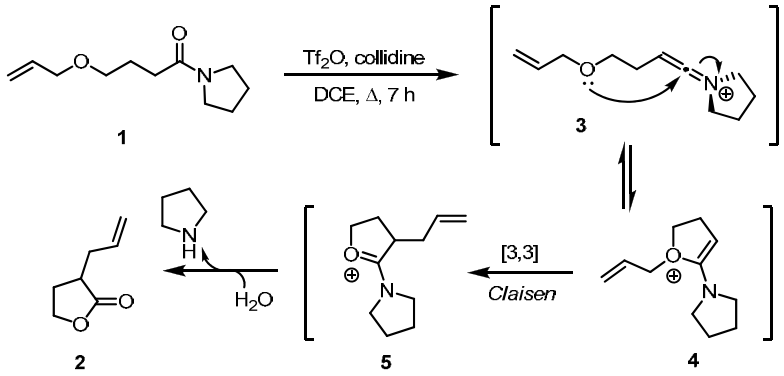

Scheme 2

In this reporting period, a "benzyl Claisen" rearrangement – a transformation that has been scarcely investigated prior to our work – was developed starting from readily available benzyl ether starting materials **6**. As depicted, ω-benzyloxyamides smoothly rearranged to α-arylated lactone products **7** in moderate to excellent yields (Scheme 3). Particularly interesting was the beneficial effect of an ester appendage at the benzylic position, leading to much improved yields of the products **7c-e**. This "metal-free" arylation process would later inspire us to explore related sulphur-based rearrangement sequences (cf. Section 2.2.10 – Sulfur area).

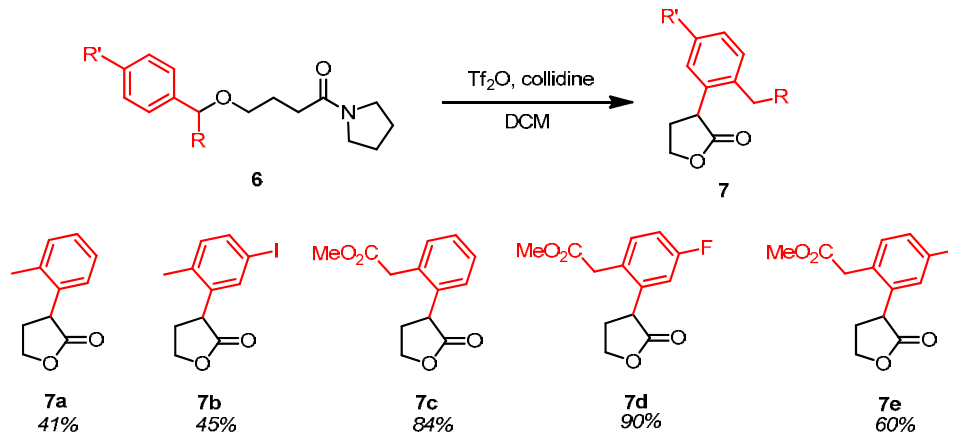

Scheme 3

In addition, we were also able to study an intriguing THF- and THP-migration from simple protected alcohols **8** into complex lactone products **9**. In this reaction (Scheme 4), an otherwise innocuous and benign protecting group actually functions as a reactive handle for a pivotal C–C bond forming transformation.

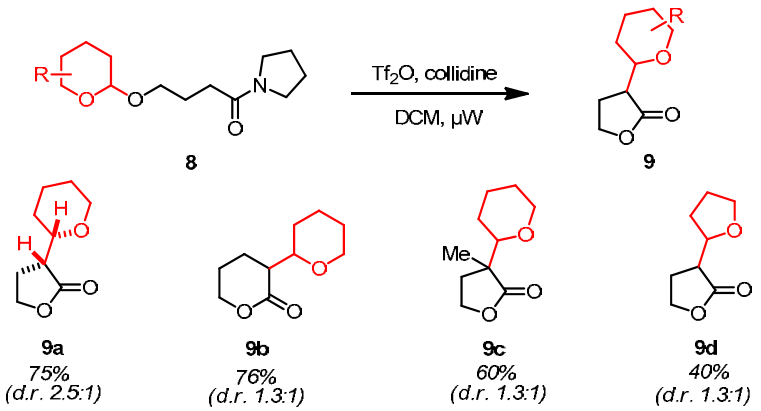

Scheme 4

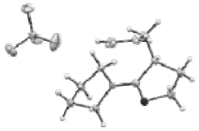

5.BF$_4$

Scheme 5

Further investigations on the original transformation revealed that, if the hydrolysis step is avoided, isolation of iminium ether **5** (as the BF_4 salt) is possible and its structure was unambiguously elucidated by single-crystal X-ray analysis (Scheme 5). This suggested opportunities for further functionalization.

We were guided by the recognition of **5**'s *a priori* ambident electrophilicity at either C_1 or C_4, the former being what had been realized through hydrolysis (formal addition of water at C_1, path a, Scheme 6). The range of products **10**/**11** available by realization of this concept has significantly expanded the utility of the original reaction.

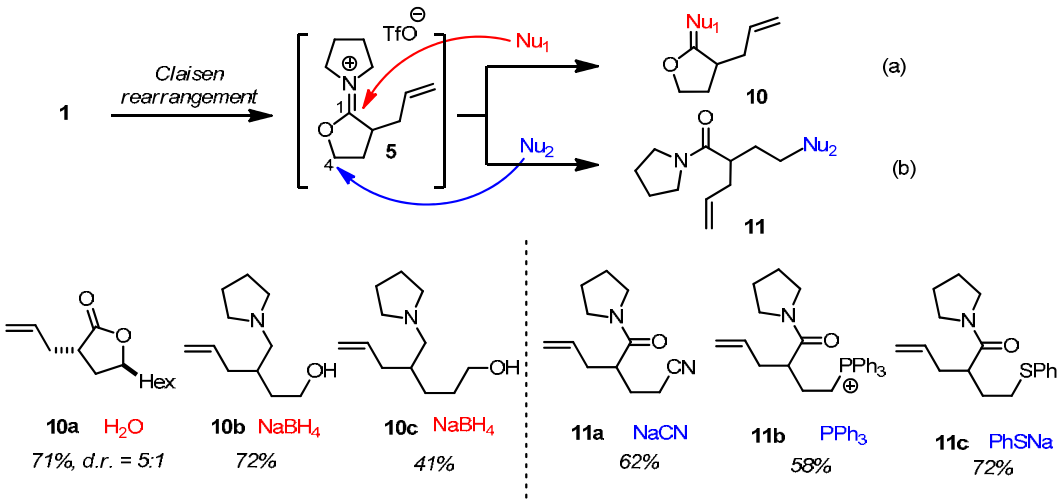

Scheme 6

We also acknowledged the intrinsic C–H acidity of intermediate **5** and speculated that it might lend itself to deprotonation and electrophilic capture (Scheme 7). The product of such a reaction would be the new iminium ether **13**, allowing us to achieve consecutive electrophilic/nucleophilic tandem functionalization sequences. The final products thus obtained are highly decorated derivatives showcasing the ability to achieve multiple (up to three), different C–C bond forming events in a one-pot manner through this process.

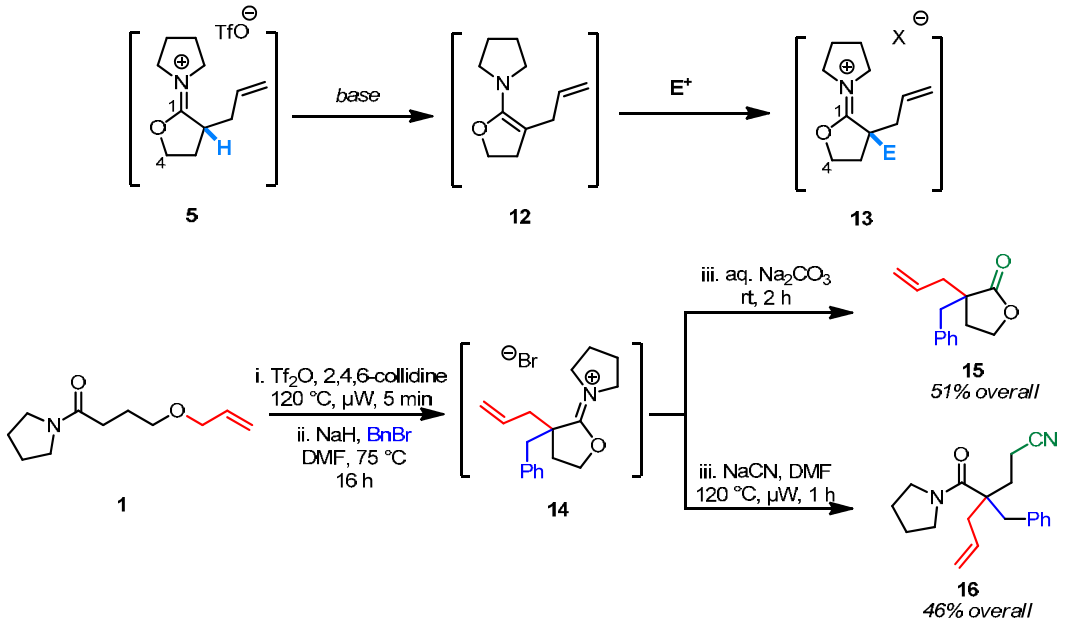

Scheme 7

Finally, we recently developed a novel methodology for direct lactonization of ethers and alcohols onto amides, hinging on our realization that the activation of amide **1** in the absence of a base smoothly led to unsubstituted lactone **17** as the single reaction product after hydrolysis (Scheme 8).

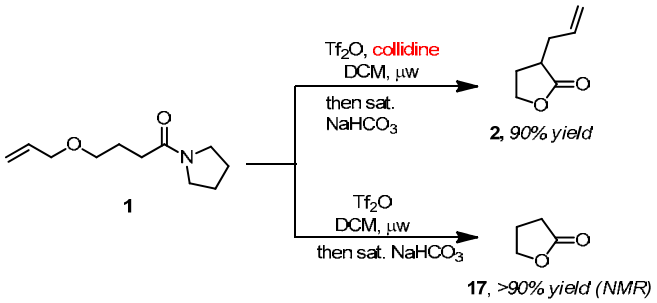

Scheme 8

Through this procedure, within 1 hour at room temperature rings as large as 14 members can be smoothly formed. Mechanistic studies support a pathway consisting of amide activation and intramolecular nucleophilic attack in the case of ether substrates. This direct lactonization allows the synthesis of lactones **18** from fully protected precursors without the need for individual deprotection steps, an advantage that could prove useful in the context of multistep target-oriented synthesis (Scheme 9).

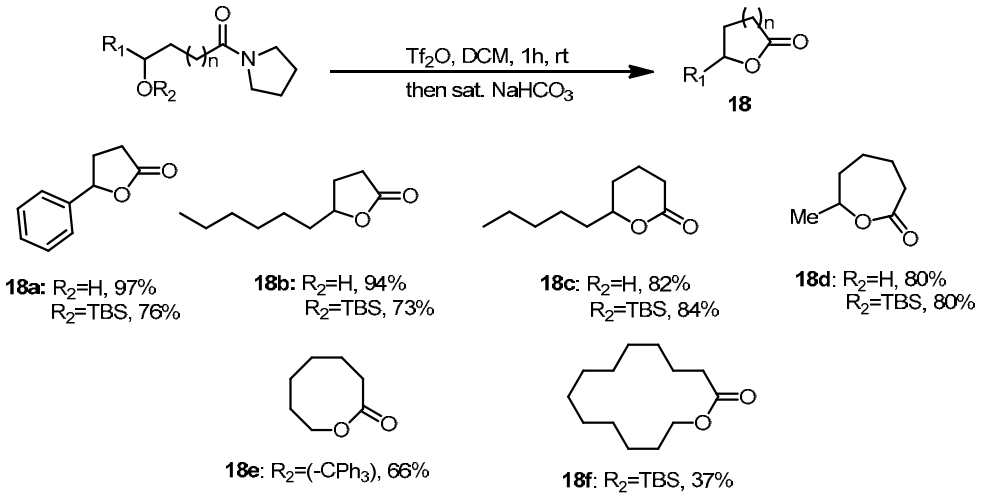

Scheme 9

Continuously guided by intuition and serendipitous discovery, the developments described herein form a coherent approach to the synthesis of lactones in general. Future work will focus on broadening the scope of these methodologies and installing asymmetric variants that enable the preparation of optically enriched products in a traceless manner.[64]

Publications resulting from this research area: 50, 51, 55, 62, 64

External funding: Deutsche Forschungsgemeinschaft, Alexander von Humboldt Foundation (stipend to C. Madelaine), Ecole Polytechnique (stipend to I. D. Jurberg), FCT (stipend to L. Carvalho), FCI

Cooperations: L. Veiros (Lisbon, PT), M. M. B. Marques (Lisbon, PT)

2.2.9 Research Area "Catalytic Stereoselective Synthesis and Chemistry of Cyclobutenes" (N. Maulide)

Involved: L. G. Alves, D. Audisio, H. Faustino, F. Frébault, M. Luparia, A. Misale, S. Niyomchon, M. T. Oliveira, M. Padmanaban, C. Souris, E. Wöstefeld, L. Xie

Objective: The preparation of small rings has been a pervasive topic in organic synthesis ever since chemists realized the potentialities and fascinating properties associated with their inherent ring strain. Nevertheless, there is a serious lack of general methodologies for the preparation of optically active functionalized cyclobutane and cyclobutene derivatives. This project aims at the development of a catalytic asymmetric synthesis of cyclobutene building blocks starting from 2-pyrone and the study of their chemistry.

Results: 2-Pyrone **1** is known to undergo photomediated isomerization to the unstable oxabicyclo[2.2.0]hexane **2** (Scheme 1). Historically, this reaction has been the subject of considerable scrutiny, since to date it still constitutes the surest path to the synthesis of the elusive anti-aromatic compound cyclobutadiene (*via* decarboxylation of **2**).

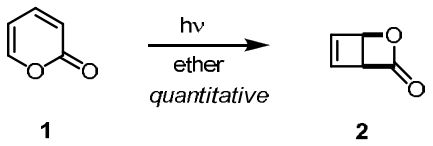

Scheme 1

This project has its origins on our realization that compound **2** is, structurally, an allylic ester susceptible of ionization by a suitable zero-valent, electron-rich transition metal. We have previously achieved catalytic stereoselective transformations of **2** employing several nucleophiles, enabling a synthesis of functionalized cyclobutenes in only two operations from 2-pyrone (Scheme 2).

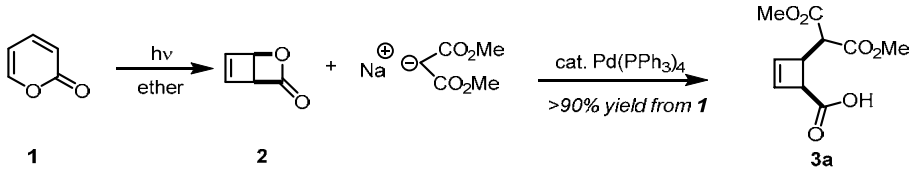

Scheme 2

The translation of this chemistry to a catalytic asymmetric version offered opportunities to establish a deracemization process. Indeed, the putative allyl-metal complex **4** formed on interaction of lactone **2** with the palladium catalyst has a plane of symmetry that

effectively erases the stereochemical information contained in the (chiral) racemic starting material. By employing optically pure ligands, one could then envisage the re-inscription of chiral information upon nucleophilic attack and, thus, the obtention of >50% yields of optically enriched cyclobutene products **5** (Scheme 3).

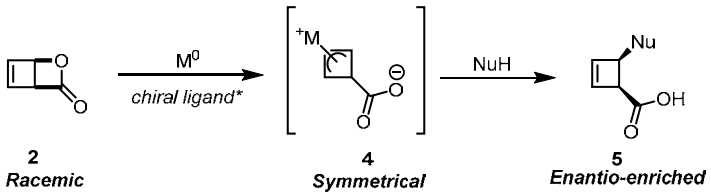

Scheme 3

The reduction of this plan to practice involved the comprehensive screening of a large library of chiral ligands and led to the serendipitous discovery of an unusual ligand-dependent stereochemical outcome. As shown in Scheme 4, phosphoramidites **L1** were highly effective in converting racemic lactone **2** into the *cis*-configured cyclobutene products **6**. The attainment of yields consistently above 50% with very high enantioselectivities confirmed the operation of a dynamic deracemization.

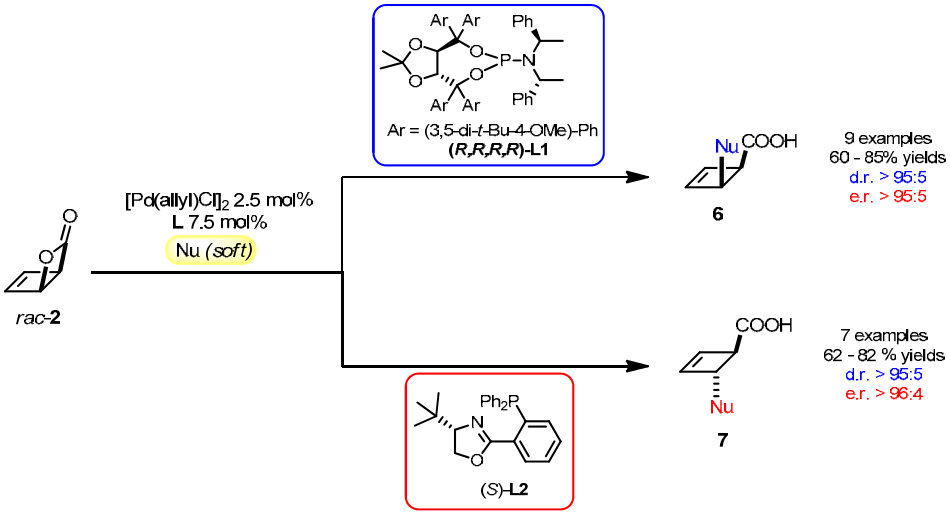

Scheme 4

To our surprise (Scheme 4), the ligand family typified by ligand **L2** proved to be selective for the opposite diastereoisomer, and produced the *trans*-disubstituted cyclobutenes in equally high yields and exquisite selectivities.

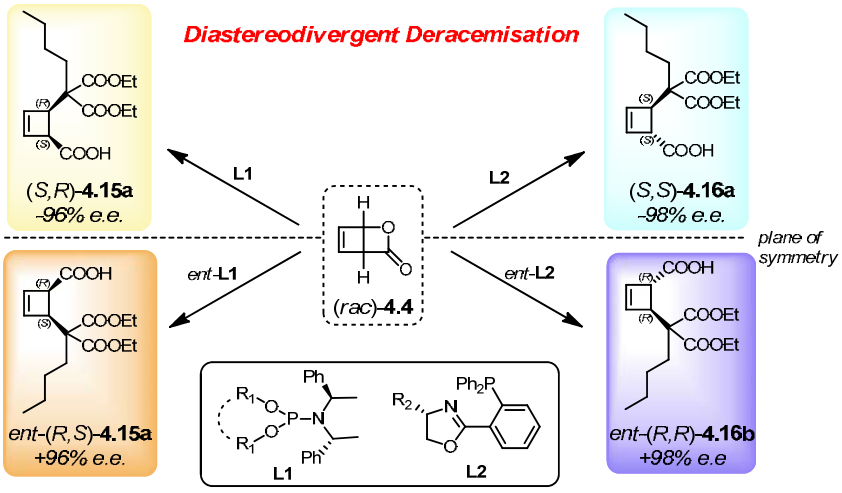

This novel phenomenon was termed "*Diastereodivergent Deracemization*".

Scheme 5

Through this process, we have been able to convert a racemic substance bearing a number n ($n \geq 2$) of stereogenic centers into each and every one out of the 2^n stereoisomers of the product, at will and by simple modification of the chiral ligand employed, an unprecedented observation in allylic alkylation chemistry (Scheme 5).

Subsequently, we have extended this concept to the Deracemization of epimers, or De-epimerization. The "*Diastereodivergent De-epimerization*" portrayed in Scheme 6 is a novel type of transformation allowing the synthesis of diverse stereoisomers of the product regardless of the stereochemical information contained in the starting materials – a rare metal-catalysed asymmetric transformation that permits the use of diastereomeric mixtures of racemic compounds as substrates.

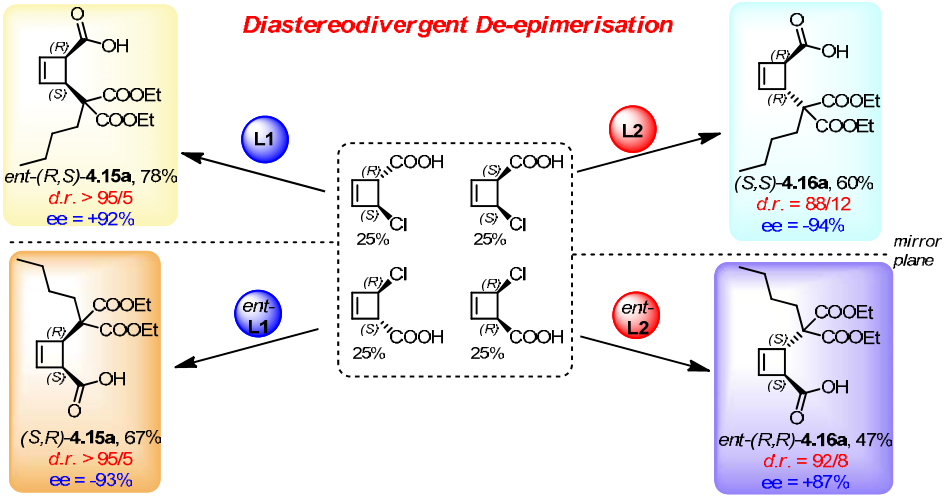

Scheme 6

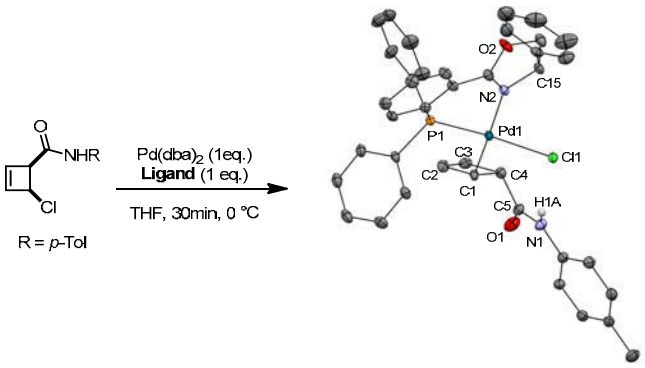

Scheme 7

More recently, we have uncovered several interesting structural features of this system. In this context, rare examples of cyclic σ-allyl palladium complexes were encountered and the first structural (X-ray) and reactivity studies of such species were reported (Scheme 7).

Asymmetric allylations of these and other cyclobutene electrophiles have also been realized.

In addition, we have exploited the potential of stereochemically defined cyclobutenes as starting materials for the synthesis of geometrically pure diene subunits. This has enabled us to prepare aryloxy- and azido-substituted dienes, interesting building blocks for synthetic and biological applications (Scheme 8).

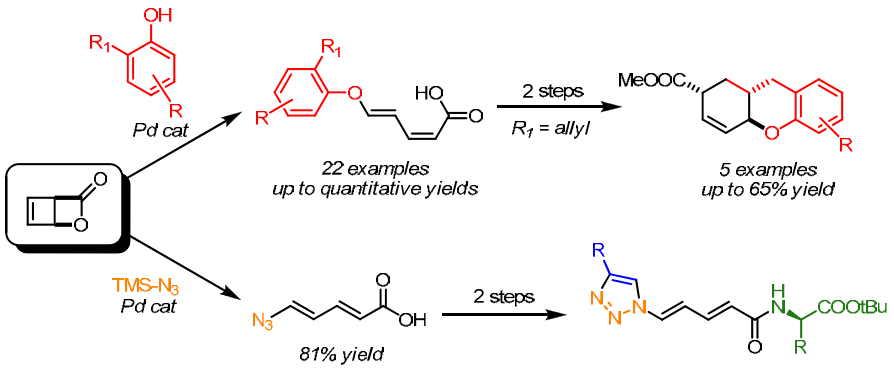

Scheme 8

The use of halogenated cyclobutenes as starting materials enables the synthesis of versatile scaffolds for cross-coupling chemistry. This leads to applications in total synthesis of polyenic natural products, as exemplified with Inthomycin C (Scheme 9).

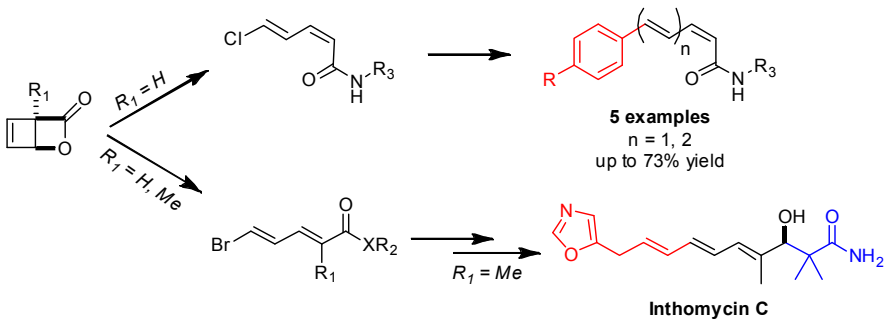

Scheme 9

In summary, we have developed a novel catalytic asymmetric synthesis of cyclobutenes, leading to serendipitous discoveries of relevance to the field of asymmetric catalysis. We have thus developed a rare *Diastereodivergent Deracemization* and the first example of a *Diastereodivergent De-epimerization*. Mechanistic studies have revealed unprecedented structural features and additional research in this direction is in progress. Furthermore, the potential of cyclobutenes as starting materials for the preparation of dienes has just barely been tapped as we are currently pursuing further modular and concise applications in total synthesis.

Publications resulting from this research area: 52, 53, 57, 58, 65-71

External funding: ERC Starting Grant, Deutsche Forschungsgemeinschaft, SusChemSys, Alexander von Humboldt Foundation (stipend to M. Luparia), FCT (stipends to M. T. Oliveira, L. G. Alves, H. Faustino)

Cooperations: W. Thiel (Mülheim, D), C. Farès (Mülheim, D), R. Goddard (Mülheim, D), A. M. Martins (Lisbon, PT), K. N. Houk (UCLA, USA), José Luis Mascareñas (Compostela, ESP)

2.2.10 Research Area "New Perspectives in Sulfur(IV) Chemistry" (N. Maulide)

Involved: L. Gomes, X. Huang, S. Klimczyk, F. Kulewei, M. Luparia, B. Peng, J. Sabbatani

Objective: The aim of this project is the development of novel C–C bond forming transformations exploiting the unique properties of sulfur(IV) intermediates.

Results: Inspired by the Benzyl-Claisen transform developed in the Electrophilic Amide Activation project, we speculated that a carbonyl compound with a favorable enol content (such as β-ketoester **1a**) might be amenable to form a sulfonium-substituted intermediate **2** upon interaction with a suitable sulphur(IV) electrophile (depicted as **S(IV)** in Scheme 1). The vinylallyl ether moiety of **2** should then eventually rearrange into the α-arylated product **4** *via* the dearomatized intermediate **3**.

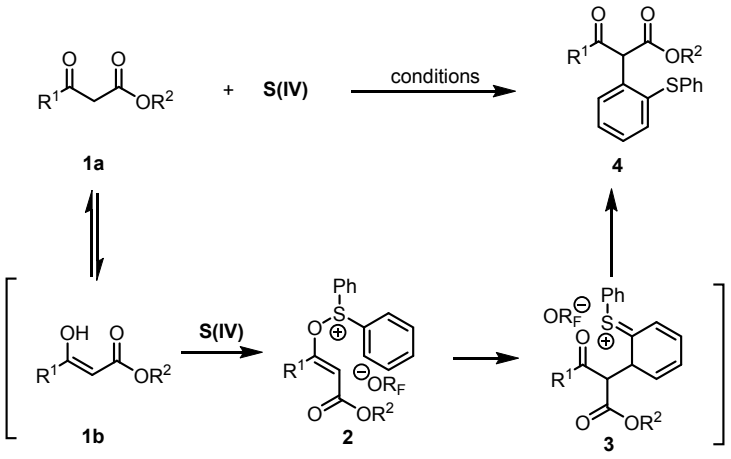

Scheme 1

This simple yet conceptually appealing hypothesis led us to select Martin's sulfurane **5** as a commercially available, suitable diphenylated sulphur(IV) electrophile and to perform the reaction depicted below. As shown in Scheme 2, admixing the β-ketoester **1a** with Martin's sulfurane **5** led to a single product in essentially quantitative yield – the sulfur ylide **6a**.

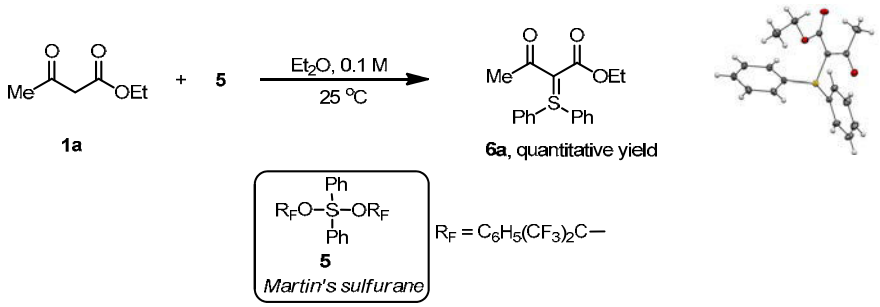

Scheme 2

This fortuitous observation paved the way for the development of a process we termed "ylide transfer", as already communicated in the previous progress report.

Several lateral observations made during this study prompted us to explore the ylide transfer reaction further. For one, the use of a substituted (cyclic) ketoester under various conditions resulted in the formation of multiple products with rapid consumption of sulfurane **5**. In addition, the relatively high cost of this sulfurane stimulated a search for surrogates.

Treatment of a mixture of ethyl acetoacetate **1a** and diphenyl sulfoxide **7a** with 2.0 equivalents of triflic anhydride led to the corresponding sulfonium ylide **6a** in moderate 51% isolated yield along with several additional, highly polar compounds (Scheme 3a). However, and to our surprise, when ethyl 2-oxocyclohexanecarboxylate **1b** was exposed to similar conditions, the α-arylated ketoester **8a** was isolated in 66% yield, and its structure was unambiguously confirmed by single-crystal X-ray analysis (Scheme 3b).

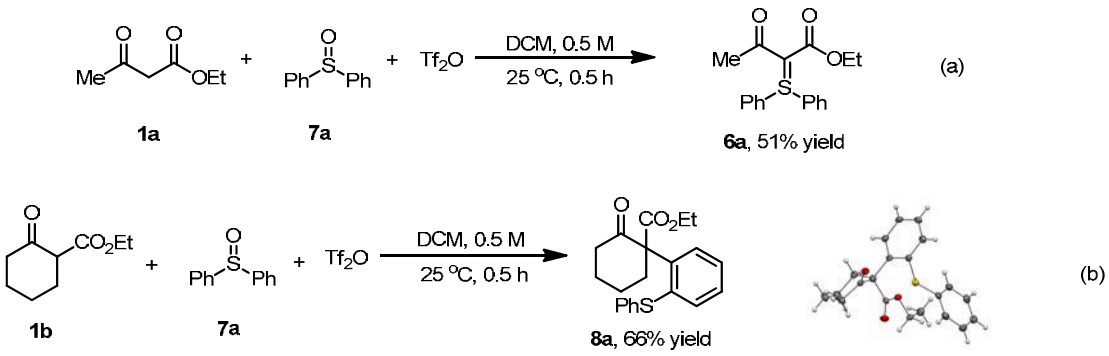

Scheme 3

In addition to six-membered cyclic β-ketoesters, various other active methylene compounds can be employed in this highly regio- and diastereoselective transformation (Scheme 4).

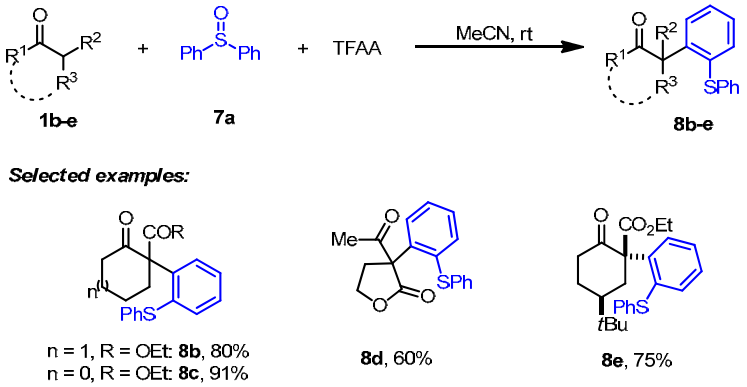

Scheme 4

Aryl alkylsulfoxides could also be employed as donors. The use of phenyl methyl sulfoxide **7b** led to arylated product **9a** as the major adduct of the reaction, together with traces of the "normal" Pummerer product **10a** detected in the reaction mixture (Scheme 5a).

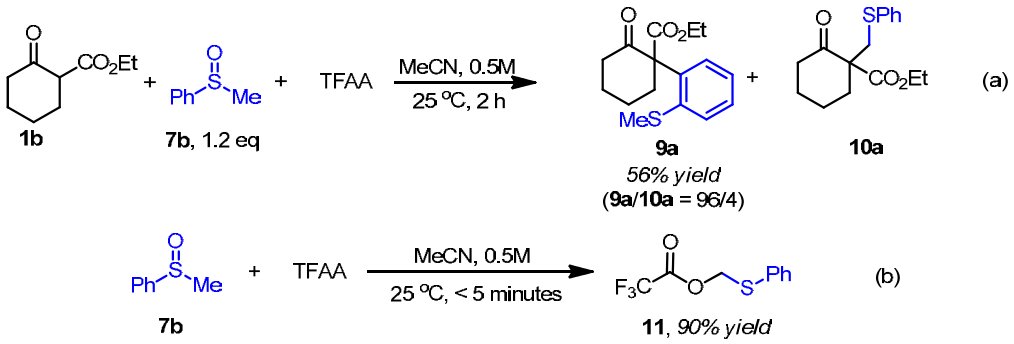

Scheme 5

This result is all the more noteworthy taking into account that exposure of sulfoxide **7b** to the action of TFAA *in the absence of nucleophile* almost instantaneously generates the trifluoroacetate **11** in very high yield (Scheme 5a). Clearly, the mechanism of these arylations is fundamentally different from the classical Pummerer reaction.

We recently discovered that the stable, easily handled ylide products prepared by our ylide transfer methodology can be activated in the presence of gold catalysts (Scheme

6). In particular, it is possible to perform a formal [3+2] cycloaddition of an ylide **6a** with alkynes such as phenylacetylene **12a**, leading to a trisubstituted furan **13a**.

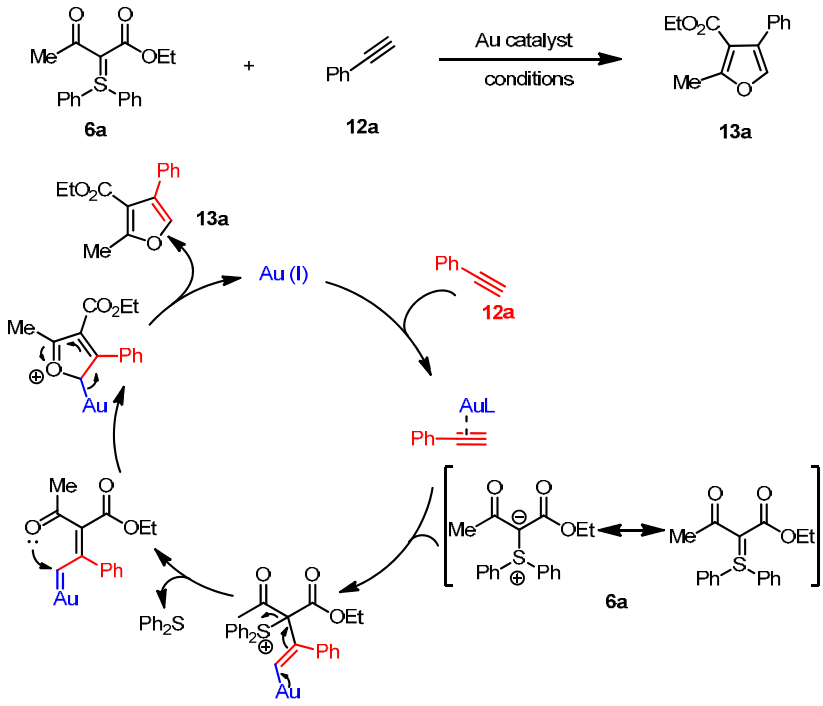

Scheme 6

We further realized that changing the ester moiety of the ylide partner to an allyloxycarbonyl group (as in **6**) induced a subsequent, consecutive rearrangement of the allyl residue, generating a furanone **14** bearing a quaternary center (Scheme 7). As shown, this reaction leads to 3 distinct bond-forming events (highlighted in bold typeset) and holds promise as a general method for preparation of such scaffolds.

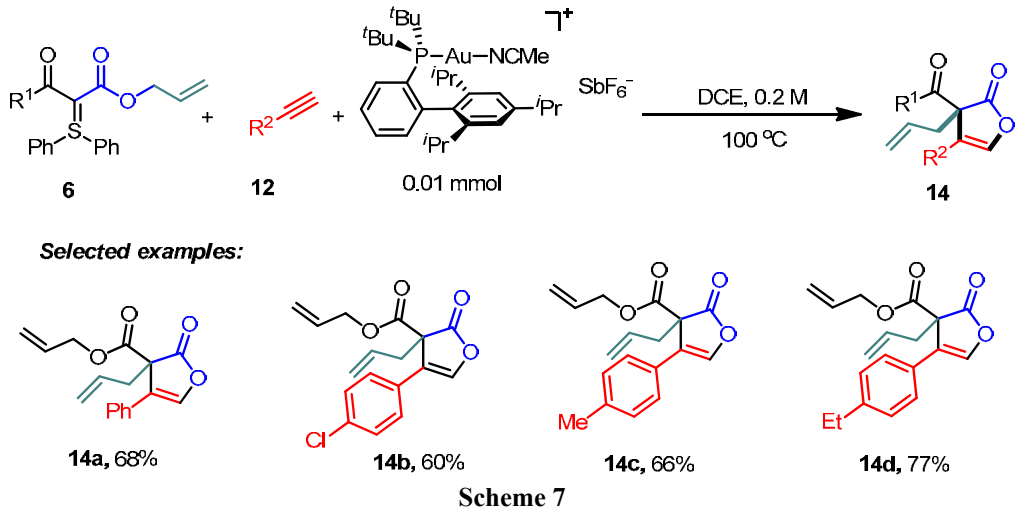

Scheme 7

During these studies, we made another serendipitous observation. As portrayed in Scheme 8, the use of less reactive aliphatic alkynes in the abovementioned furanone synthesis leads to a low yield of the product **14e** as well as an unforeseen by-product: the cyclopropane **15a**!

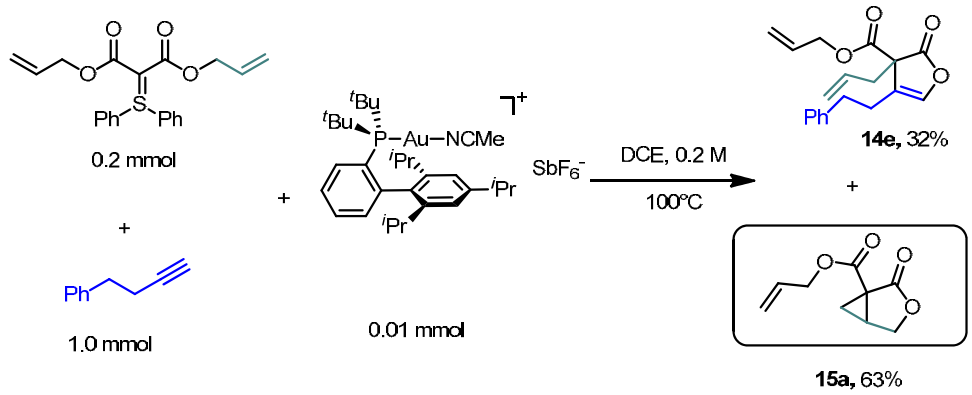

Scheme 8

Omitting the alkyne from the equation above led exclusively to cyclopropane **15a** in quantitative yield. This laid the ground for the development of an unusual gold-catalysed intramolecular cyclopropanation of sulfonium ylides (Scheme 9).

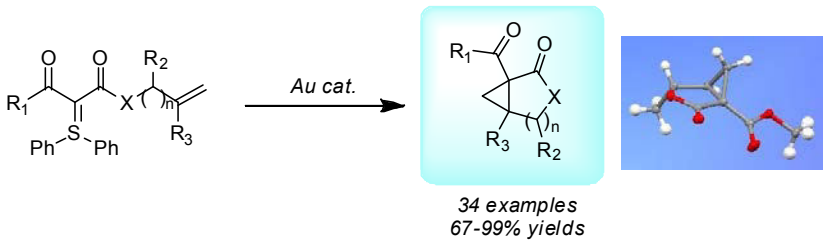

Scheme 9

Mechanistic studies revealed that this reaction is highly stereoselective and proceeds by an unconventional mechanism implying olefin activation rather than ylide decomposition to a metal carbene.

In summary, we have developed an ensemble of sulfur(IV)-mediated transformations that yield very diverse products (as are sulfonium ylides and α-arylated carbonyl derivatives), yet proceed by interconnected pathways. Subsequently, the unique structural features of the ylide products obtained were exploited in the context of gold-

catalysed transformations. The transformations reported herein should find growing synthetic utility among the community.

Publications resulting from this research area: 54, 59-61, 63, 72, 73

External funding: Deutsche Forschungsgemeinschaft, FCT (stipend to L. Gomes), Alexander von Humboldt Foundation (stipend to M. Luparia)

Cooperations: R. Goddard (Mülheim, D), W. Thiel (Mülheim, D), C. Afonso (Lisbon, PT), L. Veiros (Lisbon, PT)

2.2.11 Research Area "Redox-Neutral C–C bond forming reactions" (N. Maulide)

Involved: I. D. Jurberg, B. Peng, S. Shaaban, M. Wasserloos, E. Wöstefeld

Objective: The emergence of so-called "redox-neutral" transformations proceeding by intramolecular hydride shift processes has led to several intriguing developments. In this project, we aim to exploit the potential of hydride-shift C–H activation processes to achieve simultaneous, *intermolecular* bond formation en route to streamlined total syntheses of bioactive natural products.

Results: C–H functionalization is an attractive strategy for the efficient and environmentally friendly preparation of organic compounds. We were particularly intrigued by the possibilities afforded through nucleophilic C–H functionalization α- to nitrogen (Scheme 1).

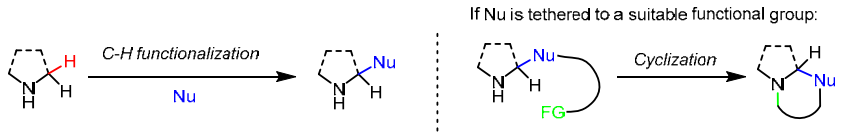

Scheme 1

As shown, judicious functionalization of nitrogen-containing heterocycles should allow the rapid assembly of bicyclic structures found in a plethora of naturally occurring alkaloids.

With this aim in mind, we designed a redox-neutral triggered C–C bond forming strategy. This concept would entail a two-stage sequence comprising redox isomerization and nucleophilic α-functionalization.

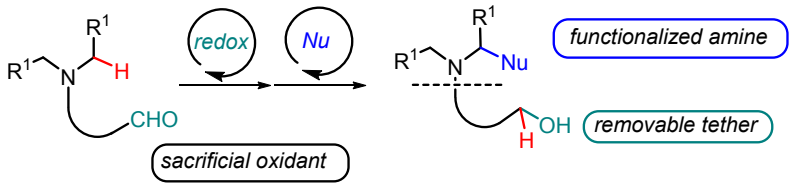

Scheme 2

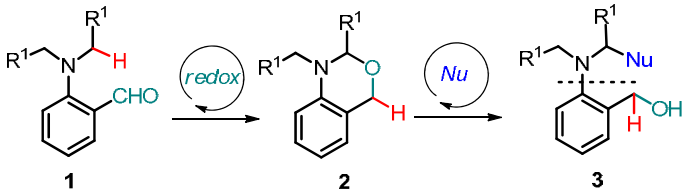

Scheme 3

The proof-of-principle validation of this concept was then designed on aryl-tethered aminoaldehydes such as **1** (Scheme 3).

We realized that the intermediacy of benxozazine **2** would, in principle, enable the formation of α-functionalized products **3** through *in situ* nucleophilic addition.

After optimization, we established that the redox-neutral isomerization could be brought about by the action of a mild Lewis Acid, such as scandium(III) triflate. Direct addition of a Grignard reagent led to the functionalized products in moderate to excellent yield (Scheme 4).

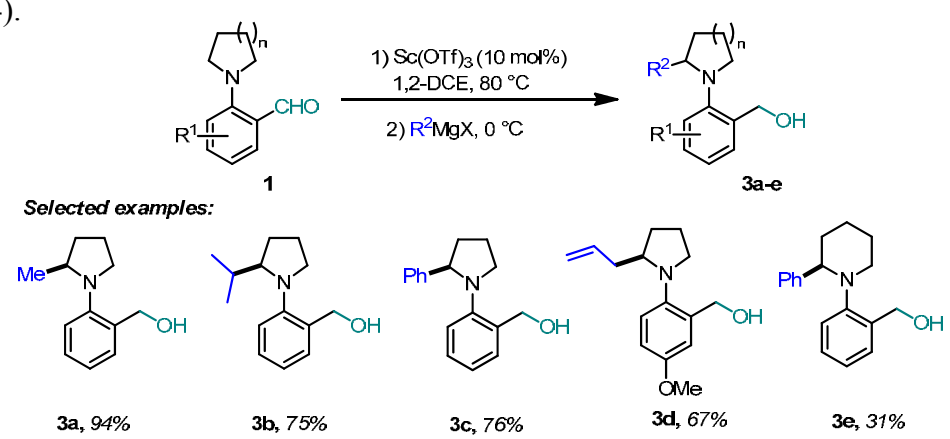

Scheme 4

Alternatively, the construction of sp–sp^3 bonds was also possible by addition of lithium alkynyltrifluoroborates as nucleophiles. The corresponding alkynylated products **4** were formed in a smooth and efficient manner (Scheme 5).

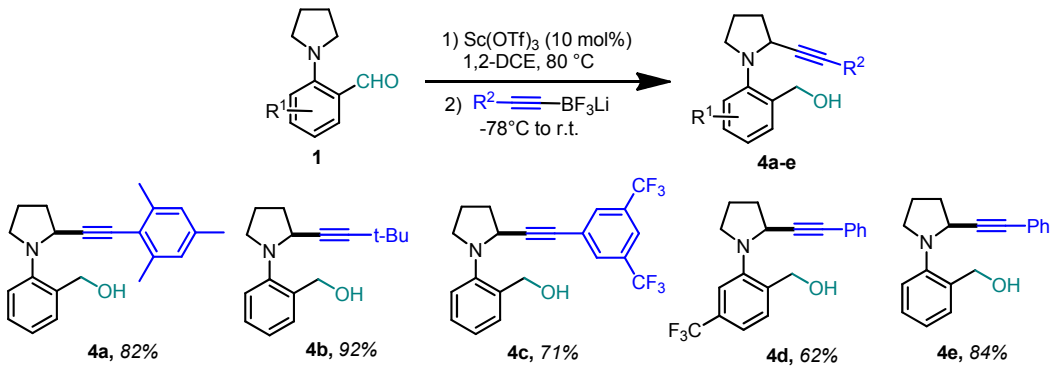

Scheme 5

This strategy was exploited in a short total synthesis of indolizidine 167B (Scheme 6). As depicted, the use of a dioxolanyl-functionalized nucleophile sets the stage for clean deprotection of the *p*-methoxy-substituted aromatic tether under oxidative conditions.

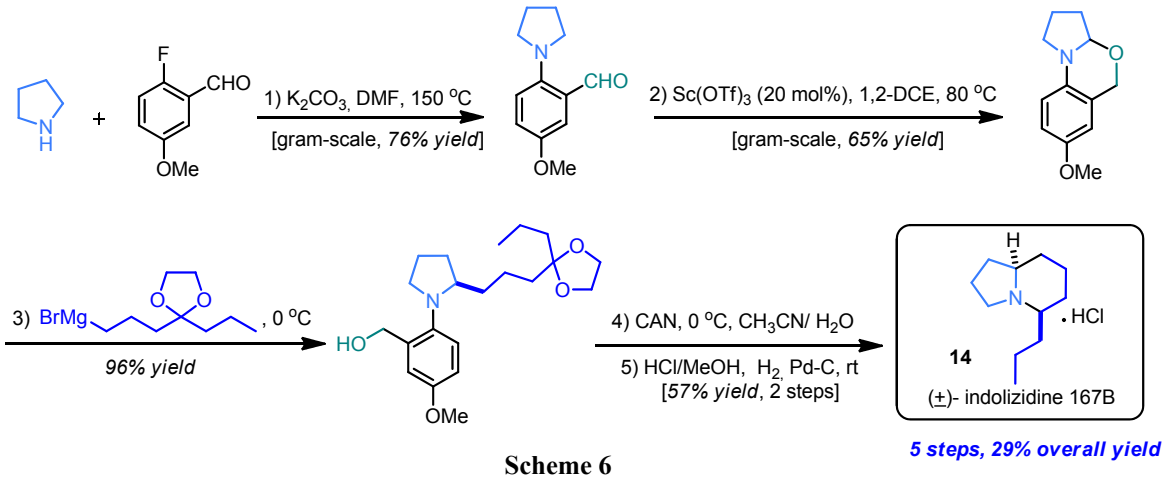

Scheme 6

Simple reductive amination under aqueous acidic conditions directly furnishes the natural product in only 5 steps from pyrrolidine (Scheme 6).

In summary, we have developed a novel approach to C–H functionalization relying on a Lewis-Acid catalysed redox-neutral isomerization. This method opens up interesting perspectives for the direct synthesis of naturally occurring alkaloids. Further steps towards advancing this strategy to asymmetric variants and exploring other redox-neutral transformations are currently underway.

Publications resulting from this research area: 56, 74, 75

External funding: Ecole Polytechnique (stipend to I. Jurberg)

Cooperations: none

2.2.12 Research area "Bispidine analogs of Cisplatin, Carboplatin, and Oxaliplatin" (K.-R. Pörschke)

Involved: H. Cui, W. Gamrad, R. Goddard

Objective: Cisplatin is the leading antitumor drug. There are, however, substantial side-effects associated with its administration. Additional major problems are an inherent platinum resistance (esp., toward colon cancer) and the development of an acquired platinum resistance of refractory tumors. Related developments are carboplatin and oxaliplatin. Present research on platinum-based drugs is directed at the reduction of side-effects and the enlargement of the spectrum of activity. Since the parent bispidine (3,7-diazabicyclo[3.3.1]nonane) has become available to us from previous work, we have used it as a possible "carrier ligand" and synthesized the corresponding analogs of cisplatin, carboplatin, and oxaliplatin.

Results: Reaction of (1,5-hexadiene)$PtCl_2$ with bispidine ($C_7H_{14}N_2$) in DMF afforded large pale yellow crystals of the DMF adduct ($C_7H_{14}N_2$)$PtCl_2$·DMF (**1b**) in 87% yield. Recrystallization from the less basic *N*-methyl formamide gave solvent free ($C_7H_{14}N_2$)$PtCl_2$ (**1a**) and from water the trishydrate ($C_7H_{14}N_2$)$PtCl_2$·$3H_2O$ (**1c**) was obtained. Similarly, the Pt–bispidine analogs of carboplatin, both solvent-free ($C_7H_{14}N_2$)Pt{$(O_2C)_2C_4H_6$} (**2a**) and the pentahydrate ($C_7H_{14}N_2$)Pt{$(O_2C)_2C_4H_6$}·$5H_2O$ (**2b**), and the analog of oxaliplatin, solvent-free ($C_7H_{14}N_2$)Pt(C_2O_4) (**3**), were prepared.

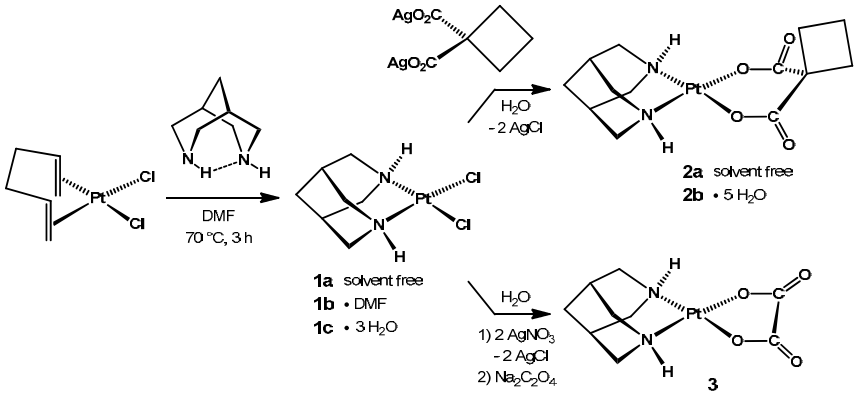

Of particular interest are the structures of the hydrates **1c** and **2b**. In the solid chloride **1c** the complex molecules are linked by parallel N–H···Cl hydrogen bonds to give infinite bands, which are accompanied on both sides by zigzag-shaped strings of water molecules (Figure 1). In contrast, in crystals of the 1,1′-cyclobutanedicarboxylate **2b** the

complex molecules are monomeric and completely surrounded by a shell of water molecules, easily explaining the enhanced water solubility of this complex (Figure 2).

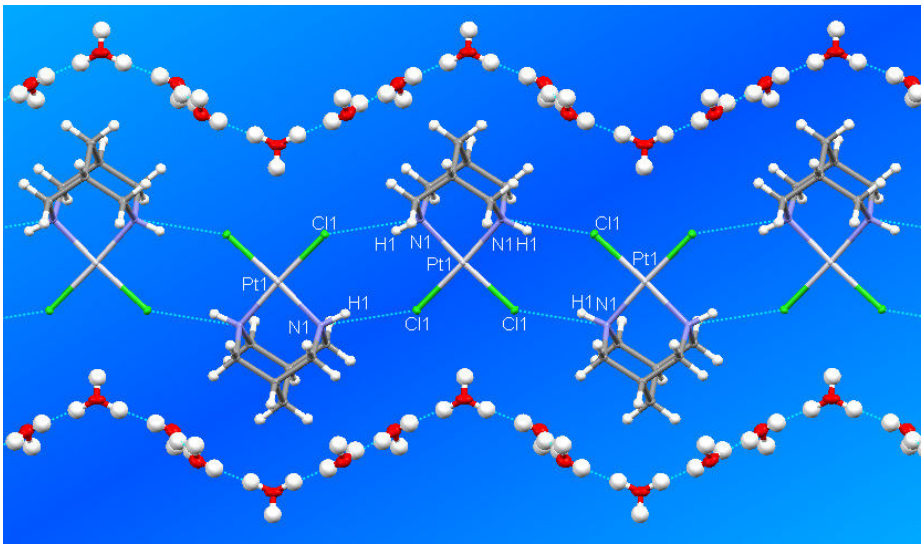

Figure 1. Crystal structure of $(C_7H_{14}N_2)PtCl_2 \cdot 3H_2O$ (**1c**).

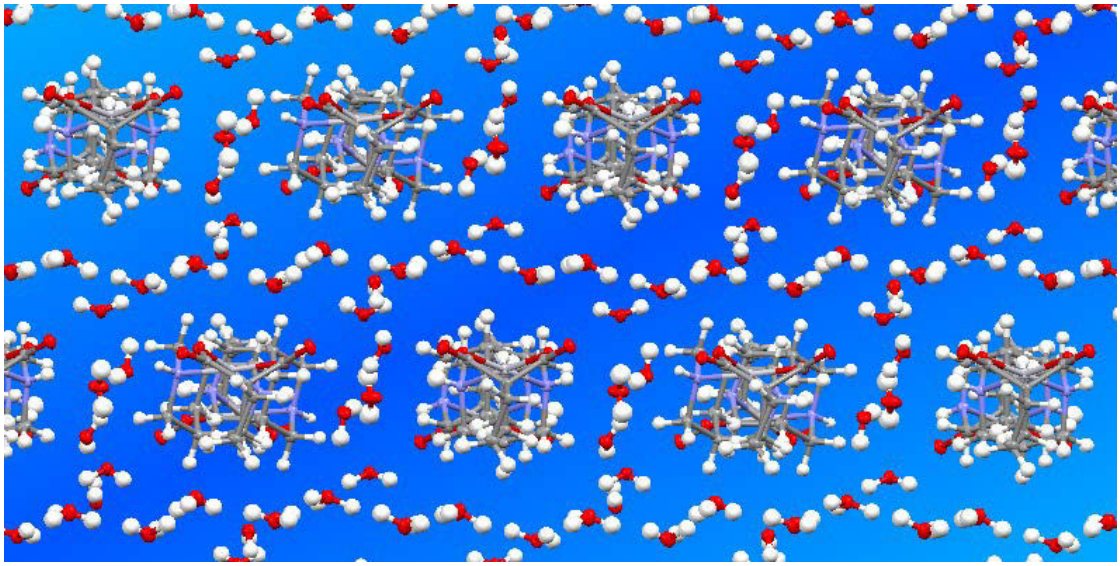

Figure 2. Crystal structure of $(C_7H_{14}N_2)Pt\{(O_2C)_2C_4H_6\} \cdot 5H_2O$ (**2b**).

Cytotoxicity of **1**, **2**, and **3** was tested against human cancer cell lines K562 (chronic myeloid leukemia), A2780 (ovarian cancer), and its cisplatin-resistant subline A2780 CisR. All bispidine–Pt complexes showed significant cytotoxic activity in the μM range. While the cytotoxic potency compared to their parent analogs was somewhat reduced, except for **1** toward A2780 CisR, the resistance factor of **1** for A2780 and its subline

A2780 CisR was significantly smaller (more favorable) than for cisplatin. This appears relevant to the problem of platinum resistance and encourages further studies.

Subsequently, two hydroxy groups were introduced as substituents in 9-position of the bispidine to improve solubility. This was achieved by converting the bispidin-9-one **4** with glycol into spiro[3,7-diallylbispidin-9,2′-[1,3]dioxolane] (**5**) and cleavage of the substituents at N to give crystalline spiro[bispidin-9,2′-[1,3]dioxolane] dihydrate (**6b**), which was dehydrated to anhydrous crystalline **6a**.

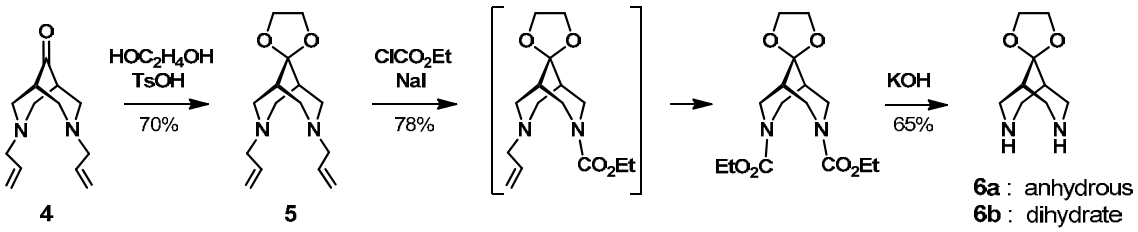

The ketal **6a** was reacted with (1,5-hexadiene)$PtCl_2$ to form water-insoluble **7**, which excludes its application as a possible antitumor drug. Hydrolytic cleavage of the glycolic protecting group in **7** gave yellow needles of anhydrous (bispidin-9,9-diol)-platinum(II)dichloride (**8**) which dissolves moderately in water. From **8** the carboplatin derivative **9a**, forming dihydrate **9b**, and the oxaliplatin derivative **10** are accessible.

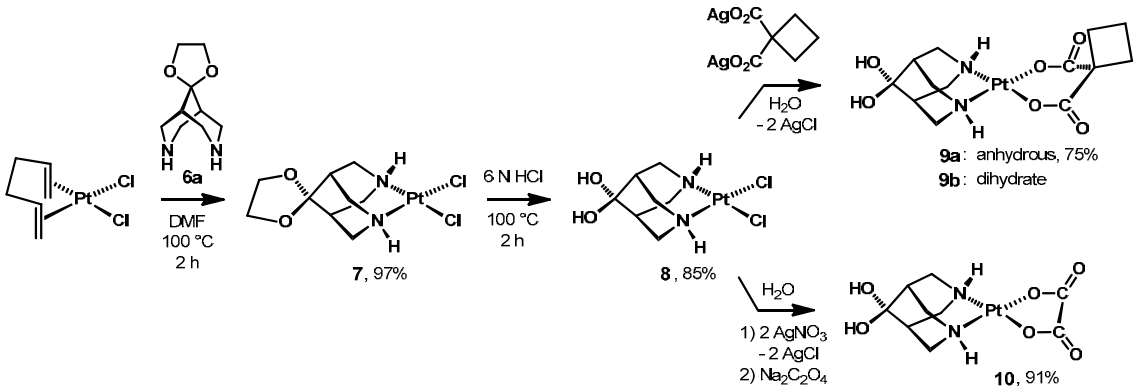

In the crystal, the molecules of **8** are pairwise associated by twofold OH···O* hydrogen bonds between the geminal diol groups (Figure 3). These dimeric entities are further associated by hydrogen bonds to form infinite strands. A similar association is found in crystals of the dihydrate **9b**, whose water molecules are clustered in pockets (Figure 4).

While **10** is virtually insoluble in water, precluding biological studies, the possible anticancer potency of **8** and **9b** is presently under investigation.

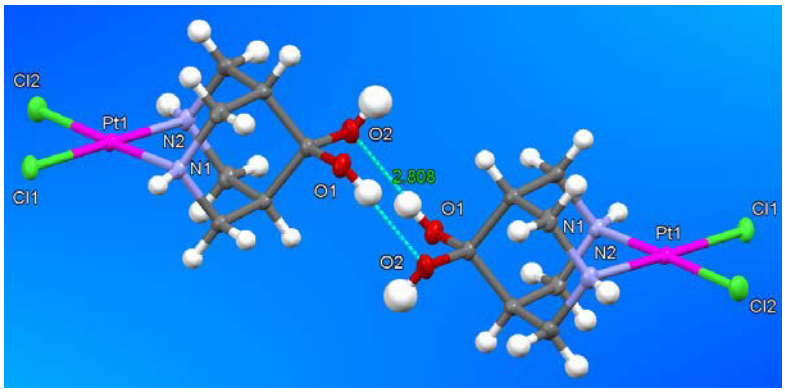

Figure 3. Crystal structure of $\{(HO)_2C_7H_{10}(NH)_2\}PtCl_2$ (**8**)
(shown is the dimerization *via* twofold OH···O* hydrogen bonds).

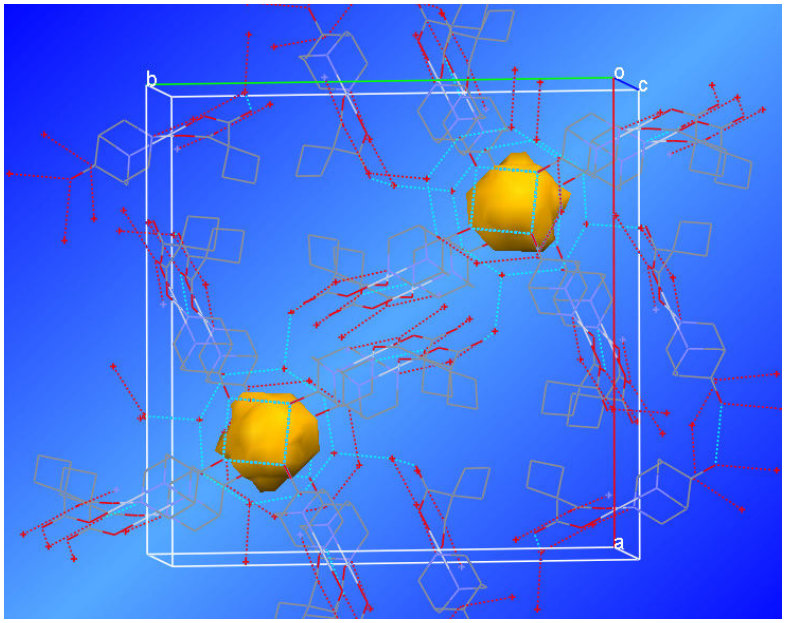

Figure 4. Crystal structure of $\{(HO)_2C_7H_{10}(NH)_2\}Pt\{(O_2C)_2C_4H_6\}\cdot 2H_2O$ (**9b**)
(shown is the association of complex molecules around the water pockets).

Future directions: Currently, cisplatin analogs containing 9-oxabispidine as a ligand are being prepared and their structural and biological properties are being studied.

Publications resulting from this research area: none in the present time frame.

External funding: none

Cooperation: M. Kassack, A. Hamacher, Institut für Pharmazeutische und Medizinische Chemie der Universität Düsseldorf (D)

2.2.13 Research area "Structure and Solubility of 4-Oxopiperidinium Salts" (K.-R. Pörschke)

Involved: A. Dreier, W. Gamrad, R. Goddard

Objective: 9-Bispidinone, which contains two fused 4-piperidone rings, easily undergoes hydration to form 9,9-bispidindiol. In order to better understand this ketone hydration, we turned our attention to "4-piperidinone hydrate hydrochloride", which is a chemical feedstock in the pharmaceutical industry. We anticipated that this compound is actually 4,4-dihydroxypiperidinium chloride and became interested in the factors which render this quite simple geminal diol stable.

Results: Commercial "4-piperidinone hydrate hydrochloride" (**A**) is extremely soluble in water, but insoluble in all organic solvents. From DMF/water or acetone/water mixtures single-crystals of **A** have been obtained. X-ray structure analysis proved **A** to be 4,4-dihydroxypiperidinium chloride in which the cations are fourfold NH···Cl and OH···Cl hydrogen bonded to chloride anions in a 3D network (Figure 1). Dehydration with $SOCl_2$ afforded the ketone 4-oxopiperidinium chloride (**B**), which gave single-crystals from anhydrous DMF. Crystalline **B** forms infinite double-strands of molecules which are associated *via* NH···Cl···HN bridges, whereas the keto functions are not involved (Figure 2). Solid **B** is strongly hygroscopic and the hydration reaction **B**→**A** of the single-crystals can be followed under a microscope in a short time. Intriguingly, in a solution of either **A** or **B** in pure water (where chloride becomes hydrated) the ketone is only partially hydrated to give an about 9:1 geminal-diol/ketone mixture. This indicates that it is essentially the OH···Cl hydrogen bonds which stabilize crystalline **A**.

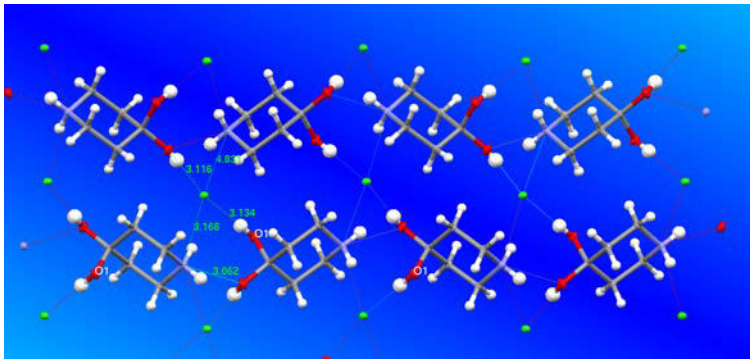

Figure 1. 3D-Structure of the diol **A**.

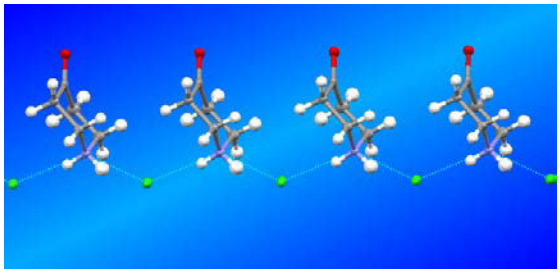

Figure 2. Linear association of the ketone **B**.

By anion exchange the 4-oxopiperidinium salts $[(O=)C_5H_8NH_2]X$ with weakly coordinating anions X = BF_4, ClO_4, OTf, and NTf_2 have been prepared. These solids are non-hygroscopic and their properties in aqueous solution are the same as for **A** and **B**. For $[(O=)C_5H_8NH_2]$OTf (**C**) and $[(O=)C_5H_8NH_2]NTf_2$ (**D**) chain structures similar to that of **B** have been determined. Thus, in these compounds the anions X bridge the ammonium groups by acting as "hydrogen bond acceptors" toward the ammonium protons (NH···X hydrogen bonds). The anions are apparently not basic enough to stabilize also the corresponding geminal diols by OH···X hydrogen bonds, which therefore are not formed.

The anion X = $Al\{OC(CF_3)_3\}_4$ is even less basic. When the anion exchange is carried out in either diethyl ether or CH_2Cl_2 as a solvent, the solute complexes $[(O=)C_5H_8NH_2(OEt_2)_2][Al\{OC(CF_3)_3\}_4]$ (**E**) and $[(O=)C_5H_8NH_2(CH_2Cl_2)]$-$[Al\{OC(CF_3)_3\}_4]$ (**F**) can be crystallized. The cocrystals of **E** consists of separate cations and aluminate anions, and two ether molecules are bound to the ammonium group *via* NH···O(ether) hydrogen bonds. Interestingly, pairs of piperidinium cations appear to be stabilized by N–CH···O(ketone) hydrogen bonds (Figure 3).

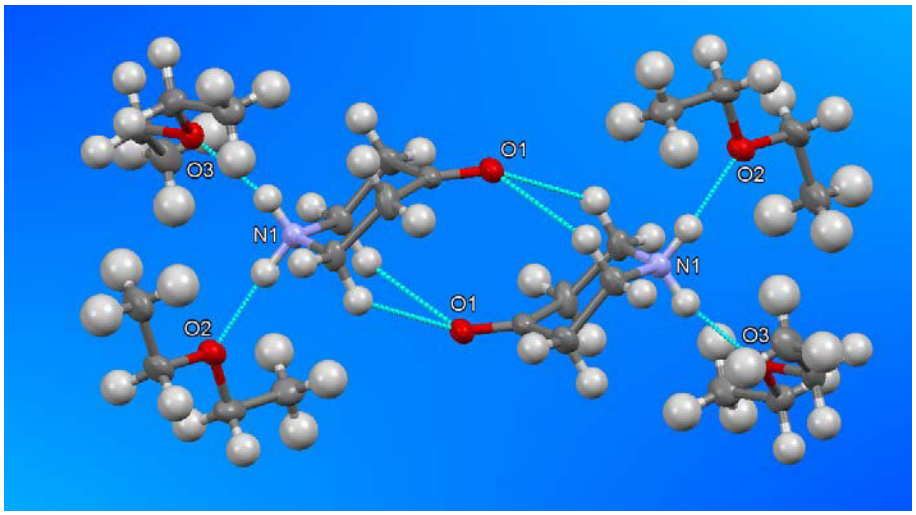

Figure 3. Structure of the piperidinium bis(etherate) **E** (shown are two cations).

Future directions: Ongoing studies on the 9,9-bispidindiol ligand in cisplatin analogs are currently in progress (see corresponding section).

Publications resulting from this research area: none in the present time frame.

External funding: none

Cooperation: none

2.2.14 Research area "Ni(0) Complexes of Polyunsaturated Aza Ligands" (K.-R. Pörschke)

Involved: W. Gamrad, R. Goddard

Objective: There is an enduring interest in zero-valent Ni(0), Pd(0), and Pt(0) complexes, since these are active precursor complexes for catalytic reactions. While typical ligands (e.g. COD) have ene functions in 1,5-sequence, we have studied cyclic and acyclic polyunsaturated aza molecules having two ene and one yne function in 1,6,11-sequences and used them as ligands for nickel(0). Mixing alkene and alkyne functions will introduce different carbon hybridization states into the ligands and should induce different conformations of the chain, together with associated variable donor–acceptor properties. A detailed conformational analysis was performed on the resulting product complexes.

Results: In the first part of the project (*E*,*E*,*E*)-1,6,11-tris(4-tosyl)-1,6,11-triazacyclopentadeca-3,8,13-triene (**A**) was coordinated to Ni(0), supplementing previous studies for Pd(0) and Pt(0) by A. Roglans. The structure of the uncoordinated macrocycle **A** can be thought of as (idealized) C_2-symmetrical, with the C_2-axis passing through the center of one C=C bond and the opposite N-atom. The NMR spectra indicate rotations of the C=C moieties about their vinylic C–C bonds, resulting in 60° jumps of the C_2-axis.

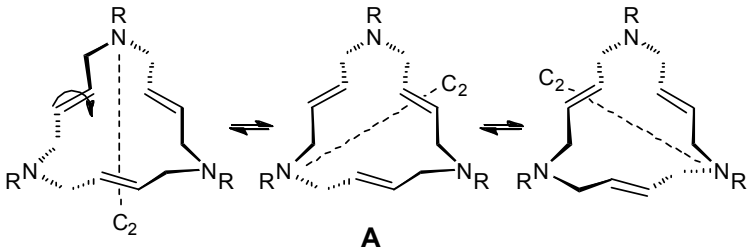

When **A** is coordinated to a metal center such as Ni(0), rotations about the vinylic C–C bonds are no longer possible. The triazacyclotriene ligand in **B** forms three formal azanickelacyclohexanic rings with the metal in a chair–chair–twist (c,c,t) conformational combination, resulting in an overall rigid C_2 symmetrical structure and the presence of a pair of enantiomers.

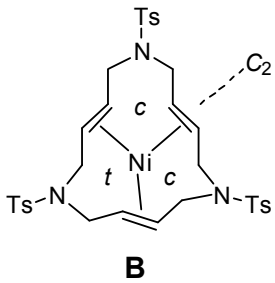

Reacting (*E,E*)-1,6,11-tris(4-tosyl)-1,6,11-triazacyclopentadeca-3,8-diene-13-yne (**C**) with Ni(0) affords mononuclear **D**, which can accept a further Ni(0) to give the dinuclear **E**. The structure of **D** is C_S-symmetrical and resembles a chair, with the 15-membered ring providing the seat, the two tosyl groups at $NCH_2C{\equiv}CCH_2N$ representing the front legs, and the other tosyl group forming the back rest (Figure 1).

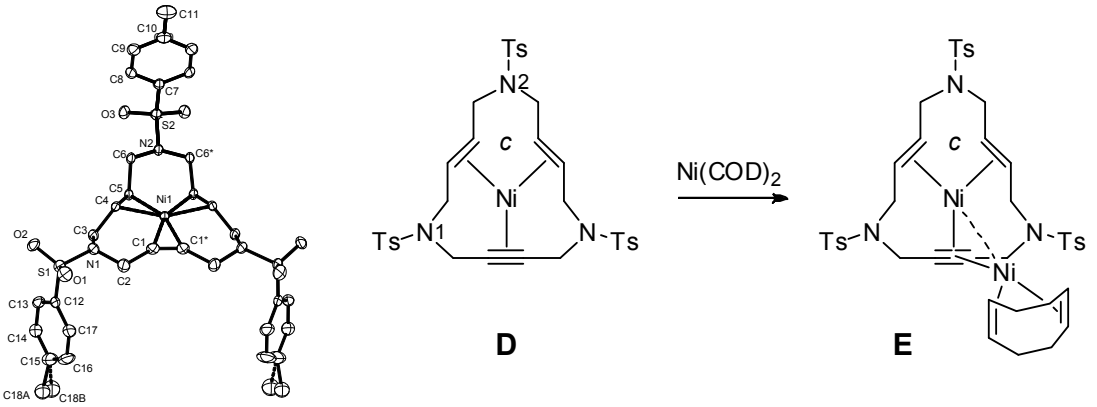

Figure 1. Structure of **D**.

Isolation of **D** and **E** raised the question as to how the structure and properties of these complexes are affected by replacing the cyclic ligand by *acyclic* analogs. Formal excision of a $CH_2N(TS)CH_2$ entity can occur at two sites to give ligands **F** and **G**, for which complexes **H–K** have been synthesized.

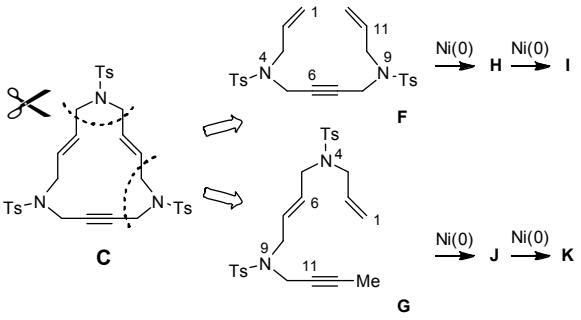

Complex **H** shows a C_2-symmetrical structure and packs in parallel columns, made up of identical C_2 symmetrical molecules having the same chirality and orientation (Figure 2). These are stacked such that the phenyl groups of adjacent molecules lie almost parallel to one another. The dinuclear **K** (Figure 3) crystallizes in well-formed spherulites (Figure 4).

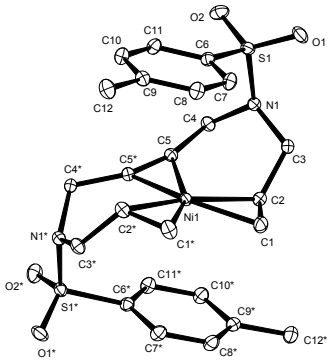

Figure 2. Structure of **H**.

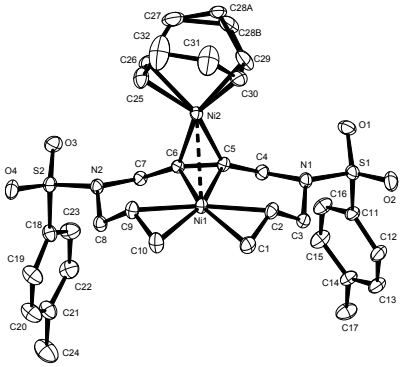

Figure 3. Structure of **K**.

Figure 4. Spherulites of **K**.

Publications resulting from this research area: 77, 79

External funding: DAAD (Acciones Integradas Hispano-Alemanas, 2011–2012)

Cooperations: A. Roglans, A. Pla-Quintana, University of Girona, Spain

2.2.15 Publications 2011-2013 from the Department of Homogeneous Catalysis

List group

(1) Ratjen, L.; García-García, P.; Lay, F.; Beck, M. E.; List, B. *Angew. Chem., Int. Ed.* **2011**, *50,* 754-758.

(2) Lee, A.; Michrowska, A.; Sulzer-Mosse, S.; List, B. *Angew. Chem., Int. Ed.* **2011**, *50,* 1707-1710.

(3) Jiang, G.; List, B. *Adv. Synth. Catal.* **2011**, *353*, 1667-1670.

(4) List, B. *Synlett* **2011**, *4,* 462-463.

(5) Jiang, G.; List, B. *Chem. Commun.* **2011**, *47,* 10022-10024.

(6) Jiang, G.; List, B. *Angew. Chem., Int. Ed.* **2011**, *50,* 9471-9474.

(7) Lifchits, O.; Demoulin, N.; List, B. *Angew. Chem., Int. Ed.* **2011**, *50,* 9680-9683.

(8) Jiang, G.; Halder, R.; Fang, Y.; List, B. *Angew. Chem., Int. Ed.* **2011**, *50*, 9752-9755.

(9) Müller, S.; Webber, M. J.; List, B. *J. Am. Chem. Soc.,* **2011**,*133,* 18534-18537.

(10) List, B. (Vol. Ed.) "Asymmetric Organocatalysis 1: Lewis Base and Acid Catalysts" in *Science of Synthesis,* Georg Thieme Verlag KG, Stuttgart, **2012**.

(11) Čorić, I.; List, B. *Nature* **2012**, *483,* 315-319.

(12) Lee, A.; Reisinger, C.; List, B. *Adv. Synth. Catal.* **2012**, *354,* 1701-1706.

(13) Liao, S.; Čorić, I.; Wang, Q.; List, B. *J. Am. Chem. Soc.* **2012**, *134*, 10765-10768.

(14) Guin, J.; Rabalakos, C.; List, B. *Angew. Chem., Int. Ed.* **2012**, *51,* 8859-8863.

(15) Mahlau, M.; List, B. *Isr. J. Chem.* **2012**, *52,* 630-638.

(16) List, B. *Beilstein J. Org. Chem.* **2012**, *8,* 1358-1359.

(17) Liao, S.; List, B. *Adv. Synth. Catal.* **2012**, *354,* 2363-2367.

(18) Demoulin, N.; Lifchits, O.; List, B. *Tetrahedron* **2012**, *68,* 7568-7574.

(19) List, B.; Liao, S.; Shirakawa, S.; Maruoka, K.; Gong, L.-Z.; Xiao, W. (Ed. Ding, K.; Dai, L.-X.) *Wiley-VCH, Weinheim,* **2012**.

(20) Maruoka, K.; List, B.; Yamamoto, H.; Gong, L. *Chem. Commun.,* **2012**, *48,* 10703.

(21) Lee, J.-W.; List, B. *J. Am. Soc. Chem.* **2012**, *134,* 18245-18248.

(22) Mahlau, M.; List, B. "Asymmetric Counteranion-Directed Catalysis (ACDC)" in *Asymmetric Synthesis II (Ed. M. Christmann, S. Bräse)* Wiley-VCH, Weinheim, **2012**, 79-84.

(23) Mahlau, M.; García-García, P.; List, B. *Chem. – Eur. J.* **2012**, *18,* 16283-16287.

(24) Mahlau, M.; List, B. *Angew. Chem., Int. Ed.* **2013**, *52,* 518-533.

(25) Guin, J.; Varseev, G.; List, B. *J. Am. Chem. Soc.* **2013***, 135,* 2100-2103.
(26) Gandhi, S.; List, B. *Angew. Chem., Int. Ed.* **2013***, 52,* 2573-2576.
(27) Čorić, I.; Vellalath, S.; Müller, S.; Cheng, X.; List, B. *Top. Organomet. Chem.* **2013***, 44,* 165-193.
(28) Čorić, I.; Kim, J. H.; Vlaar, T.; Patil, M.; Thiel, W.; List, B. *Angew. Chem., Int. Ed.* **2013**, *52,* 3490-3493.
(29) Kim, J. H.; Čorić, I.; Vellalath, S.; List, B. *Angew. Chem., Int. Ed.* **2013***, 52,* 4474-4477.
(30) Lifchits, O.; Mahlau, M.; Reisinger, C. M.; Lee, A.; Farès, C.; Polyak, I.; Gopakumar, G.; Thiel, W.; List, B. *J. Am. Chem. Soc.* **2013***, 135,* 6677-6693.
(31) Martínez, A.; Webber, M. J.; Müller, S.; List, B. *Angew. Chem., Int. Ed.* **2013***, 52,* 9486-9490.
(32) De, C. K.; Pesciaioli, F.; List, B. *Angew. Chem., Int. Ed.* **2013***, 52,* 9293-9295.
(33) Lee, J.-W.; Mayer-Gall, T.; Opwis, K.; Song, C. E.; Gutmann, J. S.; List, B. *Science* **2013***, 341,* 1225-1229.
(34) Wang, Q.; Leutzsch, M.; van Gemmeren, M.; List, B. *J. Am. Chem. Soc.* **2013***, 135,* 15334-15337.
(35) Bae, H. Y.; Hun Sim, J. H.; Lee, J.-W.; List, B.; Song, C. E. *Angew. Chem., Int. Ed.* **2013**, *52,* 12143-12147.
(36) Zhang, Z.; List, B. *Asian J. Org. Chem.* **2013***, 2,* 957-960.
(37) List, B.; Čorić, I.; Grygorenko, O. O.; Kaib, P. S. J.; Komarov, I., Lee, A.; Leutzsch, M.; Pan, S. C.; Tymtsunik, A. V.; van Gemmeren, M. *Angew. Chem., Int. Ed.* **2014**, *53*, 282-285.

Klußmann group

(38) Klussmann, M.; Sureshkumar, D. *Synthesis* **2011**, *3*, 353-369.
(39) Böß, E.; Hillringhaus, T.; Nitsch, J.; Klussmann, M. *Org. Biomol. Chem.*, **2011**, 9, *6*, 1744-1748.
(40) Boess, E.; Sureshkumar, D.; Sud, A.; Wirtz, C.; Farès, C.; Klussmann, M. *J. Am. Chem. Soc.* **2011**, 133, *21*, 8106-8109.
(41) Jones, K. M.; Karier, P.; Klussmann, M. *ChemCatChem* **2012**, 4, *1*, 51-54.
(42) Jones, K. M.; Klussmann, M. *Synlett* **2012**, 23, *2*, 159-162.
(43) Klussmann, M. "Mechanism in Organocatalysis" in *Science of Synthesis: Asymmetric Organocatalysis 2*, (Ed.: K. Maruoka), Thieme, Stuttgart, **2012**, 633-671.

(44) Pintér, Á.; Klussmann, M. *Adv. Synth. Catal.* **2012**, 354, *4*, 701-711.
(45) Boess, E.; Schmitz, C.; Klussmann, M. *J. Am. Chem. Soc.* **2012**, 134, *11*, 5317-5325.
(46) Schweitzer-Chaput, B.; Klussmann, M. *Eur. J. Org. Chem*. **2013**, 666-671.
(47) Jones, K. M.; Hillringhaus, T.; Klussmann, M. *Tetrahedron Lett*. **2013**, *54*, 3294-3297.
(48) Gulzar, N.; Klussmann, M. *Org. Biomol. Chem*. **2013**, *11*, 4516-4520.
(49) Schweitzer-Chaput, B.; Sud, A.; Pinter, Á.; Dehn, S.; Schulze, P.; Klussmann, M. *Angew. Chem., Int. Ed.* **2013**, *52*, 13228 –13232.

Maulide group

(50) Valerio, V.; Madelaine, C.; Maulide, N. *Chem. – Eur. J.* **2011***, 17,* 4742-4745.
(51) Madelaine, C.; Valerio, V.; Maulide, N. *Chem. Asian J.* **2011***, 6,* 2224-2239.
(52) Luparia, M.; Audisio, D.; Maulide, N. *Synlett* **2011**, 735-740.
(53) Luparia, M.; Oliveira, M.; Audisio, D.; Frébault, F.; Maulide, N. *Angew. Chem., Int. Ed.* **2011***, 50,* 12631-12635.
(54) Huang, X.; Maulide, N. *J. Am. Chem. Soc.* **2011***, 133*, 8510-8513.
(55) Peng, B.; O'Donovan, D.; Jurberg, D.; Maulide, N. *Chem. – Eur. J.* **2012***, 18,* 16292-16296.
(56) Jurberg, I.; Peng, B.; Wöstefeld, E.;Wasserloos, M.; Maulide, N. *Angew. Chem., Int. Ed.* **2012***, 51,* 1950-1953.
(57) Frébault, F.; Maulide, N. *Angew. Chem., Int. Ed.* **2012***, 51,* 2815-2817.
(58) Audisio, D.; Luparia, M.; Oliveira, M.; Frébault, F.; Klütt, D.; Maulide, N. *Angew. Chem., Int. Ed.* **2012***, 51,* 7314-7317.
(59) Huang, X.; Peng, B.; Luparia, M.; Gomes, L.; Veiros, L.; Maulide, N. *Angew. Chem., Int. Ed.* **2012***, 51,* 8886-8890.
(60) Klimczyk, S.; Huang, X.; Farès, C.; Maulide, N. *Org. Biomol. Chem.* **2012***, 10,* 4327-4329.
(61) Huang, X.; Klimczyk, S.; Maulide, N. *Synthesis* **2012**, 175-183.
(62) Valerio, V.; Petkova, D.; Madelaine, C.; Maulide, N. *Chem. – Eur. J.* **2013***, 19,* 2606-2610.
(63) Huang, X.; Patil, M.; Farès, C.; Thiel, W.; Maulide, N. *J. Am. Chem. Soc.* **2013***, 135,* 7312-7323.
(64) Peng, B.; Geerdink, D.; Maulide, N. *J. Am. Chem. Soc.* **2013***, 135,* 14968-14971.

(65) Oliveira, M.; Audisio, D.; Niyomchon, S.; Maulide, N. *ChemCatChem* **2013***, 5,* 1239-1247.
(66) Souris, C.; Frébault, F.; Audisio, D.; Farès, C.; Goddard, R.; Maulide, N. *Chem. – Eur. J.* **2013***, 19*, 6566-6570.
(67) Audisio, D.; Gopakumar, G.; Xie, L.; Alves, L.; Wirtz, C.; Martins, A.; Thiel, W.; Farès, C.; Maulide, N. *Angew. Chem., Int. Ed*. **2013***, 52,* 6313-6316.
(68) Souris, C.; Frébault, F.; Audisio, D.; Farès, C.; Maulide, N. *Synlett* **2013***, 24,* 1286-1290.
(69) Niyomchon, S.; Audisio, D.; Luparia, M.; Maulide, N. *Org. Lett.* **2013***, 15,* 2318-2321.
(70) Souris, C.; Frébault, F.; Patel, A.; Audisio, D.; Houk, K.; Maulide, N. *Org. Lett.* **2013***, 15*, 3242-3245.
(71) Oliveira, M.; Luparia, M.; Audisio, D.; Maulide, N. *Angew. Chem., Int. Ed.* **2013***, 52*, 13149 – 13152.
(72) Huang, X.; Goddard, R.; Maulide, N. *Chem. Commun*. **2013**, *49,* 4292-4294.
(73) Huang, X.; Klimczyk, S.; Veiros, L.; Maulide, N. *Chem. Sci.* **2013***, 4,* 1105-1110.
(74) Peng, B.; Maulide, N. *Chem. – Eur. J.* **2013***, 19,* 13274-13287.
(75) Shabaan, S.; Peng, B.; Maulide, N. *Synlett* **2013***, 24,* 1722-1724.

Pörschke group

(76) Cui, H.; Goddard, R.; Pörschke, K.-R. *Organometallics* **2011**, *30*, 6241-6252.
(77) Brun, S.; Pla-Quintana, A.; Roglans, A.; Goddard, R.; Pörschke, K.-R. *Organometallics* **2012**, *31*, 1983-1990.
(78) Cui, H.; Goddard, R.; Pörschke, K.-R. *J. Phys. Org. Chem.* **2012**, *25*, 814-827.
(79) Brun, S.; Torres, O.; Pla-Quintana, A.; Roglans, A.; Goddard, R.; Pörschke, K.-R. *Organometallics* **2013**, *32*, 1710-1720.

2.3 Department of Heterogeneous Catalysis

Director:

Ferdi Schüth (born 1960)

Further group leaders:

Frank Marlow (born 1960)

Roberto Rinaldi (born 1979)

Wolfgang Schmidt (born 1962)

Harun Tüysüz (born 1978)
group leader since 2012

Claudia Weidenthaler (born in 1965)
group leader since 2012

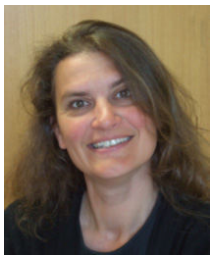

Curriculum Vitae: Ferdi Schüth

1960	Born in Allagen (now Warstein), Germany
1978-84	Chemistry studies at the Westfälische Wilhelms-Universität Münster, Diploma October 1984
1983-88	Law Studies at the Westfälische Wilhelms-Universität Münster, First State Examination February 1989
1984-88	Doctoral studies in the group of E. Wicke, Institute of Physical Chemistry, Münster, Dr. rer. nat. June 1988
1988-89	Post-doc at the Department of Chemical Engineering and Materials Science, University of Minnesota, USA, L. D. Schmidt
1989-95	Wissenschaftlicher Assistent (Assistant Professor) at the Institute of Inorganic and Analytical Chemistry of the Universität Mainz, K. Unger, Habilitation February 1995
1993	Visiting Assistant Professor at the Department of Chemistry, University of California at Santa Barbara, USA, G. D. Stucky
1995-98	Full Professor of Inorganic Chemistry at the Johann-Wolfgang-Goethe Universtität Frankfurt
1998-	Scientific Member of the Max Planck Society and Director at the Max-Planck-Institut für Kohlenforschung, Mülheim/Ruhr

Awards and Honors

1989	Award for outstanding Ph.D. thesis
1991	Boehringer-Ingelheim Research Award
2001	Award des Stifterverbandes für die Deutsche Wissenschaft
2003	Gottfried Wilhelm Leibniz Award of the Deutsche Forschungsgemeinschaft
2007	Honorary Professor of Dalian University of Technology, China
2008	Elected member of German Academy of Science Leopoldina
2009	Guest Professor Beijing University, China
2009	European Research Council Advanced Grant
2010	Heisenberg-Medaille of the Alexander von Humboldt Foundation
2010	Elected member of the Nordrhein-Westfälische Akademie der Wissenschaften und der Künste
2010	Nominated for the Deutscher Zukunftspreis 2010
2011	Ruhrpreis für Wissenschaft und Kunst (Ruhr Award for Science and Arts)

2011	Wöhler-Award for resource-saving processes
2011	Hamburger Wissenschaftspreis (Hamburg Award for Science)
2012	Wilhelm-Klemm-Preis of the GDCh
2013	Chemical-Engineering-Medal of the ETH Zürich

Other Activities / Committees

1995-1997	Managing Director of the Institute of Inorganic Chemistry, Frankfurt University
1995-2001	Coordinator of the DFG-Schwerpunktprogramm "Nanoporous Crystals"
1994	Member of the Dechema Arbeitsausschuss "Heterogene Katalyse"
1995-2005	Member of the Dechema Arbeitsausschuss "Zeolithe"
1996-2004	Member of the Dechema Arbeitsausschuss "Mikroreaktionstechnik"
1996-	Member of the Editorial Board, *Microporous Materials*
1998	Member of the Editorial Board, *Advanced Materials*
1998-2005	Chairman of the Dechema Arbeitsausschuss "Zeolithe"
1999-	Founder, Chairman of the Board and of the Scientific Advisory Board hte AG
1999-2005	Member of the Kuratorium, *Nachrichten aus der Chemie*
2000-	Member of the Dechema Board of Governors
2000-	Member of the Selection Committee for the Humboldt Award
2001-	Member of the IZA-Council
2001-	Chairman of the IZA Commission on Mesoporous Materials
2001-2006	Member of the Editorial Board, *Chemistry of Materials*
2002-	Member of the IMMA-Council
2002-2007	Member of the Selection Committee Heinz Maier-Leibniz Award
2003-2005	Managing Director of the Max-Planck-Institut für Kohlenforschung, Mülheim/Ruhr
2003-2007	Member of the Deutsche Forschungsgemeinschaft Senate Commission for SFB
2003-2010	Chairman of the Selection Committee, Alexander von Humboldt Award
2003-	Member of the Editorial Board "QSAR-Combinatorial Science"
2003-	Member of the International Expert Commission Elitenetzwerk Bayern
2004-2008	Member of the Kuratorium Universität Duisburg-Essen
2004-	Member of the Editorial Board, *Chemical Communications*
2004-	Member of the Scientific Commission of the State of Niedersachsen
2004-	Member of the GDCh Board of Governors

2004-	Chairman of the Dechema Forschungsausschuss “Chemical Reaction Engineering”
2005-	Chairman of the Investment Committee “Life Science, Materials and Energy” of the German High-Tech Fund
2005-	Member of the Editorial Advisory Board, *Chemical Engineering & Technology*
2005-	Member of the Expert Commission Elitenetzwerk Bayern
2006-	Editor, *Chemistry of Materials*
2006-	Member of the Advisory Board, *Chemistry–An Asian Journal*
2007-	Member of the Editorial Board, *Advances in Catalysis*
2007-	Member of the Hochschulrat, University Duisburg-Essen
2007-	Vice-President of the Deutsche Forschungsgemeinschaft (DFG)
2009-2012	Chairman of the Selection committee of the Communicator Award of the DFG
2009-2012	Vice-Chairman of the Scientific Council of the Max Planck Society
2009-	Vice-Chairman of Dechema
2009-	Member of the Supervisory Board of the Karlsruhe Institute of Technology (KIT)
2010-	Member of the University Council of the University of Oldenburg
2010-	Member of the Trustees of the Federal Institute of Materials Testing and Research (BAM)
2011-	Member of the Board of Trustees of the Award “Otto-Bayer-Preis”
2012-	Member of the selection committee of the “Deutscher Zukunftspreis” (Future Award of the German President)
2012-2015	Chairman of the Scientific Council of the Max-Planck-Society
2013-	Chairman of the selection committee of the “Deutscher Zukunftspreis”

Research in the Department of Heterogeneous Catalysis

The re-direction of the research of the Department of Heterogeneous Catalysis, which had already been mentioned in the last report, continued over the current reporting period and is now more or less complete, although further development is expected also in the future in order to react to new findings and new ideas. Up to about 2010 the prime focus of the Department was the synthesis, characterization and use of micro- and mesoporous materials, supplemented by activities in high throughput experimentation. These research fields have now mainly supporting character, while the focus of the work strongly shifted towards nanostructured catalysts and energy-relevant catalytic processes, for which the former research directions provide an excellent platform to build on. Methodologically, mechanochemistry/mechanocatalysis is playing an increasing cross-sectional role in three different fields: hydrogen storage, biomass conversion, and mechanocatalytical processes under in-situ ball milling conditions.

The new research directions are partly associated also with new group leaders. Roberto Rinaldi had already joined the group towards the end of the last reporting period. His activities are exclusively focused on biomass conversion, with the research on cellulose and mechanocatalytic depolymerization performed in close collaboration with the group of the director Ferdi Schüth. Roberto Rinaldi's activities on lignin conversion, on the other hand, are pursued fully independently. Regina Palkovits had research activities in the Institute in the first phase of the reporting period, although she was formally appointed professor at Aachen University at the end of 2010. Since her laboratories were not ready at that time, her research continued in Mülheim for an appreciable period of time, her last students have finished their experimental work at the end of 2012 in Mülheim. Harun Tüysüz was appointed group leader in 2012, after returning from a post-doc stay in Peidong Yang's group in Berkeley. He is ramping up activities in the field of electro- and photocatalysis with relevance for energy conversion, thus well complementing the activities of Frank Marlow, who has also moved more and more towards photocatalysis over the last years. Wolfgang Schmidt continues his activities in the field of synthesis and applications of zeolitic materials, he was appointed editor-in-chief of the most important journal in this field, Microporous and Mesoporous Materials, in 2013. Claudia Weidenthaler, who had been responsible for powder X-ray diffraction and XPS analysis in the analytical Department headed by Christian Lehmann, was promoted to a group leader position, with dual responsibilities both in pursuing research in the field of in-situ X-ray methods for applications in catalysis and in continuing to provide service in powder XRD and XPS for the Institute.

Michael Felderhoff continues to coordinate the activities in the hydride/hydrogen storage group, which is expanding also in the direction of heat storage. Due to his high international standing, he was appointed member of the hydrogen storage task force of the International Energy Agency.

The research of the Department is multi-facetted, but the core activities lie in the fields of nanostructured catalysts and biomass conversion processes. The division into the different research areas described in the following is to some extent arbitrary, since the activities are closely related and highly integrated. Nevertheless, the subdivision serves to organize the work - at least on a conceptual level – into different directions under a common topic.

Some of the activities described in this report are completely new; some of them continue work along lines established over preceding periods. For instance, in continuation of the activities covered in the last report, a deeper understanding of the solid analogue of the molecular Periana catalyst has been achieved; determination of reaction rates for this highly complex reaction has allowed to benchmark solid catalysts against the molecular system, and activity increase by almost one order of magnitude was achieved. By a wide range of analytical techniques the similarity of the coordination motifs in the solid to the molecular counterpart was proven. A relatively high level of continuity of the work can also be noticed in the synthesis and use of ordered mesoporous materials in catalysis and in the synthesis of gold-based catalysts by colloidal deposition.

While the methods for the production of ordered mesoporous materials are among the core competencies of the Department, this toolbox has been substantially extended: different methods of hard and soft templating are used for the production of catalysts with defined porosity on different levels. These porous matrices, often in the form of hollow spheres, are loaded with catalytically active compounds by different methods, with the goal of producing catalyst particles with precisely defined size and chemical composition. Exemplary important achievements of the reporting period were the production of highly active and very stable electrocatalysts for PEM fuel cells by the novel method of confined space alloying, in cooperation with the group of Karl Mayrhofer (MPI for Iron Research), or the synthesis of carbon-encapsulated PtCo alloy catalysts which allow the synthesis of the fuel molecule dimethylfuran from hydroxymethylfurfural in almost quantitative yield. The second example is also part of the overall activities on biomass conversion. A full process chain, from the mechanochemical depolymerization of native biomass, which incidentally also allows

fractionation of biomass to a cellulosic and a lignin fraction, to the conversion of the celloligomers into value added products, such as hydroxymethylfurfural, sugar alcohols or dimethylfuran, has been developed and covered in a family of patents. Notably, combining three of the processes mentioned, an overall yield of 75 % of dimethylfuran can be achieved in three steps, starting from cellulose. Also the hydrogenation process for the conversion of lignin to liquid hydrogenated products is a highly interesting achievement of the last reporting period.

The entry point into most processes for biomass conversion investigated in the Department is the mechanochemical depolymerization of cellulose and lignocellulosic biomass. This development on the one hand resulted from the experience with milling processes available in the Department, where it had been used over the last ten years as a key method for the synthesis and modification of complex hydride based hydrogen storage materials. On the other hand, the mechanocatalytic work on cellulose and hydride milling has led to transfer of the methodology to heterogeneously catalyzed gas phase reactions. Performing solid-catalyzed gas phase reactions during milling in a ball mill leads to increase in rate by more than three orders of magnitude, an effect which has not been fully understood, yet, but which is a topic of intensive current investigation.

The different groups of the Department are integrated in several bi- or multilateral national and international cooperation networks. These include an EU project on the processing of biooil (Cascatbel), BMBF and AIF grants, integration into the nano-energy program at the University Duisburg-Essen, and participation of the Department in a DFG-Sonderforschungsbereich (collaborative research center). Moreover, in the second funding period of the German Excellence Initiative the Cluster of Excellence (CoE) “Tailor made fuels from biomass” with RWTH Aachen was renewed, with the Schüth and the Rinaldi groups involved, and the CoE “Solvation Science” with the Ruhr-Universität Bochum was funded, also under participation of the Schüth, the Marlow, the Rinaldi and the Tüysüz groups. External funding for the Department was somewhat above 1 M€ per year on average during the reporting period. Integration into these and other scientific networks certainly also helped to advance the careers of several young scientists: Huaiyu Shao was appointed assistant professor in one of the Japanese World Premier Institutes at Kyushu university, Chunjiang Jia became full professor at Shandong University, and Heqing Jiang was appointed full professor at the Qingdao Institute of Bioenergy and Bioprocess Technology of the Chinese Academy of Science.

The members of the Department have been invited to numerous presentations at various institutions and conferences, among them several plenary lectures at important international meetings. Moreover, Ferdi Schüth received several awards, such as the Ruhrpreis für Wissenschaft und Kunst, the Wöhler-Prize of the German Chemical Society (GDCh), the Award of the Hamburg Academy of Arts and Science, the Wilhelm-Klemm-Prize of the GDCh, and the first Chemical Engineering Medal of ETH Zürich. Ferdi Schüth was also active in various capacities beyond the direct research activities. He has served since 2007 as vice-president of DFG, and was re-elected for another three years in 2013. He was also elected as chairman of the Scientific Council of the Max-Planck-Society, and he had a prominent role in the German Academy of Science activities in advising the German government on energy issues. The service of Wolfgang Schmidt as the editor in chief of Microporous and Mesoporous Materials and that of Michael Felderhoff in the International Energy Agency has already been mentioned. Members of the Department, notably Claudia Weidenthaler and many of the Ph.D. students and post-docs, were also very active in outreach activities, especially with the local high schools.

The future research of the Department of heterogeneous catalysis is planned to follow the directions initiated in the past several years, with strong synthetic capabilities as the backbone which serves to support the synthesis of nanostructured catalysts for specific reactions and the activities in the field of biomass conversion. It is expected that the activities directed at understanding the influence of mechanical forces on catalytic reactions will be increased, additionally, research targeted at the exploration of novel feedstocks, such as methane (via syngas) or acetylene, for chemical production is being ramped up. Especially acetylene is considered an attractive molecule, since research on acetylene conversion has been strongly neglected over the last five decades after the decline of Reppe chemistry in times of cheap naphtha feedstocks. With increasing oil prices, acetylene, be it coal based or natural gas based, could become more interesting again, and considering the tremendous progress in catalytic materials, process technology and understanding of catalytic processes, it is expected that new valorization pathways starting from acetylene can be opened.

2.3.1 Research Area "Nanoengineered Catalysts" (F. Schüth)

Involved: M. Feyen, C. Galeano, D. Gu, R. Güttel, C.J. Jia, J. Knossalla, S. Mezzavilla, M. Paul, W. Schmidt, M. Soorholtz, G. Wang, R. Wang, T. Zimmermann

Objective: The goal in this research area is twofold. On the one hand, methodological development is important in order to be able to place desired catalytic functionality at will at desired locations of catalyst materials with compositions freely chosen, on the other hand, these methods are applied for the synthesis of catalysts with high activity and selectivity for specific target reactions.

Results: One of the key synthetic approaches for the production of nanoengineered catalysts is colloidal synthesis.[3,38] This method allows the production of metal or metal oxide particles in solution, where stabilization is typically achieved by capping ligands, such as polymers, fatty acids, or related compounds. These stable nanoparticles can then be further processed in order to produce composite catalysts, or they can be deposited on pre-formed supports, which allows decoupling of the catalyst particle synthesis and the supporting step. Thus, a very high level of control is achieved which allows both fundamental studies and the synthesis of highly interesting catalyst materials.

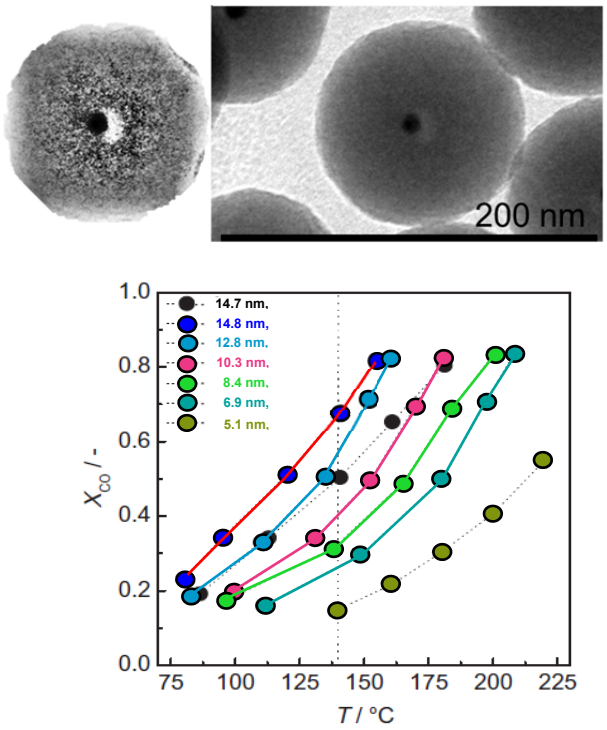

Fig. 1: Encapsulated, partially leached gold particles (top). CO conversion curves for differently sized gold-particle catalysts (bottom). Evaluation of TOFs at 140°C reveal independence of activity on size.

In the last report the synthesis of single gold colloidal particles encapsulated in hollow zirconia shells (Au, @ZrO_2; the nomenclature denotes first the encapsulated species, the blank after the comma indicates that the shell is not directly coated onto the core, and after the "@" the shell material is indicated; possible further shells are indicated by additional "@shell"-levels) had already been described. These materials are highly interesting systems for the study of effects which render

gold colloidal particles active in, for instance, CO-oxidation, since for such systems manipulation of particle sizes and doping levels is possible under precise control of the number of particles present. Such studies were therefore pursued in the reporting period after the synthesis had been well established. By controlled leaching (Fig. 1) it was shown that down to a size of 5 nm, starting from the initial size of 16 nm, the activity per gold surface site is independent of the particle size.[25] Deposition of small amounts of titania on the surface of the colloidal gold particles prior to encapsulation allows studies of the influence that this oxide has on the activity of gold-based catalysts in CO-oxidation.[5] A clear correlation between the titania doping level and the catalytic activity of the composite encapsulated gold catalysts was established which proves that titania enhances the activity, most probably by supplying oxygen species to the gold sites which are active for CO-oxidation.

If iron oxide nanoparticles instead of gold particles are encapsulated in a silica shell (the outer zirconia shell is not required in this case), very stable catalysts for ammonia decomposition, a reaction which can supply high purity hydrogen, can be synthesized.[11] Reference catalysts were produced by leaching the core of FeO_x@SiO_2 particles to produce hollow SiO_2 shells, then identical iron oxide nanoparticles are added again. This results in nominally identical catalysts as for the encapsulated system; however, in the reference catalyst the iron oxide particles are not embedded in the silica shells any more. Using such catalysts in ammonia decomposition at temperatures up to 800 °C revealed improved thermal stability for the encapsulated system.

In fortunate cases, encapsulation of metal or metal alloy nanoparticles can be achieved by simpler pathways (Fig. 2).[47] Polymerization of 2,4-dihydroxybenzoic acid and hexamethylenetetramine (resulting in a polymer resembling resorcinol formaldehyde gel) under hydrothermal conditions leads to the formation of hollow polymer shells. If during polymerization a noble metal salt is added, noble metal particles form in the

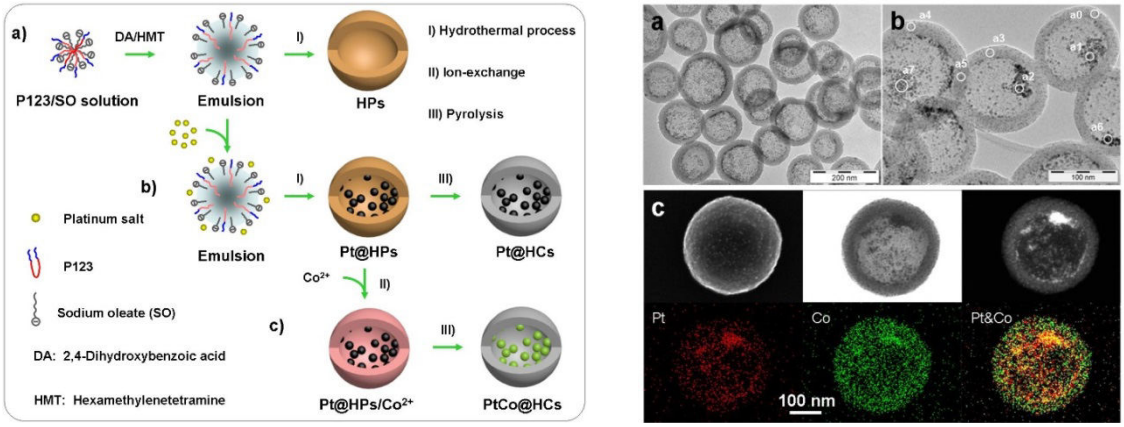

Fig. 2: Schematic synthesis pathway for the production of carbon-encapsulated alloy nanoparticles (left) and TEM, SEM and elemental mappings for encapsulated PtCo nanoparticles (right).

hollow core. Since the carboxylic acid groups in the shell provide ion exchange sites, additional metal components can be exchanged into the catalysts. For many compositions, these exchanged ions migrate into the core and form alloy nanoparticles upon calcination of the polymer shells, while the polymer is transformed into carbon. By controlling the metal concentration in the synthesis, the size of the encapsulated nanoparticles can be controlled. These systems are highly interesting for different catalytic reactions; the PtCo-system allows conversion of 5-hydroxymethylfurfural to dimethylfuran, a very interesting fuel molecule, at almost quantitative yield. In connection with the processes for cellulose depolymerization (see section on cellulose chemistry), this reaction is part of a three step sequence by which 75 % yield of the dimethylfuran fuel can be obtained from cellulose.

Carbon hollow shells are highly interesting not only for the conversion of biomass-derived compounds, but due to its conductivity, it is the support material of choice for fuel cell catalysts. The potential of hollow carbon shell materials for the production of good anode catalysts for PEM fuel cells was thus explored over the last three years. The initial idea was the replacement of the gold core of the Au, @ZrO_2 particles by platinum and to replace the zirconia shell by graphitized carbon. This was found to be possible by a series of nanocasting, leaching, and annealing steps, by which incidentally also the versatility of the synthetic method was demonstrated.[44] As a side result, it could also clearly be proven that carbon is far inferior as a support for gold particles for CO-oxidation compared to different oxides.[12] Since the gold particles are always identical, any differences in catalytic activity can be traced back to the influence of the support, so that the catalysts are ideal model systems. However, the original target, the production of highly active fuel cell catalysts, could not be reached by this approach, since the loading of the catalysts with platinum were much too low for stable shells which need a certain size of approximately 50 nm, while smaller shells, which allow platinum loadings in the 10 % range, are easily destroyed and thus do not provide sufficient stabilization.

The problem could be solved by incorporating the platinum particles not in the hollow center of the spheres, but in the mesopores of the shell itself.[29] With a suitable synthetic protocol, particles with sizes of 1-2 nm could be produced, which only grow to sizes of 3-4 nm after heat treatment at 800 °C, due to the fact that only such particles that are located in the same mesopore coalesce. These hollow graphitic shell based catalysts are excellently suited for application in fuel cells. The major degradation pathways for fuel cell catalysts are particle detachment, growth by Ostwald ripening, and platinum dissolution.[22,27] Encapsulation of the nanoparticles in the carbon matrix suppresses all three deactivation pathways, so that very active catalysts can be

synthesized, which are much more stable compared to conventional, Vulcan-carbon based catalysts, both in accelerated aging tests in rotating disc electrode (RDE) measurements and in real world single fuel cell experiments. In a series of reference experiments with solid spheres having identical pore system and with irregular, bulk mesoporous carbon with identical pore system the superiority of the hollow shell morphology could be proven. It can probably be attributed to better stabilization due to the "quasi 2-D" diffusion pathway, which platinum species have in the shell, and to improved mass transfer due to the hollow core.

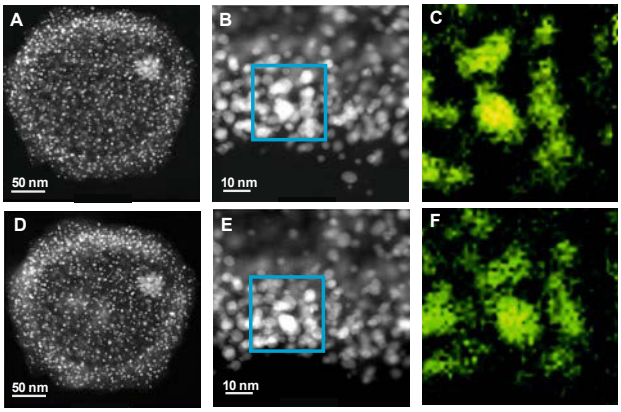

Fig. 3: Identical location TEM images of PtNi loaded hollow graphitic spheres before (top) and after (bottom) accelerated aging test. The elemental map on the left shows the nickel distribution.

This development was very encouraging, but the activity of the catalyst was lower than the DOE target for 2020 which is an important target for work in the fuel cell field. It appears clear that this can only be reached with alloy catalysts, and the work with the stable platinum catalyst inspired the idea of "confined space alloying". The problem with alloy catalysts is the fact that either a high temperature treatment is needed which leads to excessive particle growth, or that preformed alloy nanoparticles are not attached tightly, if they are later supported on a solid, so that rapid detachment occurs. However, the HGS-material provides confining pores, and alloying of individually deposited platinum and nickel precursors should thus proceed without particle growth even after high temperature treatment. The concept was proven for PtNi alloy particles. Stability of this system was so far only demonstraded in RDE measurements, but under the conditions of such experiments, neither substantial particle loss nor particle growth was observed (Fig. 3). However, much more significant is the fact that at least under the RDE conditions the mass activity exceeds the 2020 DOE target by a factor of 2.5 which makes this catalyst system highly attractive. Work is under way to investigate the transferability of the results obtained by RDE experiments to a real single cell under realistic operation conditions. Moreover, a continuous synthesis for the catalyst is being developed in order to render the production scalable.

The nanoengineered systems discussed so far were structured on the scale of several nanometers. However, there is one class of solid catalysts investigated in the Department for which control is exerted at the atomic scale. These are the solid Periana-

type catalysts, which are synthesized by adding a platinum salt to nitrogen-containing porous polymers.[37] Already in the previous reporting period it was shown that Pt-CTF (carbon triazine framework) has activities comparable to the molecular benchmark. This work has now been expanded to other polymers, and the best catalysts outperform the solid Periana system by a factor of almost ten with respect to activity. This precise analysis, however, was only possible because a set-up was built in which reaction rates for this complex reaction system could be measured reliably for the first time. Moreover, by combination of various analytical techniques, including ^{195}Pt MAS NMR, HAADF-STEM and EXAFS, partly at the very limit of what is possible today, with cooperation partners world-wide, it could be proven that the ligand environment in the solid very closely resembles that in the molecular Periana-catalyst, so that one can indeed speak of a solid single-site catalyst.

Future directions: Nanostructured catalysts hold a lot of potential for further development. While many of the methods are too complicated to lead to industrially scalable synthetic protocols, the systems synthesized could provide the blueprint for cheaper, scalable synthesis pathways. Work in this direction is underway for the HGS-based fuel cell catalysts, where a continuous synthesis is being developed. Work on nanostructured catalysts will at least continue at the same level as in this reporting period, but probably increase in importance, augmented by the availability of the new electron microscope and increasing cooperation also beyond the institute, for instance with MPI CEC and MPI-E.

Publications resulting from this research area:
3,5,7,8,10,11,12,21,22,25,27,29,35,37,38, 40,44,47

External funding: ERC Advanced Grant, DFG SFB 558, Fonds der Chemischen Industrie

Cooperations: M. Antonietti (MPI KG); B. Chmelka (UCSB); A.H. Lu (Dalian University); J. Maier (MPI FKF); K. Mayrhofer (MPI E); O. Terasaki (Stockholm)

2.3.2 Research Area "High Surface Area Materials" (F. Schüth)

Involved: D. Gu, C.J. Jia, T. Klasen, I. Lim, V. Nese, Y. Meng, C. Neudeck, A. Padovani, A. Pommerin, F. Richter, M. Ruby, L. Sahraoui, G. Wang, R. Wang

Objective: In this research area, novel methods for the synthesis of high surface area materials, both with ordered and disordered pore systems, are being developed. While in previous reporting periods mostly oxides and carbons were studied, the focus has now strongly shifted to polymeric materials, since these are being explored as catalysts for biomass conversion reactions. The work on high surface area materials is a cross-sectional activity of the Department, with substantial research efforts in the groups of W. Schmidt on zeolitic materials and H. Tüysüz, who investigates ordered mesoporous oxide composites for photochemical and electrochemical reactions. Several projects run jointly with these groups.

Results: Understanding the processes leading to the formation of high surface area materials is a long term research direction in the group. ESI-MS has been developed as a tool to study pre-nucleating solutions.[39] During the last years, it was attempted to extend the systems from silicate systems to $AlPO_4$ and MOF synthesis. In these systems, however, much less pronounced speciation is observed. In the synthesis of $AlPO_4$-18 relatively small units consisting of alternating AlO_4- and PO_4-tetrahedra of up to eleven units were observed. Other than in similar silicate systems, these are clustered with several TEA^+ templating ions, which possibly prevent the formation of higher oligomers. These findings are in line with previous studies, where the formation of $AlPO_4$s via chain and sheet structures has been suggested. Also for the synthesis of the first MOF studied, ZIF-8, condensation to only relatively small units was observed. The kinetics of ZIF-8 formation could be rationalized, since fast precipitation occurs at high imidazolium/Zn ratios, which favors imidazolium incorporation into the oligomers, while at high zinc concentration the addition of zinc is favored.

Zeolites play a major role in several catalysis projects running in the group. The synthesis activities are mostly concentrated in the group of W. Schmidt, but one project on the borderline between high surface area solids and nanoengineered catalysts is also being pursued in the group of F. Schüth. The objective of this project is to elucidate whether the Fischer-Tropsch-synthesis activity of metal particles can be combined with the molecular sieving effect of a zeolite on the level of the zeolite crystallite in order to break the Schulz-Flory-Anderson distribution. This requires the encapsulation of iron

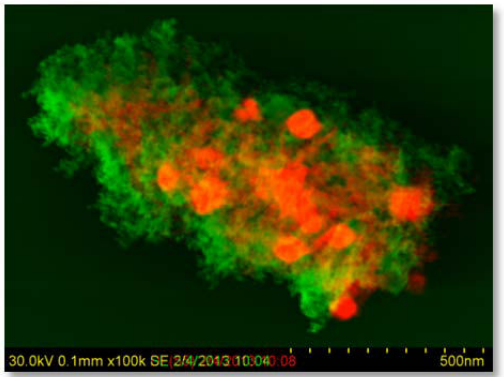

Fig. 1: SEM (green) and STEM (red) overlay of a zeolite particle with embedded iron oxide particles.

nanoparticles within a zeolite crystal which is not possible by directly adding an iron precursor to the zeolite synthesis gel. In that case, the zeolite phase forms as a distinctly separate phase next to the metal oxide, so that the intended effect cannot be exploited. This can be solved by a kind of "stealth" approach. Several years ago the Lyngby group had reported that carbon black particles ("black pearls") can be incorporated in growing zeolites; after calcination, a pronounced mesopore system is generated. If the iron oxide precursor nanoparticles would be covered by a carbon layer, they should be incorporated as well. After optimization of the rather delicate synthesis protocol, this approach proved indeed to be successful. Fig. 1 shows the overlay of an SEM/STEM image which proves the incorporation of the iron oxide nanoparticles in the zeolite. Analysis of the performance in the Fischer-Tropsch reaction is under way.

The synthesis of porous polymers with high surface areas and defined pore structure was one of the key directions of research pursued during the reporting period. The activities range from the synthesis of polymer gels over nanocasting approaches to innovative pathways, i.e. the use of Suzuki-coupling reactions for the direct synthesis of metal loaded polyphenylene. The prototypes of sol-gel porous polymers are resorcinol-formaldehyde composites. Several related compounds have been explored for different applications, but mostly they were used as precursors for high-performance carbons for different applications. The application of such carbons in the conversion of 5-hydroxymethylfurfural to dimethylfuran[47] has already been mentioned in the section on nanoengineered catalysts. A poly(benzoxazine-co-resol)-derived carbon was found to have highly favorable properties for CO_2 capture:[14] it can be obtained in mechanically very stable form, and the nitrogen functionalities introduced in the carbon framework by the addition of amine groups provide excellent adsorption sites for the capture of carbon dioxide. Capacities range up to about 5 mmol/g at 0°C and 1 bar of

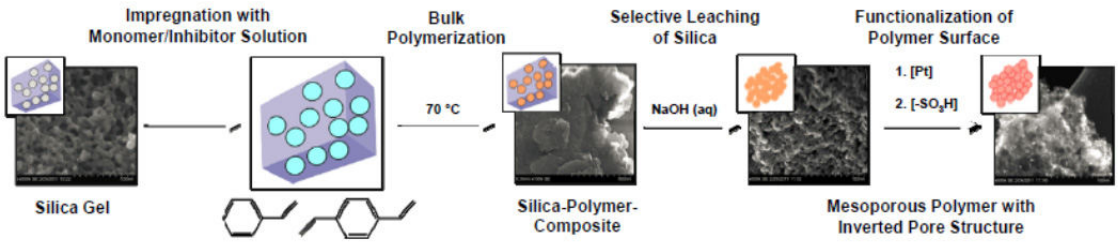

Fig. 2: Schematic representation of the process leading to porous polymer by nanocasting.

CO_2 which are record values for such materials; notably, separation of CO_2 from gas streams is even effective under moist conditions, an advantage which is provided by few sorbents only.

The most intensively studied class of porous polymers were poly(styrene-co-divinylbenzene) which were synthesized by nanocasting.[36,46] Fig. 2 schematically illustrates the process: a porous silica, which can be ordered or disordered, is filled with a polymer precursor, here styrene and divinylbenzene, then polymerization is initiated by a suitable starter. After the polymer has been formed, the silica is leached, typically by treatment with NaOH, then the polymer is ready for subsequent functionalization, which can, amongst others, be sulfonation, metal loading, oxide loading, or others. This method has proven to be extremely versatile. A wide range of different materials, with BET surface areas ranging from a few to about 500 m^2/g and acid site concentrations from about 0.6 to approximately 4.5 mmol/g is accessible by judicious choice of the synthetic parameters.[36] These catalysts proved to be excellently suited for the conversion of fructose to 5-hydroxymethylfurfural. With such a set of catalysts it was also for the first time possible to compare directly the effect of polymeric supports in the oxidation of ethanol to acetic acid and glycerol to glyceric acid against inorganic supports, such as aluminas and carbons.[46] The polymer-based catalysts outperformed the catalysts based on inorganic support: it was generally found that the resin-based catalysts combined the activity of carbon-based catalysts with the selectivity of alumina-based ones.

The most unusual polymer-based catalyst studied was synthesized by a Suzuki-coupling reaction (Fig. 3). This reaction results in a material with a BET equivalent specific surface area of about 1000 m^2/g (the value should be judged with care since the material

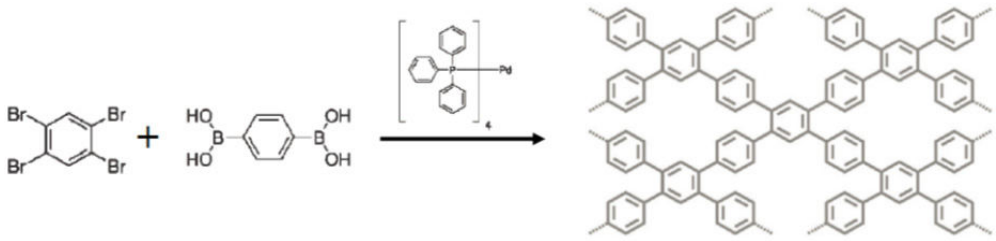

Fig. 3: Reaction scheme for the synthesis of palladium-loaded polyphenylene.

is mostly microporous) onto which at the same time palladium particles with sizes of a few nanometers were deposited. This catalyst, which is synthesized by a Suzuki-coupling, is an excellent catalyst in itself for Suzuki-coupling reactions. More importantly, however, it is one of the most active catalysts for such coupling reactions,

where even sterically highly demanding substrates and chloro-substituted aromatic compounds can be converted at high yields.

While studies into the synthesis of ordered mesoporous oxides are decreasing in importance, there are still very interesting problems to be tackled in this field.[45] These include the synthesis and characterization of composite materials based on ordered mesoporous oxides, and the study of the magnetic properties of such materials.[4] This field was to an appreciable extent developed by H. Tüysüz, while he was still a Ph.D. student in the Department. Now that he is running his own research group, studies in this direction will largely be performed by his team. However, there are a number of projects which were running in the Schüth-group in the reporting period which shall be addressed here.

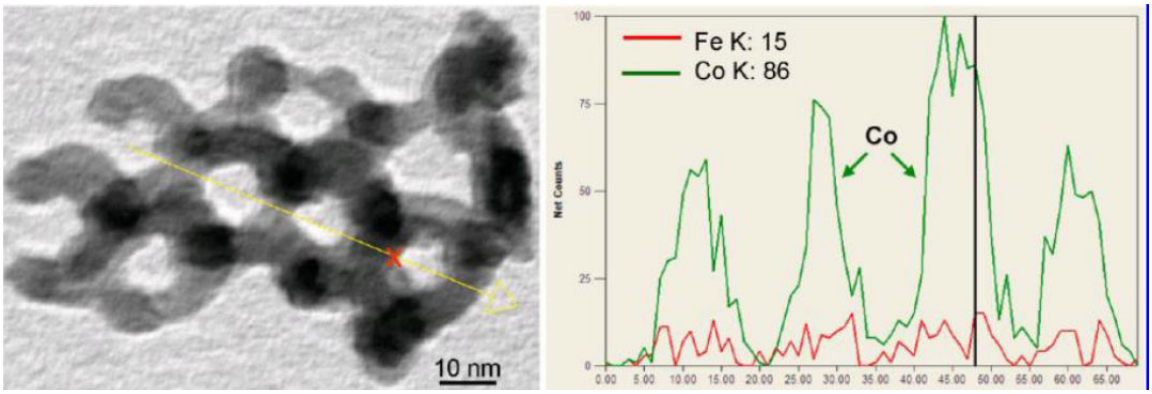

Fig. 4: TEM image of mesostructured $Co_3O_4/CoFe_2O_4$ composite with Ia3d structure (left) and elemental mapping along the yellow line (right), suggesting homogeneous iron and cobalt distribution.

On the synthesis side, methods for the preparation of unusual compositions were further explored. It was thus possible to produce CoO by a careful topotactic reduction of mesostructured Co_3O_4, a method which is not only suitable for cobalt oxides, but can probably be generalized, as shown as a further example for the case of iron oxide.[20] Synthesis of mesostructured CrO_2, a very interesting ferromagnetic material, is still not fully successful, but the CrO_2 content of the mesostructured material could be increased to above 80 %, and we are confident, that further improvements, probably up to the phase-pure material, will be possible. The magnetic properties are the feature which is the reason for exploring these synthetic pathways. Ordered mesoporous oxides provide the opportunity for the creation of magnetic heterostructures. This was exemplified for the case of a hard magnetic $Co_3O_4/CoFe_2O_4$ nanocomposite.[24] Unfortunately, the exact nanostructure – Co_3O_4 with a thin layer of $CoFe_2O_4$ or a mixed crystal – could not fully be elucidated, although the results rather suggest a homogeneous distribution of the iron in the cobalt oxide matrix (Fig. 4). It is hoped that the new electron microscope, which will be delivered in 2014, will help in elucidating the structures in more detail. Such

heterostructures are not only interesting with respect to their magnetic properties (they behave like a homogeneous exchange coupled system), but have potential for photo-electrochemical applications,[49] a research field which is now independently pursued by H. Tüysüz (see corresponding report).
Finally, high surface area Co_3O_4 based materials were also explored as catalysts for CO oxidation. If these materials are doped with small amounts of silicon, they show unprecedented activity for low temperature oxidation, reaching the activity levels of the best gold-based catalysts.[15] This high activity could to some extent be traced back to the influence of the silicon on the size of the cobalt oxide particles,[26] although deeper analysis is still required to fully understand the behavior of the system (see also report of C. Weidenthaler).

Future directions: High surface area materials belong to the core competencies of the Department. This research direction will therefore be pursued also in the future at approximately the same level as currently. However, in the future the range of materials will be substantially broadened. In addition, the focus of the work on high surface area materials will be shifted from the creation of such materials as a goal in itself and more towards the synthesis of high surface area materials for specific purposes.

Publications resulting from this research area: 1,4,14,15,18,20,24,26,28,32,45,46

External funding: ERC Advanced Grant, Fonds der Chemischen Industrie, Humboldt-Foundation, Danish Research Council

Cooperations: K.P. de Jong (Utrecht), S. Kegnaes (Lyngby), B. Weckhuysen (Utrecht), H. Zabel (Bochum), A. Fürstner (Mülheim)

2.3.3 Research Area "Novel Catalytic Concepts" (F. Schüth)

Involved: P. Djinovic, R. Eckert, S. Immohr, H. Jiang, W. Schmidt, T. Trotus, D. Wendt, T. Zimmermann

Objective: This group of projects is highly exploratory, since the target is not directly the development of novel catalytic materials or specific conversions, but the investigation of conceptually novel approaches, be it with respect to feedstocks or with respect to the way the reactions are carried out. In previous reports this section had more specific titles, such as "microreaction technology" or "high throughput experimentation", but as long as the concepts explored in this research area are not integrated more into the mainstream of the work of the Department, it is felt that the current title is more appropriate. The topics under this heading are typically investigated only by relatively small groups, on the order of two to three coworkers, in some cases only one coworker is assigned a specific topic.

Results: It is expected that the feedstock situation in the chemical industry will change in the years to come, with a shift from naphtha as the prime carbon source to methane or coal. Both methane and coal can enter the value chains of the chemical industry via syngas or acetylene, and both feedstocks are studied in several exploratory projects. Methane can also be activated by direct oxidation via SO_3, this topic has already been addressed in the section on nanoengineered catalysts.

Syngas has been explored as a feedstock in a number of different – conventional and unconventional – processes. Already in the last and next-to-last reporting periods the activities for the synthesis of methanol and the exploration of the methanol catalyst have been described. The work is now being expanded to the direct synthesis of dimethylether (DME) and oligomethyleneethers (OME). Direct DME synthesis is thermodynamically advantageous compared to the two-step process, in which first methanol is produced and in a subsequent step the methanol is coupled in an acid catalyzed reaction to DME, moreover, for direct DME synthesis a $CO:H_2$ ratio of 1:1 is required which is close to the ratio obtained from biomass gasification and by dry reforming, so that a direct DME synthesis can be coupled to innovative syngas-production routes.

Direct DME synthesis requires the combination of a CO hydrogenation function and an acid function in the catalyst. This can be realized as a mechanical mixture of, for instance, a methanol synthesis catalysts and a zeolite. Such mixtures are effective in

catalyzing the direct synthesis. It has been shown, though, that substantial amounts of carbonaceous deposits form on the catalyst under DME-synthesis conditions. This is strongly suppressed, if a catalyst consisting of a mesoporous γ-aluina loaded with copper nanoparticles is used. This catalysts, however, is somewhat less active and thus requires higher temperatures of reaction.[30] For the zeolite-based catalysts it was found that side products formed at very low concentration in the DME-synthesis reaction, such as ethylene, are the precursor for the carbonaceous deposit. This is not surprising, as olefins are prone to oligomerization and eventually coke formation, and in the methanol-to-olefin reaction a zeolitic component is used in the catalyst. Currently it is studied, how the localization of the CO hydrogenation functionality and the acid function influence the performance of the bifunctional catalyst.

Acetylene is a more unusual alternative feedstock. There are predominantly research activities in Russia and China over the last decades after Reppe chemistry was terminated in most other countries, primarily due to the vast reservoirs of coal.[48] However, acetylene could also be an interesting methane based feedstock, especially in regions with high fractions of intermittent renewable electricity, if acetylene is produced from natural gas in electric arc furnaces. Such systems could have a substantial load levelling influence, since they can be shut down and started up very rapidly. Due to this consideration, activities on acetylene conversion have been ramped up in the Department. This included the commissioning of a compressor system for the supply of high pressure acetylene. This was successful, and acetylene pressures of several ten bar can now be reached routinely in a safe manner. Moreover, an alternative high-pressure acetylene technique was established which consists of dissolving acetylene in a suitable solvent at very low temperature, followed by temperature increase, which results also in acetylene pressures of several ten bar.[48]

Initially, some of the work reported in literature was reproduced as a starting point. Trimerization of acetylene to benzene over niobium chloride could successfully be achieved even below room temperature. Also reaction of acetylene with water and carbon monoxide to result in acrylic acid was found to be possible with the nickel bromide system, which is known from literature. Using palladium acetate, diphenyl-2-pyridylphosphine and an acid with a weakly coordinating anion to catalyze the carbonylation of acetylene to methylacrylate, TOFs as high as $2500h^{-1}$ with above 99% selectivity to the desired product had been reported in literature at a temperature of 50°C. We were able to reproduce these results observing similar activity and selectivity, and also found that supported palladium nanoparticles can catalyze this transformation in the presence of the ligand. We consider this as a first proof of concept, that the reactions of acetylene, which were dominated by homogeneous catalysis in Reppe's

times are also possible over solid catalysts, so that the full tool-box of modern catalysis research can be used to explore novel transformation routes.

A very exciting, thermodynamically possible, transformation of acetylene which, to the best of our knowledge, has not been reported thus far is the reaction with ethylene to form butadiene. Using ruthenium-based metathesis catalysts we were able to show that this transformation can occur via an enyne metathesis reaction. As it is known that in enyne metathesis an excess of ethylene is beneficial, a high excess of ethylene was used, which resulted in a selectivity as high as 43% to butadiene at 93% conversion. Unfortunately, metathesis catalysts can also lead to acetylene polymerization, and generally have TOFs <1000h^{-1}, so that substantial development work is still required in this direction.

Probably one of the most exciting discoveries of the reporting period was the mechanocatalytic rate enhancement by more than three orders of magnitude in the solid-catalyzed CO-oxidation. Milling is a standard technique which is used in the Department in various projects, such as the synthesis of complex hydrides,[16] for quite some time. A first real breakthrough was achieved when the mechanocatalytic depolymerization of cellulose could be demonstrated (see research area "Cellulose Chemistry").[23] This provides a novel and unprecedented entry point into novel biorefinery schemes which has potentially also high commercial value.

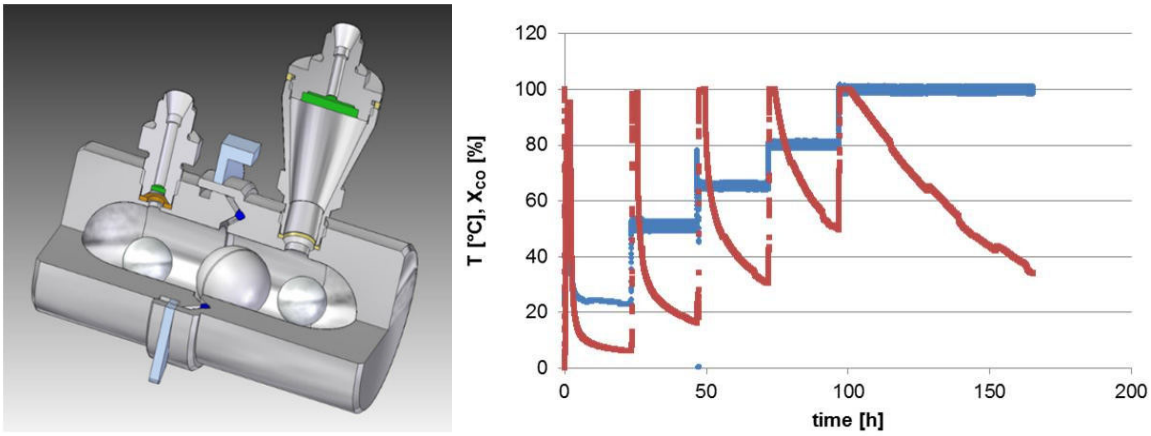

Fig. 1: Schematic drawing of the milling vial (left) and CO conversion at different temperatures during milling and after stopping the mill (right). Conversion jumps to 100 % when the mill is started and decreases after stopping the mill. Catalyst: 1 g gold powder; 50 ml/min 1 % CO in synthetic air.

Inspired by this mechanocatalytic process, the effect of milling on a solid-catalyzed gas-phase reaction was studied. Since there is substantial experience with CO-oxidation in the Department and ready-to-use flow systems were available, this was the first reaction tackled. In order to carry out the reaction under flow-through conditions, a milling vial was constructed which allows such reactions (Fig. 1). Rate enhancement during milling was observed for a number of different catalysts. Most intensively studied were Cr_2O_3

and bulk gold powder. For both systems, rate enhancement by more than three orders of magnitude was observed, which could be clearly traced back to the influence of the milling process by a number of reference experiments.[43] The reason for the enhanced reactivity is not clear, yet. Part of it is probably due to the impact induced hot spots which form between the balls during milling. However, since the activity does not immediately drop down to zero after stopping the mill, but decays over times from minutes to hours, depending on the system (Fig. 1, right), it is probable that milling induced transient defects also contribute to the increased activity. The cause of the rate enhancement is currently under study.
The effect is not confined to CO-oxidation, but is found also for other reactions, such as preferential oxidation of CO in hydrogen-rich gas streams. Moreover, milling can be used to synthesize high activity gold-based catalysts from micrometer sized gold powder, opening up a novel pathway for the synthesis of this class of catalysts which is one of the most intensively studied systems over the last decade.

Future directions: All three topics addressed in this section will be continued in the next reporting period. The work on acetylene conversion is in its early stage, and especially the use of solid catalysts for acetylene conversion will be intensively studied in the next years. Scientifically the most challenging question is the nature of the mechanocatalytic effect observed. In-situ investigations during milling are extremely difficult, and thus a reactor system is being constructed, which should allow exerting mechanical force and analyzing the effects on the catalyst structure after specific delay times.

Publications resulting from this research area: 30,42,48

External funding: ERC Advanced Grant, Industry, BMBF

Cooperations: Fraunhofer Institut UMSICHT (Oberhausen)

2.3.4 Research Area "Hydrides for Hydrogen and Energy Storage" (M. Felderhoff, F. Schüth)

Involved: K. Hauschild, D. Krech, K. Peinecke, A. Pommerin, M. Meggouh, R. Schinzel, H.Y. Shao, C. Weidenthaler, B. Zibrowius

Objective: Hydrogen storage materials based on complex hydrides for mobile applications have been in the focus of the group for more than ten years. However, it seems by now clear that the boundary conditions for on-board hydrogen storage in cars cannot be met by such materials.[50] Nevertheless, the work in this direction is continued for two reasons: first, complex hydrides are rather simple, but little explored solids, and thus the exploration of the synthesis, structures, and properties is of interest, irrespective of whether they are immediately useful. Their synthesis, for instance, poses interesting challenges with respect to pressure and temperature range which needs to be realized. Secondly, while complex hydrides and metal hydrides do not appear to have application potential for hydrogen storage, they could be highly suitable as advanced latent heat storage systems, a field that had already been initially explored by B. Bogdanovic in the institute in the 1980s.

Results: After more than a decade of intense research on $NaAlH_4$ doped with transition metals as hydrogen storage material, the actual mechanism of the decomposition and rehydrogenation reaction is still unclear. Early on, monomeric AlH_3 was named as a possible transport shuttle for aluminum, but this compound has never been observed experimentally. It was now for the first time possible to trap the volatile AlH_3 produced during the decomposition of undoped $NaAlH_4$ by an adduct of sodium alanate and crown ether.[50] The resulting $Al_2H_7^-$ anion was identified by solid-state ^{27}Al NMR spectroscopy. Based on this indirect evidence for the formation of the volatile alane, a simple description of the processes occurring during the reversible dehydrogenation of $NaAlH_4$ was possible.

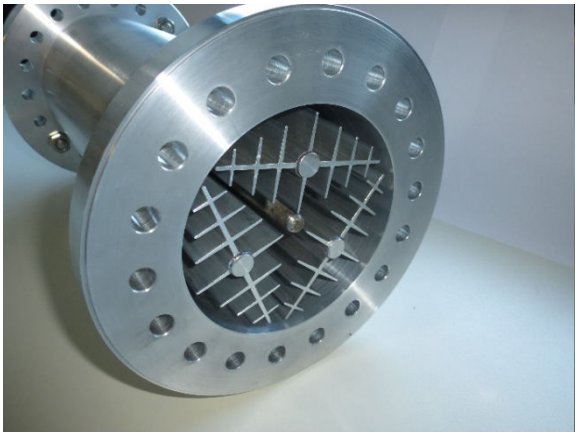

Fig. 1: Prototype of hydride storage tank without the hydride. Fins for cooling are visible.

Even if applications of complex hydrides as storage material for automotive applications appear to be remote, there are other application fields – albeit of smaller scale – where such materials

could be useful. In order to explore the technical implementation of the material in a storage system, a light-weight hydrogen storage tank, charged with Ti-doped sodium aluminum hexahydride Na_3AlH_6, was developed.[13,53] This intermediate hydride has a theoretical hydrogen storage capacity of 3 wt.% and can be operated at lower pressure compared to sodium alanate, $NaAlH_4$. Therefore the tank can be constructed from Al-alloys, with mechanical properties suitable for safe operation of the system. A prototype of the tank is shown in Fig. 1. This prototype was tested under a wide range of pressure and temperature conditions and proved to be suitable for application in combination with high temperature polymer electrolyte fuel cell systems.

Investigations were also extended to other hydrides. Rare earth alanates, such as $Eu(AlH_4)_2$ or the related alkaline earth alanate $Sr(AlH_4)_2$ were studied with respect to structure, thermodynamics and kinetics of the hydrogen release and rehydrogenation.[19] It was found that the decomposition proceeds through an intermediate phase ($EuAlH_5$ and $SrAlH_5$), which, however, is structurally rather different from the hexahydride phase observed in the $NaAlH_4$ system, as could be shown in a combination of powder XRD and solid state NMR spectroscopy. Detailed analysis of both systems revealed – as for most other hydrides – that the thermodynamic properties, but especially the gravimetric storage densities, are insufficient for use in mobile applications. Rehydrogenation of the fully dehydrogenated europium compound could only be achieved to a minor extent, even at pressures of 100 MPa of hydrogen or up to 30 MPa under milling in a pressure ball mill.

MgH_2 is a hydride which has a sufficiently high gravimetric storage capacity of approximately 7.5 wt.%. However, the temperatures for decomposition are too high, the hydrogen is only released above 300 °C. Doping this metal hydride with titanium or other compounds was investigated in order to address both the thermal stability by thermodynamic tailoring due to formation of additional compounds and to improve the kinetic behavior of the system. Direct synthesis via ball milling of magnesium and titanium powder under 30 MPa of hydrogen in a pressure mill allowed the synthesis of a nanostructured MgH_2 doped with TiH_2.[6,16] This composite released hydrogen at temperatures lower by 100°C than bulk-MgH_2, and also rehydrogenation was substantially facilitated. Detailed analysis revealed that the thermodynamic properties of the system are essentially unchanged. For the kinetics the nanostructure is less important than the catalyst, since after several cycles grain growth had occurred, while the positive effect on the kinetics was still observed. This highlights a general problem of nanostructuring hydrogen storage compounds: due to the massive mass transfer during hydrogenation/dehydrogenation cycles the nanostructures are lost in practical

operation, so that special precautions are required to maintain the positive effects of nanostructuring.

Mg-based hydrides are not only interesting for hydrogen storage, but possibly even more useful as heat storage media.[54] Intermediate heat storage for high temperature industrial applications based on thermochemical gas solid reactions possess the highest gravimetric and volumetric energy storage densities of all possible thermal energy storage methods. MgH_2 itself, but also other mixed metal hydrides, such as Mg_2FeH_6 are highly promising for such applications. In particular, Mg_2FeH_6 is suitable for temperatures exceeding 550°C; it is stable over hundreds of cycles and has a volumetric heat storage density of 1500 kWh m^{-3}. Because all experimental results published are based on small lab-scale procedures, we have started a heat storage demonstration project with the development of the tank system, the in- and out-coupling of heat with salt melts and the production of several kg Mg_2FeH_6 as heat storage material. In addition to these technical developments the understanding

$$Mg_2FeH_6 \rightleftharpoons 2\,Mg + Fe + 3\,H_2$$

of the molecular processes during charging and discharging are in the focus of the project. Since such systems have to sustain hundreds or even thousands of cycles in practical applications, full reversibility has to be guaranteed, since otherwise storage capacity will fade. This requires a full understanding of all relevant processes, from the atomic scale up to the level of the grain.

Future directions: The work in this research area will be developed in two different directions. On the one hand, fundamental studies on the synthesis and characterization of hitherto unknown complex hydrides are planned. Since it is expected that many of these materials are unstable under ambient conditions, synthetic work will be extended to low temperatures down to liquid nitrogen temperatures and high pressures up to 1000 bar of hydrogen. On the other hand, work on the use of hydrides for heat storage will be extended, possibly including the construction of a demonstration system.

Publications resulting from this research area: 6,13,16,19,43,50,51,52,53,54

External funding: AIF, Industry

Cooperations: D. Bathen (Duisburg)

2.3.5 Research Area "Nanostructured Optical Materials" (F. Marlow)

Involved: R. Brinkmann, T.-S. Deng, L. Messmer, M. Muldarisnur, D. Schunk, P. Sharifi, S. Wall

Objective: Novel functional materials consist of a hierarchy of building blocks which have to be assembled by precise and tunable methods. In this research area we investigate fundamental aspects of processing steps, nanostructured building block formation, and the tuning of properties of optical materials.

Results: *Opals.* Nanostructures with length scales in the order of the wavelength of light have specific effects on electromagnetic fields. Photonic crystals (PhCs) are highly ordered versions of them. The self-assembly of these materials, especially of artificial opals, was investigated. The improvement and understanding of one well-defined opal fabrication method developed in this institute was the focus of the research. We found that the opal lattice is strongly aligned in opals fabricated by this method (Fig. 1). This is considered as an important step to mono-crystalline opal films which are, up to now, not existing. The current opal films can be understood as intergrowth structures of two different fcc lattices, each of them interrupted by stacking faults. We found out that the fcc-fcc twinning leads to relatively big domains which are not limiting to potential applications.

The detailed understanding of the opal self-assembly process is another topic of our research. The opal formation can be divided in two temporal phases: the wet assembly and the drying. Both are of different relevance for the quality of the opals. We have followed the second phase by optical spectroscopy in-situ and found significant rearrangement processes during and after water extinction. Optical microscopy, SEM[56], optical spectroscopy[59], and neutron scattering[57,60] have been used for opal film characterization.

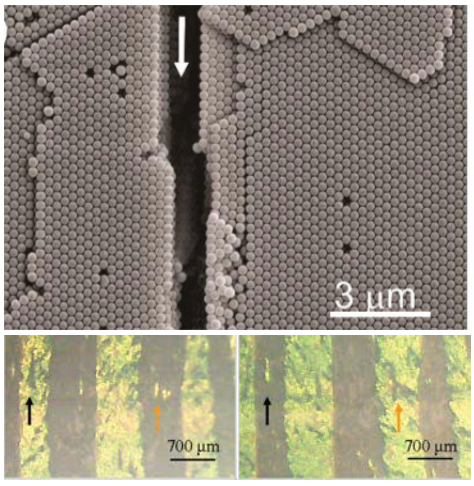

Fig. 1: Opals fabricated by the capillary deposition method (CDM). White arrow: growth direction. SEM images and optical images from two directions.[56, 59]

Core-shell particles. Core-shell particles are interesting building blocks for photonic crystals, catalysis, drug release, and corrosion protection. Their internal structure (shell thickness and composition) can, for example, be used to tune the band structure of PhCs and they are a way to avoid the inversion step which is needed for many PhC applications.[62] Moreover, it turned out that opals made from hollow shells can nearly avoid all cracks. This surprising improvement is ascribed to the enhanced mechanical flexibility of hollow spheres in comparison with solid ones.[65]

NPAs. Nano particle aggregates (NPAs) are also building blocks for photonic crystals, but they can also serve as micro lenses or special scattering particles.[61,63,64] An efficient fabrication method was developed which delivers strongly monodisperse NPAs. Also the shape tuning of NPAs was investigated.

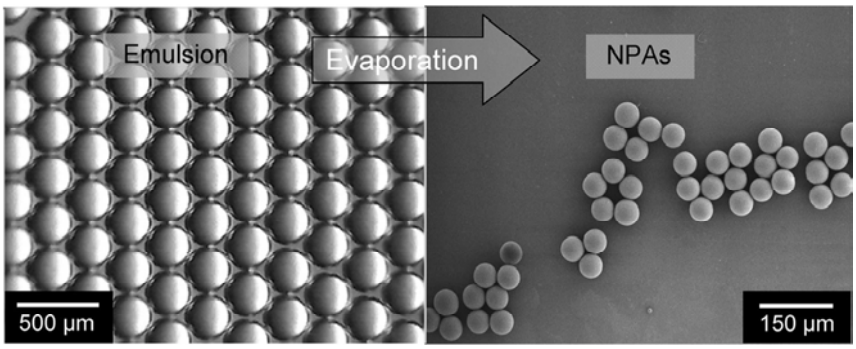

Fig. 2: The NPA fabrication process. The highly monodisperse emulsion is fabricated in a micro fluidic T-junction set-up. The drying leads to the solid NPAs.[61]

DSSCs. Dye-sensitized solar cells are a promising alternative type of solar cells. After 20 years of slow progress with these cells, the interest has increased in the last years again. We also started with works on the fabrication, characterization, and modeling of these solar cells. The key issue is the use of modified semiconductor electrodes and an improved understanding of the charge transport mechanisms in these solar cells.

Future directions: The activities in the DSSC field will be extended. Combinations of DSSCs with photonic crystals will be explored. The understanding of the working mechanism of DSSCs is regarded as a crucial issue which is not satisfactorily addressed in the literature up to now.

Publications resulting from this research area: 53, 54, 55, 56, 57, 58, 59, 60, 61, 62, 63

External funding: IMPRS “SurMat”, NETZ

Cooperations: H. Zabel (RUB, Bochum, D); H. Eckerlebe (GKSS, Geestacht, D);
H. Wiggers, Ch. Schulz, M. Winterer (UDE, Duisburg, D)

2.3.6 Research Area "Deep Depolymerization of Lignocelluloses by Mechanocatalysis" (R. Rinaldi and F. Schüth)

Involved: N. Meine, J. Hilgert, M. Käldström, M. D. Kaufman Rechulski

Objective: The utilization of lignocelluloses (*e.g.* wood, grass, crops residues and several others) shows great potential as part of the solution for decreasing the dependence of modern societies on fossil resources. In spite of this, the direct conversion of these renewable carbon sources by chemical and biotechnological processes is hindered by their complex polymeric nature. In plant biomass, three polymers – cellulose, hemicellulose and lignin – form a complex composite that creates the plant cell walls. The composite structure is highly recalcitrant so that chemical or enzymatic processes for hydrolysis of cellulose suffer from low efficacy due to harsh reaction conditions and high byproduct formation in case of the chemical methods, or high costs and long reaction times for the enzymatic methods. Thus, there is an overwhelming need for novel processes to convert the whole plant biomass, forming fermentable sugars and technical sulfur-free lignins. In this group of projects, we aim at the development of energy- and solvent-efficient processes for 'deep' depolymerization, thus leading to full substrate conversion into 'water-soluble lignocellulose.'

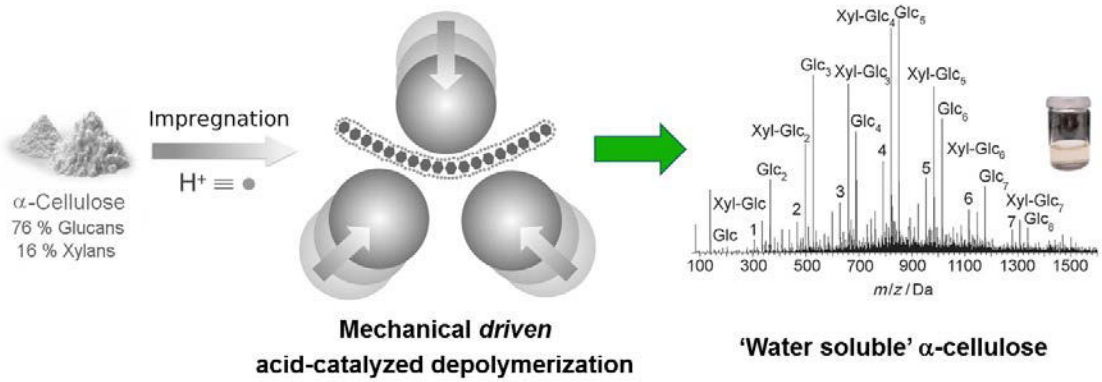

Scheme 1. The pathway towards full conversion of (ligno)cellulosic materials into 'water-soluble lignocellulose.' The substrate is impregnated with catalytic quantities of H_2SO_4 or HCl and then mechanically treated in a planetary ball mill. ESI-MS spectrum of water-soluble products obtained by milling H_2SO_4-impregnated α-cellulose for 2 h. For clarity, products containing a levoglucosan unit (LG) are represented by numbers (n), where the composition is LG-Glc_n. The m/z values correspond to $[M+Na^+]$. Insets show the appearance of products from cellulose.

The real significance of processing 'aqueous solutions of wood', instead of slurries, lies in the prevention of accumulating the highly recalcitrant lignocellulosic residues on

solid catalysts, thus enabling the development of highly efficient processes for biomass valorization by solid catalysts, which is also studied in this area.

Results: Mechanical forces have been exploited for the past few hundreds of years as a first step in wood pulping and conversion of lignocellulose. Usually, conventional mechanical pretreatments (*e.g.* ball milling) are applied to lignocelluloses in order to comminute the substrate and disrupt the crystalline domains of cellulose. As a result, the raw material becomes more amenable for the chemical or biochemical conversions. In fact, moderate hexitol yields (~ 70 %) can be obtained from cellulose conversion in the presence of Ru/C catalysts only, if cellulose is pretreated for 2 to 4 days prior to the catalytic reaction. Similar experiences in other types of conversions (*e.g.* enzymatic saccharification) created a common notion that the effective pretreatment of cellulosic materials by ball milling is always time consuming, and thus very energy intensive for large-scale purposes.

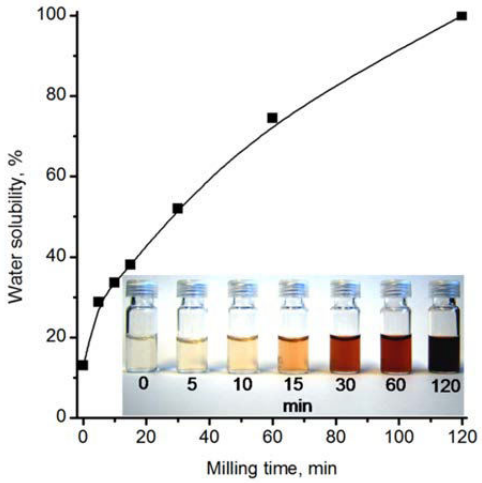

Fig. 1. Formation of water-soluble products (oligosaccharides and lignin fragments) as a function of milling time. Reaction conditions: H_2SO_4-impregnated beechwood (1 g, 0.8 mmol H_2SO_4 per gram of substrate) milled in a planetary mill at 800 rpm for the indicated duration.

'One-pot processes' that combine acid catalysis with mechanical forces thus have not yet been extensively explored for the depolymerization of lignocelluloses. We were the first to demonstrate the full conversion of lignocellulose into 'water- soluble lignocellulose' can easily be achieved by mechanocatalysis within milling durations as short as 2 h.[23] We found that the simple impregnation of substrate fibers with catalytic quantities of a strong acid (e.g. HCl, H_2SO_4) holds the key for the high efficiency. This strategy alleviates the contact problems faced by the experiments performed in the presence of a solid acid. As a result, water-soluble oligosaccharides are formed in quantitative yield within milling duration of 2 h. Most interestingly, lignocellulosic substrates (e.g. sugarcane bagasse, beechwood, pinewood) are also fully converted into 'water-soluble lignocelluloses' within 2 to 3 h (Fig. 1). Remarkably, the method also solubilizes lignin, giving a red-brownish color to the solution products obtained from beechwood (Fig. 1).

Because the mechanical process does not destroy the acid catalyst, no additional acid is required in a subsequent step (taking place in aqueous phase) to hydrolyze the soluble

oligosaccharides. This fact offers an attractive and inexpensive alternative to enzymatic hydrolysis. In fact, oligosaccharides undergo hydrolysis at temperatures as low as 130 °C for 1 h, forming 91 % glucose, 8 % glucose dimers and 1 % HMF relative to the glucan fraction, and 96 % xylose and 4 % furfural relative to the xylan fraction.[23] Such high yields in monosaccharides with such a low degree of byproduct formation using such a simple process are unprecedented.

Even more impressive are the results for the saccharification of 'water-soluble beechwood. The reaction starting with a 10 wt% aqueous solution of depolymerized beechwood (pH 1, at 140 °C for 1 h) also resulted in high yields of monosaccharides (84 % glucose and 89 % xylose, relative to the glucan and xylan fractions, respectively). However, the saccharification led to an unexpected result – the precipitation of a *sulfur-free* lignin (Fig. 2). The separation of lignin from the monosaccharide solution becomes thus feasible by simple filtration.

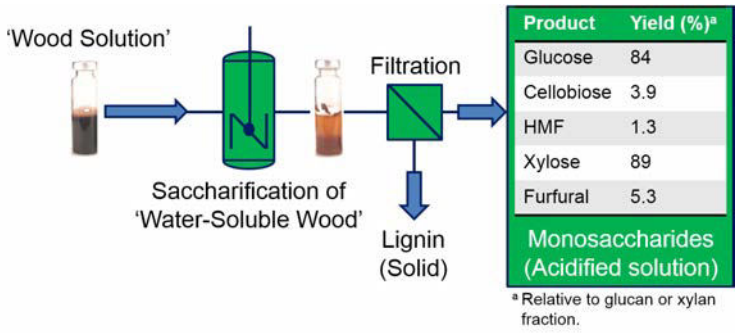

Fig. 2. Fractionation of beechwood into fermentable sugars and sulfur-free lignin by saccharification of 'water-soluble beechwood.'

The absence of sulfur in these lignin precipitates distinguishes these materials from technical lignins obtained by current pulping processes (*e.g.* kraft and sulfite processes, which may contain up to 10 wt.% sulfur). Furthermore, it is conducive to advanced utilization of the lignin precipitates for the production of high value products (*e.g.* chemicals, fuel additives and carbon fibers).

We also demonstrated the deep deploy-merization as a unique entry-point process for efficient production of sugar alcohols from cellulosic substrates.[34] Under low-severity

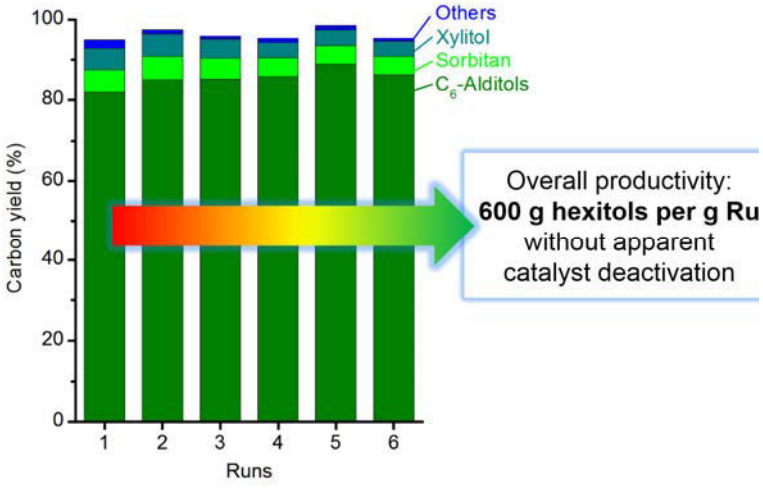

Fig. 3. Recycling of Ru/C. Reaction conditions: 500 mg depolymerized microcrystalline cellulose, 10 mL water, 100 mg Ru/C, 50 bar H_2 (r.t.), at 160 °C for 1 h.

conditions, 94 % yield of hexitols was obtained from the depolymerized microcrystalline cellulose, in the presence of a pre-activated Ru/C, by a batch reaction at 150 °C for 1 h. Noteworthy, such a high yield was achieved in an overall time of only 3 h, that is, *24-36 times faster* than the best examples reported so far. Indeed, a commercial Ru/C catalyst was fully compatible with the presence of H_2SO_4 in the reaction medium. The catalytic activity of Ru/C was fully maintained throughout six runs at 160 °C for 1 h each, as seen in Fig. 3. In the recycling experiments, the cumulative productivity achieved about 600 g of hexitols per g of Ru. As the catalyst is still highly active at the sixth reaction run, this value will be much higher in an extended recycling test.

In a joint research project with J. A. Dumesic (U. Madison-Wisconsin), we also demonstrated the high-yield production of furfurals starting with mechanocatalytically depolymerized substrates.[41] This reaction is conducted in a biphasic reactor containing an organic phase (4-propylguaiacol) and an aqueous salt phase comprising the sugar oligomers. Short reaction times are possible with the use of microwave heating and limit the extent of degradation reactions. Remarkably, at a conversion of glucans of 94% or higher, the isolated yield of HMF reached 60 and 69% in the experiments beginning with water-soluble products from beechwood and sugar cane bagasse, respectively. These yields are remarkably high, as similar studies have reported HMF yields of ~35% when starting from pinewood. Full conversion of xylose with high selectivity for furfural was achieved for the lignin-containing substrates. Again, the current yields of furfural (74 – 84 %) are also higher than those previously reported for the direct processing of solid lignocellulosic substrates (~ 65 %).

One may argue that milling would not be a feasible solution on the scale required for bulk processing of lignocellulosic biomass. Amidst the several conditions studied for the mechanocatalytic depolymerization, we found good correlations of the estimated energy dose, transferred to the substrate, with the achieved solubility of the products. Table 1 compares the milling energy input required for full conversion of the substrate into water-soluble products with the substrate energy content. Most importantly, we have found that the method would be, indeed, already feasible on a kilogram-scale, as indicated by the lower energy demand of the method (by a factor of 0.3-0.7) relative to the substrate energy content.

Table 1. Comparison of the energy demand for the milling process at several method scales.

Method scale (g)	Milling energy input / substrate energy content*
2	49
40	7
100	1
1000	0.3-0.7

* Values estimated considering an average energy content of dry wood of 18 MJ/kg.

Future directions: The results clearly demonstrate the mechanocatalytic depolymerization as a highly promising method for full conversion of plant biomass into water-soluble products. The 'water-soluble lignocelluloses' easily undergo saccharification, producing fermentable sugars and sulfur-free lignin in high yields. Accordingly, the future direction of this research is the exploitation of the produced sugars and lignin in novel catalytic processes currently under development in the Department (*e.g.* hydrogenolysis and oxidation). Importantly, special attention will also be paid to the fundamental aspects concerning the scale-up of the mechanocatalytic process, since we already could demonstrated its feasibility on a kilogram-scale. Most importantly, since we dispelled the common notion that milling processes are time-consuming and very energy demanding, we envisage the development and understanding of basic science towards the better utilization of renewable waste resources by mechanocatalytic reactions, such as the lignin conversions as well as sugar reactions (*e.g.* non-specific synthesis of oligosaccharides for low-cost applications in surfactant and cement industry).

Publications resulting from this research area: 23, 34, 41.

External funding: Alexander von Humboldt Stiftung; Cluster of Excellence "Tailor made fuels from biomass" RWTH Aachen; ERC Advanced Grant

Cooperations: J. A. Dumesic and R. Carrasquillo-Flores (Wisconsin-Madison, USA).

2.3.7 Research Area "New Catalytic Methodologies for Valorization of Lignin" (R. Rinaldi)

Involved: X. Wang, P. Ferrini, G. Calvaruso, N. Ji, H. J. Estevez-Riveira, J. Geboers

Objective: Lignin occurs alongside hemicellulose and cellulose in the plant cell walls. Chemically, lignin is a network polymer made of phenylpropenyl units (*i.e.* coumaryl, syringyl and coniferyl alcohols) that are randomly connected by C—C and C—O bonds (Scheme 1). This biopolymer corresponds to up to 30 % of the plant biomass composition and 40 % of the energy content of lignocellulose. Hence, to find outlets for technical lignins is clearly required for lignocellulose utilization to become carbon economic and energy efficient. At the first sight, the structural model of a native lignin suggests that this feedstock could serve as a raw material for the production of phenols. In this context, hydrogenolysis of aryl alkyl ethers is a reaction receiving increasing attention because of the large fraction of lignin subunits connected by such ether bonds (Scheme 1). However, the lack of catalytic methodologies able to transform the polymeric lignin into solely a class of monomeric products present a major barrier to exploit the potential of this feedstock to the fullest. In this group of projects, we aim to establish a world-class laboratory on catalysis for lignin valorization. The mission of this laboratory, supported by the Alexander von Humboldt Foundation through the Sofja Kovalevskaja Award 2010 given to Rinaldi, is to contribute to the foundations for the rational design of catalytic systems for efficient lignin conversion. Accordingly, we rely on two main strategies to develop catalysis for lignin conversion. First, to understand the solvent effects on the hydrogenolysis/hydrogenation of lignin in the presence of Raney Ni and other Ni catalysts. Second, to design reaction pathways for the molecular simplification of lignin feeds (organosolv lignin and biogenic phenols from bio-oil) based on catalytic hydrogen transfer.

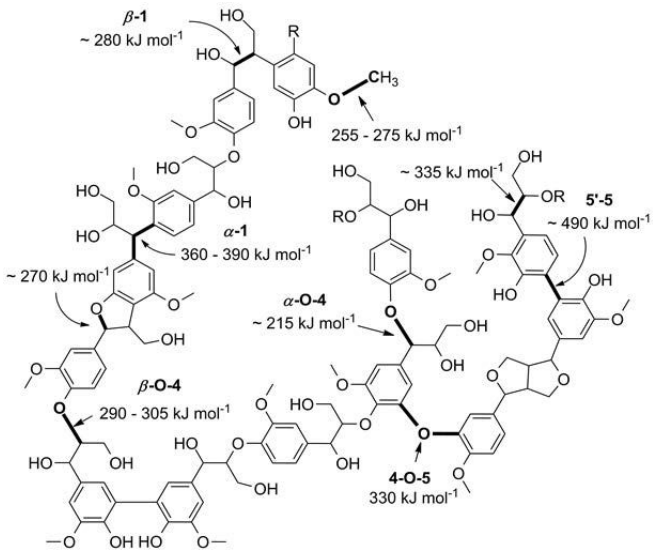

Scheme 1. Example of lignin structure depicting some of the primary inter-unit linkages and the corresponding average values of bond dissociation enthalpy.

Results: Solvents play an important role in catalytic hydrogenations. So far, however, there has been almost no discussion on the influence of solvents in the catalytic hydrogenolysis of lignin or related model compounds. Aiming to ultimately assess the solvent effects on the hydrogenolysis of lignin, we first examined the influence of several solvents in a model reaction using diphenyl ether, a substrate comprising a very strong C–O bond (analogous to 4-O-5, Scheme 1). In the exploratory study, Raney Ni was chosen for several reasons. Unlike noble metals, which show usually a high chemoselectivity towards hydrogenation or hydrogenolysis, Raney Ni is a relatively less expensive material and a 'promiscuous' catalyst in regard to its chemoselectivity. Hence, Raney Ni is able to tackle the structural complexity of lignin, thus showing great potential for lignin conversion.

As expressed by a solvent parameter called 'donor number', the Lewis basicity of the solvent was identified as one of the most important parameters accounting for the activity and selectivity of Raney Ni in the conversion of diphenyl ether. In non-basic solvents (*e.g.* 1,1,1,3,3,3-hexafluoro-2-propanol and alkanes), Raney Ni is an extremely active catalyst for hydrogenolysis and hydrogenation, as shown by the full conversion of diphenyl ether into saturated products. In basic solvents, however, Raney Ni is less active, but a much more selective catalyst for hydrogenolysis of the C—O bonds.

Lignin conversion can be performed even in solvents in which lignin is insoluble. Indeed, lignin starts to undergo thermolysis at temperatures as low as 160 °C. This non-catalyzed process brings aromatic fragments into solution and, consequently, enables the action of solid catalysts. Nonetheless, for high conversion of solid lignin, the process should be performed at temperatures above 250 °C, although such a requirement increases the energy demand of the process. We found that subjecting organosolv lignin to Raney Ni in methanol under an initial H_2 pressure of 7 MPa *(r.t.)* at 300 °C for 8 h is an effective strategy to produce a complex mixture of phenols from lignin. In turn, if saturates are the desired products, solvents possessing no Lewis basicity (*e.g.* methylcyclohexane) are the best choices for the lignin conversion.[71]

Raney Ni is able to catalyze the reduction of many organic functionalities by transfer hydrogenation using 2-propanol as an H-donor. These reactions usually take place under reflux conditions. The transfer hydrogenations with Raney Ni have not

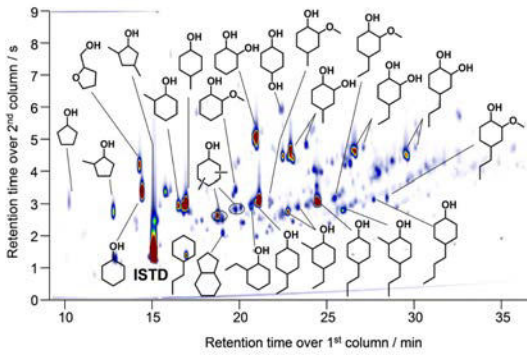

Fig. 2. GC×GC image of bio-oil processed by transfer hydrodeoxygenation using 2-propanol as solvent and H-donor at 160 °C for 3 h.

found extensive uses in organic synthesis due to the lack of chemoselectivity, very often leading to defunctionalization of complex molecules. This 'disadvantage' attracted our attention because the upgrade of highly functionalized phenols, such as those found for the lignin substructures or bio-oil, requires catalysts capable of simultaneously reducing several functionalities under low-severity conditions.

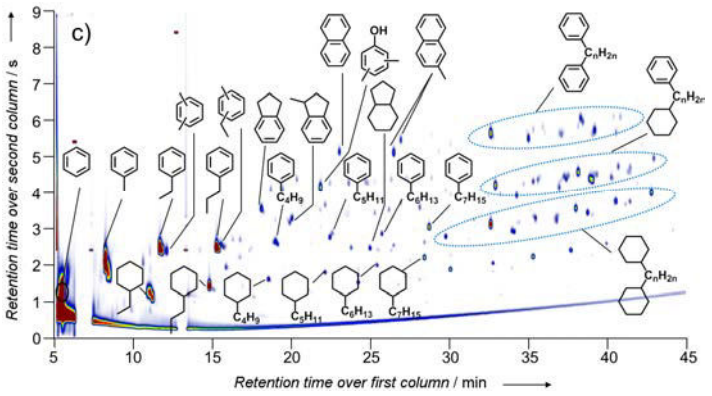

Fig. 3. GC×GC-MS of lignin products obtained from the tandem dehydroxylation of phenols. Reaction conditions: Raney Ni (0.6 g), H-BEA-35 (0.050 g), substrate (0.1 g), 2-PrOH (0.50 g), *n*-pentane (7 mL) processed at 160 °C for 2 h and sequentially at 240 °C for an additional 2 h.

We demonstrated the transfer hydrodeoxygenation of the phenolic fraction of bio-oil to a mixture of cyclic alcohols and diols to be feasible under unprecedented low-severity conditions (*e.g.* 160 °C and autogeneous pressure).[70] In spite of the importance of the aforementioned findings, we realized that the even in the best cases, the formation of mixtures of oxygenated products from lignin (*e.g.* phenols, cyclohexanols and cyclohexanones) still does not suffice for utilization of lignin by the chemical industry. This is because the cracking of the complex structure of lignin leads to very complex product mixtures having only low content of individual components. In effect, since the oxygenated lignin products have high boiling points (*e.g.* phenol, 182 °C), the product separation is very difficult to envision on such a large scale as needed for the lignocellulosic biorefinery. Thus, the complex mixture of oxygenated products would be mostly destined for low-value purposes. Alternatively, the conversion of lignin yielding

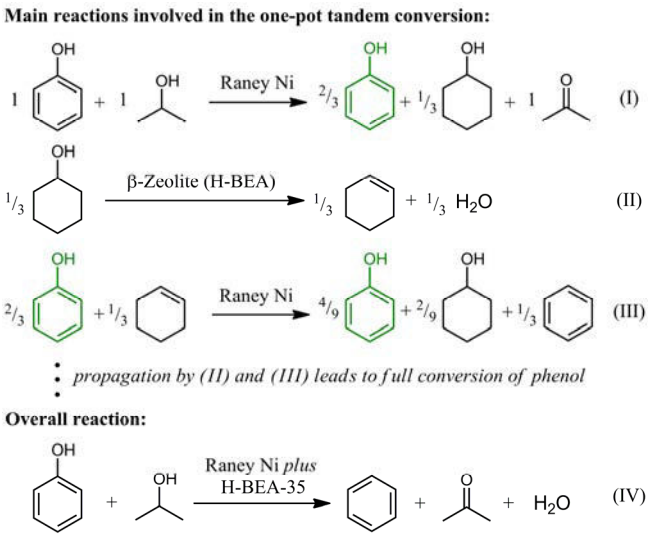

Scheme 2. Simplified pathway for the dehydroxylation of phenols to arenes by catalytic tandem reactions with concurrent use of Raney Ni and β-zeolite (H-BEA-35). The structure in *green* corresponds to the unconsumed phenol by (I) and (III).

arenes with low boiling point could greatly facilitate the fractionation and further processing of the arene mixtures into chemical commodities (*e.g.* benzene, toluene, ethylbenzene and xylenes) by conventional refinery and petrochemical routes.
In spite of the potential in lignin and bio-oil valorization, the dehydroxylation of phenols is a very challenging chemical transformation. In fact, the Ar—OH bond has a bond dissociation enthalpy of 465 $kJ \cdot mol^{-1}$, which is even higher than that of a C—H bond in methane (439 $kJ \cdot mol^{-1}$). In organic synthesis, there are few methods available for phenol dehydroxylation. Typically, they require the derivatization of the Ar-OH group with an electron withdrawing group for weakening the C—O bond. As such, the derivatization enables the hydrogenolysis of the C—O bond with the use of Pd/C and H_2, thus forming the corresponding arenes. It is understandably difficult to envision the utilization of these procedures on a large scale, since they generate stoichiometric quantities of waste.

We demonstrated a novel pathway as highly useful for the depolymerization of lignin and removal of its oxygen-containing functionalities in addition to dehydroxylation of phenols.[73] The novel approach for phenol dehydroxylation (Scheme 2) consists in coupling (I) hydrogenation of phenol to cyclohexanol and (II) dehydration of cyclohexanol to cyclohexene with (III) dehydrogenation of cyclohexene to benzene. Under H_2 pressure, the combination of steps (I) and (III) in a one-pot procedure is impossible. However, steps (I) and (III) become compatible in a one-pot procedure when the reactions are performed by *H-transfer in the absence of* H_2. The conversion of phenol continues by the utilization of cyclohexene formed by (II) because the reaction (III) is thermodynamically more favorable than (I). Therefore, the formation of arenes occurs by the propagation of the reaction chain by (II) and (III). The one-pot procedure is carried out in the presence of Raney Ni and β-zeolite using 2-propanol solely as a starting H-donor, that is, in a molar ratio 2-propanol-to-phenol below 3. Applying the catalytic procedure to organosolv lignin (Fig. 3) resulted in an isolated yield of about 40 wt% colorless oil (78 % of the detected products are arenes, 18 % alkanes, and only 4 % are phenols). Similar results were obtained from the upgrade of the phenolic fraction of bio-oil. Overall, if one considers that the lignin has 70 % of C-content, and the products, 80 - 90 %, isolated yields of ca. 50 % corresponds to a very good carbon yield of *ca.* 70 - 80 %.
In conclusion, the unprecedented high selectivity to arenes obtained under low-severity conditions provides a new route in stark contrast to emerging approaches for catalytic upgrade of bio-oil or other methods using H-transfer which are performed under extremely harsh conditions (5 – 20 MPa, 300 – 500 °C). Finally, even if the isolated

yield of the products is insufficient to give a suitable return in today's chemical industry, the mixture of arenes and aliphatics could very well serve as valuable bio-additives to synthetic fuels produced by the Fischer-Tropsch process, which lack aromatic and branched hydrocarbons required for high-performance of fuels for aviation or Otto-engines.

Future directions: The future directions for this research field is the integration of the transfer hydrogenation concept into the fractionation of plant biomass. Preliminary results show that this new research approach leads to the isolation of the lignin fraction as a mixture of low molecular weight phenolic compounds. In effect, the further understanding of the H-transfer methodologies may provide a fundamental platform for innovative industrial processes for the direct extraction of lignin as arenes and cyclic aliphatics. This could then hold well the key for the fundamental research on lignin conversion to allow applications on a large-scale.

Publications resulting from this research area: 70, 71, 73

External funding: Alexander von Humboldt Stiftung; Cluster of Excellence "Tailor made fuels from biomass" RWTH Aachen;
Cooperations: C. Farès (NMR Department, MPI KOFO)

2.3.8 Research Area "Understanding the Mechanisms of Dissolution and Hydrolysis of Cellulose in Electrolytes" (R. Rinaldi)

Involved: H. F. Nunes de Oliveira, A. Carvalho, N. Meine

Objective: Native cellulose is, for several reasons, often unsuitable for technical applications. Accordingly, the dissolution of cellulose is essential to reshape the natural fibers, thus providing materials with the desired properties. Furthermore, in solution, cellulose is not physically protected by its supramolecular structures, thus enabling the direct investigation of its chemical reactivity. In this group of projects, research into new solvents for cellulose and mechanisms of cellulose dissolution and hydrolysis have been performed.[75]

Results: In 2011, a significant breakthrough was achieved by us,[67] we introduced a novel class of solvent systems for cellulose (Fig. 1). We demonstrated organic electrolyte solutions, which contain just a minor mole fraction of ionic liquid (χ_{IL}), as better solvents for cellulose than the parent ionic liquids (ILs) themselves. These solutions are able to instantaneously dissolve cellulose in concentrations as high as 25 wt%. This striking finding overcomes the major drawbacks that the dissolution of cellulose in neat ILs faces (*i.e.* the slow rate of dissolution, the high viscosity of the solutions obtained, the limited solubility of cellulose and not to mention the high costs of ILs). Indeed, the dissolution of cellulose in neat 1-butyl-3-methylimidazolium chloride (BMIMCl) is a process well-known to take more than 10 h.

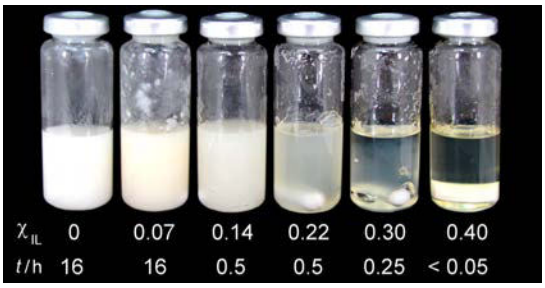

Fig. 1. Appearance of the mixtures containing microcrystalline cellulose (Avicel, 10 wt %), 1,3-dimethyl-2-imidazolidinone and 1-butyl-3-methyl-imidazolium chloride after stirring at 100 °C for the time indicated in the figure. Note that there is a magnetic bar at the bottom of the vials.

Upon dissolving easily 10 wt% cellulose in few minutes (Fig. 1), the simultaneous use of BMIMCl and 1,3-dimethyl-2-imidazolidinone (DMI) brought enormous benefit to the process. Moreover, the use of 1-ethyl-3-methylimid-azolium acetate (EMIMAcO) as IL in the solvent system allows instantaneous dissolution of cellulose at 100 °C. This feature enabled the determination of $\chi_{EMIMAcO}$ at which the dissolution of cellulose was achieved in the molecular solvents at 100 °C (Fig. 2).

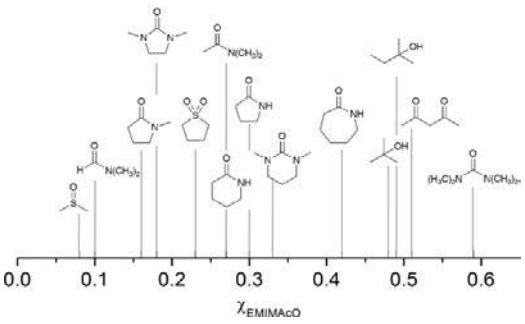

Fig. 2. Mole fraction of 1-ethyl-3-methyl-imidazolium acetate ($\chi_{EMIMAcO}$) required for the instantaneous dissolution of Avicel in several molecular solvents at 100 °C.

As we demonstrated in several contributions published in 2008-2010, the supramolecular structure of cellulose is fully disassembled upon dissolving the biopolymer in ILs, and as a result, cellulose displays reactivity similar to cellobiose. Nonetheless, even in solution, the hydrolysis of 1,4-*β*-glucans needs a strong acid catalyst ($pK_a \leq 3$) to proceed at reasonable reaction rates. This fact suggests that there should be other factors contributing to the high resistance of 1,4-*β*-glucans to hydrolysis.

In the period from 2011-2013, we have been working on a fruitful joint project with AK Thiel. We explored the electronic structure of cellobiose by DFT at the BB1K/6-31++ G(d,p) level.[74] The predictions suggest that cellulose is protected against hydrolysis not only by its supramolecular structure, as currently accepted, but also by its electronic structure, in which the anomeric effect plays a key role. The DFT studies provide very important insights on the hurdles that hydrolysis of cellulose faces (Fig. 3):

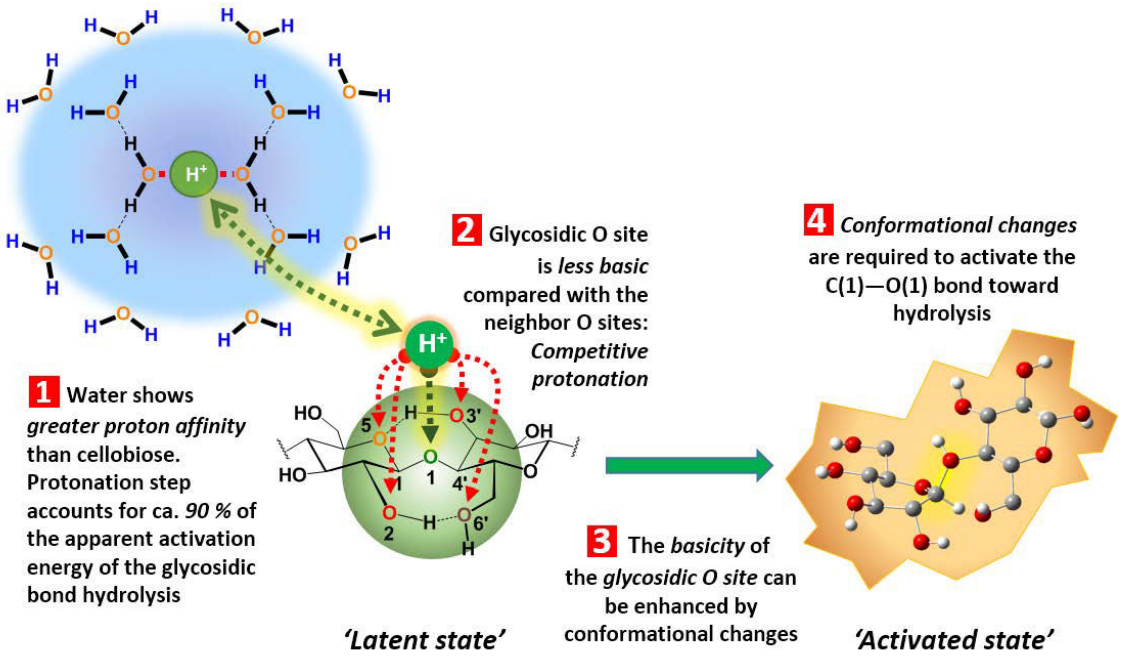

Fig. 3. Overcoming the chemical barriers of cellulose hydrolysis by mechanocatalysis.

These DFT predictions also shed light on the results recently reported for the solvent-free, mechanocatalytic depolymerization of cellulose, in which the biopolymer can be

fully converted into water-soluble oligosaccharides in the presence of a strong acid. The general mechanistic aspects of the hydrolysis of cellobiose strongly suggest that the hydrolysis of cellulose depends heavily upon conformational changes. Accordingly, we propose that mechanical forces serve to activate the 'latent state', i.e. the protonated cellobiose subunits occurring in the cellulosic chain, thus inducing the required conformational changes for the cleavage of the glycosidic linkage. Nonetheless, the reaction still requires a strong acid, which is conveniently provided by impregnation of cellulose with H_2SO_4 or HCl. Indeed, milling cellulose without additives leads mainly to the destruction of the crystalline domains. In this case, there is only little depolymerization, with very low yields of water-soluble products.

Future directions: The future directions for this research field is exploitation of salts effects in the 1,4-*β*-glucan chemistry. Studies are in progress on the assessment of the IL effects on the solubilization and hydrolysis of cellulose. In addition, a collaboration, within Cluster of Excellence "Ruhr Explores Solvation" Ruhr Universität Bochum, with Prof. Havenith should shed light on solvation of cellulose by the electrolyte solutions by means of THz spectroscopy.

Publications resulting from this research area: 67, 68, 69, 72, 74, 75

External funding: Alexander von Humboldt Stiftung; Cluster of Excellence "Tailor made fuels from biomass" RWTH Aachen; Cluster of Excellence "Ruhr Explores Solvation" Ruhr Universität Bochum

Cooperations: W. Thiel, C. Loerbroks, C. Farès (Muelheim/Ruhr, DE), M. Havenith (Ruhr Universität Bochum, DE).

2.3.9. Research Area "Formation of Nanoporous Silicates" (W. Schmidt)

Involved: X. Gu, M. Castro, I. Lim

Objective

Nanoporous silicates possess pores with sizes equivalent to molecular dimensions and serve as molecular sieves and selective catalysts in various applications. Pore diameters as well as pore shapes and pore organization determine the interaction with molecules from fluid phases. Crucial factors that affect the properties of such materials are composition, pore sizes, particle sizes and morphologies. They determine adsorptive and diffusional properties as well as catalytic activity. Understanding the formation processes of nanoporous silicates is subject of this research area.

Results: Zeolites are well known adsorbents and highly efficient catalysts in petrochemistry. Nevertheless, their nucleation and crystallization processes remain still not well understood. The formation of early silicate species in the crystallization of zeolites has been investigated by a combination of liquid state ^{29}Si, ^{27}Al, and ^{1}H nuclear magnetic resonance (NMR) spectroscopy, small angle X-ray scattering (SAXS), dynamic light scattering (DLS) and electrospray ionization mass spectroscopy (ESI MS) in collaborations with colleagues from the Universities of Versailles, France, and Leuven, Belgium.

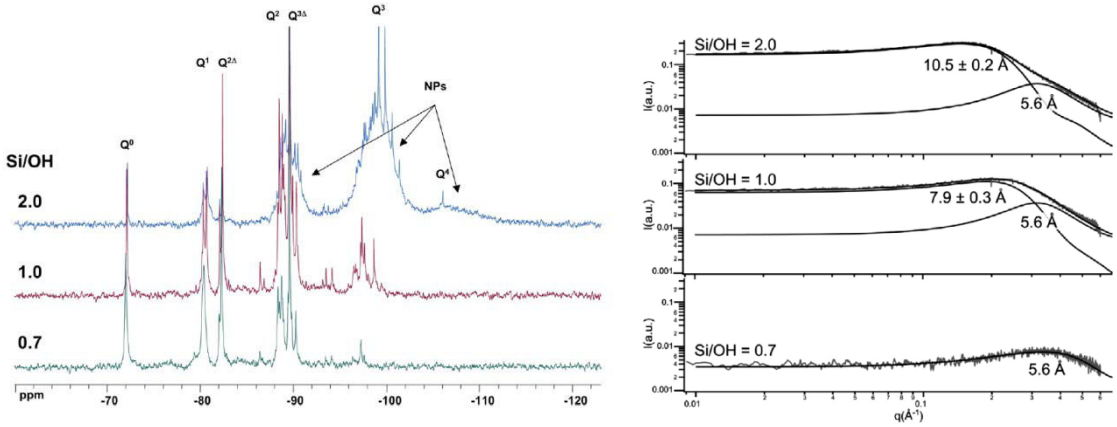

Fig.1. ^{29}Si NMR spectra (left) and SAXS data (right) measured on synthesis mixtures for zeolite beta with different Si/OH ratios prior to heating of the solutions (particle radii are given under the SAXS curves).[83]

Starting from clear reaction solutions with tetraethylammonium hydroxide (TEAOH) as the structure directing template, the silicate speciation has been monitored [83]. The appearance of nanoparticles, indicated by very broad NMR signals, depends strongly on the Si/OH ratio of the reaction mixture as illustrated in Fig. 1. At low Si/OH ratios, no nanoparticles are observed in reaction mixtures prior to hydrothermal reaction whereas at Si/OH > 1 nanoparticles are observed already at room temperature. The NMR line broadening is caused by restriction of the rotational freedom of the silicate species in the emerging solid particles. These observations are corroborated by ESI MS, DLS, and SAXS data. The SAXS curves, as shown in Fig. 1, can be modeled by populations of spherical nanoparticles. In addition, SAXS reveals individual silicate species with sizes of about 1 nm for solutions with Si/OH <1. They can be either larger silicate oligomers or very small silicate nanoparticles that also condense into amorphous nanoparticles upon hydrothermal treatment. ^{1}H NMR and ^{27}Al NMR reveals that the amorphous nanoparticles contain a fraction of the structure directing agent tetraethylammonium hydroxide (TEAOH) and all aluminum present in the reaction mixture. Crystallization of zeolite beta upon hydrothermal heating proceeds then from the amorphous particles and nucleation of the zeolite appears to proceed on the silicate nanoparticles.

Mixing of tetraalkylammonium molecules with an amphiphilic template results in mesoporous silicate with microporous pore walls. That has been investigated in collaboration with the colleagues from the Ruhr University in Bochum. Precursor solutions with tetrapropylammonium hydroxide (TPAOH) have been synthesized and mixed with solutions containing cetyltrimethylammonium bromide (CTAB). In contrast to conventional ordered mesoporous silicates such as MCM-41 and MCM-48, the resulting materials possess microporous walls as could be shown by a combination of analysis techniques, including wide and low angle XRD, adsorption studies, and ^{129}Xe NMR spectroscopy[81]. Analysis of the pair distribution function (PDF) of high resolution XRD data showed that the structure of the silica in the pore walls resembles that of MFI zeolites even though no distinct XRD reflections are observed.

Using the same combination of CTAB and TPAOH in combination with NaF as mineralizing agent, ordered mesoporous aluminosilicate (OMA) with exceptional hydrothermal stability could be synthesized in our laboratory. Structural integrity is maintained in boiling water for at least 5 days as well as upon exposure to water vapor at 600°C for a couple of hours [78]. The silica is formed as spherical particles within radial mesopores (Fig. 2 left) and a large fraction of the aluminium in the pore walls was found to be coordinated tetrahedrally (54 ppm signal in ^{27}Al MAS NMR spectrum, Fig. 2 right). Only a smaller fraction is found in octahedral coordination (signal at 0 ppm). The IR spectrum of pyridin adsorbed on that aluminosilicate showed signals

typical for both, Bronsted and Lewis acid sites, indicating that the obtained aluminosilicate probably also contained structural units similar to those in the MFI zeolite.

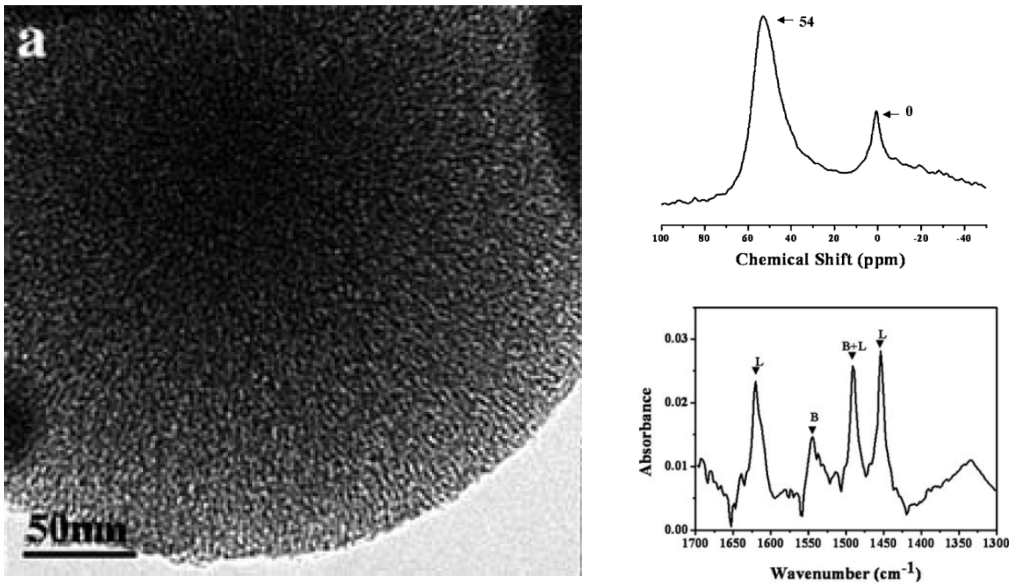

Fig. 2. TEM image of radial channels in ordered mesoporous aluminosilica from CTAB-TPAOH-NaF system (left) and ^{27}Al MAS NMR spectrum (top right) and IR spectrum of adsorbed pyridine (bottom right). [78]

Benzylation of toluene with benzyl alcohol is catalyzed by Bronsted acid sites and the OMA showed more or less quantitative conversion and high selectivity to benzyl toluene (S_{BT} > 70%) whereas commercial ZSM-5 mainly produced benzyl ether (S_{BE} > 90%) at very moderate conversion (C_{BzOH} < 5%). The large mesopores in OMA promote mass transfer and the acidity of the aluminosilicate facilitates the benzylation of toluene.

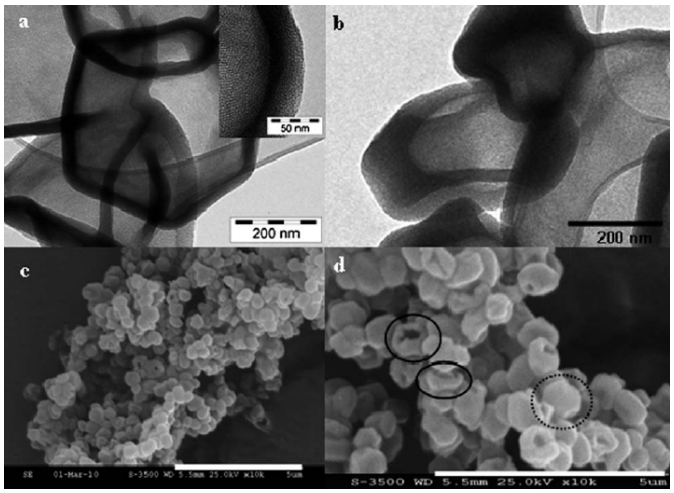

Fig. 3. TEM and SEM images of hollow mesoporous aluminosilicates. [79]

Replacing TPAOH by NaOH in the same reaction mixture as used for the synthesis of the OMA, hollow aluminosilica polyhedra with very thin walls are formed as he hollow polyhedra depends on the thermal reaction at 140°C, the solid

phase is MCM-41 and consists of particles with similar shapes as the final products. The hollow cores are formed during hydrothermal treatment of the aluminosilicate particles. The aluminum-rich outer rims of the MCM-41 particles withstand dissolution whereas the siliceous centers are dissolved. The presence of regular wormhole-type pores with 2-3 nm in diameter indicates a rearrangement of the aluminosilicate in the remaining part of the particles.

The studies on the different silicates allow for a better understanding of formation processes of porous silicates involving particle formation and nucleation. In addition the effect of different mineralizing agents has been evaluated. Dissolution and re-crystallization processes play a crucial role in the later stages of silicate formation. Nanoscopic zeolite particles grow into larger particles via such processes and partial dissolution of larger particles results in largely extended pores as exemplified on the hollow shell materials that could be obtained in a one pot reaction.

Future perspectives

In order to fully understand the formation of silica-based catalysts, investigations on silicate formation and nucleation will be continued. On short term level, investigations will be extended to amphiphilic organic molecules, such as for example 4,4′-trimethylenebis[1-CH_3-1-{CH_2-C_6H_6-CH_2-$N^+(CH_3)_2$-C_6H_{12}-$N^+(CH_3)_2$-$C_{22}H_{45}$} piperidinium]OH_6, that template both microporous zeolites and silica mesostructures. On long to mid-term level, that type of investigation will be extended to complementary reaction systems that are used in zeolite synthesis (e.g. formation of zeolites from solid silicate precursors) to fully understand silicate formation.

Publications resulting from this research area:

77, 78, 79, 81,83

WSCH01, WSCH02, WSCH05, WSCH07, WSCH12

External Funding: Ministerium für Innovation, Wissenschaft und Forschung NRW, Ziel2.NRW, EU.

Cooperations: Y. Wang (Shanghai, CN), H. Gies (Bochum, DE), W. Grünert (Bochum, DE), M. Houas (Versailles, FR), F. Taulelle (Versailles, FR), E. Breynaert (Leuven, BE), G. Brabants (Leuven, BE), C. Kirschhock (Leuven, BE), W. Park (Daejeon, Korea), R. Ryoo (Daejeon, Korea)

2.3.10. Research Area "Photocatalysis on Transition Metal containing Microporopus Silicates" (W. Schmidt)

Involved: U. Wilczok, X. Gao, H. Tüysüz

Objective

Quantum chains in microporous titanosilicate materials absorb light and create hole and electron pairs allowing photocatalytic conversion of substrate molecules on terminal sites of the quantum chains. Then investigation of photocatalytic conversions on such titanosilicates is subject of this research area.

Results: Titanium incorporation into the MFI structure results in a zeolite in which the titanium is present in tetrahedral coordination. Octahedral coordination of titanium is observed the microporous titanosilicate ETS-10 as illustrated in Fig. 4.

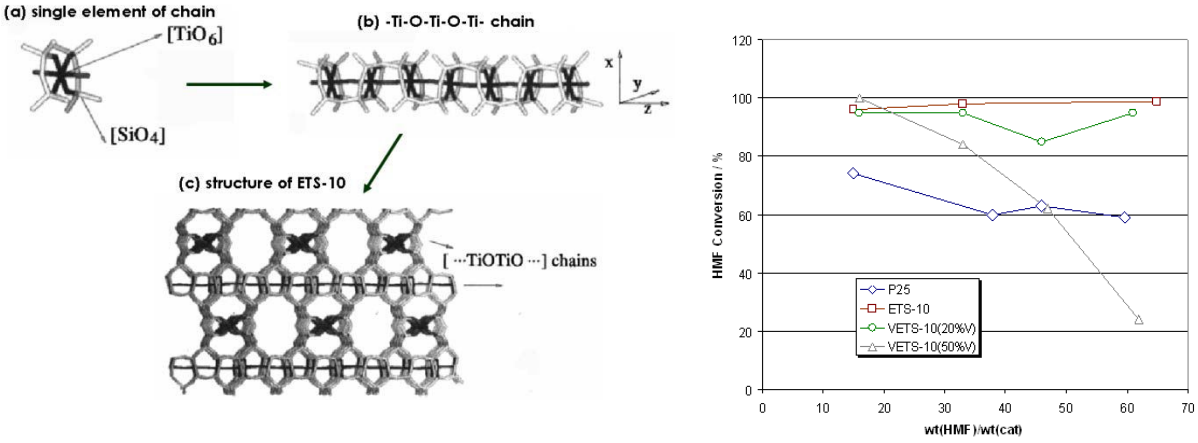

Fig. 4. ETS-10 structure (left) and photocatalytic conversion after 8h reaction time of HMF over different photocatalysts (right).

Extended titanate chains are separated by a silicate framework and thus act as quantum chains with semiconductor properties. Illumination with UV light causes charge separation and as the consequence ETS-10 is a microporous photocatalyst. In an ongoing research project the capability of ETS-10 based photocatalysts is explored. The aim is conversion of molecules that are formed in the product chain of biomass derived molecules into platform molecules for further processing. Selective oxidation of 5-hydroxymethyl furfural, a product of the conversion of sugar, to 2,5-furandicarboxylic acid is under investigation. Different ETS-10 materials have been synthesized including

materials in which titanium was replaced partially by vanadium (20% and 50% replacement of Ti by V). In comparison with the standard TiO_2 reference catalyst P25, ETS-10 based catalysts performed well and showed high conversion under UV radiation. Vanadium containing V-ETS-10 with 20% replacement of Ti by V showed conversion similar to that of the normal ETS-10 whereas V-ETS-10 with 50% replacement of Ti by V showed lower conversion at higher concentrations of HMF. Analysis of the reaction products revealed that the major reaction products were organic acids with low molecular weight. Formic acid is one of the main products whereas little conversion to carbon dioxide is observed. Thus, HMF can be efficiently converted under UV radiation but the aimed product, namely 2,5-furandicarboxylic acid, is formed only in small amounts. It seems that the primary oxidation products get fragmented and formic acid is then found as the major product.

Future perspectives

On short term, modified ETS-10 catalysts that absorb visible light, such as V-ETS-10 or transition metal exchanged Ti-ETS-10, will be investigated in photocatalytic conversion of HMF under visible light in order to explore their ability to transform HMF to larger HMF oxygenates under these conditions. On a longer term the investigations of photocatalytic reactions will shift to other substrates accompanied with spectroscopic investigations to achieve a more detailed insight into the role of the transition metal chains in the catalyst.

External Funding: Ministerium für Innovation, Wissenschaft und Forschung NRW, Ziel2.NRW, EU

2.3.11 Research Area "Supported Transition Metal Oxide Catalysts for Low Temperature Application" (W. Schmidt)

Involved: J. Tseng, C. Weidenthaler, A. Pommerin, C. Gawlik

Objective

Certain transition metal oxides, such as cobalt oxide, have been shown to be efficient catalysts for the conversion of CO at ambient conditions. The investigation of supported transition metal based catalysts as low temperature catalyst for alternative conversions is subject of this research area.

Results: Transition metal catalysts that are supported on activated carbons have been synthesized and tested for the conversion of NO_2 under ambient conditions. The research focuses on potential catalysts that can catalyze reactions at ambient conditions. The working principal comprises two steps, i.e. adsorption of noxious gases on an activated carbon followed by catalytic decomposition of the molecules on the catalyst

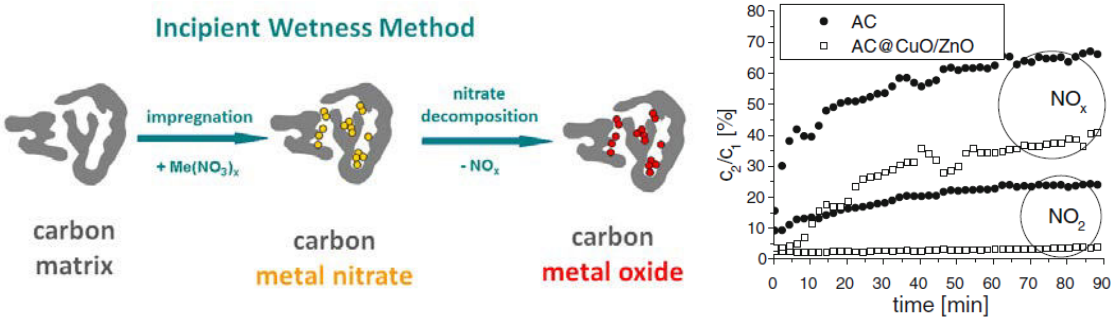

Fig. 1. Preparation of activated carbon (AC) supported transition metal catalyst via wet impregnation (left) and breakthrough curves of NO_x and NO_2 through AC@CuO/ZnO and AC after 6 cycles (right, 23 °C, 50 % r. H., c_1 NO_2 = 4 ppmV, v = 0.2 m/s). [81]

deposited within the pores of the carbon. Different methods for the deposition of pure transition metal oxides (see Fig. 1, left) as well as mixtures thereof have been investigated, i.e. liquid phase impregnation with aqueous transition metal salts or alternatively deposition of oxide precursors via chemical vapor phase deposition [76,82]. The investigations have been performed in collaboration with the Institut für Energie- und Umwelttechnik (IUTA, Duisburg) and the University of Duisburg-Essen.

Hopcalite and mixed CuO/ZnO catalysts showed best performance, especially after successive adsorption cycles as shown in Fig. 1 for CuO/ZnO on activated carbon [82]. In comparison to the pure activated carbon, the NO_x concentration could be reduced significantly. NO_2 is reduced to NO at the carbon surface, a reaction that is also

observed for pure activated carbon. However, the breakthrough curve showing NO_x as the sum of NO_2 and NO for AC@CuO/ZnO proves that the amount of total NO_x is reduced in the presence of the transition metal oxide catalysts.

Transition metal catalysts that are deposited within activated carbons via chemical vapour phase deposition have also been tested for the conversion of NO_2 at a somewhat higher temperature of 150°C. Under these conditions also iron oxide nanoparticles in activated carbon showed conversion of NO_2 to NO that was followed by decomposition of NO to N_2 and CO_2.

Further perspectives:
In order to understand the catalytic processes within the materials under investigation, analysis of the transition metal oxide nanoparticles within the pores of the activated carbons is indispensable. In collaboration with Dr. C. Weidenthaler the different materials will be investigated on a mid-term perspective. Aim of these studies will be evaluation of microstructure properties of the transition metal oxide nanoparticles within a support matrix with diffraction methods. Once this method will be established and evaluated, it will be a valuable tool for investigation of supported catalyst systems in general.

Publications resulting from this research area:
76, 82
External Funding: Arbeitsgemeinschaft industrieller Forschungsvereinigungen (AiF)
Cooperations: U. Sager (Duisburg, DE), F. Schmidt (Duisburg, DE), M. Busch, (Duisburg, DE), B. Atakan (Duisburg, DE), M. Winterer (Duisburg, DE)

2.3.12 Research Area "Design of Nanostructured Materials with High Surface Area for Photo-Electrochemical Water Splitting" (H. Tüysüz)

Involved: G. Dodekatos, T. Grewe, X. Deng

Objective: In this ongoing and planned research project, a systematic and integrated approach encompassing materials synthesis, *in-situ* structural and electrochemical characterization, as well as catalytic and photocatalytic evaluation particularly for water splitting, which is one of the appealing reactions toward development of sustainable energy sources, is carried out. The main goals of this research are design and development of highly active nanocrystals and ordered mesoporous composite (binary and ternary) electro- and photo-catalysts with heterojunctions by using templating processing and post-treatment, in addition to establishment of design rules in terms of particle size, morphology, pore volume and size, surface area, crystallinity and composition for engineered ordered mesoporous photocatalyst materials, and the study of individual effects of material's properties that are responsible for the effective charge separation and catalytic activity.

Results: Even two decades after the discovery of ordered mesoporous materials (OMMs), there is still a great interest in design of OMMs and improvement of synthetic approaches. This class of material supplies many fascinating properties that make them outstanding in a range of applications, in particularly in heterogeneous catalysis as support and catalyst.[32] Some of our efforts are devoted to better understanding of the nanocasting methodology and development of novel functional high surface area materials based on transition metal oxides[4,20,28]. A significant effect has been discovered for the replication of ordered mesoporous Cr_2O_3 and iron doped Co_3O_4. In contrast to the published studies, when cubic ordered mesoporous KIT-6 with 100°C aging temperature is used as a hard template, a cubic ordered mesoporous Cr_2O_3 replica with an uncoupled sub-framework structure that possesses an additional (110) reflection and reduced symmetry is obtained. Furthermore, it is noticed that the structure, morphology and symmetry of the Co_3O_4 replica can be tuned by iron doping during the nanocasting process. A small addition of iron during the impregnation forces Co_3O_4 to develop only in one pore system of the double gyroid silica template in some regions of the parent template, resulting in a replica with lower symmetry, higher pore volume and bi-modal pore size distribution. These findings demonstrate for the first time that the growth mechanism of metal oxides in the channels of the gyroid silica is not only

related to the interconnectivity of the silica template, it also depends on the type and nature of the metal oxide precursor.

We aim to develop novel ordered mesoporous composite materials and examine them as photo and electro-catalyst for water splitting. We initialized our first electrochemical study on ordered mesoporous Co_3O_4.[85] A series of Co_3O_4 with different morphologies, symmetries, surface areas and particle sizes has been prepared by changing the textural parameters of the silica hard template via nanocasting. These materials were tested as electrocatalysts for water splitting. The highest catalytic activity was achieved in a more concentrated alkali solution with Co_3O_4 that has an open sub-framework structure and high surface area. Co_3O_4 with the highest surface area has much better activities than its bulk counterpart and slightly higher activity than material with nanoparticle morphology. The nanocast Co_3O_4 has excellent structural stability that is retained during the electrolysis of water. This material holds promise as a cheap anode for overall water splitting.[85]

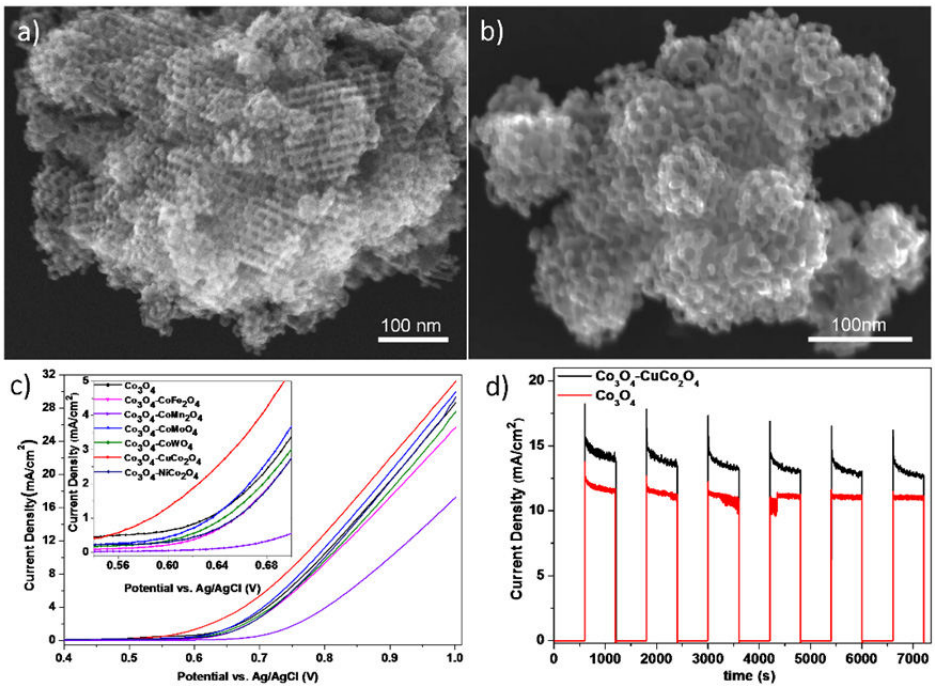

Figure 1. HR-SEM images of ordered mesoporous Co_3O_4 (a) and Co_3O_4-$CuCo_2O_4$ (b) that has been prepared via nanocasting by using silica as hard template. Oxygen evolution currents of as-made Co_3O_4, Co_3O_4-CoM_2O_4 (M= Fe, Mn), Co_3O_4-$CoMO_4$ (M = Mo, W) and Co_3O_4-MCo_2O_4 (M = Cu, Ni) composites dispersed on glassy carbon electrode in 0.1 M KOH electrolyte (c), the inset figure shows the current increment in a narrow voltage range (0.54 ~ 0.70 V vs. Ag/AgCl). Chronoamperometric measurement of Co_3O_4 and Co_3O_4-$CuCo_2O_4$ under a bias of 0.8 V vs. Ag/AgCl for 6000 sec (d) indicating stability of the materials.

Our further study was on enhancement of the electrocatalytic activates of nanocast Co_3O_4. The second generation electrocatalysts are based on binary mixed ordered mesoporous oxides. The surface of nanocast Co_3O_4 could be successfully modified by a

solid-solid reaction with various transition metal salts [24]. The novel method that we develop provides a blueprint for the production of composite materials based on ordered porous oxides that could have interesting physical and chemical properties (Figure 1a-b).[49]

The catalytic activity of the composite materials was studied in electrochemical water splitting, and the Co_3O_4-$CuCo_2O_4$ was found to be most active, with a lower onset potential and higher current density than pure Co_3O_4 (Figure 1c-d). This work opens up new possibilities in developing functional materials with ordered structure and high surface area based on non-precious metal catalysts.[46] A further study concerning the combination of this anode material with a high surface area semiconductor material for photo–electrochemical water splitting is in progress.

The design of third generation electrocatalysts will be based on ternary mixed metal oxides. A study concerning the fabrication of novel ordered mesoporous metal oxide/alloys is in progress as well. In particularly, Co_3O_4/CoPt, CuO/CuPt materials are thought to be remarkable as electrocatalyst based on the previously obtained results. Besides the synthesis and catalytic investigation, a study concerning the conductivity and charge transport on the prepared materials is planned to be carried out to understand the main reason for the catalytic enhancement. For that purpose, there will be an external collaboration with Dr. Steven J. Konezny (Yale University, USA).

Some part of our research is also focused on development of semiconductor nanostructured materials where the effects of junctions between two crystal structures for photocatalytic hydrogen production is studied. A project in collaborating with Prof. C. Chan (Arizona State University, USA) has been started on sodium tantalum oxide based materials since they are among the most stable and active photocatalysts. By a novel method, precisely controlling the reaction parameters, we could fabricate amorphous porous $NaTaO_x$, crystalline $NaTaO_3$ and crystalline $Na_2Ta_2O_6$ with morphologies that consist of a porous structure with interconnected nanoparticles or nanoparticles only. The photocatalytic investigation for overall water splitting indicated that catalytic activity highly depends on the crystal structure and morphology of the samples, with a maximum catalytic activity obtained for crystalline $Na_2Ta_2O_6$ with a nanoparticle and porous matrix structure. It seems that the junctions between two phases or morphologies of sodium tantalum oxides have an important effect on the material's catalytic behavior.[86]

Following this observation, a novel series of sodium tantalum oxide is fabricated to investigate the junctions between two different sodium tantalates.[87] It was shown that the crystal structure, band gap, morphology and textural parameters of sodium tantalates

can be controlled via a feasible hydrothermal route by changing the pH and reaction time. $Na_2Ta_2O_6$ with pyrochlore-type structure, that has an average particle size of around 27 nm, is synthesized at low alkali concentration. By slightly increasing the alkali concentration, another $Na_2Ta_2O_6$ sample with an average particle size of 15 nm and higher surface area is prepared (Figure 2a). Further increasing the alkali concentration results in a series of composite materials based on a mixture of $Na_2Ta_2O_6$ and $NaTaO_3$ (Figure 2b-c). In addition, large $NaTaO_3$ cubes are prepared at very high alkali conditions (Figure 2d). The catalytic activities of the prepared samples are investigated for photocatalytic hydrogen production and their efficiencies are correlated to the composition, surface area and junction between the two crystal structures of the materials (Figure 2e). The highest photocatalytic activity is achieved with $Na_2Ta_2O_6$ nanoparticles with the highest surface area. It is noticed that the hydrogen production rate is not only correlated to the high surface areas of the materials, an enhanced H_2 production is obtained for composite materials that is attributed to junctions between the pyrochlore and perovskite phases of sodium tantalite.[87]

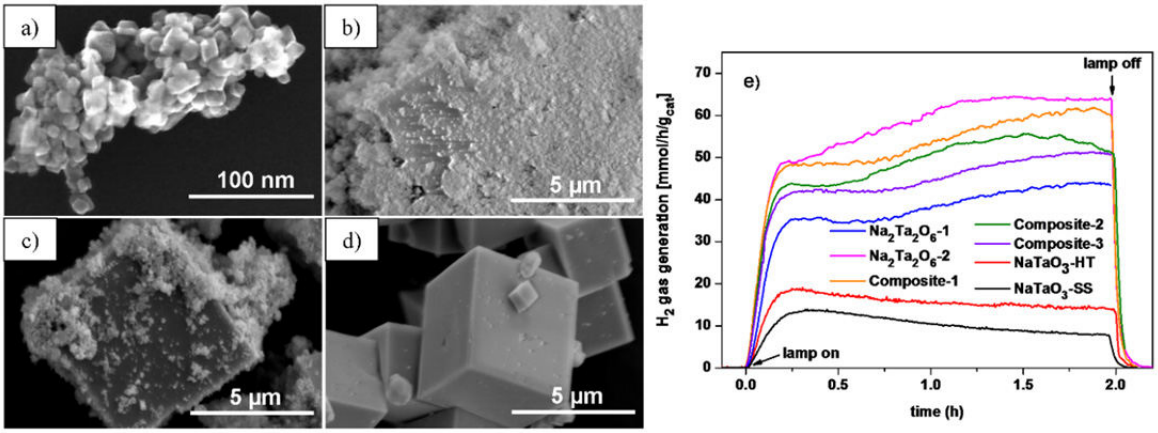

Figure 2. SEM images of $Na_2Ta_2O_6$-2 (a), Composite-2 (b), Composite-3 (c) and $NaTaO_3$-HT (d). Hydrogen production rate of the sodium tantalates prepared by hydrothermal route and the reference material $NaTaO_3$ produced via a solid-solid state.

The above investigations have proven that there is a clear effect of the junctions between two crystal phases of sodium tantalum oxide, which is mainly due to the better charge transfer and separation of electron and holes. A better junction may affect photo-catalytic activity of the material even stronger. In order to study that, systematic studies on design of nanocrystals that have two crystal phases in the same particle are in progress. In addition, a composite material in an ordered mesoporous form might provide much better catalytic activity due to the distinctive material properties like high surface area (provides higher catalytic site), tailored porosity and narrow pore size distribution (allow preparation of composite structure with high heterojunction area and incorporation of catalytically active and selective species such as co-catalysts or

plasmonic nanoparticles), controllable composition and crystallinity (provide flexible composition and crystallinity control that affect material's physical properties including light absorption efficiency and charge transfer). For this purpose, a study related to the preparation of ordered mesoporous composite tantalum oxide and sodium tantalum oxide is in progress as well.

Future directions: The future direction of the research will be focussed on better understanding of the nanocasting process and the design of more efficient materials for electro- and photochemical water splitting. The emphasis will be on fabrication of binary/ternary mixed oxides where a better charge transfer is expected.

Publications resulting from this research area: 4, 20, 24, 28, 32, 49, 84, 85, 86, 87
External funding: Fonds der Chemischen Industrie, DFG Research Fellowship, DFG Cluster of Excellence RESOL
Cooperations: F. Schüth, C. Lehmann, C. Weidenthaler (Mülheim, DE), C. Chan (Arizona State University, USA) Dr. Steven J. Konezny (Yale University, USA), P. Yang (UC Berkeley, USA), M. Wark (Bochum, GE)

2.3.13 Research Area "Advanced X-ray Diffraction Techniques" (C. Weidenthaler)

Involved: A. Dangwal Pandey, M. Felderhoff, U. Holle, C.J. Jia, A. Pommerin, W. Schmidt, V. Tagliazucca, J. Ternieden, J.C. Tseng, H. Tüysüz, A. Wosylus

Objective: Advanced laboratory X-ray diffraction techniques are crucial for the understanding of complex systems and for the establishment of structure-property relationships in catalysis. In-situ techniques and sophisticated data analysis methods are applied in close cooperation with the catalysis groups in order to elucidate the structural details of catalytic materials and to correlate them with the performance of the solids in the catalytic reactions. Moreover, also the limits of the methods are being extended, with a focus on laboratory techniques.

Results: As a continuation of detailed crystallographic investigations of complex aluminum hydrides (see report 2008-2010), powder diffraction studies were extended to aluminum hydrides with cations of higher atomic numbers $(EuAlH_4)_2$, $Sr(AlH_4)_2$.[19] The crystal structures of new members of the family of aluminum hydrides could be solved from heavily overlapping and less resolved XRD patterns by simulated annealing. A major focus of the studies was on the understanding of phase and structure changes during the decomposition of complex aluminum hydrides by means of in situ high temperature X-ray diffraction. The studies reveal also the appearance of new intermediate hydride structures which could be studied in detail. Knowledge about the crystal structures and their structural relationships contributes to the fundamental understanding of the crystal chemistry and the chemical properties of complex aluminum hydrides.

Many of the studies of hydrides have to be carried out in a controlled sample environment. This is even more important in heterogeneously catalyzed reactions. Such in-situ experiments are mostly performed at large facility synchrotron radiation sources providing high intensity radiation and a very flexible experimental setup. However, the experimental time at such facilities is very restricted. Over the last year, a reaction chamber has been adapted on a conventional laboratory powder diffractometer. The catalysis chamber is linked to a gas distribution station which allows the adjustment of the reaction gas flows accordingly to conventional catalysis experiments. This setup enables in situ investigations of catalysts during a catalytic reaction on laboratory instruments also over a long and flexible time period and with high quality data.

Nanostructured hematite (Fe_2O_3), encapsulated in a porous silica shell, was studied in detail with respect to structural changes during the decomposition of ammonia.[11] The sample was prepared on a sieve plate into a ceramic sample holder and heated up from room temperature to 800 °C in a dry NH_3 atmosphere. The reaction gas flowed through the sample with a flow rate set to 15000 cm^3/g h. The analysis reveals a complex sequence of crystalline iron oxide, iron nitride, and metallic iron phases. Additionally, the chemical composition and the crystal structures of the iron nitrides formed between 450 and 700°C change with temperature and time exposed to ammonia. In comparison to the in situ studies, ex situ diffraction experiments performed in parallel emphasize, that phase changes can occur after removing samples from the reaction environment.

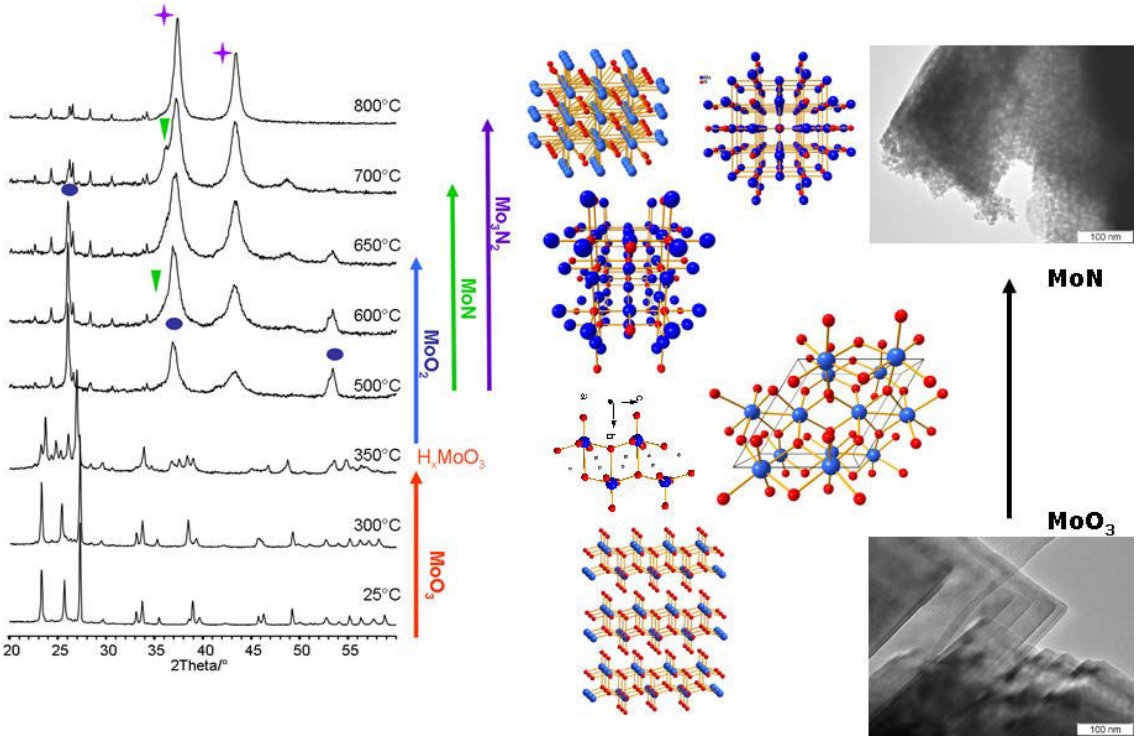

Fig. 1: In situ investigations of the formation of nanosized Mo_xN_y catalysts during the ammonolysis of large MoO_3 crystals

Another type of material investigated as potential catalysts for ammonia decomposition were nanostructured molybdenum nitrides. The entire formation pathway of the nitrides by ammonolyses of oxides was studied qualitatively and quantitatively by in situ XRD and the data were correlated with the catalytic performance (Fig. 1).[40]

These in-house experiments do not only provide a qualitative information on the crystalline catalyst phases involved, but also a quantitative analysis of the sample composition over the entire temperature range. The variation of the chemical composition of the individual phases can be analyzed in detail, and microstructure properties, such as size and defect concentrations, can be evaluated in parallel. The

comprehensive dataset of structural properties can be directly related to the catalytic properties of a distinct catalyst (Fig. 2).

However, it is not only the chemical and the phase composition which influence catalytic performance, it is widely accepted that the microstructure of solid catalysts (defined as domain size and different types of defects) also significantly influence the catalytic properties.

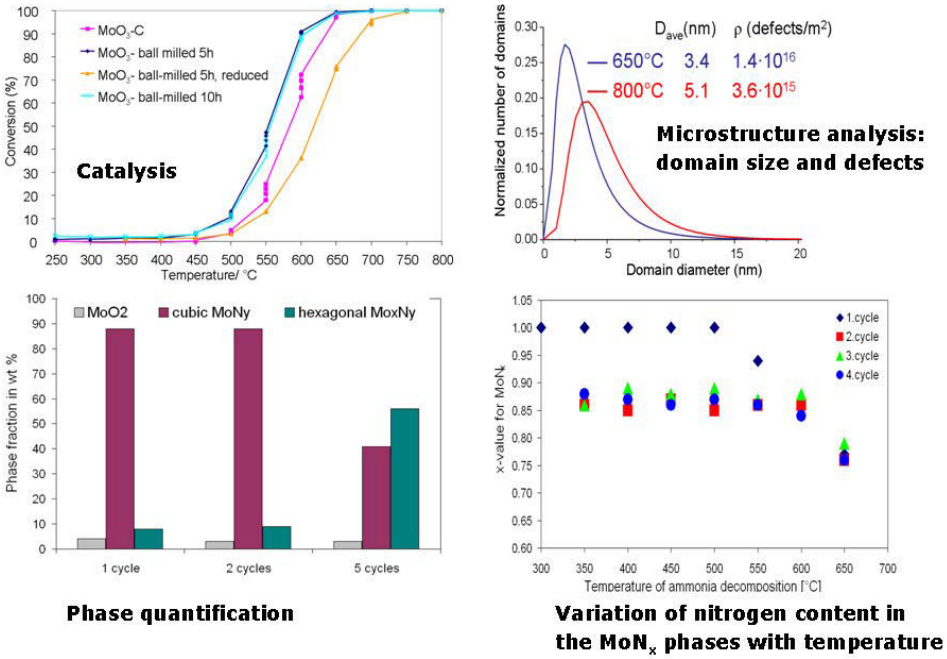

Fig. 2: Results obtained from diffraction experiments and catalytic testing.

Usually, the different types of defects are analyzed by electron microscopy techniques. However, electron microscopy images are often not representative for the entire catalyst sample. To overcome this problem, modern approaches for the evaluation of microstructure properties from powder diffraction data (line profile analyses) have been implemented in the group. The method was used to study the influence of the microstructure of Co_3O_4 on the catalytic performance for CO oxidation. It has been shown, that the addition of small amounts of silica during synthesis enables the size-control of Co_3O_4 catalysts. The domain size and the size distribution were calculated from the diffraction data.[26] The most preferable size distribution with respect to the catalytic performance was obtained for Si:Co of 0.5. Without addition of silica the mean domain size is large (40 nm) and the distribution is very broad. The activity is rather low compared to the samples with narrow size distribution and small mean domains (2-4nm) (Fig. 3). Additionally, microstructure changes taking place under non ambient conditions are more than difficult to monitor by electron microscopy methods. One big advantage of line profile analyses methods is that in addition to the atomic structures

also changes of defect concentrations and/or domain size changes under reaction conditions can be investigated.[43]

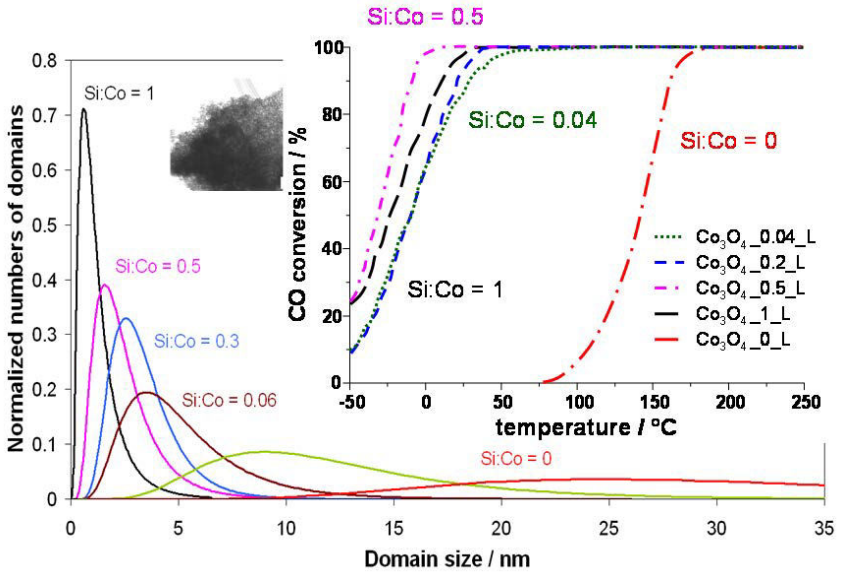

Fig. 3: Variation of size distribution in dependence of Si:Co ratio and influence on low temperature CO oxidation properties.

Microstructure changes of Cr_2O_3 due to ball milling or different temperature treatments have been intensively studied by diffraction methods. In situ studies of mesostructured Cr_2O_3 with interesting magnetic properties performed at lower temperatures (between 220 and 360 K) trace structural changes depending on the synthesis temperatures.[28] In addition to differences on the atomic level, also temperature dependent changes of the crystallite shape are detected (Fig.4).

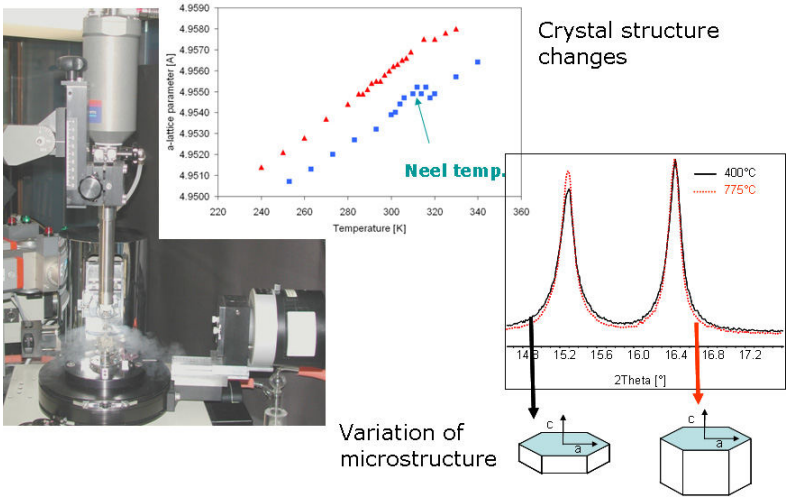

Fig. 4: Diffraction experiments performed in-house at low temperatures, dependence of microstructure properties (morphology changes) on the change of the synthesis temperatures.

Future directions: For synchrotron radiation sources the combination of different analytical methods within one experimental setup is available. However, due to experimental limitations the combination of conventional laboratory diffractometers with other analytical tools is extremely difficult and the technical realization requires extensive efforts. The projected coupling of an in situ XRD reaction chamber with a gas chromatograph will make the simultaneous analysis of structure characteristics and catalytic properties of catalysts feasible. In addition, novel and non-commercial sample cells will be designed to enable the preparation and measurement of metastable, air sensitive compounds under cryo-conditions or elevated gas pressures.
Usually, conventional diffraction experiments and evaluation methods provide information on the average structure only for crystalline materials. In the future, our crystallography studies will be also extended to disordered or partially crystalline nanostructured materials with interesting properties. This will be realized by application of laboratory-scale small angle scattering experiments and the implementation of modern pair distribution function methods.

Publications resulting from this research area: 6, 11, 15, 18, 19, 20, 26, 28, 40, 42, 43, 44, 49, 51, 88, 89, 90

External funding: AiF Arbeitsgemeinschaft industrieller Forschungsvereinigungen

Cooperations: M. Leoni (University Trento), Terry Francombe (ANU Canberra)

2.3.14 Publications 2011-2013 from the Department of Heterogeneous Catalysis

The publications are listed separately for each group of the Department. Many of the publications result from more than one group and therefore appear more than once. In order to avoid the impression that more publications are listed than have actually appeared, such publications are assigned identical numbers. As a consequence the numbering does not appear strictly ascending in this list.

Schüth Group

(1) Onfroy, T.; Li, W.-C.; Schüth, F.; Knözinger, H. *Top. Catal.* **2011**, *54*, 390-397

(2) Schüth, F. *Chem. Ing. Tech.* **2011**, *83*, 1984-1993

(3) Jia, C.J.; Schüth, F. *Phys. Chem. Chem. Phys.* **2011**, *13*, 2457-2487

(4) Benitez, M.; Petracic, O.; Tüysüz, H.; Schüth, F.; Zabel, H. *Phys. Rev. B* **2011**, *83*, 134424-134424

(5) Güttel, R.; Paul, M.; Schüth, F. *Catal. Sci. Technol.* **2011**, *1*, 65-68

(6) Shao, H.; Felderhoff, M.; Schüth, F.; Weidenthaler, C. *Nanotechnol.* **2011**, *22*, 235401/1-235401/7

(7) Wang, G.H.; Li, W.C.; Jia, K.-M.; Lu, A.H.; Feyen, M.; Spliethoff, B.; Schüth, F. *NANO* **2011**, *6*, 469-479

(8) Asahina, S.; Uno, S.; Suga, M.; Stevens, S.M.; Klingstedt, M.; Okano, Y.; Kudo, M.; Schüth, F.; Anderson, M.; Adschiri, T. *Microporous Mesoporous Mater.* **2011**, *146*, 11-17

(9) Schüth, F. *Prax. Naturwiss., Chem. Sch.* **2011**, *60*, 8-13

(10) Schüth, F. *Phys. Chem. Chem. Phys.* **2011**, *13*, 2447-2448

(11) Feyen, M.; Weidenthaler, C;, Guettel, R.; Schlichte, K.; Holle, U.; Lu, A.H.; Schüth, F. *Chem.-- Eur. J.* **2011**, *17*, 598-605

(12) Galeano, C.; Guettel, R.; Michael, P.; Arnal, P.; Lu, A.H.; Schüth, F. *Chem.-- Eur. J.* **2011**, *17*, 8434-8439

(13) Bathen, D.; Burfeind, J.; Felderhoff, M.; Hausschild, K.; Hesske, C.; Peil, S.; Schüth, F.; Urbanczyk, R. *Fuel Cells* **2011**, *11*, 911-920

(14) Bongard, H.J.; Hao, G.P.; Li, W.C., Lu A.H.; Qian, D.; Schüth, F; Wang, A.Q.; Wang, G.H.; Zhang, W.P.; Zhang, T *J. Am. Chem. Soc.* **2011**, *133*, 11378-11388

(15) Jia, C.J.; Schwickardi, M.; Weidenthaler, C.; Schmidt, W.; Korhonen, S.; Weckhuysen, B.; Schüth, F. *J. Am. Chem. Soc.* **2011**, *133*, 11279-11288

(16) Shao, H.; Felderhoff, M.; Schüth F. *Int. J. Hydrogen Energy*, **2011**, *36*, 10828–10833

(17) Schüth, F. *Chem. Mater.* **2012**, *24*, 1-2
(18) Kaper, H.; Grandjean, A.; Weidenthaler, C.; Schüth, F.; Goettmann, F. *Chem.--Eur. J.* **2012**, *18*, 4099-4106
(19) Pommerin, A.; Wosylus, A.; Felderhoff, M.; Schüth, F.; Weidenthaler, C. *Inorg. Chem.* **2012**, *51*, 4143-4150
(20) Tüysüz, H.; Weidenthaler, C.; Schüth, F. *Chem.--Eur. J.* **2012**, *18*, 5080-5086
(21) Schüth, F.; Palkovits, R.; Schloegl, R.; Su, D.S. *Energy & Environ. Sci.* **2012**, *5*, 6278-6289
(22) Meier, J.C.; Galeano, C.; Katsounaros, I.; Topalov, A.A.; Kostka, A.; Schüth, F.; Mayrhofer, K.J.J. *ACS Catal.* **2012**, *2*, 832-843
(23) Meine, N.; Rinaldi, R.; Schüth, F. *ChemSusChem* **2012**, *8*, 1449 - 1454
(24) Tüysüz, H.; Salabas, E.; Bill, E.; Bongard, H.; Spliethoff, B.; Lehmann, C.W.; Schüth, F. *Chem. Mater.* **2012**, *24*, 2493-2500
(25) Guettel, R.; Paul, M.; Galeano, C.; Schüth, F. *J. Catal.* **2012**, *289*, 100-104
(26) Dangwal- Pandey, A.; Jia, C.; Schmidt, W.; Matteo, L.; Schwickardi, M.; Schüth, F.; Weidenthaler, C. *J. Phys. Chem. C* **2012**, 116, 19405-19412
(27) Meier, J.C.; Katsounaros, I.; Galeano, C.; Bongard, H.; Topalov, A.A.; Kostka, A.; Karschin, A.; Schüth, F.; Mayrhofer, K.J.J. *Energy Environ. Sci.* **2012**, *5*, 9319-9330
(28) Tüysüz, H.; Weidenthaler, C.; Grewe, T.; Salabas, E.; Benitez-Romero, M.; Schüth, F. *Inorg. Chem.* **2012**, *51*, 11745-11752
(29) Galeano, C.; Meier, J.C;, Peinecke, V.; Bongard, H.; Katsounaros, I.; Topalov, A.A;, Lu, A.H.; Mayrhofer, K.J.J.; Schüth, F. *J. Am Chem. Soc.* **2012**, *134*, 20.457-20.465
(30) Jiang, H.; Bongard, H.; Schmidt, W.; Schüth, F. *Microporous Mesoporous Mater.* **2012**, *164*, 3-8
(31) Schubert, U.; Nestle, I.; Engel, K.; Schüth, F. *Nachr. Chem.* **2012**, **60**, 784 - 785
(32) Tüysüz, H.; Schüth, F. *Adv. Catal.* **2012**, *55*, 127-239
(33) Schüth, F. *Chemical Energy Storage*; Schlögl, R., Ed., De Gruyter, Berlin/Boston, **2013**, pp 35-48
(34) Hilgert, J.; Meine, N.; Rinaldi, R.; Schüth, F. *Energy Environ. Sci.* **2013***, 6*, 92-96
(35) Zheng, W.; Cotter, T.P.; Kaghazchi, P.; Jacob, T.; Frank, B.; Schlichte, K.; Zhang, W.; Su, D.S.; Schüth, F.; Schlögl, R. *J. Am. Chem. Soc.* **2013**, *135*, 3458-3464
(36) Richter, F.; Pupovac, K.; Palkovits, R.; Schüth, F. *ACS Catal.* **2013**, *3*, 123-127

(37) Soorholtz, M.; White, R.J.; Zimmermann, T.; Titirici, M.M.; Antonietti, M.; Palkovits, R.; Schüth, F. *Chem. Commun.* **2013**, *49*, 240-242
(38) Schüth, F. *Phys. Sataus Solidi B* **2013**, *250*, 1142-1151
(39) Lim, I.H.; Schrader, W.; Schueth, W. Microporous Mesoporous Mater. **2013**, *166*, 20-36
(40) Tagliazzucca, V.; Schlichte, K.; Schüth, F.; Weidenthaler, C. *J. Catal.* **2013**, *305*, 277 – 289
(41) Carrasquillo-Flores, R.; Kaldstrom, M.; Dumesic, J.A.; Rinaldi, R.; Schüth, F. *ACS Catal.* **2013**, *3*, 993 – 997
(42) Schmidt, W.; Schüth, F.; Weidenthaler, C. *Comprehensive Inorganic Chemistry II*, Poeppelmeier, K.; Reedijk, J., Eds.; Elsevier, **2013**; pp 1-24
(43) Immohr,S.; Felderhoff,M.; Weidenthaler,C.; Schüth, F. *Angew. Chem., Int. Ed.* **2013**, *52*, 12688–1269
(44) Galeano, C.; Baldizzone, C.; Bongard, H.; Spliethoff, B.; Weidenthaler, C.; Meier, J.C.; Mayrhofer, K.J.J.; Schüth, F. *Adv. Funct. Mater.* **2013**, *24*, 220–232.
(45) Gu, D.; Schüth, F. *Chem. Soc. Rev.* **2013**, *43*, 313-44
(46) Richter, F.; Meng, Y.; Klasen, T.; Sahraoui, L.; Schüth, F. *J. Catal* **2013**, *308*, 341-351
(47) Wang, G.H. ; Hilgert, J.; Richter, F.; Wang, F.; Bongard, H-J; Spliethoff, B.; Weidenthaler, C.; Schüth, F. *Nat. Mat.* **2013**, accepted
(48) Trotus, T.; Zimmermann, T.; Schüth., F. *Chem. Rev.* **2013**, DOI: 10.1021/cr400357r
(49) Grewe, T.; Deng X.; Weidenthaler, C.; Schüth, F., Tüysüz, H. *Chem. Mat.* **2013**, *25*, 4926–4935

Schüth Group / Felderhoff

(6) Shao, H.; Felderhoff, M.; Schüth, F.; Weidenthaler, C. *Nanotechnol.* **2011**, *22*, 235401/1-235401/7
(13) Bathen, D.; Burfeind, J.; Felderhoff, M.; Hauschild, K.; Hesske, C.; Peil, S.; Schüth, F.; Urbanczyk, R. *Fuel Cells* **2011**, *11*, 911-920
(16) Shao, H.; Felderhoff, M.; Schüth F. *Int. J. Hydrogen Energy*, **2011**, *36*, 10828–10833
(19) Pommerin, A.; Wosylus, A.; Felderhoff, M.; Schüth, F.; Weidenthaler, C. *Inorg. Chem. **2012**, 51, 4143-4150*
(43) Immohr,S.; Felderhoff,M.; Weidenthaler,C.; Schüth, F. *Angew. Chem., Int. Ed.* **2013**, DOI: 10.1002/ange.201305992

(50) Felderhoff, M.; Zibrowius, B. *Phys. Chem. Chem. Phys.* **2011**, *13*, 17234–17241
(51) Weidenthaler, C.; Felderhoff M. *Energy Environ. Sci.* **2011**, *4*, 2495–2502.
(52) Felderhoff, M.; Urbanczyk, R.; Peil, S. *H_2 – Das Magazin für Wasserstoff und Brennstoffzellen* **2011**
(53) Urbanczyk, R.; Peinecke, K.; Felderhoff, M.; Hauschild, K.; Peil, S. *Wasserstofftechnik*; Lehmann, J., Luschtinetz, T., Eds.; Fachhochschul.: Stralsund, **2012,** 111 - 115
(54) Felderhoff, M.; Urbanczyk, R.; Peil, S. *Green* **2013**, *3*, 113–123

Marlow group

(55) Khan, T. R.; Erbe, A.; Auinger, M.; Marlow, F.; Rohwerder, M. *Sci. Technol. Adv. Mater.* **2011**, *12*, 1-9
(56) Muldarisnur, M.; Marlow, F. *J. Phys. Chem. C* **2011**, *115*, 414–418
(57) Marlow, F.; Muldarisnur M.; Sharifi, P.; Zabel, H. *Phys. Rev. B* **2011**, *84*, 073401-073404
(58) Khan, T., Vimalanandan, A.; Marlow, F.; Erbe, A.; Rohwerder, M. *ACS Appl. Mater. Interfaces* **2012**, *4*, 6221-6227
(59) Muldarisnur, M.; Popa, I.; Marlow, F. *Phys. Rev. B* **2012**, *86***,** 024105
(60) Sharifi, P.; Eckerlebe, H.; Marlow, F. *Phys. Chem. Chem. Phys.* **2012**, *14*, 10324–10331
(61) Schunk, D.; Hardt, S.; Wiggers, H.; Marlow, F. *Phys. Chem. Chem. Phys.* **2012**, *14,* 7490 – 7496
(62) Deng, T.S.; Marlow, F. *Chem. Mater.* **2012**, *24*, 536-546.
(63) Schunk, D.; Marlow, F. *NanoEnergie* **2012**, *7* (CENIDE Newsletter Juni 2012)
(64) Wiggers, H.; Schunk, D.; Marlow, F. *Unikate Universität Duisburg-Essen* **2013,** *43,* 42-51
(65) Deng, T.S.; Sharifi, P.; Marlow, F. *ChemPhysChem* **2013**, *14*, 2893-2896
(66) Khan, T.R.; Vimalanandan, A.; Erbe, A.; Marlow, F.; Rohwerder, M. *Z. Phys.Chem.* **2013**, *227*, 1083-1095

Rinaldi group

(23) Meine, N.; Rinaldi, R.; Schüth, F. *ChemSusChem* **2012**, *5*, 1449-1454
(34) Hilgert, J.; Meine, N.; Rinaldi, R.; Schüth, F. *Energy Environ. Sci.* **2013**, *6*, 92-96

(41) Carrasquillo-Flores, R.; Käldström, M.; Schüth, F.; Dumesic, J.; Rinaldi, R. *ACS Catal.* **2013**, *3*, 993−997

(67) Rinaldi, R. *Chem. Comm.* **2011**, *47*, 511-513

(68) Jäger, G.; Girfoglio, M.; Dollo, F.; Rinaldi, R.; Bongard, H.; Commandeur, U.; Fischer, R.; Spiess, A. C.; Büchs, J. *Biotechnol. Biofuels* **2011**, *4*, 33

(69) Engel, P.; Bonhage, B.; Pernik, D.; Rinaldi, R.; Schmidt, P.; Wulfhorst, H.; Spiess, A.C. *Comput-Aided Chem. Eng.* **2011**, *29*, 1316-1320

(70) Wang, X.; Rinaldi, R. *Energy Environ Sci* **2012**, *5*, 8244-8260

(71) Wang, X.; Rinaldi, R. *ChemSusChem* **2012**, *5*, 1455-1466

(72) Rinaldi, R. *J. Chem. Eng. Data* **2012**, *57*, 1341-1343

(73) Wang, X.; Rinaldi, R. *Angew. Chem., Int. Ed.* **2013**, *52*, 11499-11503

(74) Loerbroks, C.; Rinaldi, R.; Thiel, W. *Chem.--Eur. J.* **2013**, *19,* 16282-16294

(75) Rinaldi, R.; Reece, J. Catalysis for the Conversion of Biomass and Its Derivatives. In *Max Planck Research Library for the History and Development of Knowledge, Proceedings 2,* Behrens, M.; Abhaya D., Eds.;. Berlin **2013**

Schmidt group

(15) Jia, C.J.; Schwickardi, M.; Weidenthaler, C.; Schmidt, W.; Korhonen, S.; Weckhuysen, B.; Schüth, F. *J. Am. Chem. Soc.* **2011**, *133*, 11279-11288

(26) Dangwal- Pandey, A.; Jia, C.; Schmidt, W.; Matteo, L.; Schwickardi, M.; Schüth, F.; Weidenthaler, C. *J. Phys. Chem. C* **2012**, *116*, 19405-19412

(30) Bongard, H.; Jiang, H.; Schmidt, W.; Schüth, F. *Microporous Mesoporous Mater.* **2012**, *164*, 3-8

(42) Schmidt, W.; Schüth, F.; Weidenthaler, C. *Comprehensive Inorganic Chemistry II*, Poeppelmeier, K.; Reedijk, J., Eds.; Elsevier, 2013; pp 1-24

(76) Busch M.; Bergmann, U.; Sager, U.; Schmidt, W.; Schmidt, F.; Notthoff, C.; Atakan, B.; Winterer, M. *J. Nanosci. Nanotechnol.* **2011**, *11*, 7956 – 7961

(77) Gu, X.; Zhu, W.; Jia, C.R.; Zhao, R.; Schmidt, W.; Wang, Y. *Chem. Commun.* **2011**, *47*, 5337 – 5339

(78) Gu, X.; Jiang, T.; Tao, H.; Zhou, S.; Liu, X.; Ren, J.; Wang, Y.; Lu, G.; Schmidt, W.
J. Mater. Chem. **2011**, *21*, 880 – 886

(79) Gu, X.; Tao, H.; Schmidt, W.; Lu, G.; Wang, Y. *J. Mater. Chem.* **2012**, *22*, 2473 – 2477

(80) Schmidt, W. in *Ion-exchange Technology: Theory, Materials and Applications* eds. Inamuddin, I.; Luqman, M., Eds.; Springer; **2012**, pp 277–298

(81) Reichinger, M.; Schmidt, W.; Narkhede, V.V.; Zhang, W.; Gies, H.; Grünert, W. *Microporous Mesoporous Mater.* **2012**, *164*, 21–31

(82) Sager, U.; Schmidt, W.; Schmidt, F.; Suhartiningsih *Adsorption* **2013***, 19*, 1027–1033

(83) Castro, M.; Haouas, M.; Taulelle, F.; Lim, I.; Breynaert, E.; Brabants, G.; Kirschhock, C.E.A.; Schmidt, W. *Micropor. Mesopor. Mater.*, **2013**, online available 03 Sep 2013

Tüysüz group

(4) Benitez, M.; Petracic, O.; Tüysüz, H.; Schüth, F.; Zabel, H. *Phys. Rev. B* **2011**, *83*, 134424-134424

(20) Tüysüz, H.; Weidenthaler, C.; Schüth, F. *Chem.--Eur. J.* **2012**, *18*, 5080-5086

(24) Tüysüz, H.; Salabas, E.; Bill, E.; Bongard, H.; Spliethoff, B.; Lehmann, C.W.; Schüth, F. *Chem. Mater.* **2012**, *24*, 2493-2500

(28) Tüysüz, H.; Weidenthaler, C.; Grewe, T.; Salabas, E.; Benitez-Romero, M.; Schüth, F. *Inorg. Chem.* **2012**, *51*, 11745-11752

(32) Tüysüz, H.; Schüth, F. *Adv. Catal.* **2012***, 55*, 127-239

(49) Grewe, T.; Deng X.; Weidenthaler, C.; Schüth, F., Tüysüz, H. *Chem. Mat.* **2013**, DOI: 10.1021/cm403153u

(84) Deng, Y.; Tüysüz, H.; Henzie, J.; Yang, P. *Small,* **2011**, *7*, 2037-2040

(85) Tüysüz, H,: Hwang, Y.; Khan, S. B.; Asiri, A. M.; Yang, P. *Nano Res.* **2013**, *6*, 47-54

(86) Tüysüz, H.; Chen, C. *Nano Energy* **2013**, *2*, 116-123

(87) Grewe, T.; Meier, K.; Tüysüz, H. *Catal. Today* **2013**, DOI:10.1016/j.cattod.2013.10.092

Weidenthaler group

(6) Shao, H.; Felderhoff, M.; Schüth, F.; Weidenthaler, C. *Nanotechnol.* **2011**, *22*, 235401/1-235401/7

(11) Feyen, M.; Weidenthaler, C;, Guettel, R.; Schlichte, K.; Holle, U.; Lu, A.H.; Schüth, F.: *Chem.-- Eur. J.* **2011**, *17*, 598-605

(15) Jia, C.J.; Schwickardi, M.; Weidenthaler, C.; Schmidt, W.; Korhonen, S.; Weckhuysen, B.; Schüth, F.: *J. Am. Chem. Soc.* **2011**, *133*, 11279-11288

(18) Kaper, H.; Grandjean, A.; Weidenthaler, C.; Schüth, F.; Goettmann, F. *Chem.--Eur. J.* **2012**, *18*, 4099-4106

(19) Pommerin, A.; Wosylus, A.; Felderhoff, M.; Schüth, F.; Weidenthaler, C. *Inorg. Chem.* **2012**, *51*, 4143-4150

(20) Tüysüz, H.; Weidenthaler, C.; Schüth, F. *Chem.--Eur. J.* **2012**, *18*, 5080-5086

(26) Dangwal- Pandey, A.; Jia, C.; Schmidt, W.; Matteo, L.; Schwickardi, M.; Schüth, F.; Weidenthaler, C. *J. Phys. Chem. C* **2012**, *116*, 19405-19412

(28) Tüysüz, H.; Weidenthaler, C.; Grewe, T.; Salabas, E.; Benitez-Romero, M.; Schüth, F. *Inorg. Chem.* **2012**, *51*, 11745-11752

(40) Tagliazucca, V.; Schlichte, K.; Schüth, F.; Weidenthaler, C. *J. Catal.* 2013, *305*, 277-289

(42) Schmidt, W.; Schüth, F.; Weidenthaler, C. Diffraction and Spectroscopy of Porous Solids In: *Comprehensive Inorganic Chemistry II*, Poeppelmeier, K.; Reedijk, J., Eds.; Elsevier, 2013; pp 1-24

(43) Immohr, S.; Felderhoff, M.; Weidenthaler, C.; Schüth, F. *Angew. Chem., Int. Ed.* **2013**, DOI: 10.1002/ange.201305992

(44) Galeano, C.; Baldizzone, C.; Bongard, H.; Spliethoff, B.; Weidenthaler, C.; Meier, J.C.; Mayrhofer, K.J.J.; Schüth, F. *Adv. Funct. Mater.* **2013**, DOI: 10.1002/adfm.201302239

(49) Grewe, T.; Deng X.; Weidenthaler, C.; Schüth, F., Tüysüz, H. Chem. Mat. 2013, DOI: 10.1021/cm403153u

(51) Weidenthaler C.; Felderhoff M. *Energy Environ. Sci.* **2011**, *4*, 2495-2502

(88) Weidenthaler, C *Nanoscale* **2011**, *3*, 792 – 810

(89) Gesing, T.M.; Schowalter, M.; Weidenthaler, C.; Murshed, M.M.; Nénert, G.; Mendive, C.B.; Curti, M.; Rosenauer, A.; Buhl, J.C.; Schneider, H.; Fischer, R.X.F.
J. Mater.Chem. **2012**, *22*, 18814-18823.

(90) Antic, B.; Kremenovic, A.; Jovic, N.; Pavlovic, M.B.; Jovalekic, C.; Nikolic, A.S.; Goya. G.F.; Weidenthaler, C. *J. Appl. Phys.* **2012**, *111*, 074309

Others

(91) Czuprat, O.; Jiang, H.Q. *Chem. Ing. Tech.* **2011**, *83*, 2219 – 2228

(92) Liang, F.Y.; Jiang, H.Q.; Luo, H.X.; Caro, J.; Feldhoff, A. *Chem. Mat.* **2011**, *23*, 4765 – 4772

(93) Rose, M (Rose, Marcus)[1] ; Palkovits, R *Macromol. Rapid Commun.* **2011**, *32*, 1299 – 1311

(94) Neudeck, C.; Kim, Y.Y.; Ogasawara, W.; Shida, Y.; Meldrum, F.; Walsh, D. *SMALL* **2011**, *7*, 869 – 873

(95) Palkovits, R. *Chem. Ing. Tech* **2011**, *83*, 411 – 419

(96) Palkovits, R.; Tajvidi, K.; Ruppert, A.M.; Procelewska, J. *Chem. Comm.* **2011**, *47*, 576 – 578

(97) Van de Vyver, S. ; Helsen, S. ; Geboers, J. ; Yu, F. ; Thomas, J. ; Smet, M.; Dehaen, W.; Roman-Leshkov, Y.; Hermans, I. ; Sels, B.F. *ACS Catal* **2012**, *2*, 2700 – 2704

(98) Sun, L.M. ; Zhao, X.; Jia, C.J.; Zhou, Y.X.; Cheng, X.F.; Li, P.; Liu, L.; Fan, W.L. *J. Mat. Chem.* **2012**, *22*, 23428 – 23438

(99) Cao, Z.W.; Jiang, H.Q.; Luo, H.X.; Baumann, S.; Meulenberg, W.A.; Voss, H.; Caro, J. *Catal. Today* **2012**, *193*, 2 - 7

(100) Liang, F.Y.; Jiang, H.Q.; Luo, H.X.; Kriegel, R.; Caro, J. *Catal. Today* **2012**, *193*, 95 – 100

(101) Li, P.; Zhao, X.; Jia, C.J.; Sun, H.G.; Li, Y.L.; Sun, L.M.; Cheng, X.F.; Liu, L.; Fan, W.L. *Cryst. Growth Des.***2012**, *12*, 5042 – 5050

(102) Mezzavilla, S.; Zanella, C.; Aravind, P.R.; Della Volpe, C.; Soraru, G.D. *J. Mat. Sci.* **2012**, *47*, 7175 – 7180

(103) Luo, H.X.; Jiang, H.Q.; Klande, T.; Cao, Z.W.; Liang, F.Y.; Wang, H.H. ; Caro, J. *Chem. Mat.* **2012**, *24*, 2148 – 2154

(104) Tajvidi, K.; Pupovac, K.; Kukrek, M.; Palkovits, R. *Chemsuschem* **2012**, *5*, 2139 – 2142

(105) Ruppert, A.M.; Weinberg, K.; Palkovits, R. *Angw. Chem., Int. Ed.* **2012**, *51*, 2564 – 2601

(106) Rose, M.; Palkovits, R. *Chemsuschem* **2012**, *5*, 167 – 176

(107) Sun, Q. ; Guo, CZ . ; Wang, G.H.; Li, W.C. ; Bongard, H.J. ; Lu, A.H. *Chem.--Eur. J.* **2013**, *19*, 6217 – 6220

(108) Luo, F.; Jia, C.J.; Liu, R.; Sun, L.D. ; Yan, C.H. *Mater. Res. Bull.* **2013**, *48*, 1122 – 1127

(109) Schulte, J.P.; Grass, S.; Treuel, L. *J. Raman Spectrosc.* **2013**, *44*, 247 – 254

(110) Li, P.; Zhao, X.; Jia, C.J.; Sun, H.G.; Sun, L.M.; Cheng, X.F. ; Liu, L.; Fan, W.L. *J. Mat. Chem.* **2013**, *1*, 3421 – 3429

(111) Liang, F.Y.; Partovi, K.; Jiang, H.Q.; Luo, H.X.; Caro, J. *J. Mat. Chem.* **2013**, *1*, 746 – 751

(112) Op de Beeck, B.; Geboers, J.; Van de Vyver, S.; Van Lishout, J.; Snelders, J.; Huijgen, W.J.J.; Courtin, C.M.; Jacobs, P.A.; Sels, B.F. *Chemsuschem* **2013**, *6*, 199 – 208

2.4. Department of Organometallic Chemistry

Director:

Alois Fürstner (born 1962)

Further group leaders:

Manuel Alcarazo (born 1978)
Group leader since December 2008

Curriculum Vitae: Alois Fürstner

1962	Born in Bruck/Mur, Austria
1980-1987	Studies at the Technical University Graz, Austria; Ph.D. with Prof. H. Weidmann
1990-1991	Postdoctoral Fellow, University of Geneva, Switzerland, with Prof. W. Oppolzer
1987-1992	"Habilitation", Technical University Graz, Austria
1993-1997	Research group leader at the Max-Planck-Institut für Kohlenforschung, Mülheim/Ruhr, Germany
1998-	Director at the Max-Planck-Institut für Kohlenforschung, Mülheim/Ruhr, and affiliated as Professor ("apl. Prof.") with the TU Dortmund University, Germany
2009-2011	Managing Director of the Institute

Awards and Honors

1994	Chemical Industries Prize ("Dozentenstipendium"), Chemical Industry Fund
1998	Ruhr Prize for Arts and Sciences, Mülheim/Ruhr
1999	Leibniz Award, German Research Foundation
2000	Thieme-IUPAC Prize for Synthetic Organic Chemistry
2000	Astra-Zeneca Award for Organic Chemistry
2001	Victor Grignard - Georg Wittig Lecture, Société Francaise de Chimie
2002	Arthur C. Cope Scholar Award, American Chemical Society
2002	Member, National Academy of Sciences Leopoldina
2004	Centenary Lecture, Royal Society of Chemistry
2004	Member, North Rhine-Westphalian Academy of Sciences, Humanities and the Arts
2004	Corresponding Member, Austrian Academy of Sciences
2004	Tetrahedron Chair
2005	Junior Award, International Society of Heterocyclic Chemistry
2005	First Mukaiyama Award, Society of Synthetic Organic Chemistry, Japan
2006	Otto Bayer Prize
2006	Heinrich Wieland Prize
2008	Janssen Pharmaceutica Prize for Creativity in Organic Synthesis
2009	Lord Todd-Hans Krebs Lectureship, RSC
2011	Lilly European Distinguished Lectureship Award

2011	Prelog Medal, ETH Zurich, Switzerland
2013	Elhuyar-Goldschmidt Lectureship, Royal Spanish Society of Chemistry
2013	Prix Jaubert, University of Geneva, Switzerland
2013	Karl Ziegler Prize, German Chemical Society
2013	Kitasato Medal, Tokyo, Japan

Special Activities

2001-2006	Member, Board of Editors of "*Organic Syntheses*"
2001-2007	Scientific Editor, "*Chemical Communications*"
2002-2009	Member of the Scientific Advisory Board, Leibniz Institute for Catalysis at the University of Rostock (LIKAT Rostock)
2002-2010	Member and since 2006 Chairman of the Selection Committee of the Alexander-von-Humboldt Foundation (Feodor-Lynen-Program)
2004-2011	Member, Board of Governors, German Chemical Society
2008	Member of the Search Committee, Institute of Science and Technology Austria (ISTA)
2012-	Member of the Scientific Advisory Board, ISIQ Tarragona, Spain
2013-	Chairman, Editorial Advisory Board of *Angewandte Chemie*

Member of the International Advisory Boards of: "*Topics in Organometallic Chemistry*" (1997-); "*Advanced Synthesis & Catalysis*" (2000-); "*Journal of Organic Chemistry*" (2002-2004); "*Progress in Heterocyclic Chemistry*" (2005-); "*ChemMedChem*" (2006-); "*Nachrichten aus der Chemie*" (2007-2012); „*Synthesis*“ and „*Synlett*“ (2009-); „*ChemCatChem*“ (2009-); „*Israel Journal of Chemistry*“ (2010-), "*Angewandte Chemie*" (2010-), "*ChemPlusChem*" (2012-), "*Comptes Rendue de Chimie*" (2013-)

Organometallic Chemistry

The research in the Department is focused on the development of organometallic catalysts of preparative relevance and the investigation of their mode of action. Prof. Fürstner was appointed Director in 1998; since then, the Department has hosted several young scientists at the outset of their independent academic careers. First in line was Prof. Frank Glorius (2001-2004) who is currently Full Professor at the University of Münster; he was followed by Prof. Stefan Hecht (2005-2006), now Full Professor at the Humboldt-University of Berlin, and Dr. Lisbet Kvaerno (2007-2008), who decided to accept a position in industry after her short stint in Mülheim.

Since December 2008, Dr. Manuel Alcarazo is affiliated with the Department. His group has grown to a considerable size, not least because of his winning of a European Research Council Starting Grant in 2011. The work of Dr. Alcarazo is mainly focused on the design of new ligand structures and their use in homogeneous catalysis. His agenda encompasses the development of catalysts of exceptionally strong π-acidity and their applications in organic synthesis, the exploration of novel "frustrated" Lewis pairs for metal-free hydrogenation and related processes, the exploration of main-group elements in low oxidation states, as well as the investigation of new bonding modes (C–M dative double bonds, for example). This program nicely complements the activities of the Fürstner group.

In methodological regard, the major lines of research in the Fürstner group comprise investigations in the following fields of catalysis research, which are partly interwoven:

- alkene and alkyne metathesis
- carbophilic Lewis acid catalysts
- organoiron chemistry and catalysis
- novel reactivity patterns and ligand design

The 2011-2013 evaluation period has seen activities in each of these areas, although with an uneven emphasis. This is partly due to the fact that an important breakthrough was accomplished in the field of alkyne metathesis which therefore attracted much of our attention. Alkyne metathesis is one of the oldest projects in the group that had been initiated over a decade ago. At that time we had to use catalysts that were exceptionally sensitive and therefore difficult to work with. We now managed to develop a new class of catalysts that are not only considerably more active and selective, but can also be

rendered bench-stable; we thought of this as inconceivable before. Because of their largely superior properties, these new tools (which have recently also been commercialized) turn out to be exceptionally versatile and open many new vistas. This is particularly true if alkyne metathesis is used in combination with carbophilic Lewis acid catalysis for the selective manipulation of the resulting products. Considerable efforts were made during the report period to illustrate this notion. In any case, attempts at integrating alkyne metathesis and gold/platinum catalysis gave access to some of the most complex targets that the Fürstner group has ever been able to conquer.

Yet, the 2011-2013 evaluation period has also seen forays into entirely new methodologies, which might eventually lead to new long-term projects. Driven by the need to convert alkynes into *E*-alkenes under conditions that are compatible with sensitive functionality, we were able to demonstrate that metal catalyzed hydrogenation reactions can be carried out in a *trans*-selective fashion. This highly unorthodox outcome challenges the fundamental *cis*-addition rule that dominates heterogenous as well as homogenous hydrogenation since Sabatier's groundbreaking work. Our current mechanistic hypothesis suggests that other reactions could possibly also be forced to follow a non-conventional *trans*-addition mode. Indeed, we have recently managed to reduce the first *trans*-hydroborations of internal alkynes to practice.

As already briefly alluded to above, the methodologies of interest are scrutinized by applications to the total synthesis of structurally complex natural products of biological significance. Because the target molecules themselves are often highly precious and hardly available otherwise, we team up with external cooperation partners to probe their biochemical/biological properties. Where deemed appropriate, we are prepared to adjust the original syntheses such that they allow for larger material throughput and/or for the preparation of non-natural analogues ("diverted total synthesis"). The present evaluation report contains two such case studies, which were chemically highly rewarding but led to stunning biological results.

Over the years, close collaborations with Prof. Thiel and coworkers became an integral part of many of our projects. This mutually beneficial work has again resulted in joint publications during the report period. Moreover, it is emphasized that our work would not be possible without the excellent support by the different analytical groups of the Institute.

2.4.1. Research Area "Metathesis" (A. Fürstner)

Involved: D. Gallenkamp, J. Heppekausen, V. Hickmann, A. Kondoh, J. Llaveria, R. Llermet, P. Persich, G. Seidel, R. Stade

Objectives: Teaching olefin metathesis "simple" stereochemistry is arguably the single most important issue of contemporary metathesis research. Whereas other laboratories managed to develop prototype examples of *Z*-selective alkene metathesis catalysts, our group pursues complementary approaches which also furnished some rewarding results.

Results: The development of an efficient and scalable synthesis of ***lactimidomycin*** was a major preoccupation of the group during the report period. This exceedingly rare compound had been claimed to be a highly potent inhibitor of cell migration and might therefore serve as a lead in the quest for anti-metastatic agents. Because of the dauntingly high ring strain of its polyunsaturated macrolide core, we conceived different routes toward this exigent target.

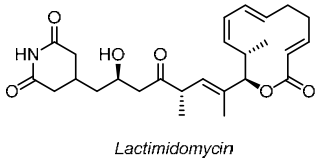

Lactimidomycin

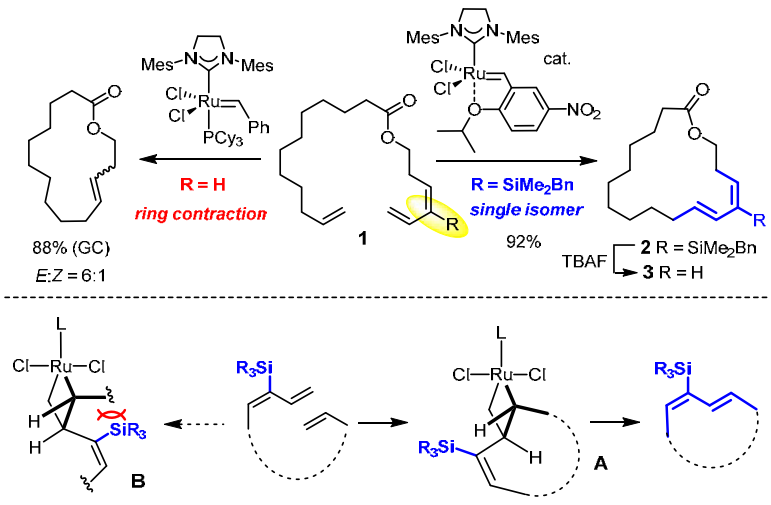

One of them envisaged closure of the 12-membered ring by ordinary olefin metathesis at the diene subunit. 1,3-Dienes, however, are notoriously difficult to make by RCM, because Grubbs-type catalysts are unable to distinguish between the different olefinic sites and therefore often lead to ring contraction; moreover, they are usually stereo-unselective. We conjectured that the introduction of a strategically placed C-silyl group in the substrate might allow these deficiencies to be overcome. In fact, reaction of a model substrate such as **1** (R = $SiMe_2Bn$) with a second generation ruthenium carbene complex furnishes a single metathesis product **2**, from which the desired *Z,E*-diene **3** can be released by protodesilylaton. The multitasking silyl group protects the inner double bond against attack by the catalyst and simultaneously acts as a stereo-directing substituent that favors metallacycle **A** over its diastereomer **B**. This tactics turned out to

be general; indeed, it opened a first successful route to lactimidomycin. Moreover, silylated products such as **2** can also be subjected to post-metathetic transformations other than protodesilylation.

This success notwithstanding, we pursued a second entry into lactimidomycin based on alkyne metathesis (see Chapter 2.4.4). In the end, this route provided the better solution because it is shorter and scales particularly well; it has powered an extensive investigation of the putative cell migration inhibition properties of this class of compounds and ultimately led to the revision of this claim.

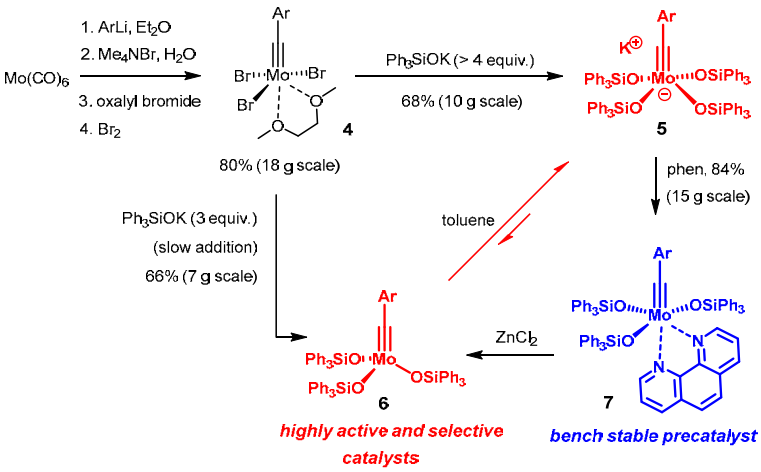

Key to success was a considerable advancement in catalyst design. In the previous evaluation report we had already mentioned that silanolate ligands impart truly outstanding activity onto molybdenum alkylidynes. Following this lead observation, considerable efforts were devoted to this new class of reactive species. To this end, their preparation was fully optimized and can now be carried out on a multi-gram scale. The best entry follows a literature route that allows readily accessible Fischer carbynes to be oxidized to the corresponding Schrock tribromo-alkylidynes **4**. Subsequent ligand exchange via salt metathesis gave access to a large panel of molybdenum alkylidynes in anionic (**5**) or – preferentially – in neutral (**6**) format and allowed the silanolate to be systematically varied. From the application point of view it is rewarding that cheap triphenylsilanol and tris(*p*-methoxyphenyl)silanol gave the most active and selective catalysts.

Importantly, addition of 1,10-phenanthroline or 2,2'-bipyridine provides bench stable adducts **7**. Upon reaction with metal salts ($ZnCl_2$, $MnCl_2$ etc.) that bind phenanthroline more tightly, however, the active alkylidyne **6** can be released undamaged and hence the excellent application profile of these powerful catalysts be harnessed without any special precautions or recourse to Schlenk techniques.

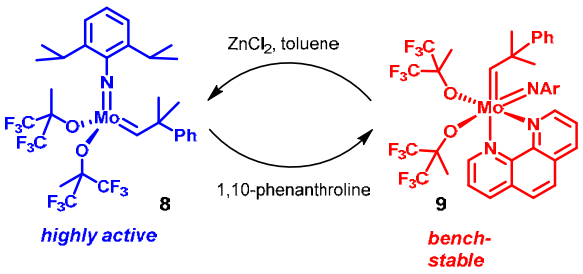

The underlying idea turned out to be more general: Schrock molybdenum alkylidenes such as **8** are amongst the most powerful olefin metathesis catalysts known to date, but mandate very careful handling. This inconvenience can be circumvented via the corresponding phenanthroline- or bipyridine adducts **9**, which are bench-stable and hence very user-friendly; once again, the active species can be regenerated on treatment with $ZnCl_2$ in toluene.

Alkylidynes endowed with silanolate ligands catalyze many alkyne metathesis reactions with unprecedented rates at or even below room temperature; under these conditions however, the released 2-butyne by-product does not evaporate (bp = 27 °C) and hence full conversion would not be reached. It was shown that this problem is easily fixed upon addition of molecular sieves (MS 5Å) which traps 2-butyne; moreover, this additive retards the eventual hydrolytic cleavage of the silanolate ligands and hence exerts a positive effect on the catalyst lifetime.

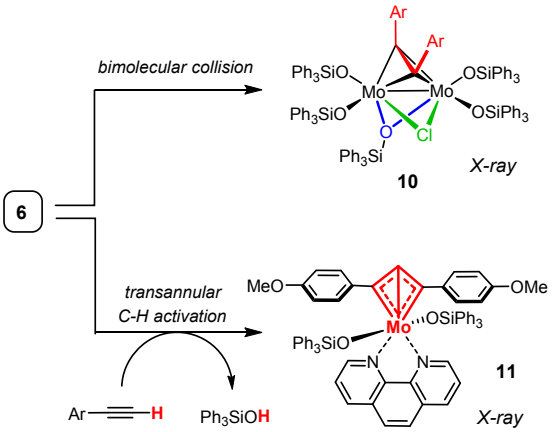

The major decomposition pathways of these catalysts were also carefully investigated. Other than by hydrolysis, they primarily decay via bimolecular collision with formation of dimetallatetrahedrane complexes **10**; gratifyingly though, the "peripheral" bulk of the R_3SiO-groups disfavors this process. Another decomposition pathway operates with terminal alkynes, which are subject to transannular C-H activation after the initial [2+2] cycloaddition; this process, however, requires gentle heating and is retarded due to the fairly low basicity of the silanolates.

Importantly, structural and spectroscopic data gave valuable insights into the origins of the remarkable synergy between silanolate ligands and the operative molybdenum alkylidyne unit. It is believed that their "adaptive electronic properties" are the single most important feature. Thermal motion results in constant stretching and bending of the Mo–O–Si hinges, which gently modulates the donor properties of the ligands and hence the Lewis-acidity of the central metal. This, in turn, allows the catalyst to meet

the different electronic optima of the individual steps of the catalytic cycle and therefore renders the turnover very facile.

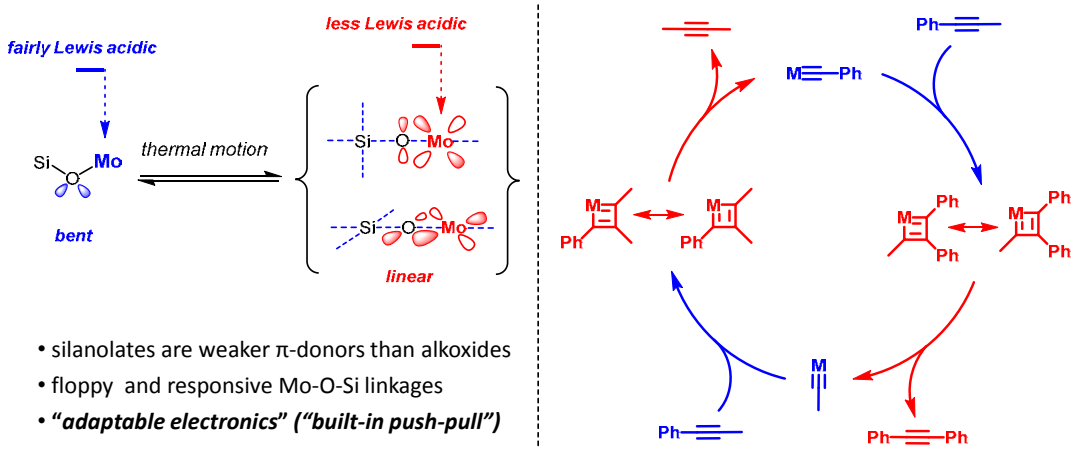

The arguably most rewarding aspect is the outstanding functional group compatibility of **6** and congeners. Although these catalysts comprise a cheap and early transition metal, their tolerance is reminiscent of what one usually expects from noble metals. Even commonly problematic groups such as basic amines or divalent sulfur seem to pose no problem. Limitations are encountered with substituents that are able to protonate the silanolate ligands off as well as with sterically very hindered substrates. Current efforts are directed towards closing these few remaining gaps in coverage.

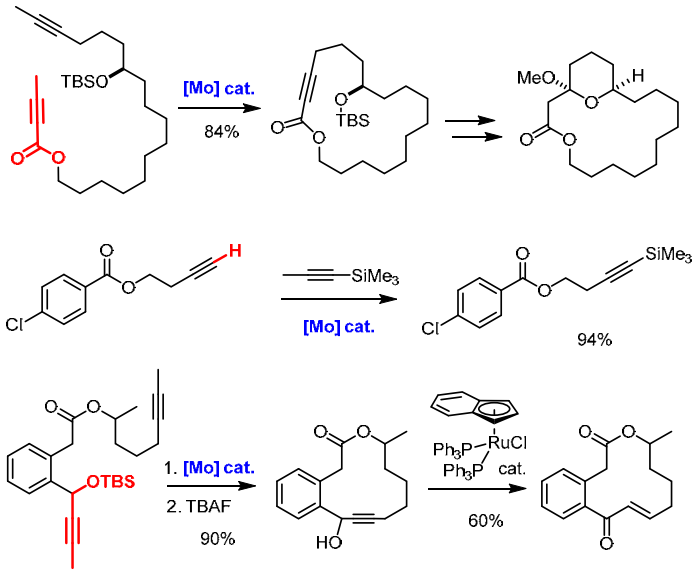

Furthermore, **6** is sufficiently reactive to accept substrates that were problematic or even totally inert before. This includes electron rich as well as electron poor acetylenes, propargyl alcohol derivatives, and even terminal alkynes. Moreover, the first successful examples of ring opening alkyne cross metathesis reactions could be achieved. This largely increased substrate scope opens many new opportunities.

Importantly, the new alkyne metathesis catalysts rigorously distinguish between the π-systems of alkynes and alkenes; the latter remain untouched independent of whether

they are terminal, internal or conjugated to a functional group. Likewise, only the triple bond of an 1,3-enyne will react. This remarkable chemoselectivity profile predestines alkyne metathesis for applications to polyunsaturated targets as well as to the synthesis of 1,3-dienes, independent of whether they are *E,E*-, *E,Z*- or *Z,Z*-configured.

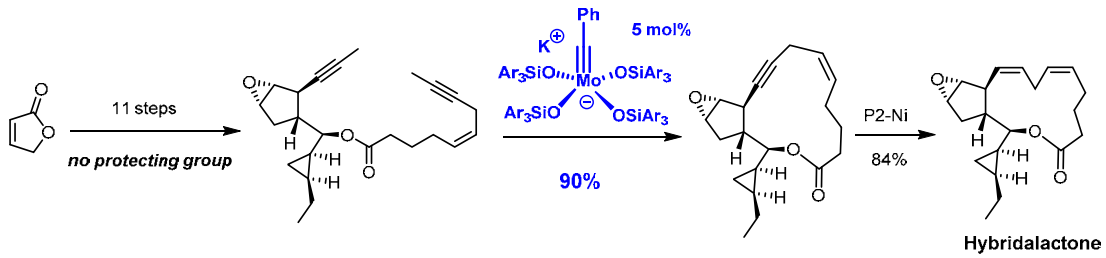

This notion is corroborated by several advanced syntheses (see the following Chapters). An illustrative example is the protecting-group free approach to the rather fragile marine prostanoid ***hybridalactone***. Attempts at forging the macrocyclic frame containing two *Z*-configured olefins with the help of (*Z*-selective) alkene metathesis catalysts result in instantaneous ring contraction. In contrast, alkyne metathesis allows the site of ring closure to be unambiguously defined. Furthermore, this example showcases that the functional group tolerance of silanolate bearing catalysts is largely superior to that of the classical Schrock alkylidyne (tBuO)$_3$W≡CCMe$_3$, which destroys the acid sensitive cyclopropylmethyl carbinol subunit in the cyclization precursor.

Since acetylenes are privileged substrates for gold/platinum catalysis, alkyne metathesis is obviously serviceable in this context too; several examples compiled in the following Chapter illustrate this aspect. Additional applications to bioactive target molecules, including the scalable route to ***lactimidomycin*** and analogues, are found in Chapter 2.4.4.

Finally, we note that other groups start to use our new alkyne metathesis catalysts, as evident from several applications published in the recent literature. It is hoped that the commercial availability of **6** and the stabilized variant **7** will help to make these powerful tools more popular.

Future directions: Fill the few remaining gaps with regard to functional group tolerance, optimize the activation mode for the bench stable pre-catalysts, find additional applications were alkyne metathesis might be uniquely enabling.

Publications resulting from this research area: 4, 7, 9, 10, 16, 21, 28, 30

External funding: Alexander von Humboldt Foundation (fellowship to J. Llaveria), SusChemSys (Ziel 2 Programm NRW, fellowship to J. Heppekausen), Chemical Industry Fund

Cooperations: none

2.4.2. Research Area "π-Acid Catalysis" (A. Fürstner)

Involved: S. Benson, L. Brewitz, W. Chaladaj, M.-P. Collin, M. Corbet, T. de Haro, J. Llaveria, L. Mantilli, K. Radkowski, C. Regens, G. Seidel, H. Teller, G. Valot, A. Yada

Objective: Guided by our own early mechanistic proposal on how gold-, silver- or platinum-based π-acidic catalysts might operate, we continue to investigate the true nature of the reactive intermediates. In parallel, we try to showcase the significance of carbophilic catalysis by implementations into the late stages of multistep total syntheses. Another line of research concerns asymmetric gold catalysis.

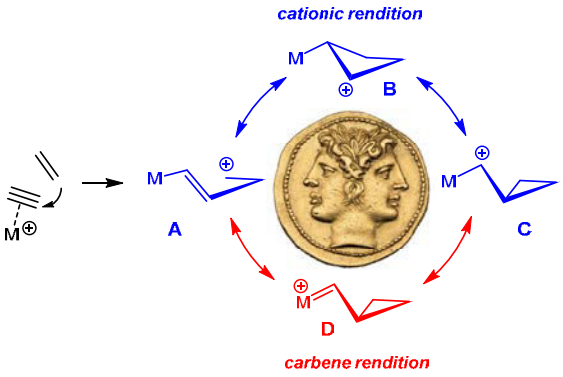

Results: As early as 1998, we proposed a unifying mechanism for π-acid catalyzed addition reactions to alkynes. It implied the intervention of carbenoid species as reactive intermediates which closely resemble (non-classical) cations stabilized by the transition metal center. Although the involvement of carbenoids is now generally accepted, the true nature of such species continues to be a matter of debate. This is largely due to the fact that gold carbenoids basically escaped spectral and structural analysis. The only fully characterized examples pertinent to mechanistic discussion were previously prepared by our group via rearrangement of substituted cyclopropene derivatives such as **1** at low temperature. The resulting products **2**, however, must be viewed as alkenylgold complexes carrying positive charge on the ligand since they exhibit only marginal C–Au double bond character. Other authors have objected that the oxygen substituents – which are needed to avoid substrate polymerization – might unduly disfavor the carbene resonance form.

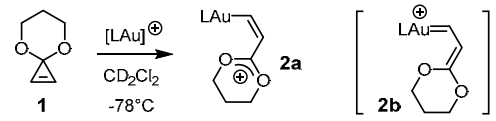

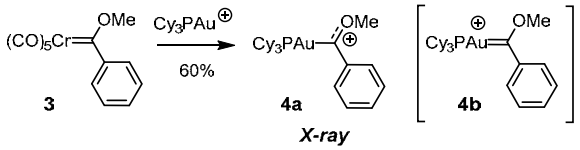

As a consequence, we pursue several complementary approaches towards *unstabilized* gold carbenoids, most notably via carbene transfer. It is well precedented in the literature that Fischer

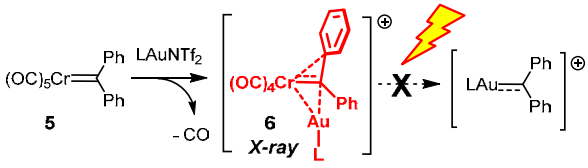

carbenes of tungsten or chromium can be "transmetalated" on treatment with Au(+1). First, we convinced ourselves of the exceptional ease of this reaction, which allowed complex **3** to be transformed into **4** even at –50 °C. As expected, the latter shows a long C–Au but a short C–O bond and is thus best viewed as an oxocarbenium cation in the coordination sphere of gold. When applied to the diphenylchromium carbene **5** however, an analogous transmetalation fails. Rather, the quite unusual bimetallic complex **6** is formed, as confirmed by X-ray diffraction. Although one of the CO ligands of the starting material is lost, breakdown with release of an unstabilized gold "carbene" does not take place; rather, the chromium center engages in a weak interaction with one of the phenyl groups which arguably provides more steric shielding than electronic compensation. Extensive DFT calculations allowed the bonding situation in this and related complexes to be deciphered. Overall, complex **6** basically represents a chromium carbene carrying an η^2-bound gold unit but has little to do with an unstabilized gold carbene. Such species therefore continue to remain elusive form the experimental vantage point, since three of the very best entries into carbene complexes failed to deliver (diazo decomposition, cyclopropene rearrangement, carbene transfer).

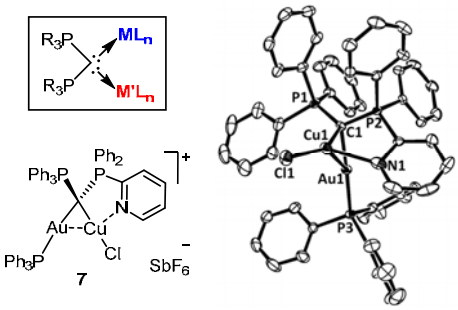

Earlier studies from this laboratory had indicated the possible intervention of *gem*-diaurated complexes in certain gold catalyzed reactions. During the current report period, many additional examples of such species were prepared. Moreover, it was found that *gem*-heterobimetallic complexes are also easy to make. A particularly interesting example is the gold/copper complex **7**, which carries a non-symmetrical carbodiphosphorane ligand (prepared in cooperation with the Alcarazo group). As its central atom C-atom is formally zerovalent, **7** is the first example of a chiral "carbone" complex in which all bonds about the metalated center are arguably capto-dative.

Alkenyl gold species with an oxygen substituent at the β-position are particularly prone to *gem*-diauration. Since the resulting complexes are surprisingly unreactive, we proposed that they might actually be off-cycle and hence constitute unproductive sinks for the precious gold catalysts. This hypothesis allowed the advantageous effect of acetic acid on a conceptually new approach to 4-hydroxypyrones to be rationalized. Driven by the need to make the heterocyclic nucleus of the naturally occurring cyclophane derivative ***neurymenolide A*** under notably mild conditions (this target is

unusually sensitive by virtue of its skipped polyene backbone), we conjectured that alkynyl ketoesters such as **8** might be adequate starting materials.

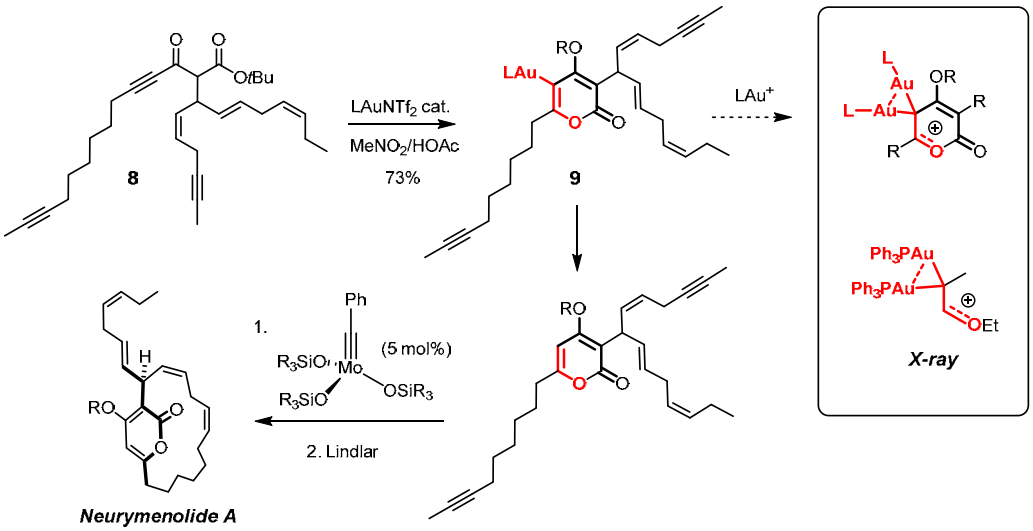

Activation of compound **8** with a carbophilic π-acid engenders a 6-*endo* cyclization with formation of the desired heterocyclic ring. In neutral media, the reaction proceeds rather slowly (12-24 h), whereas addition of small amounts of HOAc results in a dramatic rate acceleration (ca. 15 min). Control experiments suggest that the acid favors the proto-demetalation of the gold complex **9** primarily formed over competing *gem*-diauration. This preparative set-up was quintessential for the total synthesis of neurymenolide, which capitalizes on a substrate containing no less than six different non-conjugated sites of unsaturation (not counting the highly enolized β-oxoester). Alkyne metathesis of the resulting diyne **10** forged the macrocyclic perimeter while leaving all preexisting alkene sites untouched, independent of their configuration.

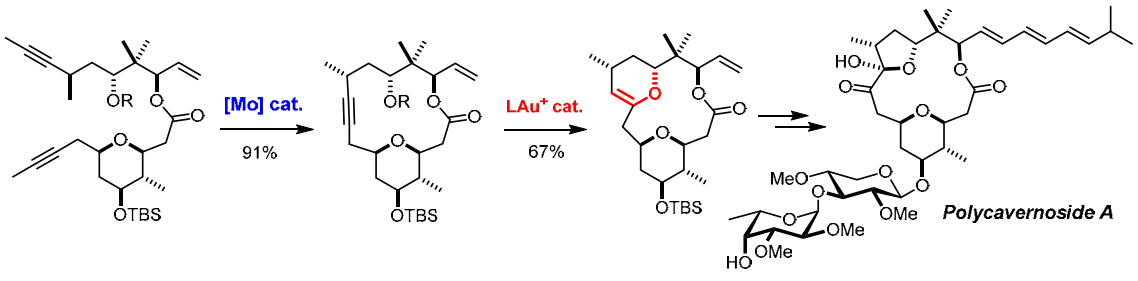

The interplay between alkyne metathesis and alkyne functionalization with the aid of π-acidic catalysts also formed the conceptual basis of several other total syntheses. The most demanding ones were those of ***polycavernoside A***, ***amphidinolide F*** and ***spirastrellolide F***. The densely functionalized macrocyclic frames of these intricate targets could invariably be closed by alkyne metathesis using the newly developed

molybdenum alkylidynes endowed with silanolate ligands, which attests to the excellent performance and functional group tolerance of these new catalysts.

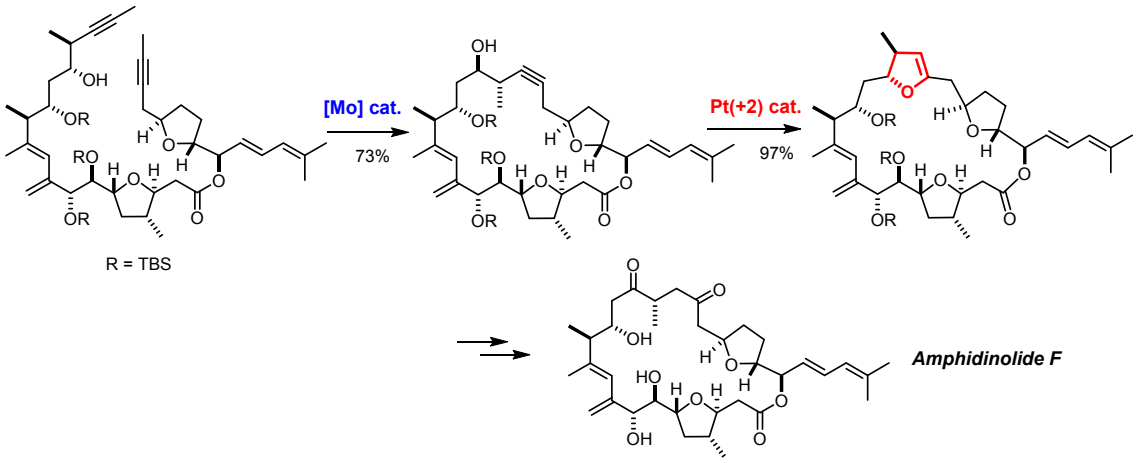

In case of polycavernoside A and amphidinolide F, the resulting cycloalkynes were subjected to exquisitely selective transannular hydroalkoxylation reactions catalyzed by Au(+1) and Pt(+2), respectively. In case of spirastrellolide F, a gold catalyzed spiroketalization was envisaged. Because of severe steric hindrance about one of the two hydroxyl groups, however, the addition stopped at the enol ether stage; yet, the oxygen pattern got properly set and hence a simple Brønsted acid sufficed to complete the acetalization.

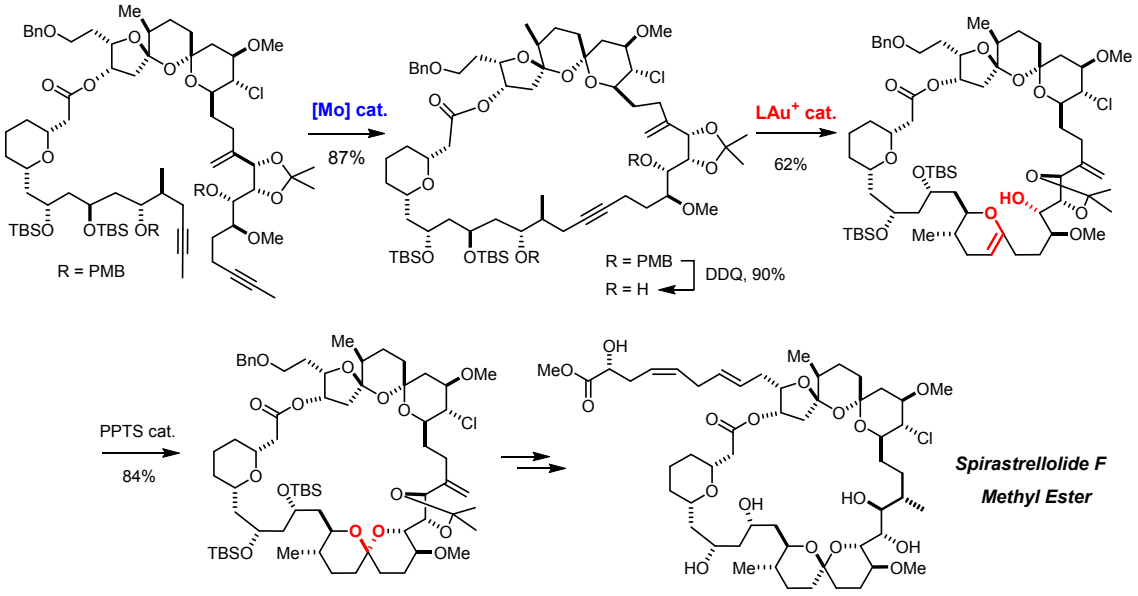

In addition to these massive projects, we were exploring several other opportunities of how metathesis and π-acid catalysis might be integrated in preparatively meaningful

ways. Some of these exploratory studies have already transfigured into “real” synthesis projects in the recent past.

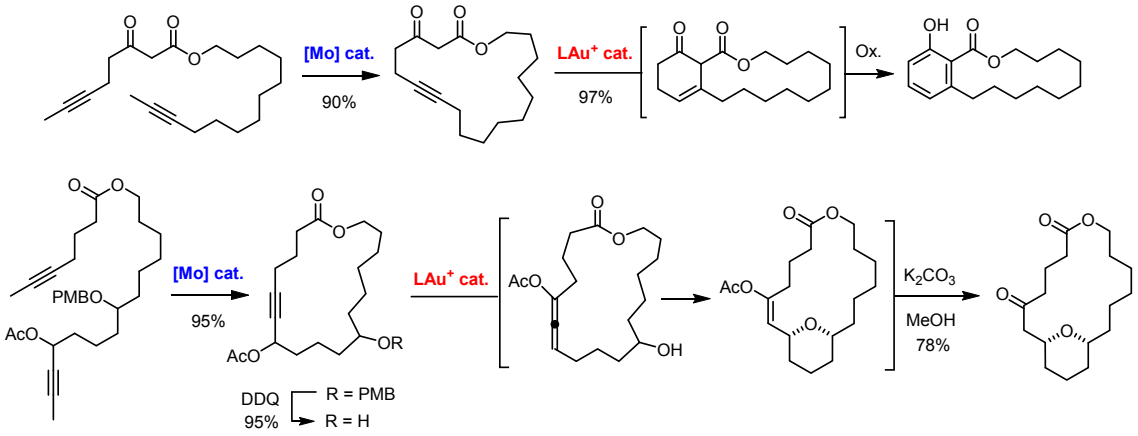

Another important topic is asymmetric gold catalysis, which is particularly challenging due to the peculiarities of the coordination chemistry of Au(+1) and the outer-sphere nature of gold catalyzed processes. In the last evaluation report, we disclosed our basic ligand design that consists of one-point binding phosphoramidites comprising a TADDOL-related scaffold with an acyclic backbone.

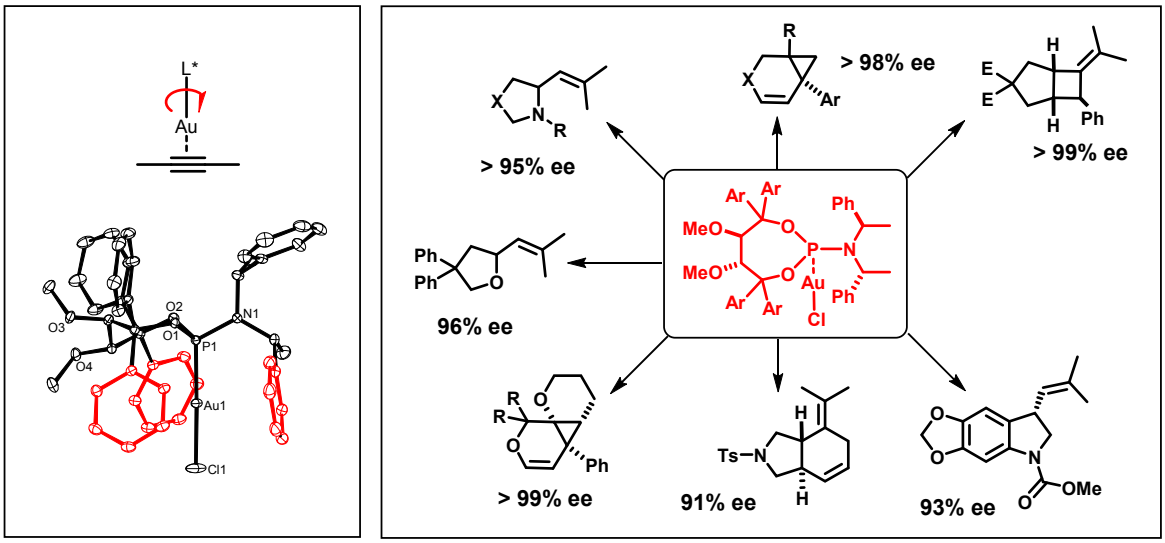

This latter structural element is essential, as it allows three of the aryl substituents to craft an effective C_3-symmetric binding site that is deep enough to reach over the gold center and impose asymmetry on the ensuing reaction. Moreover, these ligands are fairly easy to make, allow for substantial structural variation, and have molecular weights that are considerably smaller than those of competing ligands currently used in asymmetric gold catalysis. We optimized their synthesis and extensively studied their

performance. They were shown to impart outstanding enantioselectivities upon a number of mechanistically different transformations, including [2+2] and [4+2] cycloadditions, indoline formations, as well as intramolecular hydroaminations and hydroalkoxylations of allenes. Likewise, they excel in the cycloisomerization of enynes, which enabled a remarkably efficient synthesis of the antidepressive agent (–)-GSK 1360707. Moreover, our understanding of the origin of stereoselectivity has been considerably refined. In cooperation with the Thiel group, we learned how the initially C_3-symmetric pocket of such gold complexes becomes C_1-symmetric after substrate binding, and how a unidirectional rotatory motion of an enyne substrate within this ligand environment explains the enantioselectivity of the ensuing cycloisomerization.

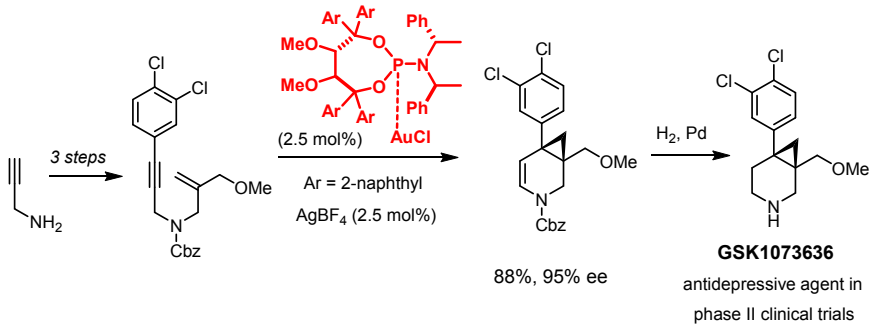

Future directions: Refine our mechanistic understanding of π-acid catalysis, expand the scope of asymmetric gold catalysis and scrutinize the methodology by advanced applications.

Publications resulting from this research area: 8, 11, 15, 18, 23, 24, 27, 29

External funding: Alexander von Humboldt Foundation (fellowship to J. Llaveria), Chemical Industry Fund (stipends to S. Benson and H. Teller), Swiss National Science Foundation (fellowships to T. de Haro and L. Mantilli), Uehara Memorial Foundation (fellowship to A. Yada).

Cooperations: W. Thiel (Mülheim/Ruhr, DE), M. Alcarazo (Mülheim/Ruhr, DE)

2.4.3. Research Area: "New Reaction Modes" (A. Fürstner)

Involved: L. Leseurre, K. Lehr, A. Kondoh, H. Krause, R. Mariz, K. Radkowski, G. Seidel, C.-L. Sun, B. Sundararaju

Objective: We try to find potentially useful transition metal catalyzed reactions that have little or no precedent in the literature.

Results: Despite the exceptional level of sophistication in the area of cross coupling chemistry in general, reactions of substrates that contain the leaving group as integral part of a heterocyclic scaffold are extremely scarce. During the report period, we managed to develop a formal ring opening/cross coupling process of 2-pyrones that epitomizes this largely underrepresented reaction mode. Specifically, it was shown that 2-pyrones react with Grignard reagents in the presence of cheap and benign $Fe(acac)_3$ to give diene carboxylic acids after work up. In all cases investigated, the reaction was stereospecific, in that the incoming nucleophile replaces the lactone leaving group with retention of configuration. Although the overall transformation hence formally represents a "cross coupling" process, it likely proceeds by a sequence of 1,6-addition followed by electrocyclic ring opening. First applications to the synthesis of the indole alkaloid granulatamide B and to a configurationally labile subunit of the potent translation-initiation inhibitor pateamine A augur well for future projects.

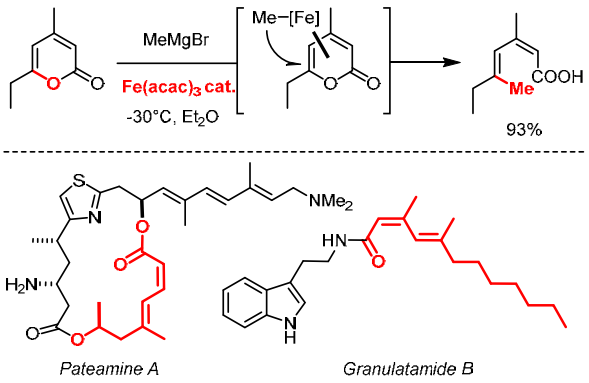

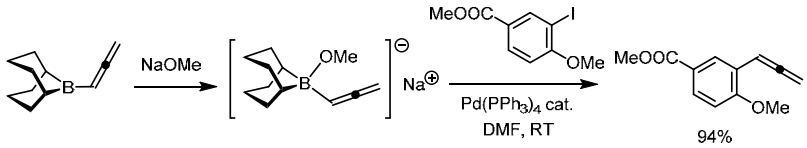

Driven by the need to prepare various types of allenes for use in gold and platinum catalysis, we noticed that cross coupling reactions of allene donors are rare. Despite the tremendously wide scope of the venerable Suzuki–Miyaura reaction, boron-mediated allenylations are basically unknown. We were able to close this gap in structural coverage by demonstrating that the borate complex formed in situ from B-allenyl-9-

BBN and NaOMe in DMF allows aryl- and heteroaryl iodides to be allenylated under mild conditions with good to excellent yields.

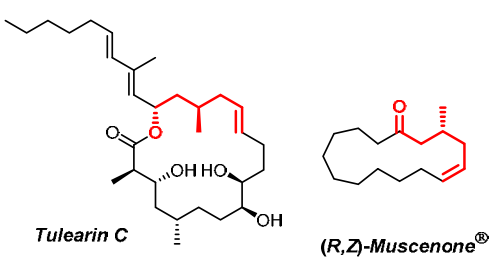

As briefly mentioned in Chapter 2.4.1, the recent literature has witnessed considerable progress toward the development of efficient *Z*-selective alkene metathesis catalysts, whereas inherently *E*-selective catalysts remain elusive. This lack surfaced in an attempted synthesis of ***tulearin C***, where closure of the macrocyclic ring at the *E*-alkene embedded into its framework by RCM afforded poor results. Challenged by this outcome, we devised an alternative entry based on alkyne metathesis followed by formal *trans*-reduction via a hydrosilylation/protodesilylation sequence, which delivered tulearin C in good overall yield and excellent selectivity. In addition, this extensive project had two rewarding methodological spin-offs.

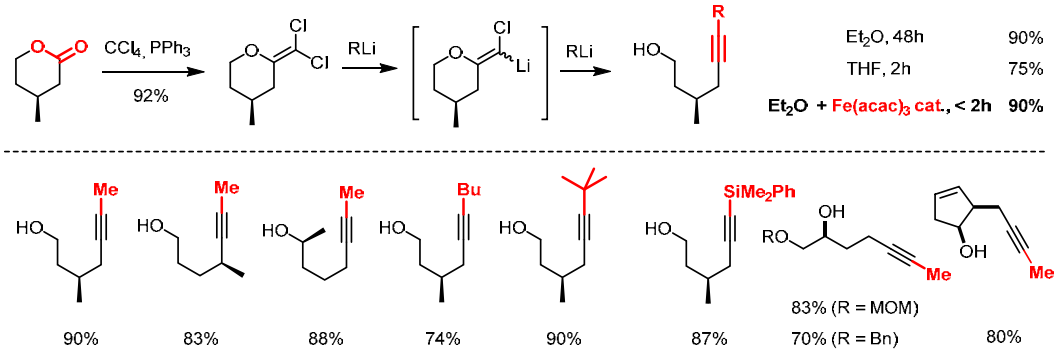

First, we developed a high yielding route to non-terminal alkynes starting from lactones. Transformation into the corresponding *gem*-dichloroalkenes by a literature procedure followed by treatment with an alkyllithium reagent RLi primarily generates lithium carbenoids that are sufficiently electrophilic to intercept an additional equivalent of RLi prior to collapse and release of the product. Although the reaction proceeds uncatalyzed in Et_2O or THF, it is best performed in the presence of $Fe(acac)_3$ as a cheap and benign catalyst (in some cases, copper catalysts are optimal). Under these conditions, the method is quite general and does not lead to epimerization of chiral centers. Although parts of this investigation have already been published, the major body of work still needs to be disclosed. One of the alkyne products thus formed on large scale served as a valuable building block in the total synthesis of ***tulearin C*** mentioned above as well as in a particularly short synthesis of the valuable perfume ingredient ***muscenone***® in optically and isomerically pure form.

The tulearin case study relied on a formal *trans*-reduction of the cycloalkyne formed by RCAM via hydrosilylation/proto-desilylation. Although this sequence originally pioneered by Trost and coworkers served our group well on this and several other occasions, we became interested in developing possible alternatives.

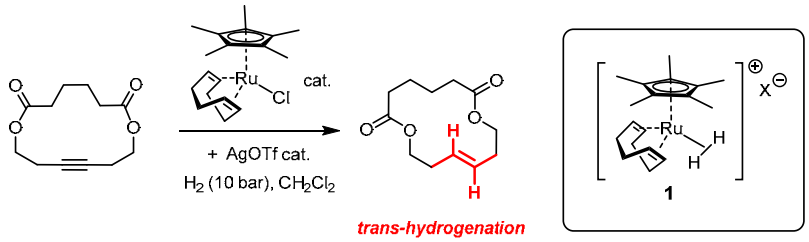

After various unsuccessful trials, we were able to find conditions that allow internal alkynes to be hydrogenated with good to excellent levels of *trans*-selectivity. Although we still need to further improve this transformation (in some cases, over-reduction is observed), it basically constitutes the first broadly applicable and functional group tolerant method that breaks the stereochemical dogma of suprafacial delivery of the two H-atoms to the π-system of the substrate; this rule had remained largely unchallenged for more than a century since Sabatier's groundbreaking work.

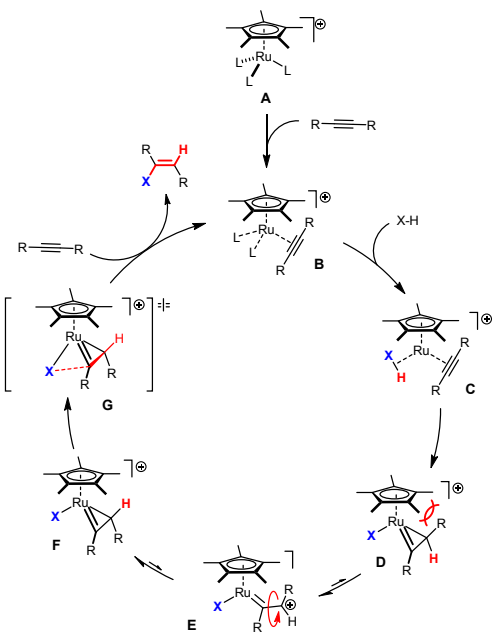

Preliminary mechanistic data suggest that a non-classical hydrogen complex might be the active species (or a precursor to it). We assume that binding of an alkyne forms a loaded complex **C**, in which the acetylene moiety acts as a four-electron donor; this explains why alkenes do not react well under the chosen conditions. This particular bonding situation facilitates an inner-sphere delivery of the hydride with formation of a metalla-cyclopropene **D** (η^2-vinyl complex) without prior generation of a discrete Ru–H species. It is well precedented in the literature that the substituents at the β-carbon atom of such complexes are configurationally labile and easily swap places via a $\eta^2 \rightarrow \eta^1 \rightarrow \eta^2$ hapticity change. Because they are approximately orthogonal to the plane of the metallacyclopropene, the sheer size of the Cp* ring will exert a massive influence on the stereochemical outcome. As a result, isomer **F**, in which the hydrogen rather than

the R group is oriented towards the bulky lid, will be largely favored over **D**. The trajectory of the ensuing reductive elimination places the X-group *anti* to the already transferred H-atom and hence leads to an *E*-configured alkene if X = H.

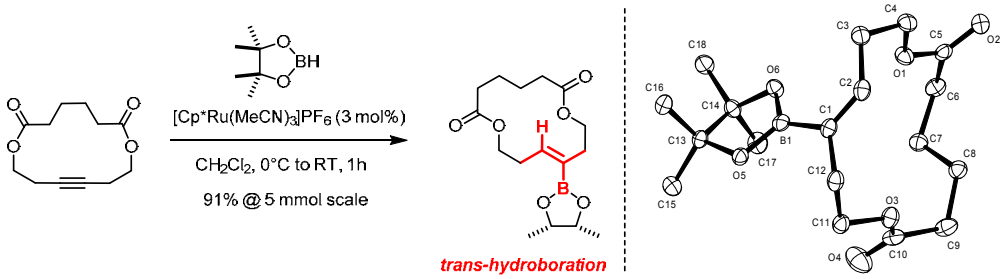

This rationale suggests that reagents H–X with X ≠ H should also be amenable to *trans*-additions across alkynes, provided they are able to form analogous σ-complexes. Indeed, we were recently able to perform the first recorded examples of *trans*-hydroborations of internal alkynes using pinacolborane as a versatile and user-friendly reagent. This transformation is pleasingly facile, rapid, tolerant and high yielding, and might therefore be of some interest. Control experiments showed that the net *trans*-addition observed under our conditions is not the result of a secondary isomerization. From the conceptual viewpoint, this *trans*-addition mode challenges the equally fundament rule that hydroboration proceeds by a *syn*-delivery of boron and hydrogen via a four-membered frontier-orbital controlled transition state. Ongoing investigations intend to explore the scope of these versatile new reactions in more detail. Furthermore, preliminary data suggest that reagents X–H other than H_2 and pin–H can also be forced to follow *trans*-addition pathways.

Future directions: Rejuvenate our program on iron catalysis and explore the scope and limitations of the ruthenium catalyzed *trans*-addition reactions.

Publications resulting from this research area: 2, 12-14, 17, 20, 31

External funding: Alexander von Humboldt Foundation (fellowships to C.-L. Sun and B. Sundararaju), Chemical Industry Fund

Cooperations: none

2.4.4 Research Area "Catalysis Based Syntheses and Evaluation of Bioactive Natural Products" (A. Fürstner)

Involved: A. Arlt, S. Benson, S. Handa, N. Kausch-Busies, A. Kondoh, J. Llaveria, K. Micoine, P. Persich, S. Schulthoff, J. Willwacher

Objectives: We pursue the synthesis of complex natural products by catalysis-based routes, evaluate their biochemical and biological properties in cooperation with external partners, and investigate structure/activity relationships by molecular editing.

Results: As already mentioned in Chapter 2.4.1, ***lactimidomycin*** and related glutarimide macrolides constituted an important focal point of our synthetic work. Although this compound was claimed to be the most potent cell migration inhibitor of a fairly large family of natural products, it had never been made before. In order to close the supply chain and gain access to non-natural analogues for testing, we pursued different routes that might allow the strained head group of this enticing target to be closed. Although the RCM-based entry summarized in Chapter 2.4.1 provided a decent solution, an alternative entry using ring closing alkyne metathesis (RCAM) was ultimately more satisfactory.

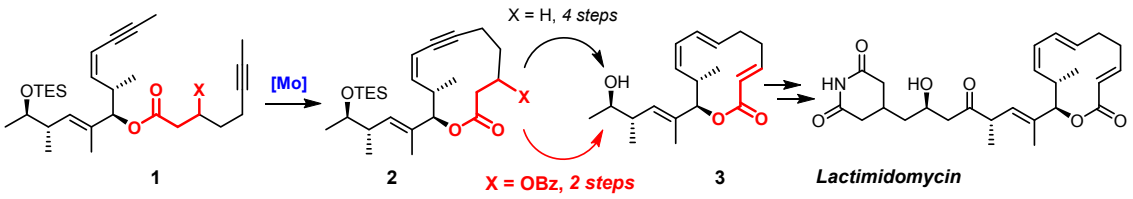

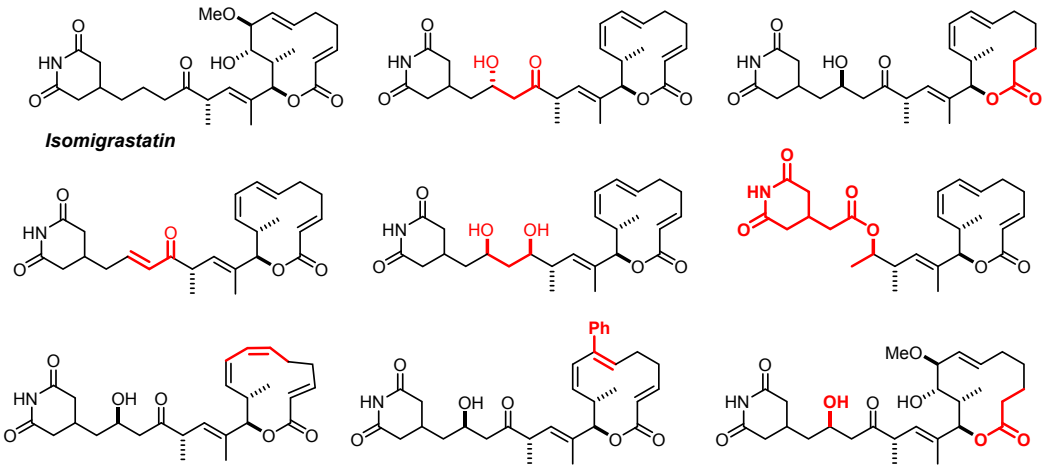

In our first attempt, the macrocyclic ring was closed starting from diyne **1** (X = H), followed by *trans*-reduction of the resulting cycloalkyne **2** (X = H) to set the *E*-configured site of the diene entity. A sequence of selenylation/oxidative deselenylation was then needed to install the yet missing enoate moiety. Although this chemistry worked reasonably well and gave first crops of lactimidomyin for biological testing, it is certainly not ideal for scale-up. Therefore, we pursued a modified route that avoids the selenium chemistry altogether. To this end, the enoate of the target was encoded as an aldol ester derivative. Gratifyingly, RCAM of diyne **1** (X = OBz) with the new molybdenum catalyst still proceeded smoothly (85% @ 2 g scale), without any premature elimination occurring. Subsequent *trans*-hydrosilylation of **2** (X = OBz) followed by treatment with TBAF furnished the key intermediate **3** in excellent overall yield; note that TBAF effects a C- and an O-desilylation as well as concomitant benzoate elimination with formation of the enoate, all in one pot. With the access to **3** being secured, we were not only able to make substantial amounts of lactimidomycin itself, but could also prepare its sister compound ***isomigrastatin*** and a panel of non-natural analogues by diverted total synthesis. These compounds powered an extensive biological (re)assessment of these putative cell migration inhibitors (in cooperation with Pfizer Oncology), which led to a revision of the claims made in the literature; rather, lactimidomycin and analogues were found "just" acutely cytotoxic. Although this was certainly not the expected outcome, their particular mode of action as eukaryotic ribosome inhibitors is perhaps equally interesting.

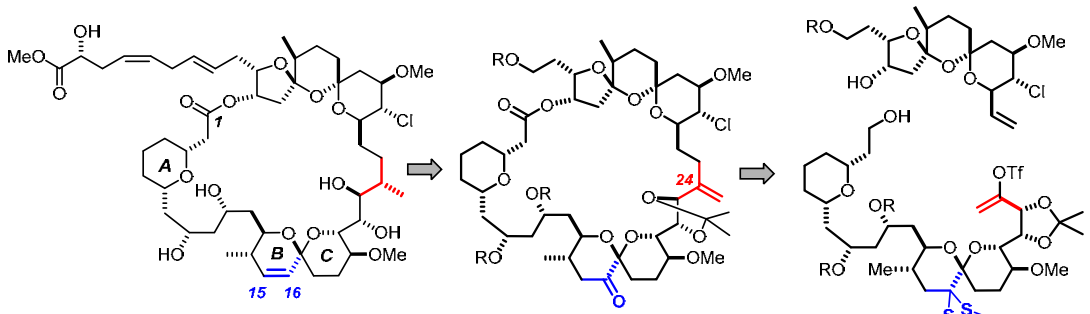

Spirastrellolide A Methyl Ester

In Chapter 2.4.2, our total synthesis of the potent phosphatase inhibitor ***spirastrellolide F methyl ester*** has been summarized that involves an RCAM reaction followed by a gold catalyzed transannular spiroketalization. In parallel work – but through largely different chemistry – we also managed to make the sister compound ***spirastrellolide A methyl ester***, which contains an additional $\Delta^{15,16}$ double bond within the B-ring. The assembly of this exigent target that exhibits no less than 21 chiral centers plus three

olefinic sites within its complex polyketide frame centered on a late-stage unveiling of the signature C15-C16 alkene, only after the methyl branch at C24 had been properly set by a highly selective substrate-controlled hydrogenation. The elaborate *exo*-methylene precursor was formed by a convergent route using dithiane chemistry, an alkyl-Suzuki coupling, and a Yamaguchi lactonization.

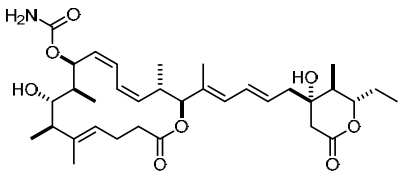

Leiodermatolide

Another massive project concerned the first total synthesis of the antimitotic agent ***leiodermatolide***, an extremely scarce metabolite derived from a marine sponge, whose stereostructure could not be fully established by the isolation team. This macrolide comprises a fragile non-thermodynamic *Z,Z*-diene subunit, which remains beyond reach of any alkene metathesis catalyst known to date. Once again, alkyne metathesis opened a very effective entry into this delicate target and allowed its stereostructure to be unambiguously determined. This compound currently undergoes biological testing (Pfizer Oncology); because of some very encouraging preliminary data, we are now optimizing our route and enter the phase of analogue-making by late-stage digression from the underlying synthesis blueprint.

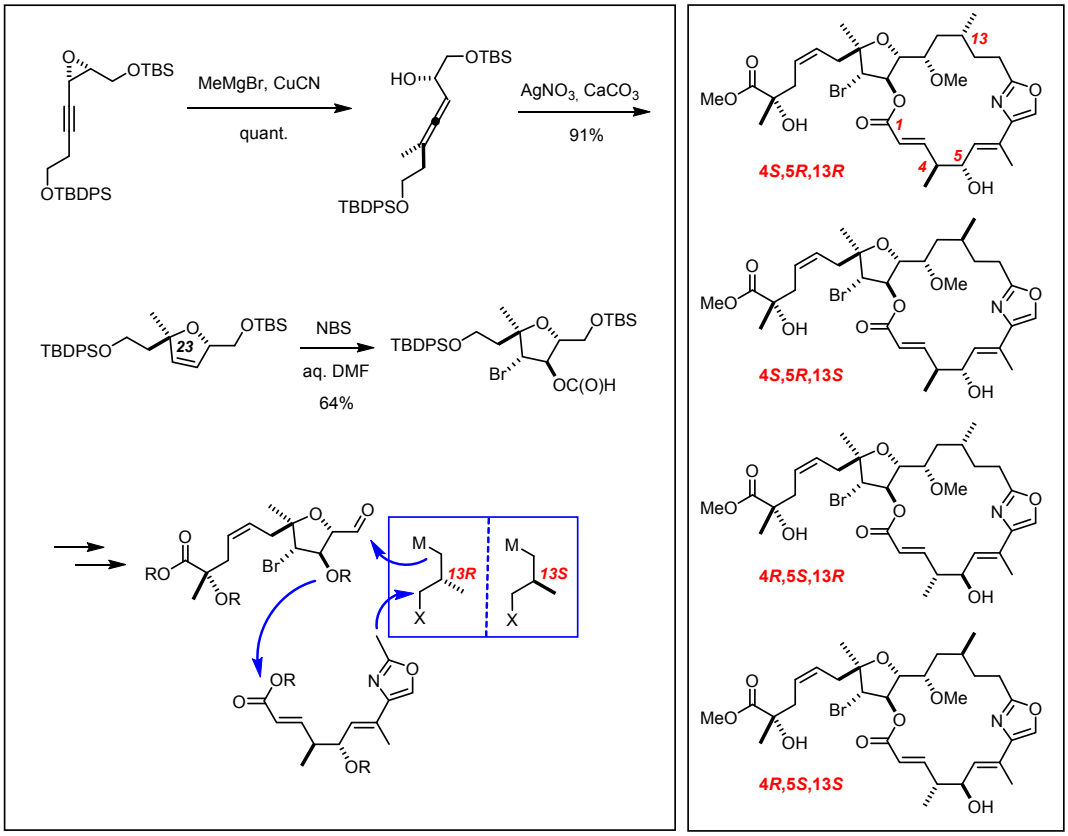

Another deep-sea sponge harvested by submersible in deep waters is the source of ***leiodolide B***, an intricate macrolide of mixed polyketide/non-ribosomal peptide synthetase origin. It attracted our attention because it is practically inaccessible from the producing organism but supposedly very active in the NCI 60 tumor cell line screen. From the purely chemical viewpoint, we felt that the brominated tetrahydrofuran subunit comprising a *tert*-ether site at C23 poses an interesting synthetic challenge. An effective way to form this motif starts off with the vinylogous opening of a propargyl epoxide with a methylcopper reagent, followed by a silver-mediated hydroalkoxylation of the resulting product. This sequence allows for an efficient chirality transfer from a readily available epoxide to the quaternary chiral center using the axial chirality of the allene as a relay. Although this tactics worked exceedingly well and a variety of other problems en route to the target could also be solved, the data of synthetic leiodolide B were not identical with those of the natural product. Careful analysis made us believe that the chiral centers at C4, C5 and C13 are the most likely sites of misassignment by the isolation team. Therefore we went on to make 4 different diastereomers of this complex target through total synthesis; unfortunately, none of them matched the reported data sufficiently closely to claim identity. Since the isolation group could neither provide an authentic sample nor even copies of the original spectra, we felt unable to solve the puzzle.

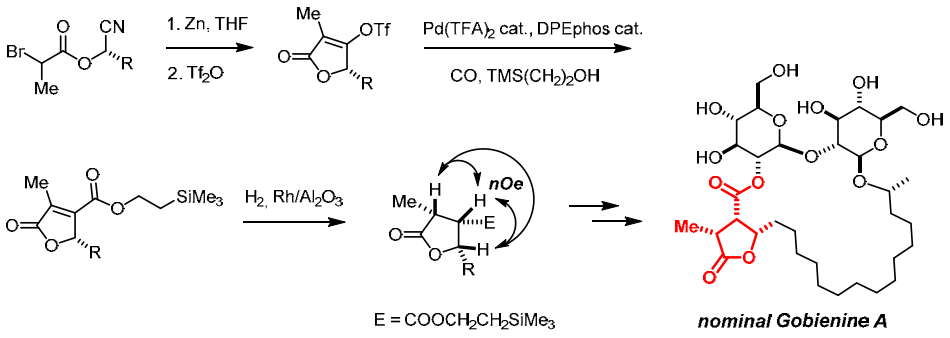

A totally different chemical challenge was encountered during the synthesis of nominal ***gobienine A***, a rather unique lichen-derived glycolipid. It contains an all-*cis* substituted butyrolactone substructure within a macrocyclic frame, which is very epimerization-prone; actually, a literature survey showed no good entry into such a motif. We found a decent solution based on an intramolecular Blaise reaction of an optically active cyanohydrin bromopropionate followed by in situ quenching of the resulting tetronic acid with triflic anhydride. Subsequent methoxycarbonylation and hydrogenation of the resulting tetrasubstituted alkene over Rh/Al_2O_3 gave the desired all-*cis*-configured product in respectable yield and excellent selectivity. This building block was then

attached to an appropriate disaccharide building block and the macrocycle was closed by RCM before a final hydrogenation released nominal gobienine A. Unfortunately, the structure of this natural product has also been mis-assigned by the isolation team; we could show through extensive studies that the flaw must be "deep seated". Here again, the lack of authentic reference material makes it impossible for us, without undue effort, to identify the mistake(s) made by the isolation team.

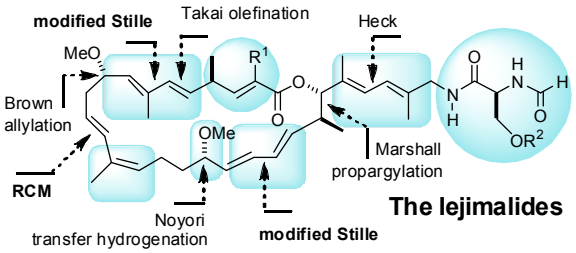

As already mentioned in the previous evaluation report, our group devoted considerable time and effort to the ***iejimalides***, which were reported to exhibit appreciable anti-tumor activities *in vivo* but cannot be obtained in sufficient quantity from the producing sponge for state-of-the-art preclinical studies. After we had demonstrated that it is possible to forge such polyunsaturated products by ring closing olefin metathesis, in which two out of ten different double bonds in the cyclization precursor have to be selectively activated, we were intrigued by the highly promising biological results obtained in the first round of testing. Iejimalide B and several synthetic analogues showed cytotoxicities in the sub-nanomolar (!) or single-digit nanomolar range as well as an encouragingly differential profile with regard to the responsive human tumor cell lines. Therefore we decided to prepare this demanding marine natural product on a gram scale (16 steps longest linear sequence, ca. 42 steps overall) together with a panel of ca. 20 non-natural analogues that map the entire pharmacophore. During the report period, these compounds were extensively tested in tumor colony formation assays, the results of which were at least as encouraging as the original cell-based screens. The most active compounds were then tested in a mouse model, unfortunately with little success. This result corrects the claim of the isolation team that had insinuated an appreciable *in vivo* activity of the natural lead.

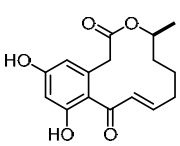

Dehydrocurvularin

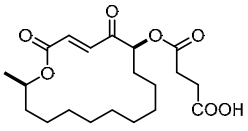

(–)-A26771B

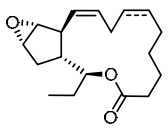

Ecklonialactone A ($\Delta^{6,7}$)
Ecklonialactone B

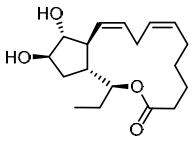

Ecklonialactone C

Additional total synthesis projects completed in between 2010-2013 were concerned with the tubulin-binding agent dehydrocurvularin, the antibiotic A26771B, and the

marine oxylipins of the ecklonialactone family; all of these compounds were prepared in optically pure form. They served to scrutinize various aspects of the metathesis chemistry developed in this laboratory.

Future directions: Identify, synthesize and evaluate (hopefully) relevant targets; prepare functional analogues by diverted total synthesis; sustain the network of collaborations with academic and industrial partners to ensure professional testing.

Publications resulting from this research area: 1, 3, 5, 6, 10, 19, 22, 25, 26, 29

External funding: Alexander von Humboldt Foundation (fellowship to J. Llaveria), Chemical Industry Fund (fellowships to A. Arlt, S. Benson and J. Willwacher), Japan Society for the Promotion of Science (fellowship to S. Handa)

Cooperations: Oncotest GmbH (Fribourg, DE), Pfizer Oncology (Groton, US)

2.4.5 Research Area "Cationic Ligands: Synthesis and Applications of Extreme π-Acid Catalysts" (M. Alcarazo)

Involved: J. Petuškova, J. Carreras, E. González, L. Gu, Á. Kozma, P. Linowski, G. Mehler, H. Tinnermann, C. Wille, T. Deden, A. Gimeno, P. Gualco, A. Zanardi

Objective: The goal of this project is the synthesis of extreme π-acceptor phosphines through the introduction of positively charged homo- or heteroaromatic substituents directly attached to the phosphorus atom. By exploiting this property, new Au and Pt catalysts have been developed that display a dramatically enhanced capacity to activate π-systems.

π-Acid catalysis, mainly with Au(I) and Pt(II) based species, has emerged in the last decade as one of the most efficient tools for the promotion of rearrangements in unsaturated organic substrates, which provide an exquisite entry to the synthesis of intricate skeletons that may be otherwise difficult to prepare. The generally accepted mechanism that governs most of these transformations involves three main steps: (i) coordination of the π-acid metal to the alkyne or allene moiety present in the starting material, (ii) nucleophilic intra- or intermolecular attack to the activated substrate forming a vinyl-metal species, and (iii) protodemetallation of the vinyl intermediate with concomitant regeneration of the active catalyst. It seems reasonable to expect that the first two of these steps may be accelerated by strong π-acceptor ancillary ligands, which should increase the Lewis acidity of the metal center they coordinate. In striking contrast, potent σ-donating ligands will weaken the M-C bond in the vinyl intermediates by their *trans*- influence and thus facilitate the protodemetallation step. Hence, the selection of the most appropriate ligand for a particular transformation can only be done based on an in-depth understanding of the nature of the rate-determining step.

Very recently, we reported the synthesis of the first ever isolated carbene-stabilized P_1-centered trication $[L_3P]^{3+}$ (L = 2,3-dialkylaminocyclopropenium) **1** by reaction of the 1-chloro-2,3-(dimethylamino) cyclopropenium salt **2** and $P(SiMe_3)_3$ (Scheme 1). Despite the three positive charges on the groups directly attached to the P atom, this compound can still serve as a ligand for π-acidic metals such as Pt. Thus, when **1** is treated with K_2PtCl_4 in acetonitrile, the bench stable complex **3** is formed. More interestingly, charge decomposition analysis of the metal-ligand interaction in **3** gave the surprising result that the total L→M σ-donation (0.31 *e*) is lower than the M→L π-back donation (0.43 *e*) into the very low-lying LUMO of **1**, which must hence be regarded as the main

interaction in **3**. This unconventional situation in which the P-ligand removes net electron density from the metal suggests that compound **1** increases the natural π-acidity of Pt(II) centers. It should thus accelerate known reactions, or even permit new ones, in which either the coordination of the substrate or the nucleophilic attack to the activated substrate are the rate-determining steps.

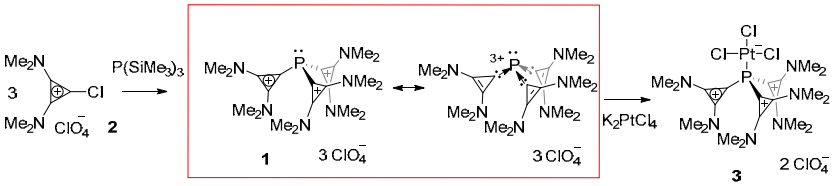

Scheme 1

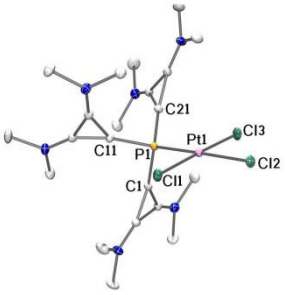

In a preliminary screening of plausible applications for these ligands, we chose the Pt-catalyzed 6-*endo*-dig cyclization of 2-ethinyl-1,1'-binaphtalene **4** into pentahelicene **5**, as model reaction for two main reasons (Scheme 2).

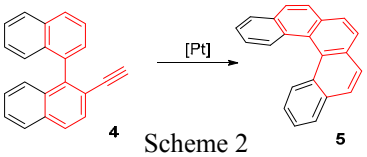

Scheme 2

(a) The interest in polycyclic homo- and heteroarenes has been refueled during the last years due to their unique optoelectronic properties and their potential applications in organic electronic devices. The chosen cyclisation is a very attractive entry for the preparation of these carbon-rich materials. Moreover, this reaction can be also used to prepare highly substituted phenanthrene moieties that are present in the structure of natural products. Therefore, expeditious syntheses to these compounds may be envisaged.

(b) Due to the relatively weak nucleophile that is employed (an aromatic ring), the nucleophilic attack is expected to be the rate-determining step for this reaction. Hence, the use of strong π-acceptor ancillary ligands such as **1** should facilitate this transformation.

Accordingly, we chose for our studies on ligand effects a series of phosphanes such as PPh_3, $P(OPh)_3$, $P(C_6F_5)_3$ and precatalyst **3** in combination with a silver salt. As expected, both $P(OPh)_3$ and $P(C_6F_5)_3$ performed better than PPh_3 in terms of reactivity (Figure 1).

Interestingly, our ligand **1** produces a much faster reaction, clearly surpassing any of the classical π-acceptor ligands. In fact, complete conversion of the model substrate to

pentahelicene **5** was achieved in less than 20 minutes under the newly developed reaction conditions.

Furthermore, the compatibility of our catalytic system with several functional groups is outstanding. Up to now, our experiments indicate that biaryl substrates containing ethers, free or silylated alcohols, esters, halogen substituents, silyl- and trifluoromethyl groups, thiophenes, and furanes are well tolerated (for representative examples see Scheme 3). Moreover, all products were obtained in few minutes with very good to excellent yields.

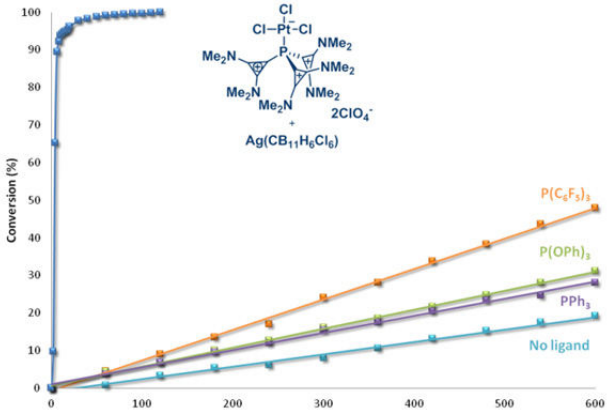

Figure 1

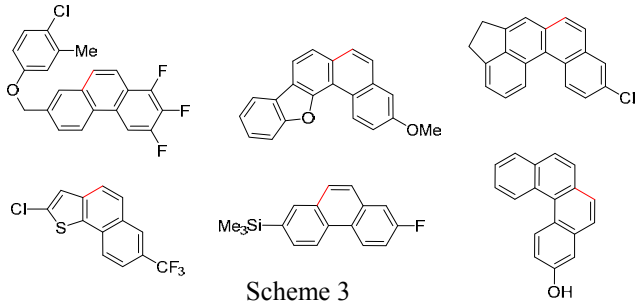

Scheme 3

However, despite of the remarkable activity depicted by **3**, there are still three main aspects regarding this catalyst that deserve further optimization:

a) Catalyst stability needs to be enhanced. With catalysts **3**, no reaction progress is observed after reaction times of about one hour, presumably due to catalysts decomposition.

b) Catalyst activity needs to be improved. Although much faster, with the newly developed catalytic system a catalyst loading of 5 mol% and high temperatures (80 °C) are still necessary. In addition no reaction is observed if bulky substituents are located at the *ortho*- positions of the biaryl starting material (See Scheme 4). The employment of a more π-acidic Au(I)-based catalysts instead of a Pt(II)-derived one might be beneficial at this point.

c) Improvement of the substrate tolerance to heteroaromatic rings such as pyridines is desirable.

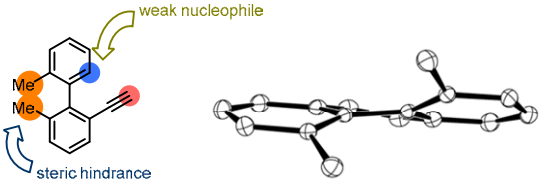

Scheme 4

As already mentioned, Au(I) based catalysts should be more active than Pt(II)-based ones due to the stronger Lewis acidity of Au(I) centers. Unfortunately, all attempts to coordinate gold to ligand **1** were unsuccessful. In contrast, dicationic ligands were found to be more appropriate in Au chemistry because: (i) their Au-derived complexes are much more stable than those derived from tricationic ligands and (ii) their reactivity is comparable. Thus, we planned to synthesize a set of dicationic ligands bearing several R substituents on the phosphorus with different steric demands and electronic nature (Ph, biphenyl, C_6F_5-, *p*-$CF_3C_6H_4$…). Up to now, compounds **6** and **7** and the Au(I) complexes thereof derived have been prepared (Scheme 5).

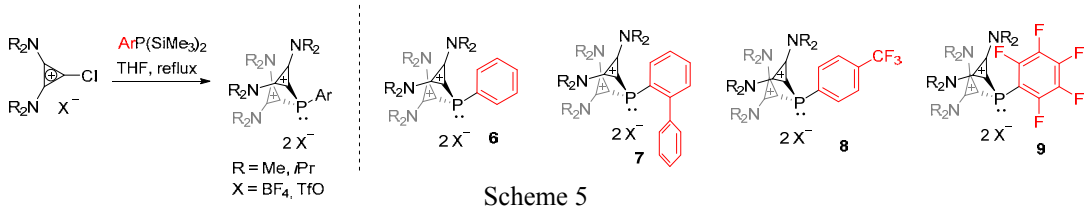

Scheme 5

To evaluate the range of application of these new Au catalysts, we focused on those substrates that were reluctant to react when the Pt-based complex **3** was employed as precatalyst; namely those with substituents in the *ortho*- positions of the biphenyl skeleton or those with electron withdrawing groups attached to the ring that has to accomplish the nucleophilic attack. Some of the substrates that could be prepared employing the new Au(I) catalysts **10** are depicted in Scheme 6.

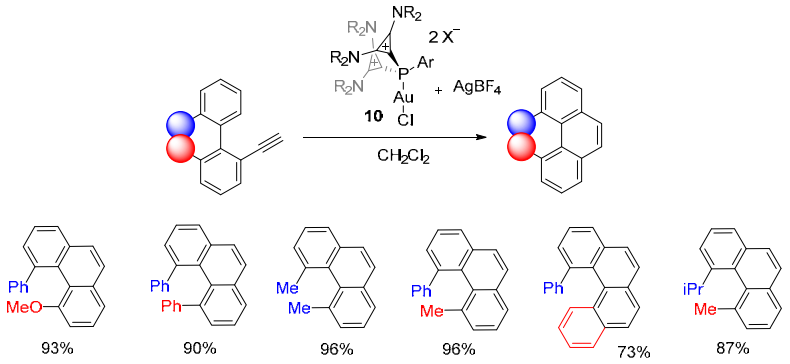

Scheme 6

In addition, our synthetic program has already benefitted from these novel tools and natural products such as Orchinol, Ochrolide, Bulbophyllantrin and Epimedoicarisoside A have been prepared using our Pt and Au catalysts for the key hydroarylation step (Scheme 7). As representative example, Scheme 8 depicts the synthesis of Epimedoicarisoside A, a

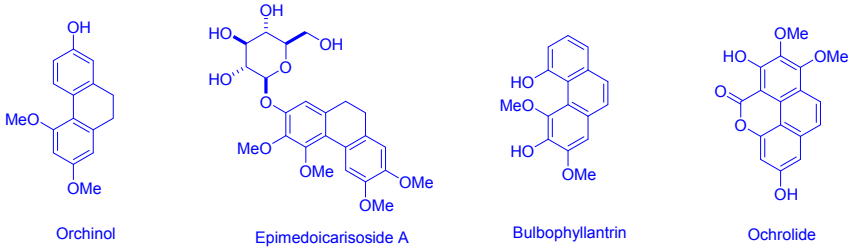

Scheme 7

compound with potential application in the treatment of cardiovascular and cerebrovascular diseases such as myocardial infection or cerebral thrombosis.

Future directions: Many transformations might benefit from the use of extremely π-acceptor ligands. At the moment we are focused on the application of our ligands in Rh and Pd-catalyzed processes. The synthesis of cationic phosphines containing other –onium substituents different than cyclopropenium is also being investigated.

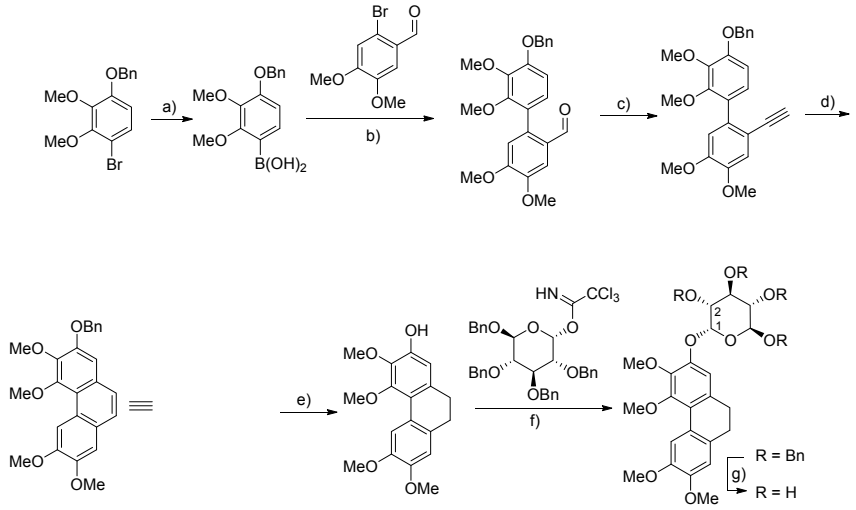

Scheme 8 a) *n*BuLi, -78 °C, $B(OMe)_3$, H^+, (59%); b) $Pd(PPh_3)_4$ (2 mol%), μwave oven, 120 °C, 25 min (98%); c) Ohira-Bestmann reagent, (3 eq.), K_2CO_3, MeOH, RT, 48 h (83%); d) **10** (2 mol%), $Cl(CH_2)_2Cl$, 80 °C, 3 h, (92%); e) H_2 (30 bar), Pd/C (20%), MeOH, RT, 48 h, (82%); f) BF_3·OEt (1 eq.), CH_2Cl_2, -20 °C, 2 h, (93%); g) H_2 (1 bar), Pd/C (10%), MeOH: AcOEt (2:1), 24 h, RT, (75%).

Publications resulting from this area: 33, 35, 37, 40, 44, 47

External funding: German Research Foundation (Project AL 1348/5-1); Chemical Industry Fund; SusChemSys (Ziel 2 Programm NRW, fellowship to E. González); Spanish Ministerio de Educación y Ciencia (fellowship to J. Carreras); German Academic Exchange Service (DAAD, fellowship to Á. Kozma)

Cooperations: W. Thiel (Mülheim/Ruhr, DE)

2.4.6 Research Area "Synthesis and applications of simultaneous σ- and π-donor ligands: C-M dative double bonds" (M. Alcarazo)

Involved: B. Inés, S. Kahn, R. Azhakar, S. Holle, F. Martín

Objective: The goal was to study new coordination modes of carbon(0) compounds.

In this area, our research has been strongly inspired by the theoretical work of Frenking about the nature of carbodiphosphorane **1** (Scheme 1). His studies revealed that in compound **1** and analogues the central carbon atom retains its four valence electrons that are thus all available for coordination. In fact, carbodiphosphoranes are known to react with two Lewis acids such as AuCl affording diaurated derivatives. However, their ability to donate their four electrons to the same electrophile in a simultaneous σ- and π-donation had not been described.

In this regard, we envisaged that the use carbodiphosphoranes may provide sufficient stabilization to attenuate the reactivity and allow the isolation of dihydrido borenium cations $[L{\rightarrow}BH_2]^+$ (L = carbodiphosphorane), a series of compounds that cannot be isolated when classical σ-donating ligands are employed.

Hence, we allowed carbodiphosphorane **1** to react with borane dimethylsulfide complex and isolated adduct **2** as a bright yellow solid in quantitative yield (Scheme 1). Upon treatment of a solution of **2** with one equivalent of $B(C_6F_5)_3$ the color smoothly vanishes. The ^{11}B-NMR spectrum indicated the generation of the borohydride anion $HB(C_6F_5)_3^-$ (δ = -24.0 ppm; $^1J(^1H,^{11}B)$ = 92 Hz) while complete consumption of $B(C_6F_5)_3$ was confirmed by ^{19}F-NMR. Additionally, the original ^{11}B-NMR resonance of **2** (δ = -22.7 ppm; $^1J(^1H,^{11}B)$ = 84 Hz) disappeared and a new broad signal (δ = 56.6 ppm) emerged. These data suggested the formation of the dihydrido borenium borohydride **3**, an interpretation that was validated by X-ray crystallographic analysis (Figure 1).

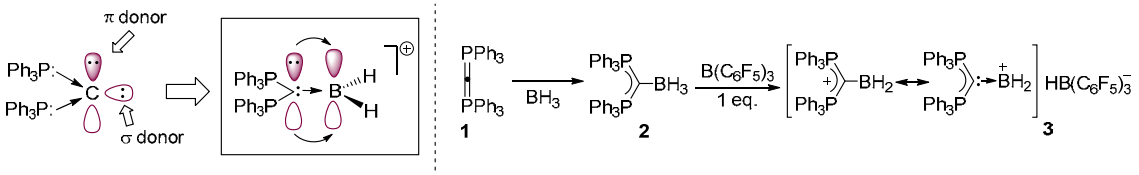

Scheme 1. Synthesis of a dihydridoborenium cation.

In an attempt to clarify the electronic nature of **3**, density functional calculations at the B3LYP/6-31G* level were performed. Inspection of the frontier orbitals reveals that the highest occupied molecular orbital (HOMO) is the C-B π-bonding orbital that is strongly polarized toward the C atom (see Figure 1). Energy decomposition analysis also indicates that σ-donation contributes about twice as much as π-donation to the stability of the C=B bond. Presently, our efforts are directed to the application of the borenium cations in fluorine-free frustrated Lewis pair chemistry as their Lewis acidity has been proved to be very similar to the one depicted by $B(C_6F_5)_3$.

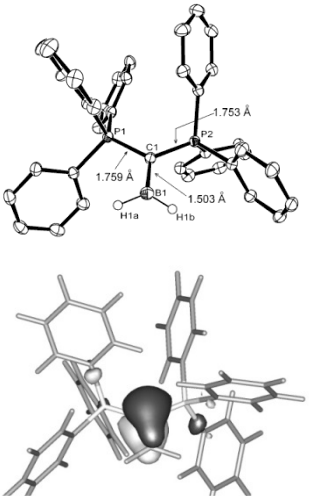

Figure 1. X-ray structure (up) and HOMO(down) of compound **3**.

The employment of **1** as both σ- and π- acceptor ligand is expected to facilitate the isolation of low coordinated p-block cations such as $Si(IV)^{+2}$ or $Ge(II)^{+2}$. Our strategy, that is already producing some positive results, is depicted in Scheme 2. In broad lines it relies on the coordination of carbodiphosphorane **1** to a germanium or silicon chloride and subsequent abstraction of the chloride anions, a task that should be facilitated by the extra π-electrons of the ancillary ligand. Up to now we have been able to synthesize compound **4** which already depicts a σ- and a π-dative bonds between the central carbon atom and the GeCl moiety. Reaction with dimethylamino pyridine affords adduct **5** where the π interaction is not existing anymore. Currently, we are trying to remove the chloride moiety from **5**. In case of success, the first dicoordinated Ge(II) dication will be isolated. The same strategy is being applied for the preparation of Si(IV) dications.

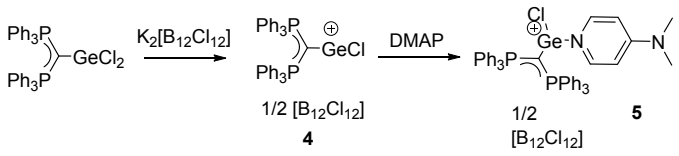

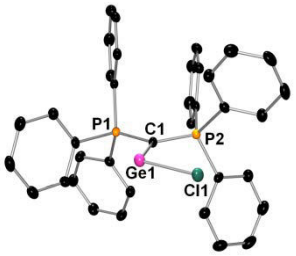

Scheme 2. Proposed synthesis of Ge(II) dications and structure of 4.

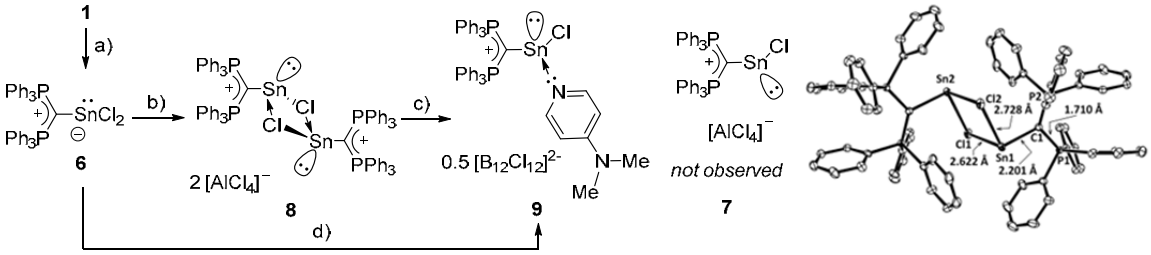

Scheme 3. a) **1**, $GeCl_2$·dioxane, DCM, RT, quant.; b) **6**, $AlCl_3$, CH_2Cl_2, 67%; c) **8**, DMAP, CH_2Cl_2, $K_2[B_{12}Cl_{12}]$ (0.5 eq.); d) **6**, DMAP, CH_2Cl_2, $K_2[B_{12}Cl_{12}]$ (0.5 eq.), 53%.

Finally, the extension of this chemistry to Sn(II) was also attempted. Reaction of **1** with $SnCl_2$ afforded the very insoluble and air-sensitive adduct **6** that was subsequently treated with $AlCl_3$. In sharp contrast to the Ge analogue previously described, abstraction of a chloride anion from **6** did not yield the expected cation **7** but its dimer **8** (Scheme 3). The steric hindrances around Ge and Sn in 4 and in a hypothetical complex 7 (see calculated structure, Figure 2) are basically identical. Therefore, the isolation of **8** indicates that the plausible stabilization provided by a π(C-Sn) bond in **7** is so feeble that it is overridden by formation of chloride bridges between the Sn atoms.

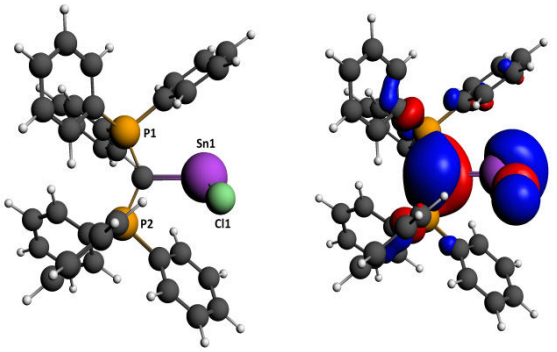

Figure 2. Calculated gas-phase structure of cation **8** (left) and plot of its HOMO (right) at BP86/6-31G* level [LANL2DZ for Sn].

Future directions: It is our intention to evaluate if other compounds containing doubly dative C=E double bonds can be isolated. In addition, the past few years have witnessed an ever-increasing interest in the chemistry of compounds that contain two or more metal centers. Specifically, heteronuclear complexes are attractive because new reactivity patterns can be expected. The ability of **1** to donate up to four electrons makes this ligand exceptionally interesting for this objective.

Publications resulting from this research area: 2, 24, 34, 42, 43

External funding: German Research Foundation (Project AL 1348/5-1); Chemical Industry Fund; Spanish Ministerio de Educación y Ciencia (fellowship to B. Inés)

Cooperations: W. Thiel (Mülheim/Ruhr, DE)

2.4.7 Research Area "Metal-free hydrogenations" (M. Alcarazo)

Involved: B. Inés, S. Holle, I. Abdellah, J. Nicasio, D. Palomas, S. Steinberg

Objective: The main objective was to expand the scope of frustrated Lewis pair chemistry to the reduction of electron poor allenes and alkenes.

Since its discovery, the chemistry of frustrated Lewis pairs (FLP) has flourished, showing exquisite reactivities towards the activation of small molecules. Thus, it has been reported in recent years that bonds such as C-O, C-H, B-H, S-S, C-C or Si-H can be activated by using this elegant concept. In spite of this, their arguably most remarkable application is still the heterolytic cleavage of H_2, and the subsequent development of metal free catalytic hydrogenations of a number or organic polar substrates such as imines, enamines, nitrogenated heterocycles or silyl enol ethers employing H_2 rather than Hantzsch esters. Surprisingly, despite these achievements, the FLP-promoted catalytic hydrogenation of electron poor unsaturated systems is still underdeveloped. In an attempt to address this limitation, we focused our efforts towards the catalytic reduction of allenes, expecting that the higher reactivity derived from their two adjacent double bonds, could make them appropriate substrates for a preliminary screen of conditions.

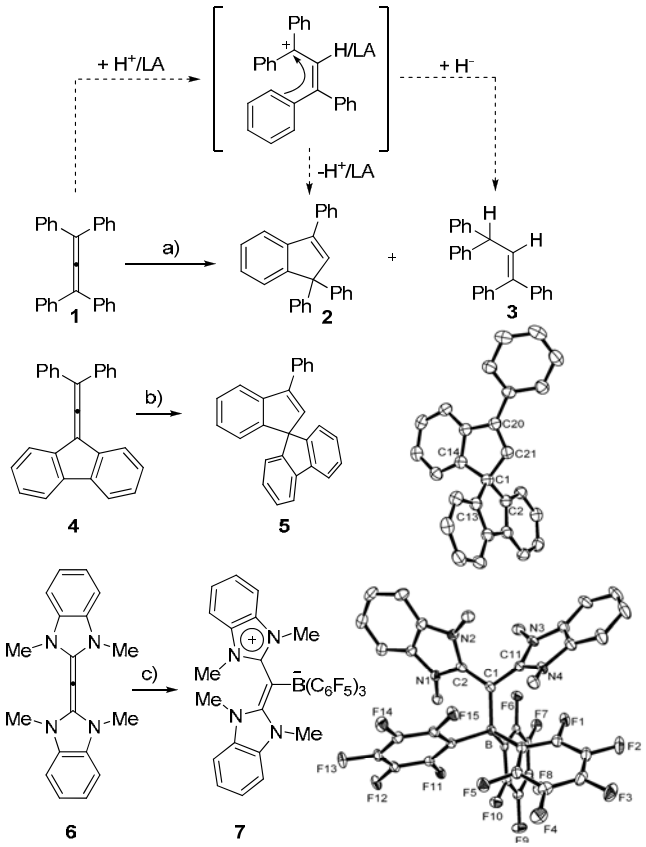

Scheme 1 Reactivity of allenes towards frustrated Lewis pairs. a) $B(C_6F_5)_3/Ph_2NMe$ (15 mol%), toluene, 80 °C, 3 days, **2** (63%), **3** (22%) or $B(C_6F_5)_3/PhNMe_2$ (15 mol%), toluene, 80 °C, 3 days, **2** (0%), **3** (96%); b) $B(C_6F_5)_3$ (15 mol%), toluene, RT, **5** (97%); c) $B(C_6F_5)_3$, toluene, RT, **7** (78%).

Thus, tetraphenylallene **1** was exposed to mixtures of $PhNMe_2$ or Ph_2NMe /$B(C_6F_5)_3$ (15 mol%) and H_2 (60 bar). Interestingly, consumption of **1** was observed and two new products **2** and **3** could be isolated from the reaction mixtures after column chromatography

(Scheme 1). While the formation of alkene **3** proves that reduction of allenes is possible by FLP chemistry, the detection of **2** suggests the existence of a competing reaction pathway. Hence, it can be envisaged that **1** is first protonated at the central carbon followed by hydride transfer to the transient cation produces **3**. Alternatively, intramolecular Friedel-Crafts alkylation affords **2**. In addition, it cannot be excluded that the undesired transformation of **1** into **2** may be directly promoted by $B(C_6F_5)_3$ without the participation of any proton since: (i) allene **4** cleanly cycloisomerizes into **5** solely in the presence of catalytic amounts of $B(C_6F_5)_3$ and (ii) the allene-borane complex **7** is obtained when the more electron rich allene **6** is employed as a substrate. These studies indicate that the hydrogenation takes probably place following a reaction pathway that starts with a Michael-type hydride addition to the allene followed by protonation.

Next, an electron deficient allene **8** unable to interact with the borane through the central carbon atom was chosen as new model substrate. In this case, hydrogenation (80 °C, 60 bar) gave the reduced product in very good yield and no traces of cyclised products were detected. Interestingly, despite the formation of ester-$B(C_6F_5)_3$ complexes is known, this process is probably reversible under the studied conditions and does not seem to affect the desired hydrogenation. Screening of different bases revealed that DABCO is most suitable for this transformation. With this optimized catalytic mixture in hand we were committed to explore the scope of this methodology. To this end, a representative set of diaryl substituted allenes **8**-**12** containing substituents of different electronic nature was synthesized and submitted to the optimized conditions (Table 1).

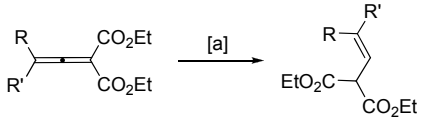

Entry	Allene	Product	Yield (%)[b]
1	**8**; R, R‘ = Ph	**13**	75
2	**9**; R, R‘ = *p*-(Me)Ph	**14**	65
3	**10**; R, R‘ = *p*-(F)Ph	**15**	94
4	**11**; R , R‘= *p*-(OMe)Ph	**16**	68
5	**12**; R-R‘ = 3,5-di(F)-9-fluorene	**17**	43[c]

Table 1. [a] Reaction conditions: Toluene, 80 °C, 3 days; H_2 60 bar and DABCO/$B(C_6F_5)_3$ (15 mol%); [b] isolated yields; [c] the low yields are probably due to dimerization of the allene at the working conditions.

In view of this reactivity, we decided to study whether the additional activation provided by the two double bonds of the allene moiety was necessary to accomplish the desired hydrogenations or if a structurally simpler alkylidene malonate or other electron poor alkenes could also undergo the same transformation.

With this idea in mind, we first carried out a series of experiments to gain some evidence about the operating mechanism. Interestingly, the equimolar reaction of

alkylidene malonate **18** with [HDABCO][DB(C_6F_5)$_3$] afforded the hydrogenated product [D_1]-**19** that bears the deuterium label exclusively in the β-position. This clearly indicates that the hydride from the borohydride anion is transferred at the electrophilic position of the substrate (Scheme 1). No reaction was detected when the reduction was attempted with K[HB(C_6F_5)$_3$] followed by quenching with DABCO·HCl, demonstrating that the $[HDABCO]^+$ cation plays an active role during the hydrogenation process. Thus, we rationalized that in this transformation the $[HDABCO]^+$ moiety should activate the substrate, presumably through the formation of a hydrogen bond, followed by nucleophilic attack of the hydride (Scheme 2).

The fact that an activation of the alkylidene malonate is necessary to carry out the desired reduction suggests that for these substrates, hydride transfer from the borohydride moiety is the rate determining step. Hence, the employment of boranes depicting weaker Lewis acidity than B(C_6F_5)$_3$ should facilitate this elemental process. However, weak Lewis acids are not the most adequate ones to promote H_2 cleavage that is necessary for the reduction to take place. Therefore, a compromise situation regarding the Lewis acidity of the borane partner had to be found in order to optimize this transformation in terms of reaction conditions and substrate scope. In our hands, borane **20** exhibits optimum properties (Scheme 3). With this compound we were able to extend this metal-free hydrogenation to alkylidene malonates, nitroalkenes and vinyl sulfones.

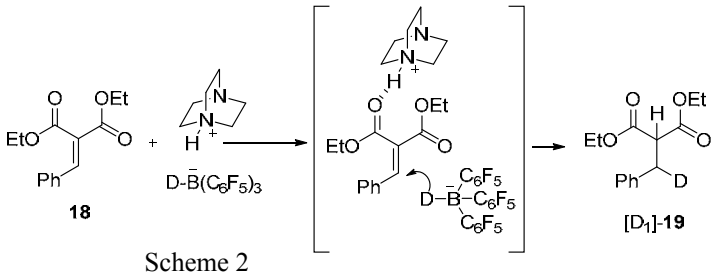

Scheme 2

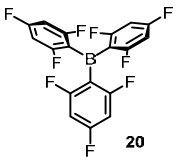

Scheme 3

Future directions: In this and many other applications of frustrated Lewis pair chemistry, the use of B(C_6F_5)$_3$ or a close derivative is essential. It is our intention to develop new boron-free Lewis acids and study if frustrated Lewis pair chemistry can be carried out with these compounds.

Publications resulting from this research area: 36, 38, 41, 45, 46

External funding: European Research Council Starting Grant (277963); Chemical Industry Fund; Spanish Ministerio de Educación y Ciencia (fellowship to D. Palomas).

Cooperations: W. Thiel (Mülheim/Ruhr, DE)

2.4.8 Publications 2011-2013 from the Department of Organometallic Chemistry

Fürstner group

(1) Larivée, A.; Unger, J. B.; Thomas, M.; Wirtz, C.; Dubost, C.; Handa, S.; Fürstner, A. *Angew. Chem., Int. Ed.* **2011**, *50*, 304-309.

(2) Alcarazo, M.; Radkowski, K.; Goddard, R.; Fürstner, A. *Chem. Commun.* **2011**, *47*, 776-778.

(3) Fürstner, A. *Isr. J. Chem.* **2011**, *51*, 329-345.

(4) Fürstner, A. *Chem. Commun.* **2011**, *47*, 6505-6511.

(5) Gagnepain, J.; Moulin, E.; Fürstner, A. *Chem.–Eur. J.* **2011**, *17*, 6964-6972.

(6) Gagnepain, J.; Moulin, E.; Nevado, C.; Waser, M.; Maier, A.; Kelter, G.; Fiebig, H.-H.; Fürstner, A. *Chem.–Eur. J.* **2011**, *17*, 6973-6984.

(7) Gallenkamp, D.; Fürstner, A. *J. Am. Chem. Soc.* **2011**, *133*, 9232-9235.

(8) Teller, H.; Fürstner, A. *Chem.–Eur. J.* **2011**, *17*, 7764-7767.

(9) Heppekausen, J.; Fürstner, A. *Angew. Chem., Int. Ed.* **2011**, *50*, 7829-7832.

(10) Hickmann, V.; Kondoh, A.; Gabor, B.; Alcarazo, M.; Fürstner, A. *J. Am. Chem. Soc.* **2011**, *133*, 13471-13480.

(11) Benson, S.; Collin, M.-P.; Arlt, A.; Gabor, B.; Goddard, R.; Fürstner, A. *Angew. Chem., Int. Ed.* **2011**, *50*, 8739-8744.

(12) Radkowski, K.; Seidel, G.; Fürstner, A. *Chem. Lett.* **2011**, *40*, 950-952.

(13) Lehr, K.; Mariz, R.; Leseurre, L.; Gabor, B.; Fürstner, A. *Angew. Chem., Int. Ed.* **2011**, *50*, 11373-11377.

(14) Seidel, G.; Fürstner, A. *Chem. Commun.* **2012**, *48*, 2055-2070.

(15) Chaładaj, W.; Corbet, M.; Fürstner, A. *Angew. Chem., Int. Ed.* **2012**, *51*, 6929-6933.

(16) Heppekausen, J.; Stade, R.; Kondoh, A.; Seidel, G.; Goddard, R.; Fürstner, A. *Chem.–Eur. J.* **2012**, *18*, 10281-10299.

(17) Lehr, K.; Fürstner, A. *Tetrahedron* **2012**, *68*, 7695-7700.

(18) Teller, H.; Corbet, M.; Mantilli, L.; Gopakumar, G.; Goddard, R.; Thiel, W.; Fürstner, A. *J. Am. Chem. Soc.* **2012**, *134*, 15331-15342.

(19) Willwacher, J.; Kausch-Busies, N.; Fürstner, A. *Angew. Chem., Int. Ed.* **2012**, *51*, 12041-12046.

(20) Radkowski, K.; Sundararaju, B.; Fürstner, A. *Angew. Chem., Int. Ed.* **2013**, *52*, 355-360.

(21) Fürstner, A. *Angew. Chem., Int. Ed.* **2013**, *52*, 2794-2819.

(22) Arlt, A.; Benson, S.; Schulthoff, S.; Gabor, B.; Fürstner, A. *Chem.–Eur. J.* **2013**, *19*, 3596-3608.
(23) Brewitz, L.; Llaveria, J.; Yada, A.; Fürstner, A. *Chem.–Eur. J.* **2013**, *19*, 4532-4537.
(24) Alcarazo, M.; Radkowski, K.; Mehler, G.; Goddard, R.; Furstner, A. *Chem. Commun.* **2013**, *49*, 3140-3142.
(25) Micoine, K.; Persich, P.; Llaveria, J.; Lam, M.-H.; Maderna, A.; Loganzo, F.; Fürstner, A. *Chem.–Eur. J.* **2013**, *19*, 7370-7383.
(26) Kondoh, A.; Arlt, A.; Gabor, B.; Fürstner, A. *Chem.–Eur. J.* **2013**, *19*, 7731-7738.
(27) Valot, G.; Regens, C. S.; O'Malley, D. P.; Godineau, E.; Takikawa, H.; Fürstner, A. *Angew. Chem., Int. Ed.* **2013**, *52*, 9534-9538.
(28) Fürstner, A. *Science* **2013**, *341*, 1229713.
(29) Persich, P.; Llaveria, J.; Lhermet, R.; de Haro, T.; Stade, R.; Kondoh, A.; Fürstner, A. *Chem.–Eur. J.* **2013**, *19*, 13047-13058.
(30) Sun, C.-L.; Fürstner, A. *Angew. Chem., Int. Ed.* **2013**, *52*, 13071-13075, DOI: 10.1002/anie.201307028.
(31) Sundararaju, B.; Fürstner, A. *Angew. Chem., Int. Ed.* **2013**, *52*, 14050-14054.
(32) Seidel, G.; Gabor, B.; Goddard, R.; Heggen, B.; Thiel, W.; Fürstner, A. *Angew. Chem,Int. Ed.* **2014**, *53*, 879-882.

Alcarazo group

(2) Alcarazo, M.; Radkowski, K.; Goddard, R.; Fürstner, A. *Chem. Commun.* **2011**, *47*, 776-778.
(10) Hickmann, V.; Kondoh, A.; Gabor, B.; Alcarazo, M.; Fürstner, A. *J. Am. Chem. Soc.* **2011**, *133*, 13471-13480.
(24) Alcarazo, M.; Radkowski, K.; Mehler, G.; Goddard, R.; Fürstner, A. *Chem. Commun.* **2013**, *49*, 3140-3142.
(33) Alcarazo, M. *Dalton Trans.* **2011**, *40*, 1839-1845.
(34) Petuškova, J.; Bruns, H.; Alcarazo, M. *Angew. Chem., Int. Ed.* **2011**, *50*, 3799-3802.
(35) Inés, B.; Patil, M.; Carreras, J.; Goddard, R.; Thiel, W.; Alcarazo, M. *Angew. Chem., Int. Ed.* **2011**, *50*, 8400-8403.
(36) Petuškova, J.; Patil, M.; Holle, S.; Lehmann, C. W.; Thiel, W.; Alcarazo, M. *J. Am. Chem. Soc.* **2011**, *133*, 20758-20760.
(37) Iglesias-Sigüenza, J.; Alcarazo, M. *Angew. Chem., Int. Ed.* **2012**, *51*, 1523-1524.

(38) Prades, A.; Peris, E.; Alcarazo, M. *Organometallics* **2012**, *31*, 4623-4626.
(39) Palomas, D.; Holle, S.; Ines, B.; Bruns, H.; Goddard, R.; Alcarazo, M. *Dalton Trans.* **2012**, *41*, 9073-9082.
(40) García-Mancheño, O.; Alcarazo, M. *Angew. Chem., Int. Ed.* **2012**, *51*, 8151-8154.
(41) Carreras, J.; Patil, M.; Thiel, W.; Alcarazo, M. *J. Am. Chem. Soc.* **2012**, *134*, 16753-16758.
(42) Inés, B.; Palomas, D.; Holle, S.; Steinberg, S.; Nicasio, J. A.; Alcarazo, M. *Angew. Chem., Int. Ed.* **2012**, *51*, 12367-12369.
(43) Kozma, Á.; Gopakumar, G.; Farès, C.; Thiel, W.; Alcarazo, M. *Chem.–Eur. J.* **2013**, *19*, 3542-3546.
(44) Khan, S.; Gopakumar, G.; Thiel, W.; Alcarazo, M. *Angew. Chem., Int. Ed.* **2013**, *52*, 5644-5647.
(45) Kozma, Á.; Petuškova, J.; Lehmann, C. W.; Alcarazo, M. *Chem. Commun.* **2013**, *49*, 4145-4147.
(46) Khan, S.; Alcarazo, M. *Top. Curr. Chem.* **2013**, *334*, 157-170.
(47) Nicasio, J. A.; Steinberg, S.; Inés, B.; Alcarazo, M. *Chem.–Eur. J.* **2013**, *19*, 11016-11020.
(48) González-Fernández, E.; Rust, J.; Alcarazo, M. *Angew. Chem., Int. Ed.* **2013**, *52*, 11392-11395.
(49) Carreras, J.; Gopakumar, G.; Gu, L.; Gimeno, A.; Linowski, P.; Petuškova, J.; Thiel, W.; Alcarazo, M. *J. Am. Chem. Soc.* **2013**, 135, 18815-18823.

2.5 Department of Theory

Director:

Walter Thiel (born 1949)

Further group leaders:

Mario Barbatti (born 1972)

Elsa Sánchez-García (born 1976)

Curriculum Vitae: Walter Thiel

1949	Born in Treysa, Germany
1966-1971	Chemistry studies at Universität Marburg
1971-1973	Doctoral studies at Universität Marburg, with A. Schweig
1973-1975	Postdoctoral fellow at the University of Texas at Austin, with M. J. S. Dewar
1975-1982	Research scientist at Universität Marburg
1981	Habilitation for Theoretical Chemistry
1983-1992	Associate Professor of Theoretical Chemistry at Universität Wuppertal
1987	Guest Professor at the University of California at Berkeley
1992-1999	Full Professor of Chemistry at Universität Zürich
1999	Director at the Max-Planck-Institut für Kohlenforschung in Mülheim/Ruhr
2001	Honorary Professor at Universität Düsseldorf

Awards and Honors

1969-1974	Studienstiftung des deutschen Volkes
1975-1977	Liebig Fellowship, Verband der Chemischen Industrie
1982	Heisenberg Fellowship, Deutsche Forschungsgemeinschaft
1988	Förderpreis, Alfried-Krupp Stiftung
1991	Member, European Academy of Sciences and Arts
2002	Schrödinger Medal, World Association of Theoretical Chemists
2007	Member, Deutsche Akademie der Naturforscher Leopoldina
2007	Member, International Academy of Quantum Molecular Sciences
2008	Member, Nordrhein-Westfälische Akademie der Wissenschaften
2009	Festschrift, Journal of Physical Chemistry A 2009, 113 (43), 11455-12044
2012	Liebig Medal, German Chemical Society
2013	ERC Advanced Grant, European Research Council

Special Activities

1986-1992	Member of the Board, Institut für Angewandte Informatik, Wuppertal
1990-1992	Speaker, DFG-Forschergruppe: Reaktive Moleküle
1997-	Advisory Editor, Theoretical Chemistry Accounts
1998-	Advisory Editor, Journal of Computational Chemistry
2000-2008	Reviewer (Fachkollegiat), Deutsche Forschungsgemeinschaft
2000-2006	Member of the Board (Lenkungsausschuss), Bavarian Supercomputer Center (Höchstleistungsrechenzentrum Bayern)

2001-2005	Chairman, Arbeitsgemeinschaft Theoretische Chemie
2002-2008	Section Editor, Encyclopedia of Computational Chemistry
2004-2007	Member, Ständiger Ausschuss der Bunsengesellschaft
2004-	Member of the Scientific Advisory Board, Lise Meitner Minerva Center for Quantum Chemistry, Jerusalem/Haifa, Israel
2006-2008	Managing Director, Max-Planck-Institut für Kohlenforschung
2006-2012	Chairman, BAR Committee of the Max Planck Society
2006-2013	Member of the Kuratorium, Angewandte Chemie
2008-	Associate Editor, WIRES: Computational Molecular Sciences
2009-	Member of the International Advisory Board, State Key Laboratory of Physical Chemistry (PCOSS), Xiamen, China
2010	Chairman, Gordon Conference on Computational Chemistry
2011-	Member of the International Advisory Board, Institute of Organic Chemistry and Biochemistry, Prague, Czech Republic
2011-	President, World Association of Theoretical and Computational Chemists
2012-2013	Editorial Advisory Board, ACS Catalysis
2012-	Editorial Advisory Board, Accounts of Chemical Research
2012-	Member of the Board of Governors, German Chemical Society

Research in the Department of Theory

The Department of Theory comprises the research group of Prof. Walter Thiel and two junior groups headed by PD Dr. Mario Barbatti and Dr. Elsa Sánchez-García.

The central research objectives in the Department are theoretical developments to extend the scope of computational methodology, and applications to study problems of current chemical interest by computation. Such applications are mostly conducted in close cooperation with experimental partners.

In the group of Prof. Thiel, the main field of research is quantum chemistry. Methodological developments and chemical applications are considered to be of equal importance. The research interests range from accurate and almost quantitative calculations on small molecules to the approximate modeling of very large molecules.

The activities of the group cover
(a) ab initio methods (e.g., coupled cluster approaches, CCSD(T)),
(b) density functional theory (DFT),
(c) semiempirical methods (MNDO and beyond),
(d) combined quantum mechanical/molecular mechanical methods (QM/MM).

Recent applications in these four areas focus on
(a) vibration-rotation and electronic spectroscopy of small molecules,
(b) catalytic reactions of transition metal compounds,
(c) electronically excited states in large molecules,
(d) reaction mechanisms in enzymes.

The group of Dr. Barbatti uses ab initio and density functional methods to study nonadiabatic processes that occur after molecular photoexcitation. Methodologically, the aim is to implement new methods and algorithms to improve excited-state simulations within the Newton-X platform and to critically assess their quality. Applications include nonadiabatic dynamics simulations of ultrafast photoinduced processes in biologically relevant molecules and in molecular photo-triggers.

The research in the group of Dr. Sánchez-García focuses on molecular interactions in organic and biological systems, in particular on the introduction of ligands capable of altering protein function, on the interaction of proteins with their biological

environment, and on designed mutagenesis for the regulation of enzymatic activity. The code development targets the implementation of coarse-grained force field methods in QM/MM approaches.

Several cooperations between the Department of Theory and the experimental groups in the Institute have been established over the past years. There have been major collaborative projects on gold catalysis (Fürstner, Alcarazo), palladium catalysis (Maulide), platinum catalysis (Alcarazo), organocatalysis (List), enzymatic catalysis (Reetz), and cellulose depolymerization (Rinaldi, Schüth). In continuation of these efforts, there are a number of ongoing joint projects that employ quantum-chemical calculations to unravel the mechanisms of catalytic reactions studied by the experimental groups in the Institute.

More detailed information on the research areas of the Department is available in the following seven individual reports and in the scientific papers published in 2011-2013. It should be noted that, for the sake of brevity, some of these papers have not been discussed in the reports on the research areas of the Department, and should therefore be consulted directly, if necessary.

The overall direction of research in the Department has remained unchanged during the reporting period, with a notable trend to put more emphasis on the study of electronically excited states and of biologically relevant systems. This is also reflected in the research of the two junior groups. For the future, we anticipate that the focus on large complex systems will remain prominent in the research of the Department, both with regard to method development and chemical applications. We expect that the scope of the research activities will continue to be as broad as in the past, but there will also be some shifts and new directions. In the Thiel group, the method development towards improved semiempirical methods will be intensified in the framework of an ERC Advanced Grant (2014-2018), and there will be more emphasis on QM/MM studies of solvent effects on enzymatic reactivity due to the participation in the RESOLV Cluster of Excellence at the University of Bochum (2012-2017) that is dedicated to solvation science. In this context, a third junior research group will be established at our Department in January 2014, which will be headed by Dr. Matthias Heyden, an expert in classical molecular dynamics simulations of solvent phenomena, who has been selected in a thematically open RESOLV competition.

2.5.1 Research area "Ab initio methods" (W. Thiel)

Involved: J. Breidung, G. Cui, Y. Lu, A. Owen, I. Polyak, T. Ribeyre, A. Yachmenev

Objective: Vibration-rotation and electronic spectra of small molecules are computed with high accuracy using high-level ab initio calculations with large basis sets. This research includes the further development of a general variational treatment of nuclear motion that allows the accurate prediction of rovibrational energies and intensities. Highly correlated ab initio methods are also applied for validation and benchmark purposes in studies on electronically excited states.

Results: The theoretical prediction of vibration-rotation spectra requires the generation of accurate potential energy and dipole moment surfaces, followed by the variational calculation of rovibrational energies and intensities. For the former task, we employ ab initio electronic structure methods, typically coupled cluster theory with complete basis set (CBS) extrapolation and corrections for core-valence correlation and relativististic effects. For the latter, we have developed and coded a variational treatment of nuclear motion that is based on the Hougen-Bunker-Johns approach with an Eckart-frame kinetic energy operator and thus also handles large amplitude motion. This has led to a general and robust variational code (TROVE) that was published in 2007.

Over the past three years, TROVE has been extended in several ways. An automated procedure has been added that permits the further refinement of ab initio potential energy surfaces against accurate high-resolution experimental data using variational rovibrational calculations [15]. Technical improvements include coverage of additional molecular group symmetries (e.g., $\boldsymbol{T}_d(M)$), extension of the Numerov-Cooley method to allow periodic solutions of the one-dimensional Schrödinger equation (e.g., for torsions), implementation of eigensolvers for very large Hamiltonian matrices (with dimensions greater than 100,000), and more efficient storage strategies. The available functionality was extended towards the calculation of the rovibrational density matrix exponential and temperature corrections to molecular electromagnetic properties as well as partition functions and thermodynamic parameters (unpublished work by A. Yachmenev and S. Yurchenko).

In the reporting period, the TROVE program has been applied to study formaldehyde [7], thioformaldehyde [12, 81], ammonia [71], and methane [76]. The most extensive project was the calculation of a comprehensive line list for thioformaldehyde (^1H_2CS)

covering all rovibrational transitions that involve states up to 5000 cm^{-1} and rotational quantum number $J = 30$ (547,926 transitions between 41,809 energy levels) [81]. The TROVE computations were based on a six-dimensional potential energy surface determined at the CCSD(T)/CBS level with corrections for higher-order valence-electron correlation (using coupled cluster excitations up to CCSDTQP), core-valence correlation, scalar relativististic effects, and diagonal Born-Oppenheimer terms [12], with a subsequent very slight adjustment of two equilibrium geometry parameters against experimental data (changes in CH bond length by 0.0016 Å and in HCS angle by 0.02º) to improve the predicted intra-band rotational energy levels [81]. The dipole moment surface was computed at the CCSD(T)/aug-cc-pVQZ level (aug-cc-pv(Q+d)Z at sulfur) [81]. The rovibrational spectra calculated at T = 300 K are in excellent agreement with the available experimental data (see Figure 1). The TROVE calculations correctly reproduce the observed resonance effects (such as intensity borrowing), thus reflecting the high accuracy of the underlying ab initio surfaces. Experimentally, many high-resolution bands are still unassigned because of the complications arising from extremely strong Coriolis coupling (as pointed out by J. M. Flaud). Our detailed theoretical predictions and analysis of the rovibrational bands up to 5000 cm^{-1} (see e.g. Figures 2 and 3) are expected to facilitate and guide future laboratory assignments [81].

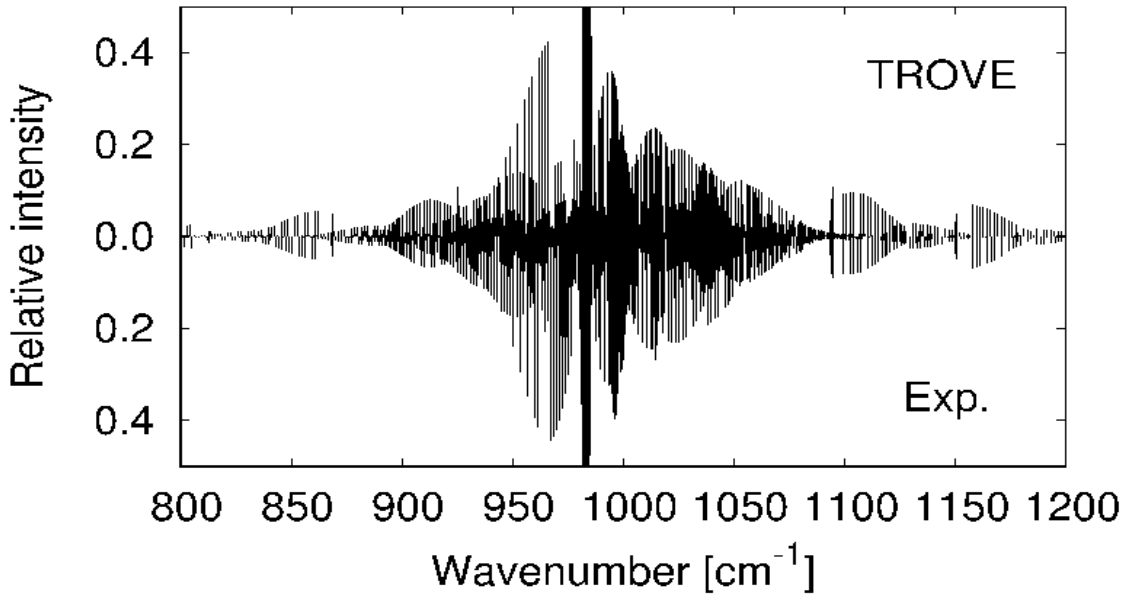

Figure 1. Comparison of the simulated absorption (T = 300 K) spectrum (TROVE) and the experimental spectrum (Exp.) of H_2CS for ν_4 and ν_6 bands [81].

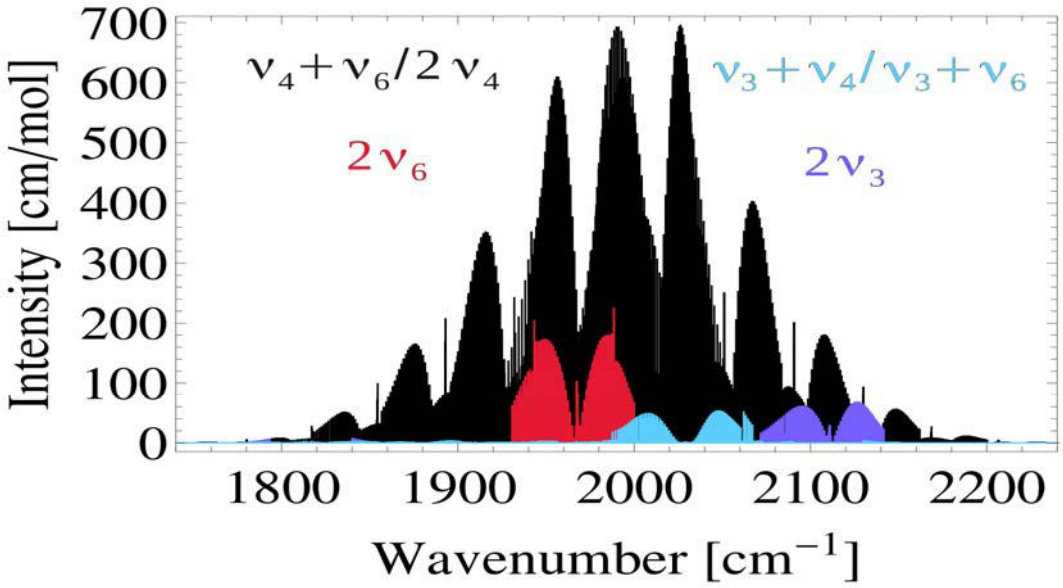

Figure 2. Overview of the simulated absorption spectrum of H_2CS at T = 300 K in the frequency range 1800-2200 cm^{-1} [81].

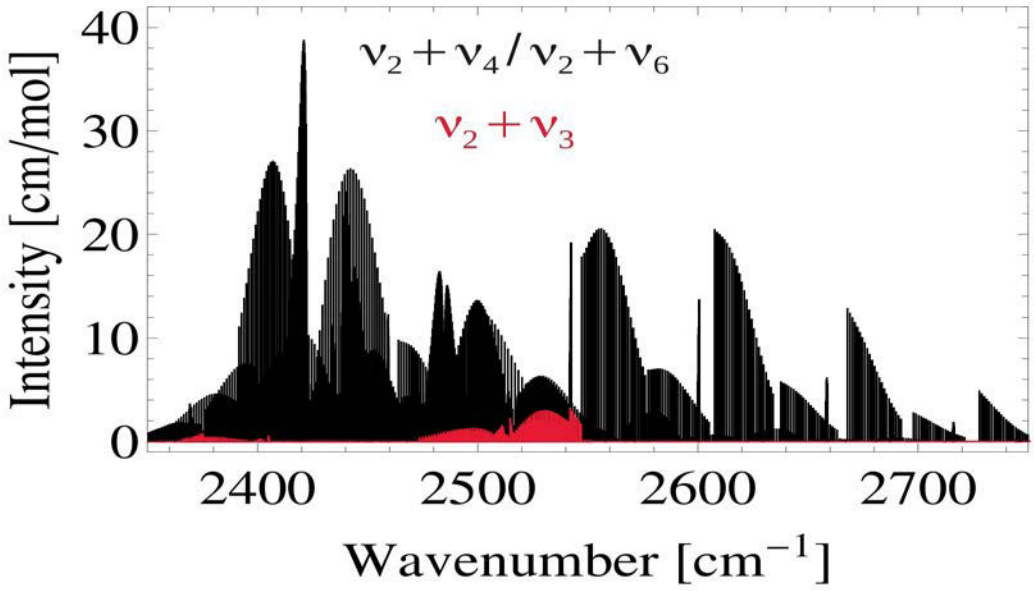

Figure 3. Overview of the simulated absorption spectrum of H_2CS at T = 300 K in the frequency range 2300-2800 cm^{-1} [81]. Please note different intensity scales in Figures 2-3.

In the case of formaldehyde H_2CO, we computed a CCSD(T)/aug-cc-pVQZ potential surface and refined it against spectroscopic data, achieving a root-mean-square (rms) deviation of 0.05 cm^{-1} for 599 rovibrational levels up to $J = 5$ [7]. In the case of ammonia, we refined our previously computed ab initio potential energy surface against accurate literature data covering transitions up to $J = 8$ and energy levels up to 10,300 cm^{-1} (with the constraint that the resulting surface remain close to the ab initio surface). This allowed us to reproduce the experimental term values of $^{14}NH_3$ with an rms

deviation of 0.05 cm^{-1} [15]. In collaborative work with the Marquardt and Quack groups, our ab initio surface was also used in the construction of an analytic, full-dimensional, and global representation of the potential energy surface of ammonia in the lowest adiabatic electronic state [71]. In the case of methane, we calculated a nine-dimensional dipole moment surface at the explicitly correlated CCSD(T)-F12c/aug-cc-pVTZ-F12 level and derived an accurate analytic representation using sixth-order polynomials, which will be used to produce comprehensive hot line lists for $^{12}CH_4$ (for astrophysical purposes such as modeling molecular opacity in the atmospheres of exoplanets and brown dwarfs) [76].

During the reporting period, we have published two reviews on ab initio rovibrational spectroscopy. The first one addresses the prediction of vibrational spectra from ab initio theory and the interplay between experiment and theory in the spectroscopic identification of new molecules, in particular reactive short-lived species [13]. The second one (together with T. J. Lee) reviews the use of quartic force fields in variational calculations of vibrational frequencies of small molecules, with emphasis on the choice of suitable coordinates with proper limiting behavior and on the accuracy that can be achieved in this manner [63].

Turning to electronically excited states and electronic spectroscopy, correlated ab initio calculations (e.g. at the MS-CASPT2 level) are performed for comparison or validation on a regular basis in excited-state projects that utilize lower-level methods (see the next chapters). In the reporting period, there have also been two ab initio application studies in this area. The first one concerned the electronically excited states and the photodissociation of benzaldehyde and acetophenone [31]. Our CASPT2//CASSCF calculations identify an $S_1/T_2/T_1$ three-state intersection area, where the T_2 state acts as a relay for an efficient $S_1 \rightarrow T_1$ intersystem crossing, followed by radical dissociation in the T_1 state. The computed pathways rationalize the experimental finding that different C-C bonds are cleaved in the photodissociation of benzaldehyde and acetophenone [31]. The second one addressed photoinduced gold(I)-gold(I) bonding in dicyanoaurate oligomers [74]. In collaboration with the Dolg and Fang groups, we assigned the band maxima of the oligomers $[Au(CN)_2^-]_n$ (n = 2-5) in aqueous solution on the basis of MS-CASPT2 calculations and explained the strengthening of the Au-Au bond upon excitation by considering the decisive orbital interactions in the leading configurations. The photodynamics in the oligomers could be well described by a three-state model for the staggered conformers and by a five-state model for the eclipsed conformers [74].

Future directions: The variational studies of vibration-rotation spectroscopy will be continued for methane, with the aim of generating comprehensive line lists at different temperatures. Further improvements and extensions of the TROVE code will be implemented as demanded by the application needs.

Generally speaking, we anticipate that the use of ab initio methods will remain important also in other projects, whenever high accuracy is needed (e.g., for validation and benchmarking purposes). This applies to all our research areas including theoretical studies on electronically excited states as well as on homogeneous catalysis and biocatalysis (see the next chapters).

Publications resulting from this research area: 7, 12, 13, 15, 31, 47, 63, 71, 74, 76, 81

External funding: None

Cooperations: M. Dolg (Köln, DE); W.-H. Fang (Beijing, CN); J.-M. Flaud (Paris, FR); P. Jensen (Wuppertal, DE); T. J. Lee (NASA Ames Research Center, US); R. Marquardt (Strasbourg, FR); M. Quack (Zürich, CH); J. Tennyson (London, UK); S. N. Yurchenko (London, UK)

2.5.2 Research Area "Density Functional Methods" (W. Thiel)

Involved: A. Anoop, T. Benighaus, D. Escudero, G. Gopakumar, J. P. Götze, B. Heggen, C. Loerbroks, M. Patil, T. Saito, K. Sen, L. Wolf

Objective: Density functional methods are applied in studies of transition metal and other compounds in order to understand and predict their properties. Much of the work on homogeneous transition metal catalysis and organocatalysis involves a close collaboration with experimental groups at our Institute and aims at a detailed mechanistic understanding of the reactions studied experimentally. Methodological advances are targeted as required by the chosen projects.

Results: In many of our applications in this area, we employ state-of-the-art density functional theory (DFT) to explore the ground-state potential energy surface and to characterize all relevant intermediates, transition states, and reaction pathways. Geometry optimizations are normally done with standard functionals (RI-BP86, B3LYP, B3LYP-D) and medium-size basis sets, followed by higher-level single-point energy evaluations that utilize either correlated ab initio methods (e.g. local CCSD(T) treatments with large basis sets) or modern density functionals (e.g., from the M06 series) with large basis sets and dispersion corrections (if appropriate). Effective core potentials are normally used to represent the core electrons of heavy elements. Thermal and entropic corrections are computed at the level applied for geometry optimization.

Joint projects with the Fürstner group: Asymmetric gold catalysis with one-point binding ligands (phosphoramidites with TADDOL-related but acyclic backbone) enables a number of difficult transformations with excellent enantioselectivity. Our DFT calculations on the cycloisomerization of enynes helped elucidate the origin of the enantioselectivity achieved with such gold catalysts [42]. Gold carbenoids are commonly considered as intermediates in many Au-catalyzed reactions. Attempts to prepare germane gold carbenoids devoid of stabilizing substituents via transmetalation led to remarkable hetero-bimetallic complexes (e.g., containing Au and Cr) that were characterized at the DFT level in terms of their electronic structure and chemical bonding [84]. In the enantioselective gold-catalyzed intramolecular etherification of allenes, the preferred enantiomer has been found to depend on the choice of solvent as well as on the temperature. Through DFT-based modeling, we attempt to help rationalize this very unusual phenomenon, which may be due to different catalyst conformations being favored in different solvents (work by L. Wolf). Further unpublished work includes theoretical studies on iron catalysis (by B. Heggen).

Joint projects with the Alcarazo group: The research in the Alcarazo group is directed towards the design and synthesis of unusual ligands and coordination compounds and their application in novel catalytic transformations. In our collaborative work, we perform DFT calculations to characterize the electronic structure of key species and to unravel the detailed mechanism of the catalytic reactions. Examples include the analysis of the electronic structure in the first observed dihydrido borenium cation [16], in carbene-stabilized phosphorus(III)-centered trications [22], in carbene-stabilized N-centered cations [54], and in cationic Ge(II) complexes [60]. In the latter case, the stability of the complexes arises from the ability of the neutral monodentate hexaphenylcarbodiphosphorane ligand to donate two electron pairs and thus simultaneously form two dative C = Ge σ and π bonds [60]. The pronounced π-acceptor properties of phosphorous trications [22] can be exploited in Pt(II) catalysis [44] and in gold catalysis [83] to enable very demanding cyclization reactions. We elucidated the underlying reaction mechanisms by computing the free energy profiles for the cyclization of 2-ethynyl-1,1'-binaphthalene into pentahelicene [44] (see Figure 4 as a typical example of such work) and of 2-ethynyl-2',6-dimethylbiphenyl into 4,5-dimethylphenanthrene [83].

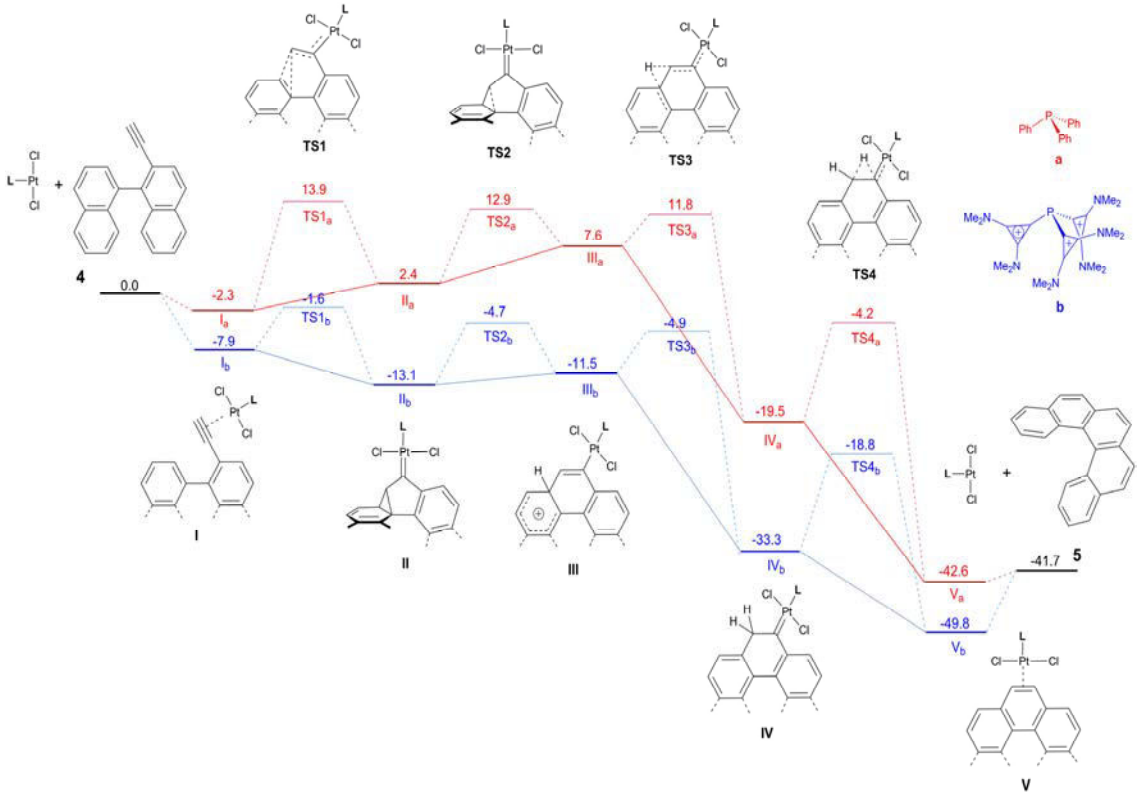

Figure 4. Free energy profiles (kcal/mol) for the cyclization of 2-ethynyl-1,1'-binaphthalene into pentahelicene, computed at the B3LYP-D level with a large basis set and PCM corrections [44]. Red: L = Ph_3P; blue: L = phosphorus trication $[R_3P]^{3+}$ with R = 2,3-dimethylamino-cyclopropenyl-1-ylidene. Calculated LUMO energies [44] for ligands L: -3.28 eV (red) vs. -11.69 eV (blue).

Joint projects with the List group: Chiral phosphoric acids are able to catalyze asymmetric S_N2-type O-alkylations, which formally involve a nucleophilic attack at the σ* orbital of a carbon electrophile. DFT calculations on the mechanism of a representative TRIP-catalyzed intramolecular alkylation show that the Brønsted acid acts as a bifunctional activator bridging the pentacoordinate transition state [52]. High stereoselectivity can be achieved in the asymmetric epoxidation and hydroperoxidation of α,ß-unsaturated carbonyl compounds using alkaloid-derived primary amines as catalysts and aqueous hydrogen peroxide as oxidant. Here, the analysis of the computed pathways led to a qualitative model of enantioselectivity based on the structure of the crucial iminium intermediate [58]. Still unpublished are further DFT investigations on the nature of the transition state in the catalytic 6π electrocyclization of unsaturated hydrazones.

Joint projects with the Maulide group: Sulfur (IV)-mediated transformations can be used to achieve direct ylide transfer to and metal-free arylation of carbonyl compounds, depending on the reagent (Martin's sulfurane or activated sulfoxides). Mechanistic studies (via NMR and DFT) support a common reaction pathway via very similar cationic S(IV) species and showcase how subtle changes in reactant properties can lead to disparate and seemingly unrelated reaction outcomes [61]. On a different front, the Maulide group has recently discovered the phenomenon of catalytic asymmetric diastereodivergent deracemization in Pd-catalyzed allylic alkylations. As part of a follow-up study, we performed DFT calculations that provide detailed insight into the Pd-catalyzed electrocyclic ring opening of cyclobutene units in large molecules, which proceeds as a conrotatory reaction in an intermediate Pd-cyclobutene complex, with competing isomer interconversion by η^1-η^3-η^1 allyl slippage [64]. Further DFT results are available on the detailed mechanism of other steps in the ligand-controlled deracemization (unpublished work by G. Gopakumar and L. Wolf).

Joint projects with the Rinaldi and Schüth groups: Cellulose consists of 1,4-β-linked glucose units, which can be converted to biofuel and industrial platform molecules. The depolymerisation of cellulose to glucose is an important part of this conversion process. As a first step in modeling this process, we have explored the electronic nature of the 1,4-β-glycosidic bond and its chemical environment in cellobiose (glucose dimer) as well as its influence on the mechanism of the acid-catalyzed hydrolysis [78]. The DFT results imply that cellulose is protected against hydrolysis not only by its supramolecular structure (as commonly accepted), but also by its electronic structure, in which the anomeric effect plays a key role [78]. Ongoing follow-up work addresses the

depolymerization of larger cellulose models (up to 40 linked glucose units) in water and in ionic liquids using QM/MM calculations on the hydrolysis mechanism as well as classical metadynamics simulations on the influence of conformational changes. In a related project, the isomerization of glucose to fructose in water has been studied at the DFT level to clarify the detailed reaction mechanism and to rationalize the observed differences in the catalytic efficiency of different metal cations (unpublished work by C. Loerbroks).

Other ground-state DFT projects: Some mechanistic DFT studies have been carried out without involvement of experimental groups from the Institute. These include calculations on the origin of selectivity in Pd-catalyzed Tsuji-Trost allylic alkylation reactions [18, 37] and on the mechanism of the stereoselective Pummerer reaction [56]. In the context of collaborative spectroscopic work with the Havenith and Sander groups (Bochum), we have performed DFT-based molecular dynamics (MD) simulations on acetylene-furan trimer formation in ultracold helium droplets to follow the aggregation process towards the global minimum [9] and on complexes between aromatic radicals and water to assess their stability at different temperatures and the population of different local minima [53].

Excited-state DFT projects: In our semiempirical excited-state work, DFT-based calculations are often carried out for comparison or validation (see the next chapter). In addition, there have been three application studies in the reporting period that mainly rely on time-dependent density functional theory (TD-DFT). In collaboration with the Barbatti group, we performed TD-DFT benchmark calculations on donor-acceptor heterojunctions composed of thiophene oligomers and C_{60} fullerene to identify the most suitable functional for studying organic solar cells of this kind [49]. The electronic excitations of two carotenoids (violaxanthine and zeaxanthine) were computed in the gas phase and in acetone using different DFT-based approaches to assess their performance, which turned out to be most favorable for the Coulomb attenuated CAM-B3LYP functional [55]. In cooperation with the Holder group, we investigated the photodeactivation pathways in a novel Ir(III) cyclometalated complex, a promising candidate for electroluminescent devices. Our DFT and TD-DFT calculations indicate that metal-centered triplet excited states play an active role in the nonradiative deactivation of this complex [77].

Analytic gradients: Unrestricted density functional theory (UDFT) is widely applied to open-shell systems. UDFT treatments often yield broken-symmetry (BS) spin-polarized

solutions that capture a certain amount of nondynamical correlation but suffer from spin contamination, which may be removed by spin projection schemes to obtain improved single-point energies. We have derived and implemented analytic gradients for BS-UDFT calculations with removal of spin contamination by Yamaguchi's approximate spin projection method [45]. The analytic gradients are more precise, robust, and efficient than the previously available numerical gradients, and they allow fast full geometry optimizations of large open-shell systems, as shown in several test applications [45].

Stochastic simulations: Motivated by experimental work in the Reetz group showing that rhodium catalysts with chiral monodentate phosphorous ligands can achieve asymmetric hydrogenation with high efficiency and enantioselectivity, we had previously computed at the DFT level the entire catalytic cycle for enantioselective hydrogenation of itaconic acid using a chiral Rh(phosponite)$_2$ catalyst. In the present reporting period, the computed relative free energies of all stationary points in the four coupled lowest-energy cycles leading to (*R*)- and (*S*)-product were refined by single-point calculations using accurate domain-based local pair natural orbital coupled cluster theory (DLPNO-CCSD and DLPNO-CCSD(T), unpublished work with the Neese group). To analyze the chemical kinetics of this reaction (with 20 stationary points in each of the four coupled cycles), we have implemented Gillespie's stochastic simulation algorithm (SSA) including various options such as τ leaping in the code. Kinetic Monte Carlo simulations with the SSA algorithm were performed to determine the enantiomeric excess (*ee*) in the products for several temperatures and for several sets of computed relative energies. The resulting *ee* values were found to be very sensitive to the input energies, and large differences were encountered for different DFT approaches. Good agreement with experiment was obtained at the coupled cluster level (unpublished work by J. Breidung).

Future directions: We plan to maintain and strengthen the existing collaborations with our experimental partners. We expect that application-driven DFT studies of catalytic processes will continue to play an important role in our future research. If warranted, they will be supplemented by combined DFT/MM calculations with a molecular mechanical (MM) description of the environment (bulky substituents or solvent), by CPMD simulations of dynamic processes, and by accurate single-point calculations using correlated ab initio methods.

Publications resulting from this research area: 9, 16, 18, 21, 22, 37, 42, 44, 45, 49, 52, 53, 54, 55, 56, 58, 60, 61, 64, 77, 78, 83, 84

External funding: SusChemSys (Ziel 2 Programm NRW)

Cooperations: M. Alcarazo (Mülheim/Ruhr, DE); M. Barbatti (Mülheim/Ruhr, DE); M. Braun (Düsseldorf, DE); A. Fürstner (Mülheim/Ruhr, DE), M. Havenith (Bochum, DE); E. Holder (Wuppertal, DE); B. List (Mülheim/Ruhr, DE); N. Maulide (Mülheim/Ruhr, DE); F. Neese (Mülheim/Ruhr, DE); T. C. Ramalho (BR); R. Rinaldi (Mülheim/Ruhr, DE); E. Sánchez-García (Mülheim/Ruhr, DE); W. Sander (Bochum, DE); F. Schüth (Mülheim/Ruhr, DE)

2.5.3 Research Area "Semiempirical Methods" (W. Thiel)

Involved: G. Cui, P. Dral, E. Fabiano, J. A. Gámez, B. Heggen, M. Korth, A. Koslowski, Z. Lan, Y. Lu, A. Nikiforov, L. Spörkel, O. Weingart, X. Wu

Objective: This long-term project aims at the development of improved semiempirical quantum-chemical methods that can be employed to study ever larger molecules with useful accuracy. This includes the development of more efficient algorithms and computer programs. Our current focus in this area is on electronically excited states.

Results: Over the past years, we have developed semiempirical methods that go beyond the standard MNDO model by including orthogonalization corrections at the NDDO level. This has led to three new approaches labelled OM1, OM2 and OM3 (orthogonalization models 1-3) that offer significant improvements over established MNDO-type methods in several areas, including conformational properties, hydrogen bonds, reaction barriers, and electronically excited states.

During the reporting period, we have rewritten our code for the multi-reference configuration interaction (MR-CI) treatment of electronically excited states. We have replaced the loop-driven by a shape-driven version of the GUGA-CI algorithm (GUGA, graphical unital group approach). We have implemented an in-core and a direct variant of the algorithm, in which the CI coupling coefficients are stored explicitly or recomputed as needed, respectively. The new code is about twice as fast as the old one (unpublished work by A. Koslowski).

In the self-consistent-field (SCF) part of our semiempirical MNDO code, we have implemented two algorithms that allow for non-integer occupation numbers of the orbitals. *Fermi smearing* introduces some occupation of virtual orbitals at high electronic temperatures and improves SCF convergence. OM2 with Fermi smearing has recently been recommended for the simulation of electron impact mass spectra of organic molecules (S. Grimme, Angew. Chem. Int. Ed. 2013, 52, 6306). The *floating occupation number SCF treatment* aims at improving the shape of the relevant active orbitals such that they are well suited for MRCI calculations on excited states. Analytic gradients have been implemented for this approach.

On the technical side, the SCF section of our semiempirical MNDO code has been ported to hybrid CPU-GPU platforms that contain a graphics processing unit (GPU) as a

co-processor [33]. The most time-consuming routines were optimized for GPUs by using suitable library routines for linear algebra tasks and locally written GPU kernels for pseudodiagonalization and for orthogonalization corrections. The overall computation times for single-point energy calculations and geometry optimizations of large molecules were reduced typically by one order of magnitude for all semiempirical methods, as compared to runs on a single CPU core [33]. This development makes it practical to study whole proteins at the semiempirical SCF level. In addition, the in-core variant of the Davidson-Liu diagonalizer was also ported to GPUs to speed up large-scale MRCI calculations (unpublished work by A. Koslowski).

For validation purposes, the accuracy of six standard semiempirical methods has been benchmarked [17] using the comprehensive GMTKN24 database for general main group thermochemistry, kinetics, and noncovalent interactions, which had originally been introduced to evaluate DFT methods (L. Goerigk and S. Grimme, J. Chem. Theory Comput. 2010, 6, 107). The OMx methods outperform AM1, PM6, and SCC-DFTB by a significant margin, with a substantial gain in accuracy especially for OM2 and OM3. These latter methods are quite accurate and robust even in comparison to DFT, with overall mean absolute deviations in the computed energies of 6.6 kcal/mol for PBE and 7.9 kcal/mol for OM3 [17].

In cases where the generic accuracy of semiempirical methods is not sufficient for a given application, it is possible to perform specific parameterizations. During the reporting period, this has been done in two collaborative projects: In the first one (with D. T. Major), specific reaction parameters (SRP) were derived in the AM1 framework for dihydrofolate reductase (DHFR) to enable accurate quantum mechanics/molecular mechanics (QM/MM) molecular dynamics (MD) simulations of the DHFR-catalyzed reaction and the evaluation of reliable kinetic isotope effects using a mass-perturbation-based path-integral approach [20]. The second project (with H. Lin) involved the reparameterization of the AM1, PM3, and OMx methods to improve their description of bulk water and of proton transfer in water. QM/MM MD simulations with the resulting SRP Hamiltonians led to significantly better results in all cases, with OM3 accounting best for the structural and dynamic properties of water and the hydrated proton [66].

Over the past three years, our semiempirical applications have focused on excited-state dynamics. We had previously implemented the trajectory surface hopping (TSH) method with the fewest switches algorithm (Tully) in the MNDO software, making use of our semiempirical in-core version of the GUGACI method that handles general CI

expansions (up to full CI) efficiently for small active spaces and provides an analytic GUGACI gradient as well as analytic nonadiabatic coupling matrix elements. Most of these studies were carried out at the OM2/MRCI level for medium-size organic molecules in the gas phase. These TSH simulations provided insight into the chiral pathways and mode-specific tuning of photoisomerization in azobenzenes [6,34,67], the mechanism of hexatriene-based fulgide photoswitches [40] and Feringa-type fluorene-based photoinduced molecular rotors [10], the complete photochemical cycle of a GFP chromophore with ultrafast excited-state proton transfer [24], the preferred relaxation pathways in the nonadiabatic dynamics in 4-N,N-dimethylamino-benzylidene malononitrile (a typical push-pull charge transfer system) [28], the photophysics of a truncated indogo model [41], the competition between concerted and stepwise mechanisms in the ultrafast photoinduced Wolff rearrangement of 2-diaza-1-naphthoquinone [48] (see Figure 5), and the photodynamics and photochromism in the prototypical Schiff base salicylidenaniline [65]. The results of these OM2/MRCI studies are generally consistent with the available experimental data and high-level static calculations, but the dynamics simulations often detect pathways and preferences between pathways that are not obvious from the static calculations. The OM2/MRCI approach has thus emerged as a suitable tool for investigating the excited states and the photochemistry of large molecules.

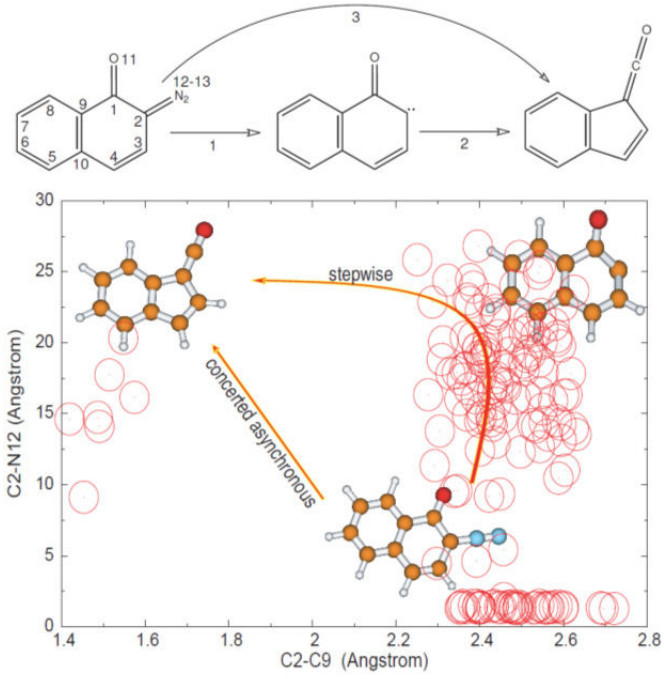

Figure 5. Top: Wolff rearrangement of 2-diazo-1-naphthoquinone (DNQ): stepwise (1-2) and concerted (3) mechanisms; the numbering scheme for the atoms is shown for the DNQ reactant. Bottom: Product distribution among 158 trajectories at the end of the 1 ps nonadiabatic simulations; red circles indicate the final geometries [48].

Note concerning Figure 5: The ketene product of the concerted Wolff rearrangement is found in 7 out of 158 trajectories; 39 trajectories return to the ground-state starting point, and the remaining 112 trajectories are roaming the carbene region. In subsequent 10 ps Born-Oppenheimer molecular dynamics for the carbene, using the final positions and velocities of the carbene fragment in the TSH trajectories as initial conditions, 36 of the 112 trajectories evolve from the "hot" carbene to the ketene region, thus increasing the overall ketene quantum yield to ca. 27% after 10 ps [48].

In the previous reporting period, we had already studied the excited-state dynamics and the photostability of the nucleobases in the gas phase. In joint work with M. Barbatti, we have thereafter carried out a thorough benchmark on *9H*-adenine [35] comparing the TSH results from ab initio MR-CIS, TD-DFT, and OM2/MRCI gas-phase simulations. The ab initio and OM2/MRCI methods predict the experimentally observed ultrafast deactivation of *9H*-adenine with similar time scales (but through different internal conversion channels), whereas the TD-DFT calculations with six different hybrid and range-corrected functionals fail to predict the ultrafast deactivation. These discrepancies were traced back to the topographies of the underlying potential energy surfaces along the relevant reaction pathways [35].

Using our TSH implementation in the ChemShell QM/MM framework, we have also studied the nonadiabatic dynamics of nucleobases in aqueous solution (adenine, guanine) and in model DNA strands (adenine). Going from the gas phase to aqueous solution, the optimized geometries of the relevant conical conical intersections and the associated relaxation paths remain qualitatively similar, but there are changes in their relative importance because of the solvent-induced shifts in the energetics. Overall, the decay times in solution are even slightly lower than those in the gas phase [8,32]. By contrast, the S_1 lifetime of adenine in a solvated B-type DNA oligomer model $(dA)_{10}$ is computed to be about ten times larger (ca. 5 ps) than in the gas phase. This is at least partly due to the higher rigidity of the DNA strand, since the two relevant conical interactions are both characterized by strong out-of-plane deformations that are more difficult to reach in the DNA environment. In our DNA double strand model, solvated $(dA)_{10}\cdot(dT)_{10}$, one of these two decay paths is suppressed because the out-of-plane motion of the amino group is impeded by inter-strand hydrogen bonding [11,30].

Ground-state MD simulations of large systems can be computationally demanding even at the QM/MM level and often become practical only with semiempirical QM methods. We use such semiempirical QM/MM MD simulations regularly in QM/MM projects [2,20,26,27,66,68,70], for example in free energy calculations or to follow the time evolution of complex systems. This work will be described in the next section.

Future directions: Research in the framework of the ERC Advanced Grant will focus on the further development and application of OMx methods. This includes a reparameterization of the existing OMx methods with inclusion of dispersion corrections aiming at a balanced treatment of ground-state and excited-state properties, the reformulation of the OMx methods with the use of MNDO-type integral approximations to facilitate the extension to heavier main-group elements and transition metals with an spd-basis, and generic as well as specific parameterizations for transition metals.

Semiempirical applications will concentrate on excited states of large complex systems (spectroscopy, photochemistry, solar cells) using both static calculations and dynamics simulations. Semiempirical methods will continue to serve as QM components in QM/MM MD studies of enzymatic reactions.

Publications resulting from this research area: 6, 8, 10, 11, 14, 17, 20, 24, 28, 30, 32, 33, 34, 35, 40, 41, 48, 65, 66, 67, 79

External funding: ERC Advanced Grant (awarded in 2013, start of funding in 2014)

Cooperations: M. Barbatti (Mülheim/Ruhr, DE); M. Filatov (Groningen, NL); B. Hartke (Kiel, DE); H. Lin (Denver, US); H. Lischka (Lubbock, US); D. T. Major (Bar-Ilan, IL)

2.5.4 Research area "Combined Quantum Mechanical / Molecular Mechanical Methods" (W. Thiel)

Involved: A. Altun, T. Benighaus, E. Boulanger, M. Doerr, E. Fabiano, J. P. Götze, B. Heggen, Y. Hsiao, B. Karasulu, Z. Lan, R.-Z. Liao, Y. Lu, S. Metz, M. Patil, I. Polyak, E. Sánchez-García, K. Sen, M. R. Silva-Junior, T. Vasilevskaya, O. Weingart, X. Wu

Objective: This research focuses on hybrid approaches for large systems where the active center is treated by an appropriate quantum mechanical method and the environment by a classical force field. It involves considerable method and code development. This approach allows a specific modeling of complex systems such that most of the computational effort is spent on the chemically important part. Current applications primarily address biocatalysis and aim at a better understanding of enzymatic reactions including the role of the protein environment.

Results: Combined quantum mechanical/molecular mechanical (QM/MM) methods have become a popular tool for studying reactions in complex systems such as enzymes. In the preceding reporting period, we had extended the two-layer QM/MM approach to a three-layer model by introducing boundary potentials that represent the outer part of the MM region and the bulk solvent. This offers two major advantages: conceptually, the long-range electrostatic interactions in a solvated enzyme are well described in this manner, and technically, the computational effort is reduced significantly by the strong reduction of the number of explicitly treated MM atoms (typically 2,000 compared with around 30,000 in standard QM/MM work). We previously implemented the generalized solvent boundary potential (GSBP), known from MM-MD simulations, in a semiempirical QM/MM framework (JCTC 2008, 4, 1600). In a second step, we developed a new boundary potential (SMBP, solvated macromolecule boundary potential) that is conceptually similar to GSBP, but can be used with any QM method and is also efficient for geometry optimization (JCTC 2009, 5, 3114). We have applied these boundary potential techniques to study the influence of long-range electrostatic interactions on the enzymatic reactions in chorismate mutase (CM) and p-hydroxybenzoate hydroxylase (PHBH) [2]. The corresponding energetic effects were found to be small for the pericyclic Claisen rearrangement catalyzed by CM (with little charge transfer), but substantial (several kcal/mol) for the hydroxylation reaction in PHBH, during which there is a formal transfer of one negative charge from the substrate to the cofactor. The QM/MM/SMBP approach provides detailed insight into the electrostatic influence of the outer MM region and the bulk solvent [2].

Our first three-layer QM/MM/continuum treatments combined the polarizable QM region with a fixed-charge MM region and a bulk solvent represented by a polarizable dielectric continuum (PDC). To arrive at a fully polarizable three-layer model, polarizable MM force fields were implemented in our QM/MM/BP approach [46] using the classical Drude oscillator (DO) model for the electronic polarizability of the MM atoms. As the mutual responses of each subsystem must be taken into account, efficient schemes were developed to converge the polarization of each layer simultaneously. This was achieved by considering the MM polarizable model as a dynamical degree of freedom in MD simulations with GSBP, and by using a dual self-consistent-field procedure for relaxing the Drude oscillators to their ideal positions and for converging the QM wavefunction in geometry optimizations with SMBP [46]. Applications with this new fully polarizable three-layer treatment are currently in progress.

The proper initial system setup for QM/MM studies is non-trivial. Starting geometries are commonly taken from classical MD simulations, but random MD snapshots may contain regions with high-energy conformations. In cooperation with the Engels group, we have proposed a new approach for the setup of water shells around proteins employing Tabu-Search global optimization techniques [50]. Comparisons with standard MD protocols for the chignolin test case show that both algorithms are capable of providing reasonable water shells. The new approach offers the advantage to generate more stable solvated systems with increased water-enzyme interactions and to enable a stepwise build-up of the solvent shell, such that the more important inner part can be prepared more carefully [50].

In QM studies of small molecules, transition states are normally verified by following the intrinsic reaction coordinate (IRC) towards reactants and products. Such IRC computations are difficult at the QM/MM level because of the high dimensionality of the investigated systems. To overcome these problems, we adopted a strategy analogous to microiterative transition state optimization. In this approach [69], the IRC equations only govern the motion of a core region that contains at least the atoms directly involved in the reaction, while the remaining degrees of freedom are relaxed after each IRC step. This strategy can be used together with any existing IRC procedure. After some proof-of-principle tests at the QM level on small gas-phase systems, the broad applicability of our implementation was demonstrated by IRC computations for two real-life enzymatic reactions using standard QM/MM setups [69].

Free energy calculations are demanding at the QM/MM level because of the need for extensive sampling. They are technically feasible with semiempirical QM components, and there are several approximate treatments available in combination with high-level

QM treatments. We designed a dual Hamiltonian free energy perturbation (DH-FEP) method for accurate and efficient evaluation of the free energy profile of chemical reactions in QM/MM calculations [70]. In contrast to existing QM/MM FEP variants, the QM region is not kept frozen during sampling, but all degrees of freedom except for the reaction coordinate are sampled. In the DH-FEP scheme, the sampling is done by semiempirical QM/MM MD simulations, while the perturbation energy differences are evaluated from high-level QM/MM single-point calculations at regular intervals, skipping a pre-defined number of MD sampling steps. The merits of the QM/MM DH-FEP approach were demonstrated by free energy calculations for an analytic model potential with an exactly known solution (validation) and for the enzymatic reaction catalyzed by CM. In the latter case, the DH-FEP approach was applied in combination with a one-dimensional reaction coordinate and with a two-dimensional collective coordinate (two individual distances), with superior results for the latter choice [70].

For the modeling of enzymatic reactions, QM-only calculations on model systems may be used as an alternative to QM/MM calculations on the full solvated enzyme. We compared these two approaches in a case study [43,75] on the formation of vinyl alcohol in the catalytic cycle of tungsten-dependent acetylene hydratase (AH). Seven QM regions were considered, containing 32 up to 657 atoms, which were selected on the basis of charge deletion analysis and distance criteria. Overall, the QM/MM energies were found to converge more smoothly than the QM-only energies upon increasing the size of QM region. At the QM/MM level, the reaction mechanism is qualitatively well described when using 157 QM atoms, whereas quantitative convergence in the computed relative energies to within 1-2 kcal/mol requires a large QM region with 407 atoms in the case of AH [43,75]. Another issue in QM-only studies of enzymatic reactions (apart from convergence with regard to model size) is the use of a coordinate-locking scheme, in which certain key atoms at the periphery of the chosen cluster model are fixed to their crystal structure positions. In a further case study on AH [57], we investigated the uncertainties introduced by this scheme, which arise from the limited accuracy of the experimental crystal structures. We found that the resulting uncertainties in the QM-only energies are tolerable for high-quality protein crystal structures (resolution better than 2.0 Å), but may become unacceptable for structures with significantly lower resolution [57].

In the preceding reporting period, we had implemented quantum refinement into our ChemShell QM/MM software. The traditional procedure for solving protein crystal structures is to supplement the X-ray diffraction data with restraints from simple MM force fields during the refinement. These restraints are taken from QM/MM energies in quantum refinement, which should thus be more reliable especially in regions that are

not well described by the available MM force fields. We applied quantum refinement in combination with classical MD simulations, QM/MM geometry optimizations, and DFT/MRCI calculations of electronic absorption spectra to reinvestigate the structure of the pB_2 species in the photocycle of the photoactive yellow protein [3] and of the blue-light sensing using flavin (BLUF) domain of the wild-type AppA protein from *Rhodobacter sphaeroides* [36]. In the pB_2 case, this led to an improvement of the chromophore geometry towards a somewhat more planar structure and the identification of a previously overlooked crystal water molecule near the phenolic OH group of the chromophore [3]. In the AppA BLUF case, there are two published crystal structures (1YRX and 2IYG) that give different side-chain orientations of key residues close to the flavin chromophore (e.g., Gln63) – our calculations slightly favor the 1YRX-type orientation [26,36].

In QM/MM studies on enzymatic reaction mechanisms, we normally use geometry optimization techniques to follow conceivable pathways on DFT/CHARMM potential energy surfaces in order to determine the most favorable one. Optimizations are normally done with efficient DFT approaches (e.g., RI-BP86 with moderate basis sets), while relative energies are determined using more refined functionals (e.g., B3LYP-D or M06 with larger basis sets) or even correlated ab initio methods (CCSD(T) or multi-reference treatments). If necessary, QM/MM free energy calculations are performed to capture entropic contributions. In the following, we first describe one such mechanistic QM/MM study in some detail and then briefly summarize several others.

Motivated by experimental directed evalution work in the Reetz group, we examined the Baeyer-Villiger oxidation reaction in cyclohexanone monooxygenase (CHMO) to elucidate its mechanism and the origin of its enantioselectivity. According to the QM/MM calculations on the wild-type enzyme [27], the enzyme-reactant complex contains an anionic deprotonated C4a-peroxyflavin that is stabilized by strong hydrogen bonds with the ARG-329 residue and the $NADP^+$ cofactor. The CHMO-catalyzed reaction proceeds via a Criegee intermediate with pronounced anionic character. The fragmentation of this intermediate to the lactone product is the rate-limiting step. The QM/MM results for the parent cyclohexanone confirm the crucial role of the ARG-329 residue and of the $NADP^+$ cofactor for the catalytic efficiency of CHMO. QM/MM calculations for the CHMO-catalyzed oxidation of 4-methylcyclohexanone reproduce and rationalize the experimentally observed (*S*)-enantioselectivity for this substrate, which is governed by the conformational preferences of the corresponding Criegee intermediate and the subsequent transition state (TS2) for the migration step [27]. A subsequent QM/MM study addressed the effect of mutations of the Phe434 residue in the active site of CHMO on its enantioselectivity towards 4-hydroxycyclohexanone

[59]. In terms of our previously established model of the wild-type enzymatic Baeyer-Villiger reaction, enantioselectivity is governed by the preference towards the equatorial ((*S*)-selectivity) or axial ((*R*)-selectivity) conformation of the substituent at the C4 carbon atom of the cyclohexanone ring in the Criegee intermediate and the rate-limiting transition state (TS2). The enantiopreference towards 4-hydroxycyclohexanone was assessed by locating all relevant TS2 structures at the QM/MM level, for the wild-type enzyme and two mutants (Phe434Ser and Phe434Ile). The experimentally observed enantioselectivity was reproduced semi-quantitatively in all three cases, including the pronounced reversed enantioselectivity in the Phe434Ser mutant. The effect of point mutations on CHMO enantioselectivity could be explained at the molecular level, by an analysis of the specific interactions between substrate and active-site environment in the TS2 structures (see Figure 6) that satisfy the basic stereoelectronic requirement of anti-periplanarity for the migrating σ-bond [59].

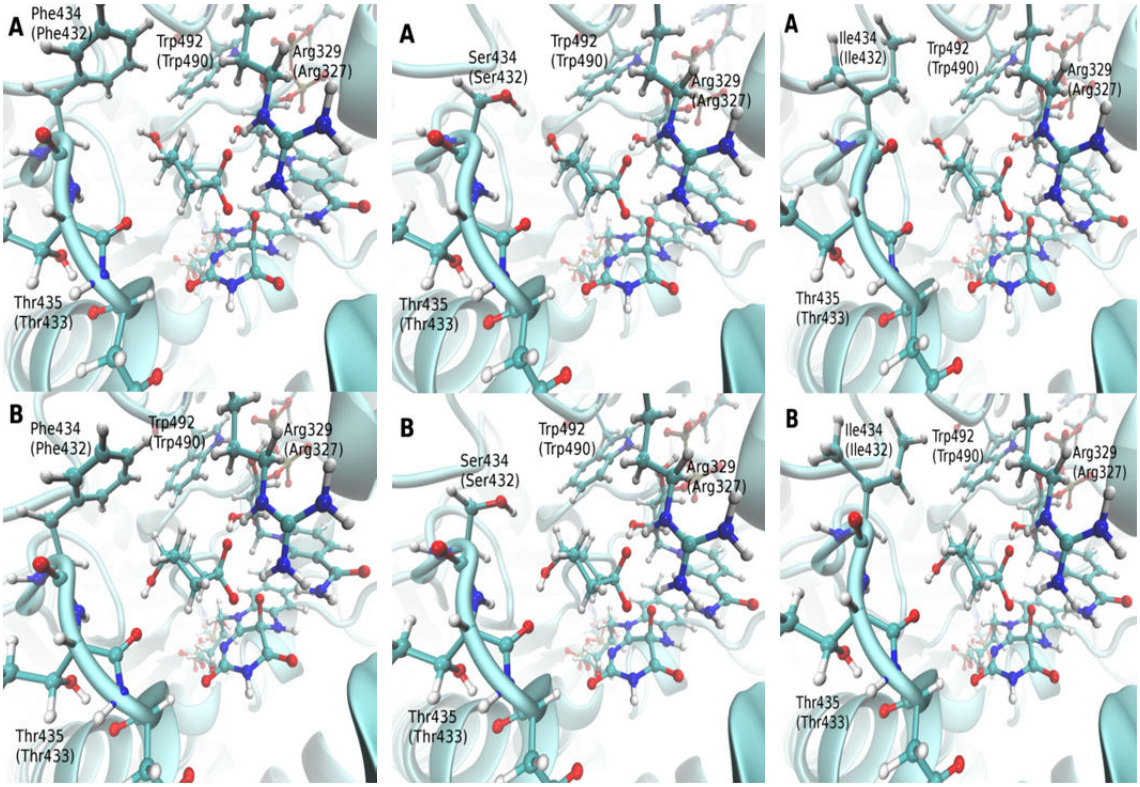

Figure 6. QM/MM optimized structures of the rate-limiting transition state for migration. Left: wild-type CHMO; middle: Phe434Ser mutant; right: Phe434Ile mutant. A (top): equatorial orientation of the substrate hydroxyl group. B (bottom): axial orientation of the substrate hydroxyl group.

Note concerning Figure 6: In orientation B, the substrate OH group always forms an H-bond with the Thr435 carbonyl oxygen atom. In orientation A, the substrate OH group interacts with the Phe434 phenyl ring of the wild-type CHMO (left), with the Ser434 OH group of the Phe434Ser mutant (middle), and with the isoleucine backbone carbonyl atom in the Phe434Ile mutant (right). The relative strength of these interactions determines the favored orientation, and hence the stereochemical outcome of the reaction. The equatorial orientation A is preferred only in the Phe434Ser mutant because of the strong H-bond between the OH groups of the substrate 4-hydroxycyclohexanone and the serine residue. Therefore, (*S*)-selectivity is only observed in the Phe434Ser mutant.

In the following, we briefly summarize the results from five other QM/MM studies on ground-state enzymatic reactions that were carried out during the reporting period.

(a) Glycosyltransferases (GTs) catalyze the highly specific biosynthesis of glycosidic bonds. We investigated the mechanism of the reaction catalyzed by Lipopolysaccharyl-α-1,4-galactosyltransferase C (LgtC) from *Neisseria meningitides* [29]. Among the three alternatives discussed in the literature, the QM/MM calculations favor a dissociative single-displacement (S_Ni) mechanism, in which the acceptor substrate attacks on the side of the UDP leaving group that acts as a catalytic base. They identify several key interactions that help this front-side attack by stabilizing the oxocarbenium ion-like transition state [29].

(b) Lysine-Specific Demethylase 1 (LSD1) catalyzes the demethylation of particular lysine residues in histone protein tails (H3K4), with flavin adenine dinucleotide (FAD) acting as cofactor. The oxidation of substrate lysine (sLys) involves the cleavage of an α-CH bond accompanied by the transfer of a hydride ion equivalent to FAD, leading to an imine intermediate. The QM/MM calculations predict this hydride transfer pathway to be clearly favored for sLys oxidation over other proposed mechanisms, including the single-electron transfer route or carbanion and polar-nucleophilic mechanisms [73]. They rationalize the activation of the rather inert methyl-CH bond in a metal-free environment through proper alignment of sLys and transition state stabilization, as well as the role of important active-site residues (Y761, K661, and W695) and of the conserved water-bridge motif [73].

(c) Fosfomycin A is a manganese-dependent enzyme that utilizes a Mn^{2+} ion to catalyze the inactivation of the fosfomycin antibiotic by glutathione (GSH) addition. According to our QM/MM calculations [51], the enzyme-catalyzed glutathione addition reaction proceeds in the sextet state. It involves an initial proton transfer from the GSH thiol group to the Tyr39 anion, followed by a nucleophilic attack of the GSH thiolate leading to epoxide ring opening. The second step is rate-limiting and is facilitated by the presence of the high-spin Mn^{2+} ion that functions as a Lewis acid and stabilizes the leaving oxyanion through direct coordination. The QM/MM calculations rationalize the observed catalytic efficiency, regioselectivity, and chemoselectivity of Fosfomycin A in terms of the influence of the active-site protein environment and the different stabilization of the distorted substrate in the relevant transition states [51].

(d) Aldoxime dehydratase is a heme-containing enzyme that utilizes the ferrous rather than the ferric ion to catalyze the synthesis of nitriles by dehydration of the substrate. Our QM/MM study of the enzymatic dehydration of *Z*-acetaldoxime covered all three

possible spin states [38]. Only one pathway was found to be feasible, starting with substrate coordination to Fe^{2+} via its nitrogen atom followed by N-O cleavage that is facilitated by a single-electron transfer from the ferrous heme to an antibonding N-O orbital in the singlet state, while His320 acts as a general acid and base by mediating the required proton transfers [38]. This scenario explains the observed oxidation state preference (Fe^{2+} vs. Fe^{3+}).

(e) Cysteine dioxygenase (CDO) is involved in the biodegradation of toxic cystein. It is a nonheme iron dioxygenase that transfers the two oxygen atoms from molecular oxygen to cysteinate to form cysteine sulfinic acid products. The mechanism for this reaction is disputed in the literature. Our QM/MM calculations [4] on substrate activation by CDO give a stepwise mechanism that takes place on several low-lying spin state surfaces via multistate reactivity patterns, starting on the singlet ground state of the iron(II)-superoxo reactant and then proceeding mainly on the quintet and triplet surfaces. An alternative pathway via a persulfenate intermediate is much higher in energy and thus not accessible [4].

In the area of ground-state enzyme reactivity, we have also published reviews on our previous QM/MM studies of molybdenum-containing enzymes [5] and on the role of single water molecules as biocatalysts in cytochrome P450cam chemistry [1]. Still unpublished is mechanistic QM/MM work on the P450eryF enzyme (by K. Sen) and on hemocyanin (by T. Saito).

Turning to QM/MM applications on electronically excited states, we have already mentioned in the preceding chapter the semiempirical QM(OM2/MRCI)/MM surface hopping studies of nucleobases in water and in DNA strands [8,11,30,32]. We have also performed QM/MM calculations of electronic absorption spectra in the condensed phase, most notably on rhodopsin mutants linked to the *Retinitis pigmentosa* disease [25], the red fluorescent protein (HcRed) from *Heteractis crisp* [39], and the blue-light photoreceptor YtvA of *Bacillus subtilis* with structurally modified flavin chromophores [72]. The QM/MM calculations of the electronic spectra mostly employed DFT/MRCI as QM component. In the latter two applications, the QM/MM calculations also covered photoinduced processes, namely the excited-state isomerization in HcRed via torsions around the two bridging bonds [39] and the competition between radiationless deactivation and photoadduct formation in photoreceptors with different flavin chromophores [72].

QM/MM techniques have also been used to address solvation effects. Concerning the modeling of zwitterions in water, we have studied the conformations and relative

stabilities of the folded and extended forms of 3-fluoro-γ-aminobutyric acid (FGABA) using discrete microsolvated QM models, a QM/MM treatment of FGABA in TIP3P water, and a standard continuum solvation treatment (PCM). Among these approaches, only the QM/MM free energy calculations gave results consistent with the experimental findings deduced from NMR spectroscoscopy [23]. As part of a study on the photochemical steps in the prebiotic synthesis of precursors from HCN, we used QM/MM MD simulations to estimate the time needed to dissipate the energy of a particular hot ground-state HCN tetramer into the solvent (water), which resulted in a very short time window for the occurrence of hot ground-state reactions during the synthesis [68]. Further ground-state QM/MM MD simulations were carried out to model proton transfer in water [66] and kinetic isotope effects in DHFR [20].

The ChemShell software that has been used in all these applications is available under a license agreement (see www.chemshell.org).

Future directions: We shall further improve ChemShell as a user-friendly and stable QM/MM environment and add features that are not yet available. QM/MM applications will continue to address ground-state enzymatic reactions where many mechanistic problems remain to be solved. In particular, the influence of solvents on enzymatic reactivity will be examined in the framework of the RESOLV Cluster of Excellence. Emphasis will also be put on QM/MM studies of electronically excited states, both for the calculation of condensed-phase electronic spectra and of excited-state reactions in biomolecules. Moreover, we are prepared to use the QM/MM technology also in other areas, e.g. in homogeneous organometallic catalysis.

Publications resulting from this research area: 1, 2, 3, 4, 5, 8, 11, 20, 23, 25, 26, 27, 29, 30, 32, 36, 38, 39, 43, 46, 50, 51, 57, 59, 66, 68, 69, 70, 72, 73, 75

External funding: Volkswagenstiftung (I/83915), German Research Foundation: RESOLV Cluster of Excellence (EXC 1069)

Cooperations: M. Bühl (St. Andrews, UK); S. de Visser (Manchester, UK); B. Engels (Würzburg, DE); J. Kästner (Stuttgart, DE); D. Kumar (Lucknow, IN); H. Lin (Denver, US); J. M. Lluch (Barcelona, ES); D. T. Major (Bar-Ilan, IL); L. Masgrau (Barcelona, ES); M. T. Reetz (Mülheim/Ruhr, DE); S. Shaik (Jerusalem, IL); S. C. Smith (Oak Ridge, US); W. F. van Gunsteren (Zürich, CH)

2.5.5 Research Area "Photoinduced Processes in Organic Molecules" (M. Barbatti)

Involved: R. Crespo-Otero, D. Asturiol, D. Mancini

Objective: After UV photoexcitation, organic molecules relax through a manifold of excited states, dissipating the absorbed energy either by photoemission or by vibrational excitation. The objective of this research area is to determine the relaxation mechanisms in two classes of organic systems: a) molecules playing roles in living organisms and b) molecules with potential application as photo-triggers. This goal is accomplished by computational simulations of excited-state dynamics, of potential-energy pathways, and of absorption and emission spectra.

Results:

a) Photophysics of life

Over the past few years, we have investigated the effect of UV radiation on nucleic acid fragments (nucleobases and backbone models) using computational chemistry. This is a topic of major interest as it allows understanding the role played by photochemistry in the biosphere and how carcinogenic and mutagenic effects are induced by radiation. Between 2011 and 2013, we have completed the mapping of the excited-state reaction pathways of cytosine, guanine and uracil (collaboration with H. Lischka). Dynamics simulations for these nucleobases on the ultrafast time-scale revealed that several reaction paths are activated and compete with each other to determine the fate of the reaction. Additionally, we showed that the ionization potentials of adenine along the main reaction paths undergo strong variations that are usually not taken into account either in experimental or in computational analysis (collaboration with S. Ullrich).

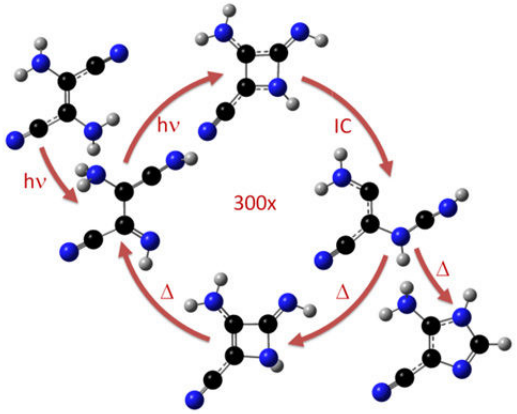

Figure 7. Photochemical steps for synthesis of an imidazole derivative from HCN.

We also investigated the photochemical step of one of the most likely pathways explaining the prebiotic origin of nucleotides on Earth (collaboration with W. Thiel and A. Anoop). This step consists of the photoinduced conversion of a HCN oligomer into an imidazole derivative. Although this photoreaction is known since the 1960s and most current prebiotic models are based on it, the exact reaction mechanism had still not been elucidated. Using dynamics, chemical kinetics, and thermodynamics, we showed that the reaction happens through a long sequence of excitations and de-excitations of an azetene derivative (Fig. 7).

Besides DNA, one of the most important UV chromophores in the skin of mammalians is urocanic acid (UA). The photophysics of this molecule is especially relevant because its *trans-cis* photoisomerization is a main factor inducing skin cancer. Another remarkable feature of UA is that its photoisomerization quantum yield decreases at short wavelengths. Although a number of models based on the topography of the excited-state potential energy surfaces have been proposed to explain this anomalous photophysics, none of them is completely satisfactory. We approached the problem in a distinct way, working under the hypothesis that the anomalous photophysics is caused by tautomeric effects. In fact, spectrum simulations of the tautomers allowed us to show that their relative spectral shift could be the cause of the anomalous photophysics.

A central process in photodynamic therapy is the generation of singlet oxygen ($^1O_2$) by a photosensitizer bound to a carcinogenic cell. Since the 1980s, porphycene (P_C) has been examined as a potentially efficient photosensitizer. We have investigated the UV absorption of P_C and the photophysics of $^1O_2$ generation via P_C sensitization. We showed that 1) there are several $^1O_2$-generation mechanisms available; that 2) the dominant mechanism is dependent on the O_2 concentration; and that 3) highly efficient $^1O_2$ generation could be obtained by encapsulating P_C and O_2 together, opening new conceptual perspectives for photodynamic therapy based on P_C.

As a last point in this research topic, we investigated the photodynamics of two simple models of molecules relevant for biological processes: the N-methyl-formamide (NMF), a model for peptide bonds; and methyl-pentadieniminium cation (Me-PSB3), a model for retinal. In both cases, ultrafast dynamics was simulated using QM/MM methods to incorporate environment effects. In the case of NMF, we showed that a caging effect enables the occurrence of reactions such as proton transfer, which are absent in the gas phase (collaboration with W. Sander). In the case of Me-PSB3, we showed that interaction with a polar solvent changes the orientation of the potential-energy

intersection cone from sloped to peaked, considerably enhancing the speed of deactivation to the ground state.

b) Molecular photo-triggers

Photo-triggers are often used for activation of molecular machines and electronic devices. They work in different ways, for instance, by inducing structural changes via isomerization or dissociation, or by promoting electronic changes via charge transport. We have been investigating a number of different photo-triggers from these two classes. Azobenzene, azomethane, ethylene, and $Cr(CO)_6$ are examples of the first class of photo-triggers. After irradiation, these molecules undergo strong structural changes, which may be communicated to neighboring molecular groups to trigger a reaction. We have simulated the photoinduced ultrafast dynamics of these molecules. In the case of azobenzene, where two nonequivalent rotational pathways corresponding to clockwise or counterclockwise rotations are available, we determined that the course of the rotational motion is strongly dependent on the initial conditions. In fact, we could even demonstrate that the occurrence of one or another pathway can be completely controlled by selecting adequate initial conditions (collaboration with J. Pittner). In the case of $Cr(CO)_6$, dynamics results were used to assign experimental time-constants corresponding to the dissociative motion through the manifold of excited states.

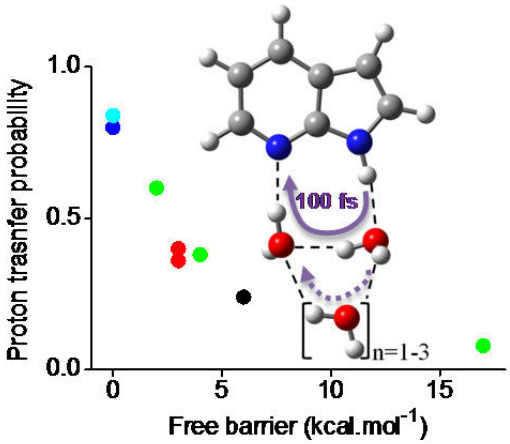

Figure 8. Excited-state intramolecular proton transfer in 7AI-water clusters.

Photoinduced excited-state intramolecular proton transfer in 7-azaindole (7AI), 2-(2′-hydroxyphenyl)benzothiazole and 1H-pyrrolo[3,2-h]quinoline are examples of the second class of photo-triggers. We have simulated the excited-state ultrafast dynamics of these three molecules within small clusters of water and methanol (collaboration with N. Kungwan). While in the gas phase the proton transfer occurs directly between the donor and acceptor groups of the molecule, within clusters the proton is transferred through the network of hydrogen bonds. For all these cases, we showed that the process

is completed within 100 fs. We also mapped the relative importance of several possible reaction pathways. In 7AI-water clusters, for instance, only the nearest two water molecules participate in the proton transfer, while the others play a passive role (Fig. 8).

Outreach: We have made an effort to communicate our results to a more general public through diverse media. Description of our research lines, main results, and new publications are constantly updated on the group homepage (sgk.mpg.de/private/barbatti). A YouTube channel dedicated to movies showing the results of dynamics simulations is also available (youtube.com/user/mbarbatti). News on our work and other relevant information for our field are delivered through our Twitter account (twitter.com/MarioBarbatti). Outstanding results from our research are communicated to general science popularization media. For this last point, we are supported by Sarah-Lena Gombert, from the press-office of our Institute.

Future directions: In the first topic, *Photophysics of life*, we are working on: 1) determination of the role of the catalytic electron for dissociation of pyrimidine dimers; 2) calculation of reaction pathways in bioluminescent proteins (collaboration with W. Thiel); 3) design of bi-fluorescent markers for proteins (collaboration with T. C. Ramalho); and 4) tautomeric effects in the deactivation of solvated adenine. In the topic *Photo-triggers*, we are working on the characterization of organic heterojunctions for organic photovoltaics (collaboration with W. Thiel) and on the photodynamics of salicylidene methylamine (collaboration with A. Sobolewski).

Publications resulting from this research area: 68, 86, 87, 88, 89, 90, 91, 92, 94, 95, 96, 98, 99, 100, 102, 103, 104, 105, 107, 108, 110, 111, 112, 113

External funding: German Academic Exchange Service (DAAD DE/HR; DAAD DE/BR; DAAD DE/EG); COST-Action CM1204

Cooperations: W. Thiel (Mülheim, DE); N. Kungwan (Chiang Mai, TH); I. Antol (Zagreb, HR); H. Lischka (Lubbock, US); A. Anoop (Kharagpur, IN); T. C. Ramalho (Lavras, BR); A. Sobolewski (Warshaw, PL); M. Elshakre (Kairo, EG); A. Castillho (Sao Carlos, BR); S. Ullrich (Athens, US); W. Sander (Bochum, DE)

2.5.6 Research Area "Development and Assessment of Methods" (M. Barbatti)

Involved: R. Crespo-Otero, T. Cardozo

Objective: Whereas state-of-the-art computational methods allow reaching chemical accuracy for the ground state, simulations of excited states bear a high level of uncertainty. This is due to the many approximations required to deal with the large density of states and the complicated electronic structures of excited states, while still keeping the simulations computationally affordable. The objectives of this research area are a) to implement new methods and algorithms to improve excited-state simulations within the Newton-X platform and b) to critically assess the quality of the calculations.

Results:

a) The Newton-X platform

Since 2005, we have been designing and developing the Newton-X platform. Newton-X is a collection of programs to perform all steps of excited-state nonadiabatic dynamics simulations, from the generation of initial conditions to the statistical analysis. The project involves collaborations with H. Lischka, J. Pittner, G. Granucci, and M. Persico. Newton-X is an open-source platform distributed free of charge. Within the last 12 months (as of October 15, 2013), 150 new downloads have been registered.

Most of new methodologies developed in our group are incorporated into Newton-X. Between 2011 and 2013, we implemented a general hybrid-gradient interface allowing dynamics with QM/MM and ONIOM approaches. We developed a general method for efficient numerical computation of nonadiabatic couplings and for dynamics using the Local Diabatization method. We also developed new interfaces for nonadiabatic dynamics with MCSCF wavefunctions using GAMESS (collaboration with T. Windus); CC2 and ADC(2) using Turbomole; and TDDFT and TDA using Gaussian 09.

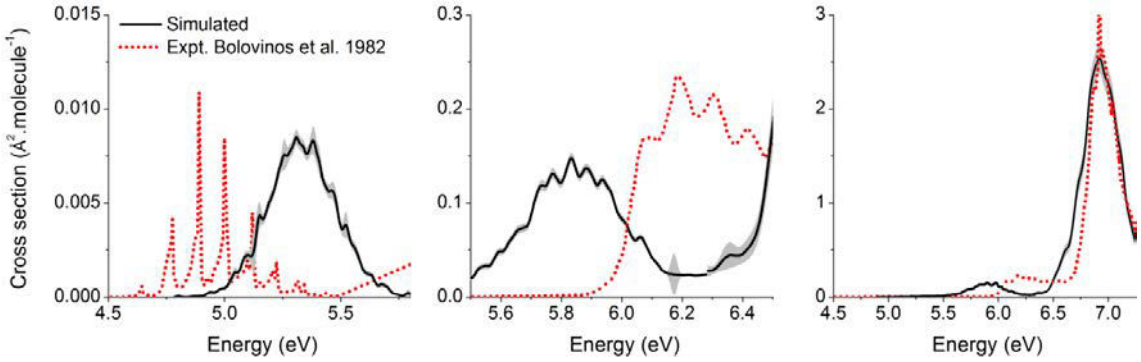

Figure 9. Simulated UV-absorption cross section of 2-phenylfuran compared to experimental results.

State classifications based on CI-type electronic densities were implemented, allowing automatic characterization of the electronic states in terms of local excitations, charge-transfer and delocalized excitations during the dynamics.

Newton-X allows spectrum simulation using ensembles of nuclear geometries. The method can provide absolute intensities, effective parameter-free band widths, and dark vibronic bands (Fig. 9). We presented a formal derivation of the method, which, although popular among several groups, had up to that point only been based on qualitative arguments. This derivation will also allow the development of new algorithms in the future.

b) Method assessment and benchmarks

To understand the impact of the active and reference spaces, we systematically investigated the dynamics of 2-aminopyrimidine at the CASSCF level and of ethylene at the MRCI level (collaboration with H. Lischka). In the first case, we found that the selection of orbitals for the active space has a strong effect on the dynamics output, up to a point where the space is saturated. Before saturation, even with the same nominal number of electrons and orbitals, the dynamics results can be very different for distinct sets of orbitals. After saturation, the results are not affected significantly even when the space is increased. In the case of ethylene, we concluded that the dynamics are influenced not only by the dynamic electron correlation within the π-system, but also within then σ-σ* subsystems and between the σ- and the π-systems. This finding allowed us to explain most of the divergences between simulated and experimental results for the excited-state lifetime of ethylene.

Dynamics simulations for adenine performed with semi-empirical and *ab initio* MRCI predicted similar lifetimes, but deactivation through different pathways. In collaboration with W. Thiel, we systematically repeated these simulations under very controlled conditions. An imbalance in the barriers along two different reaction pathways was found to be the reason for the divergence. Curiously, the imbalance was found in both methods with opposite trends. Under the same conditions, we also tested the dynamics of adenine at the TDDFT level using several functionals. All of them failed to describe the ultrafast dynamics of this molecule. Right now, we are extending these simulations to the ADC(2) level. The collection of all these simulations will provide a useful benchmark of dynamics results for small hetero-aromatic molecules.

We have also validated TDDFT for simulations of donor-acceptor (D-A) interfaces for photovoltaics (collaboration with W. Thiel). Using dimers of thiophene oligomers (D) and fullerene C_{60} (A) as prototypes, we benchmarked the vertical electronic spectra by

systematically changing a number of variables, including oligomer size, density functional (Fig. 10), polarization medium, D-A distance, and chemical functionalization of the monomers. This benchmark will guide the selection of models and computational levels in our future investigations in this field.

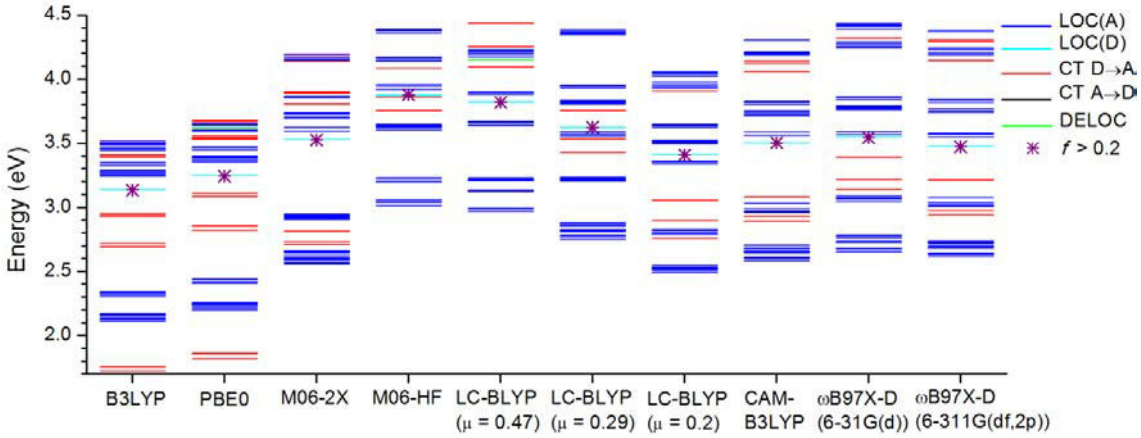

Figure 10. Benchmark of vertical excitations for a thiophene-oligomer/fullerene interface at different levels.

Outreach: Our group supervises the release and distribution of the Newton-X platform. This is done via the Newton-X webpage (www.newtonx.org), where full documentation and tutorials can be accessed. Moreover, we moderate a discussion list at goo.gl/G0H9fg, where a knowledge database is built from users and developers contributions.

Future directions: The next versions of Newton-X will include full Pump-Probe simulations, based on the computation of ionization cross sections for ensembles of dynamics snapshots. We are also starting the development of methods for automatic computation of Marcus state-transfer rates for systems with a high density of states (collaboration with W. Thiel).

Publications resulting from this research area: 35, 49, 85, 93, 97, 101, 106, 109, 113

External funding: German Academic Exchange Service (DAAD DE/HR)

Cooperations: W. Thiel (Mülheim/Ruhr, DE); H. Lischka (Lubbock, US); T. Windus (Ames, US); J. Pittner (Prague, CZ); G. Granucci and M. Persico (Pisa, IT)

2.5.7 Research Area "Molecular Interactions in Organic and Biological Systems. Applications and Methodological Implementations" (E. Sánchez-García)

Involved: K. Bravo-Rodriguez, S. Mittal, P. Sokkar, J.M. Ramirez-Anguita

Objectives: Molecular interactions (MIs) play a key role in chemical and biological processes. However, despite the many scientific advances of the last decades, understanding and predicting the effect of MIs in biological systems is still challenging. In our group we develop computational models to help regulate strategically important molecular interactions in biological systems via the rational manipulation of three factors: *1. the introduction of ligands able to alter protein function, 2. the interactions of proteins with their biological environment,* and *3. the mutagenesis of key residues*. In addition, we also investigate molecular interactions in small model systems like reactive intermediates and closed-shell molecules as a basis to understand more complex systems (Figure 11). One important goal of our research is to predict improved therapeutic agents and approaches, for example in the context of neurodegenerative diseases and the development of new antibiotics.

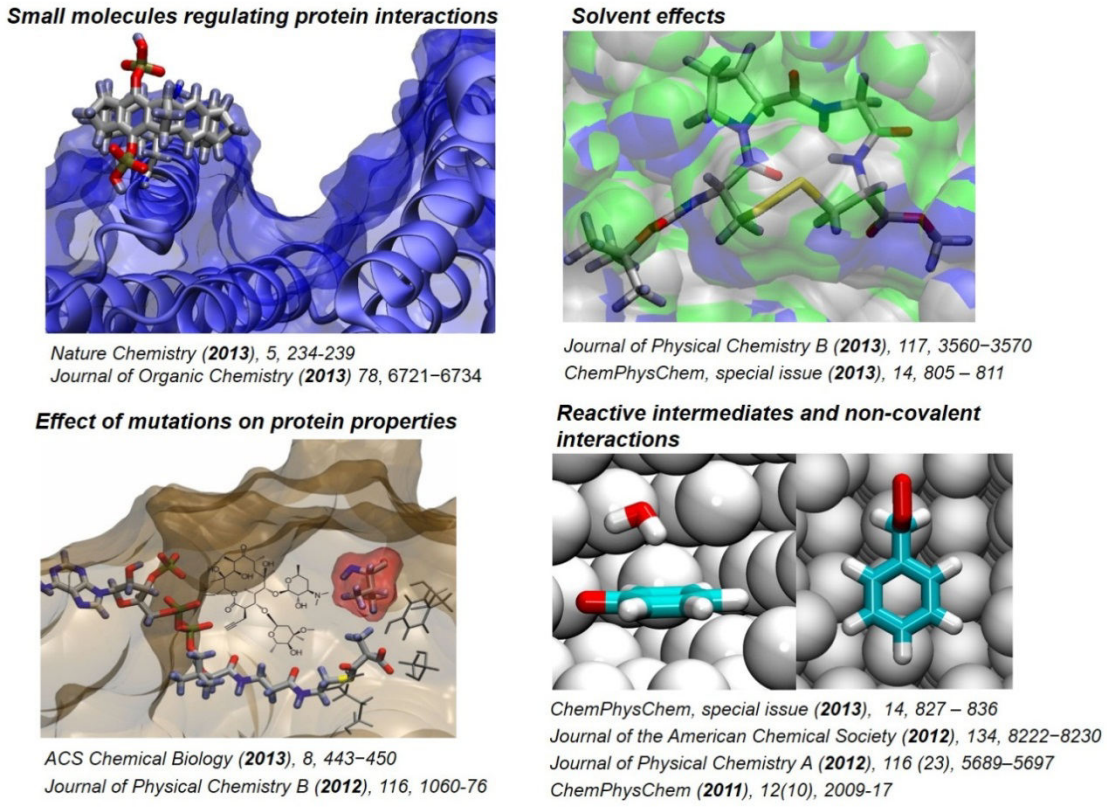

Figure 11. Main research lines and selected representative publications of our group in the last two years.

On the methodological side, we work on generalizing the combination of quantum mechanics (QM) and atomistic molecular mechanics (MM) into a triple-layer QM/MM/CG modeling approach by implementing coarse grained (CG) force fields in the ChemShell code. The aim is to extend the applicability of QM/MM computations to enable an efficient and realistic theoretical treatment of complex chemical, photochemical, and biochemical systems that are challenging for the existing computational methods.

Results:

Molecular interactions in organic and biological systems. Applications

a) Ligands for the regulation of protein properties

Ligands can be used to regulate protein aggregation, enzymatic activity, lipid attachment, and protein–protein interactions, among other important biological properties. In my group we investigate the effect of highly selective ligands such as molecular tweezers (MT) that bind specifically to lysine and arginine, as well as the effect of less specific molecules like aromatic heterocyclic derivatives.

Experimental studies have shown that MTs are able to inhibit the aggregation of Aβ (amyloidogenic peptide related to Alzheimer disease) and IAPP (islet amyloid polypeptide, related to type II diabetes mellitus) without toxic effects, which makes them promising candidates for drug development. In this context, we recently studied the binding mode of four water-soluble tweezers bearing phosphate, phosphonate, sulfate, or O-methylenecarboxylate groups at the central benzene bridge to amino acids and peptides containing lysine or arginine residues. The comparison between experimental and theoretical data provided clear evidence for the unique threading mechanism and the modulating effect of each anion on the interaction of the MTs with positively charged amino acids and peptides. These findings were explained on the basis of the host-guest complex structures obtained from molecular dynamics (MD) simulations and QM/MM methods [120].

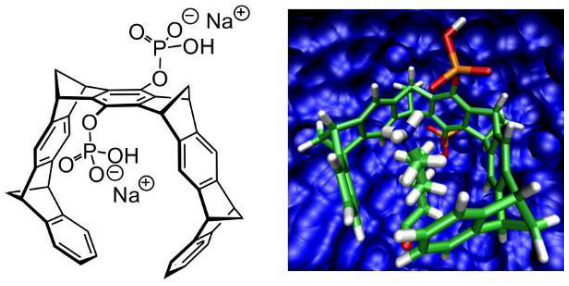

Figure 12. Bishydrogenphosphate tweezer CLR01 (left), CLR01 interacting with lysine, structure optimized in explicit water environment at the QM/MM level (right).

We also investigated the interactions of IAPP and Aβ with the bishydrogenphosphate tweezer CLR01 (Figure 12). In both, IAPP and Aβ, the selective binding to critical lysine residues is the molecular origin of the effect of the tweezers. However, there are different mechanisms that inhibit toxicity according to our calculations. In IAPP, the presence of CLR01 induces the peptide to adopt an off-pathway conformation not found in its absence. In $A\beta_{42}$, applying an excess of tweezers decreases the β-sheet content of the monomer, slowly disintegrates the oligomer structures, and leads to an alternative aggregation pathway of the monomers. Our results are in agreement with experimental findings (collaboration with G. Bitan and T. Schrader), which indicate that an excess of tweezers is necessary to inhibit toxicity in Aβ, whereas sub-stoichiometric concentrations of CLR01 are enough to achieve efficient inhibition of IAPP aggregation.

An amyloidogenic peptide closely related to the transmission of HIV-1 is $PAP_{248\text{-}286}$, a fragment of the abundant semen marker prostatic acidic phosphatase (PAP). The $PAP_{248\text{-}286}$ peptide forms amyloid fibrils (SEVI) that are believed to act as electrostatic "shield" between viral and cellular membranes. Our study of the interactions of molecular tweezers with $PAP_{248\text{-}286}$ shows that CLR01 is able to bind all positively charged residues in $PAP_{248\text{-}286}$ and that this interaction is conserved. Conversely, a spacer molecule by itself (consisting of the charged core of CLR01 with the hydrogenphosphate groups) only features labile interaction patterns with $PAP_{248\text{-}286}$, consistent with the experimentally observed lack of inhibition by such spacer molecules. Our results suggest that the lower infectivity rate found for SEVI in the presence of CLR01 can be related to the ability of the tweezer to decorate all lysine and arginine residues in $PAP_{248\text{-}286}$. This way, the addition of CLR01 changes the charge of the surface of the fibrils, thus diminishing the potential of SEVI to act as a shield between the cellular and virus membranes.

To answer the question of how the tweezers behave in the presence of complex systems with multiple lysine residues, we also studied the effect of molecular tweezers on proteins. We established that molecular tweezers are a powerful tool for regulating 14-3-3 protein-protein interactions for the 14-3-3 σ isoform via an entirely new interference mechanism. Furthermore, the combination of structural analysis and computer modeling allowed us to establish *general rules* for predicting the relative strength and type of interaction of the tweezers with lysine residues in 14-3-3 proteins [118]. Very recent unpublished studies (cooperation with C. Ottmann) show that the 14-3-3 ζ isoform also crystallizes in the presence of the tweezers in line with our computational

predictions. We are currently investigating the effect of molecular tweezers on other protein hosts like p97 and α-synuclein.

As mentioned above, we are also interested in smaller ligands with less specific binding sites and their ability to prevent toxic aggregation (cooperation with E. Wanker). O4 (2,8-bis-(2,4-dihydroxy-phenyl)-7-hydroxy-phenoxazin-3-one) is an orcein-related molecule introduced by Wanker which stabilizes the self-assembly of β-sheet-rich protofibrils and fibrils, efficiently decreasing the concentration of small toxic Aβ oligomers. Our studies of the interaction of O4 with Htt_{Gln47} (first exon of the Huntingtin protein, polyQ length of 47) using docking, MD and QM/MM MD methods confirmed the role of the N-terminus region in Htt aggregation. We showed that the binding of O4 to Htt involves simultaneous interactions with the glutamine residues of the polyQ region and with residues of the N-terminus. Our calculations also indicated that O4 binding promotes a time-dependent destruction of the initial β-sheet-rich Htt_{Gln47} structure. The effect of other novel ligands (prepared by E. Wanker) on amyloid aggregation is currently being investigated in my group.

Importantly, the study of the interaction motifs and mechanisms of small molecules with several peptide and protein hosts allows us not only to answer important questions related to these systems, but also to guide the design of improved ligands able to reach specific protein regions of biological relevance.

b) Reactive intermediates and synthetic cyclic peptides. Solvent effects

Given the importance of radicals and radical reactions in such diverse aqueous environments as biological systems or tropospheric clouds, it is highly desirable to understand the influence of water and other solvents on their chemical and physical properties. Since we are interested in using molecular interactions with the environment to tune the properties of chemical and biological systems, we study the effect of solvents on reactive intermediates (e.g., radicals) using QM, MD, and QM/MM techniques.

We investigated the complexes of phenoxyl, anilinyl, and benzyl radicals with water using QM and QM/MM MD approaches [53,116]. The influence of molecular interactions on the properties of other model systems like furan complexes [9,115] was also addressed.

Cyclic polypeptides containing a photocleavable disulfide (S-S) bridge are useful models for the study of dynamical conformational changes that convert a polypeptide chain into a three-dimensional protein structure. The conformers of a series of cyclic peptides Cys-Pro-X-Cys (X: Gly, D-Leu, L-Leu, D-Val, L-Val) were studied in the gas phase and in the solvents water and acetonitrile, using both classical MD simulations and QM/MM approaches. We elucidated the effect of the stereochemistry of just a single residue on the conformation of the peptide and on solvent–peptide interactions, and found that the solvent plays a key role for the structural and spectroscopic properties of such systems [119,120].

c) Designed mutagenesis for the regulation of enzymatic activity

Quite often, mutations have deleterious effects and dramatically alter the properties of biological systems. On the other hand, mutations are essential for evolution; and controlled mutagenesis is an important tool to selectively manipulate protein properties. Hence, mutations can be used to regulate photochemical processes, protein folding, protein-protein interactions, and enzymatic activity, among others. Computer simulations play a key role for the molecular understanding and prediction of the effect of mutations.

In our work on *computational mutagenesis*, we aim at providing a molecular understanding of the effect of mutations in biological systems and at delivering computational predictions of targeted mutations able to modify protein properties. Hence, we have investigated disease-associated mutations in rhodopsin [25,121] and the effect of mutations on structural properties of highly complex systems like p97 aggregates. Of especial interest to us are Polyketide Synthases (PKS), which are multienzyme complexes able to direct the formation of a diverse array of functional groups and stereocenters. They catalyze a cascade of Claisen condensations between the enzyme acyl thioester and malonic acid thioesters, which serve as extender units of a nascent polyketide chain. The complex process of extender unit building block selection and incorporation in PKS is mainly controlled by acyltransferase (AT) domains, which catalyze the malonylation of acyl carrier proteins (ACP). A promising option to modify building block specificity in PKS is the direct engineering of innate AT domains to alter their substrate scope by replacing selected amino acids instead of whole catalytic domains.

My group developed computational models for the last acyltransferase domain (AT6) of 6-Desoxyerythronolide B Synthase (DEBS), the key multienzyme complex in the

biosynthesis of the antibiotic Erythromycin, to provide a molecular understanding of the effect of directed mutations and the role of specific residues on the enzymatic activity. We were able not only to *rationalize* the effect of point mutations on enzymatic activity, but also to successfully *predict* which single mutation would result in the incorporation of non-native building blocks [117]. The combination of experimental sequence-function correlations (cooperation with F. Schulz) and computational modeling revealed the origins of substrate recognition in PKS domains and enabled their targeted mutagenesis. We are currently extending this research to other systems like the malonyl-CoA: acyl carrier protein transacylase (MCAT or MAT) and Premonesin (cooperation with F. Schulz).

Implementation of coarse-grained methods in ChemShell

Hybrid QM/MM methods have widespread applications to model biomolecular, organic, inorganic, and organometallic systems with explicit solvation. ChemShell is a QM/MM modular package that allows the combination of several QM and MM methods. Currently, there is considerable interest in the development of coarse-grained (CG) force fields to improve the performance and sampling in MD simulations and geometry optimizations. The CG methodology has been successfully applied to very large molecular systems (such as virus capsids), which are cumbersome to handle at the atomistic level. However, CG approaches do not allow the study of fine structural details (such as fluctuations in secondary structures) due to their approximate representation. To circumvent this problem, hybrid coarse-grained / fine-grained (CG/FG) simulation protocols have been developed.

We work on the implementation of CG force fields in the ChemShell package (cooperation with W. Thiel). By developing novel triple-layer QM/MM/CG modeling approaches, we want to extend the applicability of QM/MM computations. This scheme allows us to treat the chemically important region at the QM level, the area around the QM region at the atomistic MM level, and the rest of the outer region (far from the QM site) at the CG level. In this approach, the presence of the CG region partially eliminates artifacts that may arise from the truncation of the MM region in very large systems. For instance, to study a membrane protein, the lipid bilayer and bulk water may be represented at the CG level while the more important regions are treated at higher resolution. Introducing a CG layer will also reduce the costs of MD simulations. This is especially helpful for QM/MM MD simulations that are currently computationally very expensive, even for smaller systems. Thus, the multi-scale QM/MM/CG approach can

also be conveniently used to investigate chemical reactions in explicit solvent, with the bulk solvent being treated at the CG level.

At present, we have already developed a module for the ChemShell code that performs hybrid QM/MM/CG calculations with Martini CG water for the CG layer, which is currently at the validation and benchmarking stage. We will continue this work to include other systems and force fields in our implementation.

Future directions: I plan to continue working on the development of predictive computational models of biological systems in their native environment. This will allow me to identify common motifs of molecular interactions as a basis for the introduction of improved regulation agents and approaches. Specifically, I will further develop my main research lines: the investigation of the effect of ligands, of the molecular environment, and of selective mutagenesis on protein properties and enzymatic activity. Consequently, we will study further new guest molecules, like asymmetric molecular tweezers with specific binding anchors designed to target certain regions of interest in the protein, and additional protein hosts like *high temperature requirement A* serine proteases. The effect of co-solvents on reactivity and protein interactions will be also investigated as well as other PKS enzymes.

As mentioned above, we plan to continue our work on the implementation of hybrid QM/MM/CG schemes to include other systems and force fields. This methodology will then be used in several new projects, for example concerning solvents effects on amino-acid catalyzed reactions, reactive intermediates, and biological systems like fluorescent proteins and protein-membrane interactions.

Publications resulting from this research area: 9, 25, 53, 110, 115, 116, 117, 118, 119, 120, 121, 122

External funding: Chemical Industry Fund, German Research Foundation: RESOLV Cluster of Excellence (EXC 1069), Mercator Foundation (GYF)

Cooperations: E. Wanker (Berlin, DE); T. Schrader (Essen, DE); C. Ottmann (Eindhoven, NL); G. Bitan (Los Angeles, US); J. Münch (Ulm, DE); E. Tajkhorshid (Illinois, US); W. Sander (Bochum, DE); F. Schulz (Bochum, DE); W. Thiel (Mülheim/Ruhr, DE)

2.5.8 Publications 2011-2013 from the Department of Theory

Thiel group

(1) Kumar, D.; Altun, A.; Shaik S.; Thiel, W. *Faraday Discuss.* **2011**, *148*, 373-383.
(2) Benighaus, T.; Thiel, W. *J. Chem. Theory Comput.* **2011**, *7*, 238-249.
(3) Hsiao, Y.-W.; Thiel, W. *J. Phys. Chem. B* **2011**, *115*, 2097-2106.
(4) Kumar, D.; Thiel, W.; de Visser, S. P. *J. Am. Chem. Soc.* **2011**, *133*, 3869-3882.
(5) Metz, S.; Thiel, W. *Coord. Chem. Rev.* **2011**, *255*, 1085-1103.
(6) Weingart, O.; Lan, Z.; Koslowski, A.; Thiel, W. *J. Phys. Chem. Lett.* **2011**, *2*, 1506-1509.
(7) Yachmenev, A.; Yurchenko, S. N.; Jensen, P.; Thiel, W. *J. Chem. Phys.* **2011**, *134*, 244307/1-11.
(8) Lan, Z.; Lu, Y.; Fabiano, E.; Thiel, W. *ChemPhysChem* **2011**, *12*, 1989-1998.
(9) Metzelthin, A.; Sánchez-García, E.; Birer, Ö.; Schwaab, G.; Thiel, W.; Sander W.; Havenith, M. *ChemPhysChem* **2011**, *12*, 2009-2017.
(10) Kazaryan, A.; Lan, Z.; Schäfer, L. V.; Thiel, W.; Filatov, M. *J. Chem. Theory Comput.* **2011**, *7*, 2189-2199.
(11) Lu, Y.; Lan, Z.; Thiel, W. *Angew. Chem., Int. Ed.* **2011**, *50*, 6864-6867.
(12) Yachmenev, A.; Yurchenko, S. N.; Ribeyre, T.; Thiel, W. *J. Chem. Phys.* **2011**, *135*, 074302/1-13.
(13) Breidung, J.; Thiel, W. *In Handbook of High-Resolution Spectroscopies*, vol. 1; Quack, M.; Merkt, F., Eds.; Wiley: Chichester, UK, 2011; pp. 389-404.
(14) Fabiano, E.; Lan, Z.; Lu, Y.; Thiel, W. In *Conical Intersections: Theory, Computation and Experiment*; Domcke, W.; Yarkony, D. R.; Köppel ,H., Eds.; World Scientific Publishing: Singapore, 2011; chapter 12, pp. 463-496.
(15) Yurchenko, S. N.; Barber, R. J.; Tennyson, J.; Thiel, W.; Jensen, P. *J. Mol. Spectrosc.* **2011**, *268*, 123-129.
(16) Inés, B.; Patil, M.; Carreras, J.; Goddard, R.; Thiel, W.; Alcarazo, M. *Angew. Chem., Int. Ed.* **2011**, *50*, 8400-8403.
(17) Korth, M.; Thiel, W. *J. Chem. Theory Comput.* **2011**, *7*, 2929-2936.
(18) Meletis, P.; Patil, M.; Thiel, W.; Frank, W.; Braun, M. *Chem. Eur. J.* **2011**, *17*, 11243-11249.
(19) Thiel, W. *Angew. Chem., Int. Ed.* **2011**, *50*, 9216-9217.
(20) Doron, D.; Major, D. T.; Kohen, A.; Thiel, W.; Wu, X. *J. Chem. Theory Comput.* **2011**, *7*, 3420-3437.
(21) Ramalho, T. C.; Pereira, D. H.; Thiel, W. *J. Phys. Chem. A* **2011**, *115*, 13504-13512.
(22) Petŭskova, J.; Patil, M.; Holle, S.; Lehmann, C. W.; Thiel, W.; Alcarazo, M. *J. Am. Chem. Soc.* **2011**, *133*, 20758-20760.
(23) Cao, J.; Bjornsson, R.; Bühl, M.; Thiel, W.; van Mourik, T. *Chem.–Eur. J.* **2012**, *18*, 184-195.

(24) Cui, G.; Lan, Z.; Thiel, W. *J. Am. Chem Soc.* **2012**, *134*, 1662-1672.
(25) Hernández-Rodríguez, E. W.; Sánchez-García, E.; Crespo-Otero, R.; Montero-Alejo, A. L.; Montero, L. A.; Thiel, W. *J. Phys. Chem. B* **2012**, *116*, 1060-1076.
(26) Meier, K.; Thiel, W.; van Gunsteren, W. F. *J. Comput. Chem.* **2012**, *33*, 363-378.
(27) Polyak, I.; Reetz, M. T.; Thiel, W. *J. Am. Chem. Soc.* **2012**, *134*, 2732-2741.
(28) Lan, Z.; Lu, Y.; Weingart, O.; Thiel, W. *J. Phys. Chem. A* **2012**, *116*, 1510-1518.
(29) Gómez, H.; Polyak, I.; Thiel, W.; Lluch, J. M.; Masgrau, L. *J. Am. Chem. Soc.* **2012**, *134*, 4743-4752.
(30) Lu, Y.; Lan, Z.; Thiel, W. *J. Comput. Chem.* **2012**, *33*, 1225-1235.
(31) Cui, G.; Lu, Y.; Thiel, W. *Chem. Phys. Lett.* **2012**, *537*, 21-26.
(32) Heggen, B.; Lan, Z.; Thiel, W. *Phys. Chem. Chem. Phys.* **2012**, *14*, 8137-8146.
(33) Wu, X.; Koslowski, A.; Thiel, W. *J. Chem. Theory Comput.* **2012**, *8*, 2272-2281.
(34) Gámez, J. A.; Weingart, O.; Koslowski, A.; Thiel, W. *J. Chem. Theory Comput.* **2012**, *8*, 2352-2358.
(35) Barbatti, M.; Lan, Z.; Crespo-Otero, R.; Szymczak, J. J.; Lischka, H.; Thiel, W. *J. Chem. Phys.* **2012**, *137*, 22A503/1-14.
(36) Hsiao, Y.-W.; Götze, J.; Thiel, W. *J. Phys. Chem. B* **2012**, *116*, 8064-8073.
(37) Patil, M.; Thiel, W. *Chem.–Eur. J.* **2012**, *18*, 10408-10418.
(38) Liao, R.-Z.; Thiel, W. *J. Phys. Chem. B.* **2012**, *116*, 9396-9408.
(39) Sun, Q.; Li, Z.; Lan, Z.; Pfisterer, C.; Doerr, M.; Fischer, S.; Smith, S. C.; Thiel, W. Phys. *Chem. Chem. Phys.* **2012**, *14*, 11413-11424.
(40) Schönborn, J. B.; Koslowski, A.; Thiel, W.; Hartke, B. *Phys. Chem. Chem. Phys.* **2012**, *14*, 12193-12201.
(41) Cui, G.; Thiel, W. *Phys. Chem. Chem. Phys.* **2012**, *14*, 12378-12384.
(42) Teller, H.; Corbet, M.; Mantilli, L.; Gopakumar, G.; Goddard, R.; Thiel, W.; Fürstner, A. *J. Am. Chem. Soc.* **2012**, *134*, 15331-15342.
(43) Liao, R.-Z.; Thiel, W. *J. Chem. Theory Comput.* **2012**, *8*, 3793-3803.
(44) Carreras, J.; Patil, M.; Thiel, W.; Alcarazo, M. *J. Am. Chem. Soc.* **2012**, *134*, 16753-16758.
(45) Saito, T.; Thiel, W. *J. Phys. Chem. A* **2012**, *116*, 10864-10869.
(46) Boulanger E.; Thiel, W. *J. Chem. Theory Comput.* **2012**, *8*, 4527-4538.
(47) Yurchenko, S. N.; Thiel, W.; Jensen, P. *AIP Conf. Proc.* **2012**, *1504*, 491-494.
(48) Cui, G.; Thiel, W. *Angew. Chem., Int. Ed. 52*, **2013**, 433-436.
(49) Sen, K.; Crespo-Otero, R.; Weingart, O.; Thiel, W.; Barbatti, M. *J. Chem. Theory Comput.* **2013**, *9*, 533-542.
(50) Grebner, C.; Kästner, J.; Thiel, W.; Engels, B. *J. Chem. Theory Comput.* **2013**, *9*, 814-821.
(51) Liao, R.-Z.; Thiel, W. *J. Phys. Chem. B* **2013**, *117*, 1326-1336.
(52) Čorić, I.; Kim, J. H.; Vlaar, T.; Patil, M.; Thiel, W.; List, B. *Angew. Chem., Int. Ed.* **2013**, *52*, 3490-3493.

(53) Crespo-Otero, R.; Bravo-Rodriguez, K.; Roy, S.; Benighaus, T.; Thiel, W.; Sander, W.; Sánchez-García, E. *ChemPhysChem* **2013**, *14*, 805-811.
(54) Kozma, Á.; Gopakumar, G.; Farès, C.; Thiel, W.; Alcarazo, M. *Chem.–Eur. J.* **2013**, *19*, 3542-3546.
(55) Götze, J. P.; Thiel, W. *Chem. Phys.* **2013**, *415*, 247-255.
(56) Patil, M.; Loerbroks, C.; Thiel, W. *Org. Lett.* **2013**, *15*, 1682-1685.
(57) Liao, R.-Z.; Thiel, W. *J. Phys. Chem. B* **2013**, *117*, 3954-3961.
(58) Lifchits, O.; Mahlau, M.; Reisinger, C. M.; Lee, A.; Farès, C.; Polyak, I.; Gopakumar, G.; Thiel, W.; List, B. *J. Am. Chem. Soc.* **2013**, *135*, 6677-6693.
(59) Polyak, I.; Reetz, M. T.; Thiel, W. *J. Phys. Chem. B 117*, **2013**, 4993-500.
(60) Khan, S.; Gopakumar, G.; Thiel, W.; Alcarazo, M. *Angew. Chem., Int. Ed.* **2013**, *52*, 5644-5647.
(61) Huang, X.; Patil, M.; Farès, C.; Thiel, W.; Maulide, N. *J. Am. Chem. Soc.* **2013**, *135*, 7312-7323.
(62) Kumari, D.; Singh, H.; Patil, M.; Thiel, W.; Pant, C. S.; Banerjee, S. *Thermochim. Acta* **2013**, *562*, 96-104.
(63) Fortenberry, R. C.; Huang, X.; Yachmenev, A.; Thiel, W.; Lee, T. J. *Chem. Phys. Lett.* **2013**, *574*, 1-12.
(64) Audisio, D.; Gopakumar, G.; Xie, L.-G.; Alves, L. G.; Wirtz, C.; Martins, A. M.; Thiel, W.; Farès, C.; Maulide, N. *Angew. Chem., Int. Ed.* **2013**, *52*, 6313-6316.
(65) Spörkel, L.; Cui, G.; Thiel, W. *J. Phys. Chem. A* **2013**, *117*, 4574-4583.
(66) Wu, X.; Thiel, W.; Pezeshki, S.; Lin, H. *J. Chem. Theory Comput.* **2013**, *9*, 2672-2686.
(67) Gámez, J. A.; Weingart, O.; Koslowski, A.; Thiel, W. *Phys. Chem. Chem. Phys.* **2013**, *15*, 11814-11821.
(68) Boulanger, E.; Anoop, A.; Nachtigallova, D.; Thiel, W.; Barbatti, M. *Angew. Chem., Int. Ed.* **2013**, *52*, 8000-8003.
(69) Polyak, I.; Boulanger, E.; Sen, K.; Thiel, W. *Phys. Chem. Chem. Phys.* **2013**, *15*, 14188-14195.
(70) Polyak, I.; Benighaus, T.; Boulanger, E.; Thiel, W. *J. Chem. Phys.* **2013**, *139*, 064104/1-11.
(71) Marquardt, R.; Sagui, K.; Zheng, J.; Thiel, W.; Luckhaus, D.; Yurchenko, S.; Mariotti, F.; Quack, M. *J. Phys. Chem. A* **2013**, *117*, 7502-7522.
(72) Silva-Junior, M. R.; Mansurova, M.; Gärtner, W.; Thiel, W. *ChemBioChem* **2013**, *14*, 1648-1661.
(73) Karasulu, B.; Patil, M.; Thiel, W. *J. Am. Chem. Soc.* **2013**, *135*, 13400-13413.
(74) Cui, G.; Cao, X.-Y.; Fang, W.-H.; Dolg, M.; Thiel, W. *Angew. Chem., Int. Ed.* **2013**, *52*, 10281-10285.
(75) Liao, R.-Z.; Thiel, W. *J. Comput. Chem.* **2013**, *34*, 2389-2397.
(76) Yurchenko, S. N.; Tennyson, J.; Barber, R. J.; Thiel, W. *J. Mol. Spectrosc.* **2013**, *291*, 69-76.

(77) Escudero, D.; Heuser, E.; Meier, R. J.; Schäferling, M.; Thiel, W.; Holder, E. *Chem.–Eur. J.* **2013**, *19*, 15639-15644.
(78) Loerbroks, C.; Rinaldi, R.; Thiel, W. *Chem.–Eur. J.* **2013**, *19*, 16282-16294.
(79) Thiel, W. *Nachr. Chem.* **2013**, *61*, 1095-1096.
(80) Thiel, W.; Hummer, G. *Nature* **2013**, *504*, 96-97.
(81) Yachmenev, A.; Polyak, I.; Thiel, W. *J. Chem. Phys*. **2013**, *139*, 204308/1-14.
(82) Götze, J. P.; Karasulu, B.; Thiel, W. *J. Chem. Phys.* **2013**, *139*, 234108/1-8.
(83) Carreras, J.; Gopakumar, G.; Gimeno, A.; Linowski, P.; Petuškova, J.; Thiel, W.; Alcarazo, M. *J. Am. Chem. Soc.* **2013**, *135*, 18815-18823.
(84) Seidel, G.; Gabor, B.; Goddard, R.; Heggen, B.; Thiel, W.; Fürstner, A. *Angew. Chem. Int. Ed.*, DOI:10.1002/anie.201308842.

Barbatti group

(35) Barbatti, M.; Lan, Z.; Crespo-Otero, R.; Szymczak, J. J.; Lischka, H.; Thiel, W. *J. Chem. Phys.* **2012**, *137*, 22A503/1-14.
(49) Sen, K.; Crespo-Otero, R.; Weingart, O.; Thiel, W.; Barbatti, M. *J. Chem. Theory Comput.* **2013**, *9*, 533-542.
(68) Boulanger, E.; Anoop, A.; Nachtigallova, D.; Thiel, W.; Barbatti, M. *Angew. Chem., Int. Ed.* **2013**, *52*, 8000-8003.
(85) Barbatti, M. *WIREs: Comp. Mol. Sci.* **2011**, *1*, 620-633.
(86) Barbatti, M. *Phys. Chem. Chem. Phys.* **2011**, *13*, 4686-4692.
(87) Barbatti, M.; Aquino, A. J. A.; Szymczak, J. J.; Nachtigallová, D.; Lischka, H. *Phys. Chem. Chem. Phys.* **2011**, *13*, 6145-6155.
(88) Barbatti, M.; Szymczak, J. J.; Aquino, A. J. A.; Nachtigallová, D.; Lischka, H. *J. Chem. Phys.* **2011**, *134*, 014304/1-5.
(89) Barbatti, M.; Ullrich, S. *Phys. Chem. Chem. Phys.* **2011**, *13*, 15492-15500.
(90) Crespo-Otero, R.; Barbatti, M. *J. Chem. Phys.* **2011**, *134*, 164305/1-12.
(91) Crespo-Otero, R.; Barbatti, M.; Yu, H.; Evans, N. L.; Ullrich, S. *ChemPhysChem* **2011**, *12*, 3365-3375.
(92) Daengngern, R.; Kungwan, N.; Wolschann, P.; Aquino, A. J. A.; Lischka, H.; Barbatti, M. *J. Phys. Chem. A* **2011**, *115*, 14129-14136.
(93) Barbatti, M.; Shepard, R.; Lischka, H. In *Conical Intersections*; Domcke, W.; Yarkony, D. R.; Koppel, H., Eds.; Singapore: World Scientific, 2011; pp. 415-462.
(94) Nachtigallová, D.; Aquino, A. J. A.; Szymczak, J. J.; Barbatti, M.; Hobza, P.; Lischka, H. *J. Phys. Chem. A* **2011**, *115*, 5247-5255.
(95) Pederzoli, M.; Pittner, J.; Barbatti, M.; Lischka, H. *J. Phys. Chem. A* **2011**, *115*, 11136-11143.

(96) Szalay, P. G.; Aquino, A. J. A.; Barbatti, M.; Lischka, H. *Chem. Phys.* **2011**, *380*, 9-16.
(97) Szymczak, J. J.; Barbatti, M.; Lischka, H. *Int. J. Quantum Chem.* **2011**, *111*, 3307-3315.
(98) Barbatti, M.; Nascimento, M. A. C. *Int. J. Quantum Chem.* **2012**, *112*, 3169-3173.
(99) Barbatti, M.; Ruckenbauer, M.; Szymczak, J.; Sellner, B.; Vazdar, M.; Antol, I.; Eckert-Maksić, M.; Lischka, H. In *Handbook of Computational Chemistry*; Leszczynski, J., Ed.; Dordrecht: Springer Science+Business Media B.V., 2012; pp. 1175-1213.
(100) Borges, I.; Barbatti, M.; Aquino, A. J. A.; Lischka, H. *Int. J. Quantum Chem.* **2012**, *112*, 1225-1232.
(101) Crespo-Otero, R.; Barbatti, M. *Theor. Chem. Acc.* **2012**, *131*, 1237.
(102) Homem, M. G. P.; Lopez-Castillo, A.; Barbatti, M.; Rosa, L. F. S.; Iza, P.; Cavasso-Filho, R. L.; Farenzena, L. S.; Lee, M. T.; Iga I. *J. Chem. Phys.* **2012**, *137*, 184305/1-9.
(103) Kungwan, N.; Plasser, F.; Aquino, A. J. A.; Barbatti, M.; Wolschann, P.; Lischka, H. *Phys. Chem. Chem. Phys.* **2012**, *14*, 9016-9025.
(104) Lan, Z.; Nonell, S.; Barbatti, M. *J. Phys. Chem. A* **2012**, *116*, 3366-3376.
(105) Pederzoli, M.; Pittner, J.; Barbatti, M.; Lischka, H. *Proc. SPIE* **2012**, *8463*, 846318.
(106) Plasser, F.; Granucci, G.; Pittner, J.; Barbatti, M.; Persico, M.; Lischka, H. *J. Chem. Phys.* **2012**, *137*, 22A514/1-13.
(107) Plasser, F.; Barbatti, M.; Aquino, A.; Lischka, H. *Theor. Chem. Acc.* **2012**, *131*, 1073.
(108) Asturiol, D.; Barbatti, M. *J. Chem. Phys.* **2013**, *139*, 074307/1-7.
(109) Barbatti, M.; Ruckenbauer, M.; Plasser, F.; Pittner, J.; Granucci, G.; Persico, M.; Lischka, H. *WIREs Comp. Mol. Sci.*, DOI:10.1002/wcms.1158.
(110) Crespo-Otero, R.; Mardyukov, A.; Sánchez-García, E.; Barbatti, M.; Sander, W. *ChemPhysChem* **2013**, *14*, 827-836.
(111) Daengngern, R.; Kerdpol, K.; Kungwan, N.; Hannongbua, S.; Barbatti, M. *J. Photochem. Photobiol., A* **2013**, *266*, 28-36.
(112) Kungwan, N.; Daengngern, R.; Piansawan, T.; Hannongbua, S.; Barbatti, M. *Theor. Chem. Acc.* **2013**, *132*, 1397 (1-10).
(113) Ruckenbauer, M.; Barbatti, M.; Müller, T.; Lischka, H. *J. Phys. Chem. A* **2013**, *117*, 2790-2799.
(114) Sellner, B.; Barbatti, M.; Müller, T.; Domcke, W.; Lischka, H. *Mol. Phys.* **2013**, *111*, 2439-2450.

Sánchez-García group

(9) Metzelthin, A.; Sánchez-García, E.; Birer, Ö.; Schwaab, G.; Thiel, W.; Sander W.; Havenith, M. *ChemPhysChem* **2011**, *12*, 2009-2017.

(25) Hernández-Rodríguez, E. W.; Sánchez-García, E.; Crespo-Otero, R.; Montero-Alejo, A. L.; Montero, L. A.; Thiel, W. *J. Phys. Chem. B* **2012**, *116*, 1060-1076.

(53) Crespo-Otero, R.; Bravo-Rodriguez, K.; Roy, S.; Benighaus, T.; Thiel, W.; Sander, W.; Sánchez-García, E. *ChemPhysChem* **2013**, *14*, 805-811.

(110) Crespo-Otero, R.; Mardyukov, A.; Sánchez-García, E.; Barbatti, M.; Sander, W. *ChemPhysChem* **2013**, *14*, 827-836.

(115) Sánchez-García, E.; Jansen, G. *J. Phys. Chem. A* **2012**, *116*, 1060-1076.

(116) Sander, W.; Roy, S.; Polyak, I.; Ramirez-Anguita, J. M.; Sánchez-García, E. *J. Am. Chem. Soc.* **2012**, *134*, 8222-8230.

(117) Sundermann, U.; Bravo-Rodriguez, K.; Klopries, S.; Kushnir, S.; Gomez, H.; Sanchez-Garcia, E.; Schulz, F. *ACS Chem. Biol.* **2013**, *8*, 443-450.

(118) Bier, D.; Rose, R.; Bravo-Rodriguez, K.; Bartel, M.; Ramirez-Anguita, J. M.; Dutt, S.; Wilch, C.; Klärner, F.-G.; Sanchez-Garcia, E.; Schrader, T.; Ottmann, C. *Nat. Chem.* **2013**, *5*, 234-239.

(119) Li, F.; Bravo-Rodriguez, K.; Phillips, C.; Seidel, R. W.; Wieberneit, F.; Stoll, R.; Doltsinis, N. L.; Sanchez-Garcia, E.; Sander, W. *J. Phys. Chem. B* **2013**, *117*, 3560-3570.

(120) Dutt, S.; Wilch, C.; Gersthagen, T.; Talbiersky, P.; Bravo-Rodriguez, K.; Hanni, M.; Sánchez-García, E.; Ochsenfeld, C.; Klärner, F.; Schrader, T. *J. Org. Chem.* **2013**, *78*, 6721-6734.

(121) Hernández-Rodríguez, E. W.; Montero-Alejo, A. L.; López, R.; Sánchez-García, E.; Montero-Cabrera, L. A.; García de la Vega, J. M. *J. Comput. Chem.* **2013**, *34*, 2460-2471.

(122) Li, F.; Bravo-Rodriguez, K.; Fernandez-Oliva, M.; Ramirez-Anguita, J. M.; Merz, K.; Winter, M.; Lehmann, C. W.; Sander, W.; Sánchez-García, E. *J. Phys. Chem. B* **2013**, *117*, 10785-10791.

Publications by Other Members of the Department

(123) **Korth**, M. *ChemPhysChem* **2011**, *12*, 3131-3142.

(124) **Weingart**, O.; Altoe, P.; Stenta, M.; Bottoni, A.; Orlandi, G.; Garavelli, M. *Phys. Chem Chem. Phys.* **2011**, *13*, 3645-3648.

(125) Suardiaz, R.; **Crespo-Otero**, R.; Perez, C.; San Fabian, J.; de la Vega, J. M. G. *J. Chem. Phys.* **2011**, *134*, 061101/1-4.

(126) Ai, Y.-J.; **Liao**, R.-Z.; Fang, W.-H.; Luo, Y. *Phys. Chem. Chem. Phys.* **2012**, *14*, 13409-13414.

(127) **Götze**, J. P.; Greco, C.; Mitrić, R.; Bonačić-Koutecký, V.; Saalfrank, P. *J. Comput. Chem.* **2012**, *33*, 2233-2242.
(128) **Götze**, J. P.; Saalfrank, P. *J. Mol. Model.* **2012**, *18*, 1877-1883.
(129) Klaffki, N.; **Weingart**, O.; Garavelli, M.; Spohr, E. *Phys. Chem Chem. Phys.* **2012**, *14*, 14299-14305.
(130) Kröner, D.; **Götze**, J. P. *J. Photochem. Photobiol. B* **2012**, *109*, 12-19.
(131) Muya, J. T.; **Gopakumar**, G.; Lijnen, E.; Nguyen, M. T.; Ceulemans A. In *Vibronic Interactions and the Jahn-Teller Effect: Theory and Applications*; Atanasov, M.; Daul, C.; Tregenna-Piggott, P., Eds.; Prog. Theor. Chem. Phys., vol. 23; Berlin: Springer, 2012; pp. 265-278.
(132) Nordin, M.; **Liao**, R.-Z.; Ahlford, K.; Adolfsson, H.; Himo, F. *ChemCatChem* **2012**, *4*, 1095-1104.
(133) **Weingart**, O.; Garavelli, M. *J. Chem. Phys.* **2012**, *137*, 22A523/1-6.
(134) Yang, L.; **Liao**, R.-Z.; Ding, W.-J.; Yu, J.-G.; Liu, K.; Liu, R.-Z. *Theor. Chem. Acc.* **2012**, *131*, 1275.
(135) Muya, J. T.; Ramanantoanina, H.; Daul, C.; Nguyen, M. T.; **Gopakumar**, G.; Ceulemans, A. *Phys. Chem. Chem. Phys.* **2013**, *15*, 2829-2835.
(136) de la Vega, J. M. G.; San Fabian, J.; **Crespo-Otero**, R.; Suardiaz, R.; Perez, C. *Int. J. Quantum Chem.* **2013**, *113*, 656-660.
(137) **Liao**, R.-Z. *J. Biol. Inorg. Chem.* **2013**, *18*, 175-181.
(138) Seidel, R. W.; Goddard, R.; **Breidung**, J.; Bamfaste, P.; Neff, D.; Oppel, I. M. *Struct. Chem.* **2013**, *24*, 181-189.
(139) Krasnopolski, M.; Seidel, R. W.; Goddard, R.; **Breidung**, J.; Winter, M. V.; Devi, A.; Fischer, R. A. *J. Mol. Struct.* **2013**, *1031*, 239-245.
(140) Seidel, R. W.; Dietz, C.; **Breidung**, J.; Goddard, R.; Oppel, I. M. *Acta Crystallogr., Sect. C: Cryst. Struct. Commun.* **2013**, *69*, 1112-1115.
(141) Zhang, Z. G.; Roiban, G. D.; Acevedo, J. P.; **Polyak**, I.; Reetz, M. T. *Adv. Synth. Cat.* **2013**, *355*, 99-106.
(142) **Cui**, G.; Fang, W. *J. Chem. Phys.* **2013**, *138*, 044315/1-9.
(143) Goy, R.; Apfel, U.-P.; Elleouet, C.; **Escudero**, D.; Elstner, M.; Görls, H.; Talarmin, J.; Schollhammer, P.; González, L.; Weigand, W. *Eur. J. Inorg. Chem.* **2013**, 4466-4472.

Publications by other members of the Department (marked in bold) are included only if they carry the address of the Institute.

There are seven joint theory papers, which are listed twice but with a unique number.

Joint research projects between the Thiel group and experimental groups in the Institute are documented in fifteen joint publications, which are listed both here and in the section of the experimental partner.

CHAPTER 3

Scientific Service Units

3 Scientific Service Units

The Institute's Scientific Service Units are integral parts of the research efforts of the individual scientific groups. The highly interdisciplinary approach to catalysis requires immediate and direct access for all groups to a large and diverse pool of reaction engineering techniques ("Technical Laboratories"), of analytical methods (Chromatography, Mass Spectrometry, Nuclear Magnetic Resonance, Chemical Crystallography, Electron Microscopy), and of information or data handling systems (Library, Computer Group). A maximum standard of safety, reliability, and flexibility is essential for these units to respond to the needs of modern basic research in catalysis and related areas of chemistry.

In addition to providing the appropriate infrastructure and know-how, several service facilities are actively involved in specific projects, generally in cooperation with the scientific groups of the five Departments. For example, new techniques have been developed over the years in the fields of high-throughput screening, microfluidics, and chip-electrophoresis, to name just a few representative cases.

In order to make this approach truly successful, a long term strategy is essential for maintaining and developing the know-how and experience of the staff. This includes the active role of the Scientific Service Units in specific research projects, participation in conferences and the hosting of postdoctoral fellows with the aim of introducing new techniques.

In line with the rules stipulated by the MPG, all data recorded in the analytical departments or directly in one of the experimental groups are securely archived in electronic and/or hardcopy format for a minimum of ten years (usually much longer). With the implementation of an electronic laboratory notebook (ELN, in progress), secure data storage and retrieval will be put on a uniform basis and will be taken care of by the IT group as described in more detail in Chapter 3.7.

3.1 Technical Laboratories (N. Theyssen)

Involved: A. Brinkmann, N. Fuhrmann, N. Sadlowski, I. Sahm, M. Schalk, L. Winkel

The technical laboratory consists of a large central high pressure laboratory, several solvent purification and drying distillation apparatus (turnover ~ 13.000 L per year), large scale synthesis facilities, the necessary infrastructure for receiving and sorting the different types of waste chemicals (about 22 tons per year), two research laboratories (please see chapter 2.1.5 for further details) and office space. One chemical engineer (A. Brinkmann) and one chemical technician (L. Winkel) were mainly concerned with providing service for the scientific departments. Most recently, another chemical technician, N. Fuhrmann, has joined the group to compensate the retirement of A. Brinkmann. In 2012, N. Sadlowski, a safety engineer, became the successor of I. Sahm. Furthermore, M. Schalk changed in 2011 from house service and metal workshop to the central work safety department. He is responsible for instruction and control of employees from external companies, the test register for periodic equipment tests and coordination of First Aid courses.

As a result of ongoing core refurbishments in the laboratory building, four coworkers of Prof. Pörschke moved into the technical laboratories in 2012. Thus, one new laboratory working place had to be created, which was mainly realized with stored laboratory furniture of the former S2 laboratory. In addition, three safety cabinets and a new laboratory sink were installed in this context.

The installation of a further rectification plant for the purification of *tert*-butyl methyl ether was completed by A. Brinkmann in 2011. This measure was taken to enforce the substation of diethyl ether in order to reduce its distinct ignition hazard and peroxide formation potential. R. Thomas, our Institute's electrician, and his colleagues from the precision mechanics mounted the necessary control units.

Thanks to the contribution of R. Thomas and people from the electric department, the new MSR-technique and data saving system of the small and medium sized high pressure boxes were implemented in the reporting period and are now frequently used by the scientists of the institute. This system, operated by L. Winkel, allows the recording of pressure/temperature curves of every connected high pressure experiment. Furthermore, a steady control in terms of maximum operating pressure and temperature of the individual autoclaves is established.

In the reporting period, the central solvent drying apparatus in technical scale were equipped with a new control cabinet. Overall, this measure provided two major benefits: First, a much more precise temperature regulation could be realized in the individual oil-based tempering jackets (with hysteresis of ± 0.1 °C) which in turn allowed a systematic optimization in terms of energy efficiency and separation quality. Second, a greatly increased degree of control is now implemented in which thirteen different parameters are continuously monitored. In case that the measured values exceed or fall below permissible limits, a shutdown of an individual drying unit or the complete array is affected. Most failures are transmitted to the central building control which ensures immediate response also outside of normal working hours by our on-call service.

Since the central solvent drying unit is classified as a potentially explosive area, the electrical installation was carried out on the basis of intrinsically safe circuits. Here, the necessary safety integration level was defined for the controlling architecture (SIL 1), which was done in collaboration with the German technical inspection association (TÜV). The same agency conducted the commissioning tests as well.

In addition, the condensers of the drying apparatus were replaced with stainless steel. This measure was carried out in close cooperation of our metal workshop, our precision mechanics and A. Brinkmann. Potential water penetration in the drying containers, which would have disastrous consequences, is reliably prevented in this way.

In close cooperation with T. Zimmermann (AK Prof. Schüth), the precision mechanics and R. Thomas a fundamental retrofitting and recommissioning of an acetylene compressor was performed. Thereby the necessities of a German technical rule (TRAC 203 – acetylene compressors) were implemented as well as possible. Now, the second pressure stage of the compressor is monitored in terms of maximum temperature and pressure. In addition, the suction side is equipped with a gas failure device to prevent a diffusion of air into the acetylene pressure lines. All these components (including the control electronics) fulfill the demands for safety components in terms of failure rates, hardware-failure-tolerances and ease of operation. Moreover, a condensation of compressed acetylene is prevented in a reliable manner.

In order to reduce the risks of high pressure acetylene conversion further, the large high pressure box was equipped with a video inspection system. The analogue speed dome camera transmits video pictures of all important components of the experimental setup in high resolution. This measure was taken to decrease the necessity for a visit during a running experiment.

Publications resulting from this research area: none

3.2 Chromatography and Electrophoresis (P. Schulze)

The department of Chromatography and Electrophoresis provides analytical services for in-house scientists, e.g. qualitative and quantitative determinations, chiral analysis, preparative separation or purification of product mixtures and catalysts. For this purpose, modern chromatographic and electrophoretic separation methods as well as hyphenated techniques are applied. A section of the group is involved in development of detection technology.

Gas chromatography (U. Häusig)
Capillary GC is performed using commercial systems in diverse instrumental setups. In routine analysis most samples are analyzed using flame ionization or thermal conductivity detection, whereas unknown substances are identified using the hyphenation of gas chromatography and mass spectrometry (GC-MS). The team also develops new analytical methods, e.g. the direct analysis of small amounts of organic compounds in aqueous solution.

Liquid chromatography (A. Deege)
The LC laboratory applies a variety of (ultra) high-performance liquid chromatography techniques such as reversed / normal phase, ion exchange and size exclusion chromatography. Besides optical detection techniques, MS and electrochemical detection are utilized to detect substances lacking any UV active functional groups, e.g. cellulose decomposition products.
In addition to routine analysis and method optimization, the LC team develops column switching methods to enable sufficient separation efficiencies and to reduce analysis time of complex or crude samples. The application of capillary zone electrophoresis and micellar electrokinetic chromatography complement the tool box of liquid phase separations.
Separation of preparative sample amounts is also possible using preparative LC instruments. Usually, the purified substances are used as educts in synthesis or characterized using further analytical methods e.g. NMR or MS.

Independent research projects
1) Spectrophotometric determination of H_2O_2 in highly acidic, organoperoxide-containing media
2) Synthesis of amino-reactive fluorescence dyes designed for capillary isoelectric focusing

Future directions

To meet the requirements of increasing sample complexity in GC, we will expand the use of hyphenated techniques such as GC-MS. This helps to identify impurities or unknown sample components.
The renaissance of supercritical fluid chromatography enables highly efficient and very fast separations. This is particularly interesting with regard to preparative scale as the clean-up time of separated fractions is drastically reduced.
Furthermore the use of robust CE-MS methods for rapid analysis of crude reaction mixtures should be evaluated.

Co-workers

Georg Breitenbruch, Alfred Deege, Stefanie Dehn, Leonid Gitlin, Ulrich Häusig, Corinna Heidgen, Heike Hinrichs, Dina Klütt, Frank Kohler, Jutta Rosentreter, Sylvia Ruthe, Philipp Schulze, Marie Sophie Sterling, Maximilian Wasserloos

Publications resulting from this research area

(1) Audisio, D.; Luparia, M.; Oliveira, M.T.; Klütt, D.; Maulide, N. *Angew. Chem., Int. Ed.* **2012**, 51, 7314-7317.
(2) Schweitzer-Chaput, B.; Sud, A.; Pintér, Á.; Dehn, S.; Schulze, P.; Klussmann M. *Angew. Chem., Int. Ed.* **2013**, 52, 13228-13232.

Cooperations

M. Klussmann (Mülheim/Ruhr, DE), N. Maulide (Vienna, AU)

3.3 Mass Spectrometry (W. Schrader)

In the last three years the focus of the MS group has changed only slightly. The major task is still the service work for the groups of both Max Planck Institutes (Kohlenforschung and Bioanorganische Chemie/Chemical Energy Conversion) on the campus. While the number of samples measured for the BAC/CEC decreased in the last years this has been compensated by a much higher sample emergence from the Kohlenforschung.

Modern analytical methodologies are needed to solve the problems in the synthetic laboratories. This is achieved by providing full support in identifying unknown and new components using all ionization methods available and interpreting the obtained data. Rapid completion is a strong priority that allows the synthetic chemists to obtain the results and implement them into their work. The Institute's own data base and software package (MassLib) is constantly modernized, and different new atmospheric pressure ionization and high resolution methods have found a greater emphasis.

Standard MS: The standard program includes direct evaporation of new volatile and solid synthetic compounds. Pure liquid and volatile compounds are analyzed by direct injection and GC/MS. For polar components electrospray (ESI) MS is the method of choice for many problems.
Special measurements: High resolution mass spectrometry has become an important tool for characterization of newly synthesized compounds. FT-ICR MS is a very accurate and high resolving MS technique that allows for the investigation of a much broader spectrum of samples. The method is especially useful for the investigation of reaction mechanisms, where small intermediates are being observed in order to study how chemical reactions proceed. High-resolution MS/MS data can provide accurate structural information about unknown compounds due to fragmentation and is developing into an important tool for the investigation of chemical reactions.

The **research interests** are focusing on the investigation of complex and unusual reactions to gain information about mechanisms or formation pathways. Very often such reactions cannot be observed because potential intermediates are low in intensity or are available only for a short life-time and here mass spectrometry can play a vital role in characterizing mechanisms. One example is from a project dealing with complex organocatalytic reactions. In this project a complex organocatalytic triple cascade reaction for the stereoselective synthesis of *tetra*-substituted cyclohexene carbaldehydes

(cooperation with D. Enders within the DFG Priority Program *Organocatalysis*) was investigated (see Figure 1). The cascade starts with the activation of an aldehyde **1** by enamine formation thus allowing its addition to a nitroalkene **2** via a Michael reaction. The liberated catalyst from the hydrolysis process forms an iminium ion of an α,β-unsaturated aldehyde **3** to accomplish the conjugate Michael addition with the nitroalkane **7**. In subsequent steps, the enamine **9** leads to an intramolecular aldol condensation via **10**. The final product tetra-substituted cyclohexene carbaldehyde **11** is obtained after hydrolysis. [Alachraf-OBC 2011]

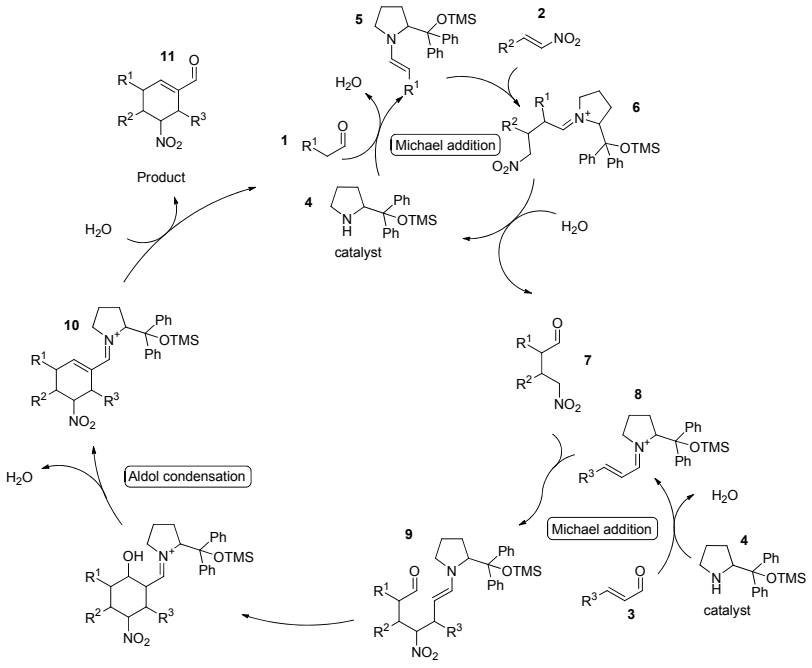

Figure 1: The proposed catalytic cycle for the complex organocatalyzed triple cascade reaction.

The intermediates of the triple cascade reaction have been intercepted through ESI-MS monitoring and structural assignments were aided by using the accurate mass data from FT-ICR MS. For each intermediate structural information was obtained from MS/MS measurements from intercepted components allowing a thorough characterization of the complex reaction. Other cooperations on organocatalytic reactions with B. List and P. Schreiner are not yet finalized.

Another project deals with the investigation, behavior and characterization of complex crude oil mixtures. Despite the continual development of renewable energy sources, energy supplies will be dependent upon the availability of crude oil for at least the next

two decades. As the remaining light crude oils diminish, previously unconventional resources will need to be upgraded into petroleum. Many of the problems associated with recovery, separation or processing of crude oils are related to the presence of high concentrations of heavy components in the crude, like asphaltenes. It was possible to study asphaltenes with a broad set of different ionization methods combined with ultrahigh resolution mass spectrometry (FT-ICR MS).

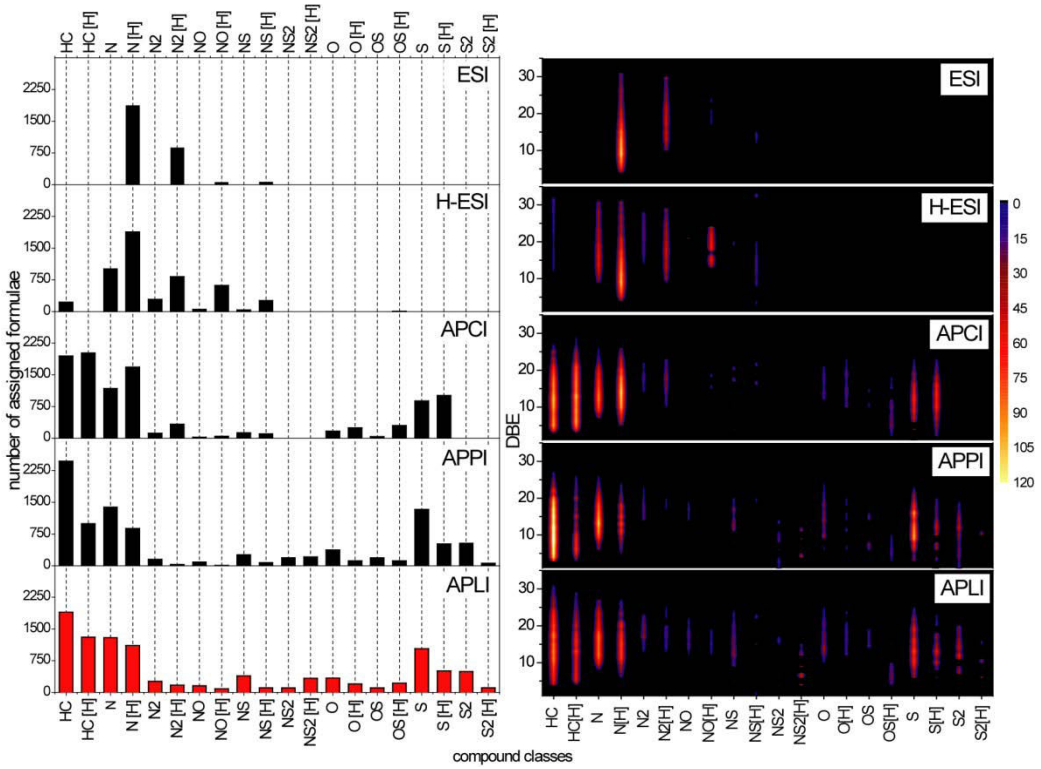

Figure 2: Population based compound classes within the assigned formulae (left) and the DBE distribution of the individual compound classes (right) using ESI (top), H-ESI, APCI, APPI and APLI (bottom) modes, according to the number of assigned molecules.

A mild, REMPI based laser ionization method was compared to electrospray-, chemical- and photo-ionization methods. The populations of the assigned molecules were found to differ substantially for each ionization method, especially in the heteroatomic and in non-heteroatomic content and in aromaticity. In maximum, more than 10,000 different components were detected and assigned for three of the five ionization methods for this asphaltene fraction, thus indicating the real complexity of the whole crude oil. An overview of the different compound classes can be obtained from Figure 2 where different classes and their respective DBE values (the number of double bonds and ring closing bonds within a molecule) are shown. [7]

Another approach of simplifying crude oil measurements was the first reported direct coupling of a normal phase liquid chromatographic separation of crude oil to an ultrahigh resolution MS. The difficulty here is that the concentration used for direct infusion experiments ranges between 100 and 500 ppm of sample. This means that each individual component is available only in minute amounts during the analysis. The mass spectrometric detection is usually carried out by adding between 100 and 500 transients to gain statistical depth. But when using LC/MS the time required to co-add a large number of transients is not available because of the associated loss of chromatographic resolution. On the other hand, when recording the spectra from an LC/MS experiment the sensitivity needs to be high enough that all the components can be detected in each individual scan and the concentration of the sample has to be at an optimum level in order to avoid overloading effects when standard chromatographic columns are used. This is one probable reason why online coupling of LC/MS for crude oil analysis is so difficult and until now all work on separation of crude oil has been done offline by collection of individual fractions. The online coupling was realized here for the group separation of nitrogen containing species using atmospheric pressure laser ionization. [1]

Additionally, the project with the Schüth group on the nucleation behavior of silicates in solution continued (for details see Chapter 2.3.2).

Publications resulting from this research area:

(1) Lababidi, S.; Panda, S.K.; Andersson, J.T.; Schrader, W. *Anal. Chem.* **2013,** 85*,* 9478−9485.
(2) Lababidi, S.; Panda, S.K.; Andersson, J.T.; Schrader, W. *Energy Fuels* **2013**, 27, 1236−1245.
(3) Lim, I.H.; Schrader, W.; Schüth, F. *Microporous Mesoporous Mater.* **2013**, 16620–36.
(4) Hegazi, A.H.; Fathalla, E.M.; Panda, S.K.; Schrader, W.; J.T. Andersson, *Chemosphere* **2012**, 89, 205–212.
(5) Gaspar, A.; Zellermann, E.; Lababidi, S.; Reece, J.; Schrader, W. *Energy Fuels* **2012**, 26, 3481−3487.
(6) Hagmeyer, D.; Ruesing, J.; Fenske, T.; Klein, H.-W.; Schmuck, C.; Schrader, W.; Minas da Piedaded, M.E.; Epple, M. *RSC Adv.* **2012**, 2, 4690–4696.
(7) Gaspar, A.; Zellermann, E.; Lababidi, S.; Reece, J.; Schrader, W. *Anal. Chem.* **2012**, 84, 5257−5267.
(8) Gaspar, A.; Schrader, W. *Rapid Commun. Mass Spectrom.* **2012**, 26, 1047–1052.
(9) Panda, S.K.; Brockmann, K-J.; Benter, T.; Schrader, W. *Rapid Commun. Mass Spectrom.* **2011**, 25, 2317–2326.

(10) Alachraf, M.W.; Handayani, P.P.; Hüttl, M.R.M.; Grondal, C.; Ender, D.; Schrader, W. *Org. Biomol. Chem.* **2011**, 9, 1047–1053.

External funding: Deutsche Forschungsgemeinschaft (Schwerpunktprogramm 1179 "Organokatalyse" SCHR 8-1, SCHR 8-2; SCHR 8-3); Project Shell Global Solutions

Cooperations: J.T. Andersson (Münster, D); T. Benter (Wuppertal, D); D. Enders (Aachen, D); B. List (Mülheim/Ruhr, D); P.R. Schreiner (Gießen, D), F. Schüth (Mülheim/Ruhr, D)

3.4 Nuclear Magnetic Resonance (NMR) (C. Farès)

The NMR department provides a broad range of specialised NMR techniques and analytical service for the entire institute. During the reporting period, approximately 60,000 NMR spectra have been recorded on a wide range of samples, going from organic and organometallic compounds in solution to porous silicas and zeolites in solids. To meet demands, the department is equipped with six NMR spectrometers with field strengths corresponding to ^{1}H frequencies of 300, 400, 500 and 600 MHz for analyses in solution and of 300 and 500 MHz for analyses in solid state. The department is also staffed with technical and scientific co-workers, skilled in NMR setup and interpretation as well as in related soft- and hardware maintenance. The department is organised in four areas of service.

(1) NMR in Full Automation (W. Wisniewski, M. Kochius)

Basic NMR measurements in liquid state can be carried out in high-throughput mode on a dedicated "open access" 300-MHz NMR spectrometers at room temperature. With minimal setup, scientific personnel from the entire institute can access this instrument around the clock and obtain NMR data which are acquired and processed fully automatically. The selection of available experiments is limited to those with high sensitivity, high information content and rapid execution with predefined parameters. These include experiments for 1D spectra of ^{1}H, ^{13}C, ^{31}P and ^{11}B. This service covers nearly 90% of all experiments run in our department.

(2) Routine NMR (W. Wisniewski, M. Kochius)

Liquid samples requiring special setup or treatment are submitted for measurement to our operators on a 400-MHz spectrometers. The most common requests are for (a) experiments or nuclear frequencies not available in the automatic mode, (b) experiments at high or low temperature, (c) advanced techniques requiring optimisation of acquisition parameters, and (d) spectroscopy of chemical reactions and kinetics followed in real time directly in the NMR tube.

(3) Advanced NMR Analyses (C. Wirtz, B. Gabor, P. Philipps, D. Bartels)

Particularly challenging NMR studies of solution compounds are accepted for advanced analysis. For these samples, our experienced staff members provide full measurement, analysis and interpretation assistance in close collaboration with the chemical research groups. The advanced techniques are carried out on one of our two dedicated

spectrometer: (a) a 600-MHz system, equipped with a cryogenically-cooled probehead, which provides exquisite sensitivity and resolution for ^{1}H, ^{13}C and ^{15}N measurements near room temperature and which is ideally suited for sub-milligram quantities of 50+ carbon organic molecules; (b) a more versatile modern 500-MHz instruments which provides the possibility to measure at high and low temperature, to cover a broad range of NMR-active isotopes, and to run advanced triple-resonance experiments. A large part of the analytical work is dedicated to determine or confirm structures, stereochemistries, conformations and dynamics. Highlights of the departments joint projects are listed here:

- The full spectroscopic characterisation of reaction products during the novel synthesis campaign of natural products, through a rigorous complete ^{1}H, ^{13}C and ^{15}N assignments. Recent projects accompanied the syntheses of Spirastrellolides Methyl Ester (A and F), Ecklonialactones (A, B and C), Leiodolide B, Tulearin C, and Amphidinolide F (Fürstner group).
- The use of unusual long-range J_{HN} couplings to help identify novel carbene-stabilized N-centered cations (Alcarazo group).
- The characterisation of intermediates in palladium-catalysed allylic substitution reaction in four-membered cyclic systems (Maulide group, Fig 1).

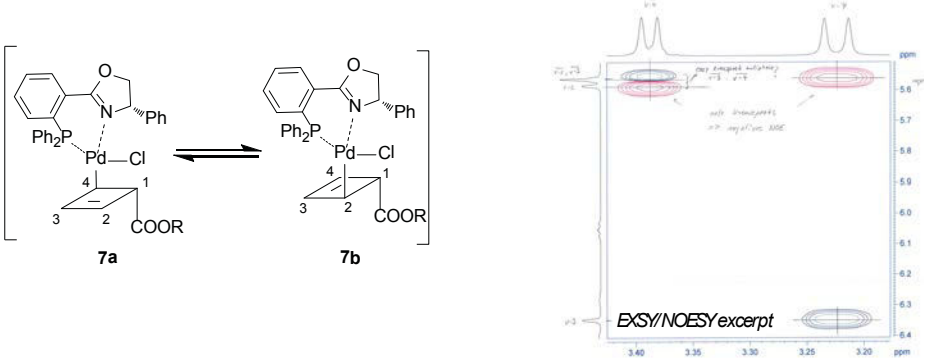

Fig 1 EXSY/NOESY of the Pd-complexed intermediate showing the dynamic exchange process in the cyclobutene ring

- The detection of key players in a Cu-catalysed aerobic oxidative coupling catalytic cycle (Klußmann group, Fig 2)

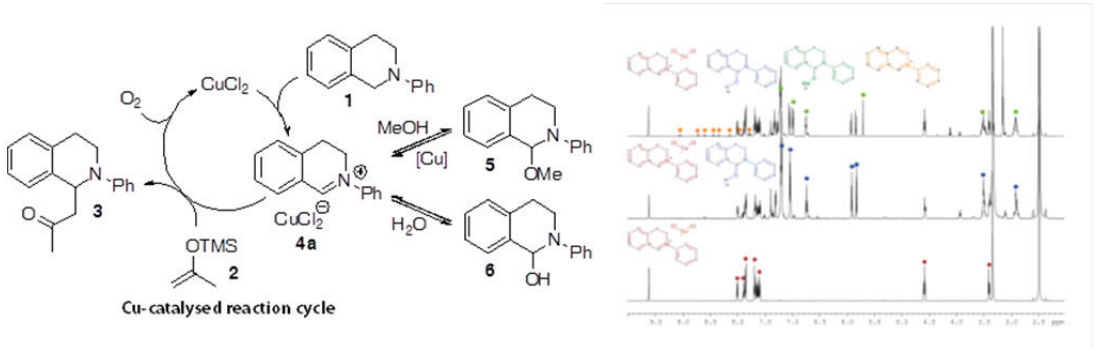

Fig 2 ^{1}H NMR assignment of the exchanging species present during the Cu-catalysed aerobic oxidative coupling reaction.

- NMR kinetic and mechanistic study in a sulphur-mediated α-arylation reaction (Maulide group, Fig 3).

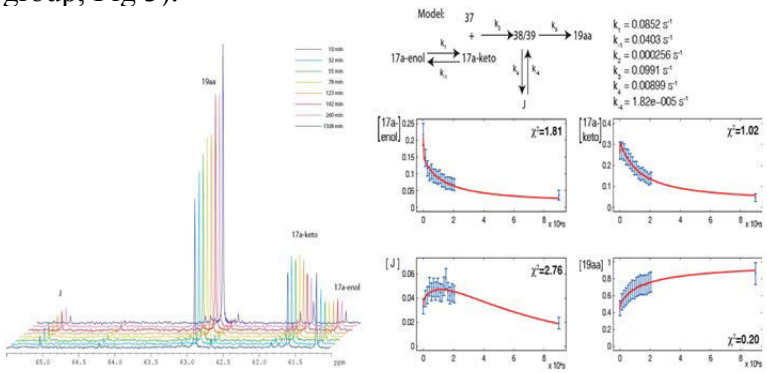

Fig 3: Kinetic profile for the direct sulfoxide-mediated arylation reaction.

- The full structural characterisation and NMR conformation of a key intermediate in primary amine-catalysed asymmetric epoxidation by NMR
- The determination of NMR fingerprint parameters to quickly determined stereochemistry in functionalised dienes (Maulide group).

(4) Solid-State NMR (B. Zibrowius)

Solid-state NMR spectroscopy remains one of the most important techniques for the characterisation of solid catalysts and other new materials synthesised in the institute (Schüth group). Both dedicated 300- and 500-MHz spectrometers are equipped with magic-angle spinning (MAS) probeheads to obtain high resolution signals from a wide range of NMR active nuclei. In continuation of work performed in previous years, solid-state NMR spectroscopy has particularly been applied in the following fields:

- Characterisation of solid catalysts prepared from mesoporous silicas or zeolites (^{29}Si, ^{13}C and ^{27}Al)

- Detailed studies of various complex aluminium hydrides and boron hydrides (mainly by ^{27}Al and ^{11}B NMR, respectively)
- Mechanistic studies on the dehydrogenation process in sodium alanate (^{27}Al and ^{23}Na).

In addition to these applications, the method has repeatedly been used to contribute to the characterisation of the following materials:

- Organic polymers synthesized as precursors for solid catalysts (^{13}C and ^{31}P)
- Solid products obtained in valorisation processes of wood and lignin (^{13}C).

Advanced Methods

The NMR department continues to develop and to establish advanced NMR methodologies as part of their collection of routine applications in order to meet the scientific requirements of the institute. A number of newly applied state-of-the-art methods that have been explored and used in the NMR department during the current reporting period.

- Residual dipolar couplings (RDC) to determine stereochemistries, to differentiate enantiomers and to provide complementary conformational and dynamic information.
- *Para*-hydrogen induced polarisation (PHIP) to follow the course of hydration reactions and to identify low amounts of intermediates.
- qNMR and DOSY to characterise and quantify the composition of complex reaction mixtures.
- Novel NMR methods to accelerate (non-uniform sampling (NUS) and ultrafast NMR) and simplify (Pureshift) multidimensional NMR and in order to better follow reactions in real-time.
- Rapid injection NMR (RINMR) for tracking catalytic transformations in “real time”.

Publications resulting from this research area

(1) Souris, C.; Luparia, M.; Frebault, F.; Audisio, D.; Farès, C.; Goddard, R., *Chem. - Eur. J.* **2013**, 19, 6566-6570.

(2) Souris, C.; Frebault. F; Audisio, D.; Farès, C.; Maulide, N. *Synlett* **2013**, 10, 1286-1290.

(3) Lifchits, O.; Mahlau, M.; Reisinger, C. M.; Lee, A.; Farès, C.; Polyak, I. *J. Am. Chem. Soc.* **2013**, 135, 6677-6693

(4) Kozma, A.; Gopakumar, G.; Farès, C.; Thiel, W.; Alcarazo, M. *Chem. - Eur. J.* **2013**, 19, 3542-3546.

(5) Kondoh, A.; Arlt, A.; Gabor, B.; Fürstner, A. *Chem. - Eur. J.* **2013**, 19, 7731-7738.

(6) Huang, X. L.; Patil, M.; Farès, C.; Thiel, W.; Maulide, N. *J. Am. Chem. Soc.* **2013**, 135, 7312-7323.

(7) Audisio, D.; Gopakumar, G.; Xie, L. G.; Alves, L. G.; Wirtz, C; Martins, A. M. *Angew. Chem., Int. Ed.* **2013**, 52, 6313-6316.

(8) Arlt, A.; Benson, S.; Schulthoff, S.; Gabor, B.; Fürstner, A. *Chem. - Eur. J.* **2013**, 19, 3596-3608.

(9) Klimczyk, S.; Huang, X. L.; Farès, C.; Maulide, N. *Org. Biomol. Chem.* **2012**, 10, 4327-4329.

(10) Andresen, C.; Helander, S.; Lemak, A.; Farès, C.; Csizmok, V.; Carlsson, J. *Nucleic Acids Res.* **2012**, 40, 6353-6366.

(11) Seidel, R. W.; Goddard, R.; Zibrowius, B.; Oppel, I. M. *Polymers* **2011**, 3, 1458-1474.

(12) Lemak, A.; Gutmanas, A.; Chitayat, S.; Karra, M.; Farès, C.; Sunnerhagen, M. *J. Biomol. NMR* **2011**, 49, 27-38.

(13) Lehr, K.; Mariz, R.; Leseurre, L.; Gabor, B.; Fürstner, A. *Angew. Chem., Int. Ed.* **2011**, 50, 11373-11377.

(14) Larivee, A.; Unger, J. B.; Thomas, M.; Wirtz, C.; Dubost, C.; Handa, S *Angew. Chem., Int. Ed.* **2011**, 50 304-309.

(15) Hickmann, V.; Kondoh, A.; Gabor, B.; Alcarazo, M.; Fürstner, A. *J. Am. Chem. Soc.* **2011**, 133, 13471-13480.

(16) Felderhoff, M.; Zibrowius, B. *Phys. Chem. Chem. Phys.* **2011**, 13, 17234-17241.

(17) Boess, E.; Sureshkumar, D.; Sud, A.; Wirtz, C.; Farès, C., Klussmann, M. *J. Am. Chem. Soc.* **2011**, 133, 8106-8109.

(18) Beckmann, U.; Eichberger, E.; Rufinska, A.; Sablong, R.; Klaui, W. *J. Catal.* **2011**, 283, 143-148.

(19) Benson, S.; Collin, M. P.; Arlt, A.; Gabor, B.; Goddard, R.; Fürstner, A. *Angew. Chem., Int. Ed.* **2011**, 50, 8739-8744.

3.5 Electron Microscopy and Chemical Crystallography (C. W. Lehmann)

Introduction: The EmRay-Group combines all electron microscopy activities of the Institute and selected areas of crystallography, namely crystal structure determination from single crystals and polycrystalline organic materials. The present research fields encompass electron density studies and crystal engineering. In addition to operating in-house facilities the group is part of a team building a dedicated chemical crystallography beamline at PETRA III in Hamburg.

Service Activities, *i) Crystallography:* The service activities focus on single crystal structure analysis and offer powder diffraction of organic compounds as an alternative method for crystal structure determination. The areas general powder diffraction and photon electron spectroscopy have been incorporated in the new research group of Dr. Claudia Weidenthaler.

For single crystal structure analysis state-of-the-art technology is employed, comprising three area detector systems. A Cu-rotating anode equipped with a four circle goniometer and a large surface area CCD-detector is used for the determination of the absolute configuration of enantiopure light atom compounds as well as for protein crystallography. Inorganic and organometallic compounds are investigated using either a Mo-rotating anode or the recently acquired molybdenum micro focus X-ray source, both equipped with four circle goniometers. All diffractometer systems employ graded multilayer optics to maximise X-ray intensities and are equipped with liquid nitrogen low temperature devices for sample cooling and stabilisation. A total of approximately 500 data sets are collected annually, however an increasing number of samples yield only very small crystals with dimensions less than 20 μm. Selected samples are analysed using synchrotron radiation, in particular using the single crystal beamline at ANKA Karlsruhe.

The crystal structures of compounds yielding crystals too small even for synchrotron radiation might be elucidated by means of X-ray powder diffraction. A pre-requisite for the determination of the crystal structures of organic molecules is the knowledge of the atom connectivity. Questions regarding the conformation of the molecules in the solid state as well as to the crystal packing can be answered by this approach. Presently the group has one powder diffractometer for analysing samples enclosed in capillaries or in transmission geometry.

ii) Electron Microscopy: The instrumentation for electron microscopy has remained unchanged during the reporting period. However, an intensive survey followed by demonstrations has been undertaken to identify a suitable microscope for sub-nanometer EDX analysis. This new electron microscope has been ordered and is currently being manufactured. Delivery is expected in the summer of 2014. Presently available electron microscopes in the group comprise a 200 kV TEM with cold field emitter gun, able to obtain micrographs with atomic resolution. Two further 120 kV TEMs supplement the set-up. One of these 120 kV transmission electron microscopes has been dedicated for self-service by trained PhD students and Post-Docs. Scanning electron microscopy is performed with an ultra-high resolution microscope, which gives a line resolution better than 0.34 nm (graphite lattice spacing). An important aspect of the electron microscopy service is the sample preparation, which forms a crucial part of the activities in the group. In addition to established coating and cutting methods, in particular ultra-microtomes, the group is constantly honing its methods and is introducing new techniques as required. Two Master Theses focussed on these aspects over the last years.

Research Projects, *Electron Density Studies (T. Dols):* The DFG priority program 1178 entitled "Experimental Charge Density as the Key to Understand Chemical Interactions" was continued. In collaboration with U. Englert (Aachen) the electron density distribution in metal organic coordination polymers new insight into non-bonding halogen-halogen and halogen-carbon interactions was gained.

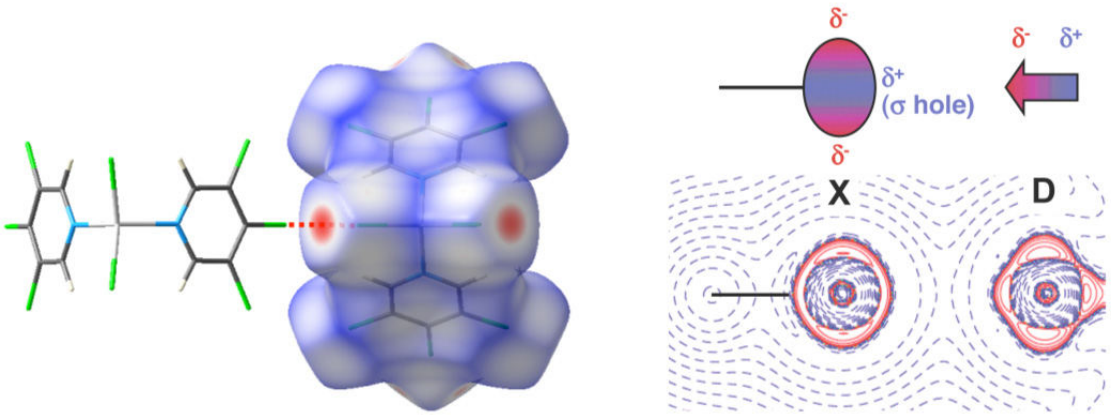

Figure 1: Hirshfeld surface of bis(3,4,5-trichloropyridinyl)zincdichloride (left) showing the short Cl…Cl interaction. Polar flattening of the acceptor halogen is clearly visible in the Laplacian of the electron density (right).

In particular the polar flattening effect postulated for covalently bonded halogen could be observed experimentally.[1] Chemically closely related monomeric zinc-halogen-dipyridyl complexes have been included lately.

Together with T. Spaniol (Aachen) the project on electron density studies of Ti-based stereotactic polymerisation catalysts of the mismatched interaction type was completed.

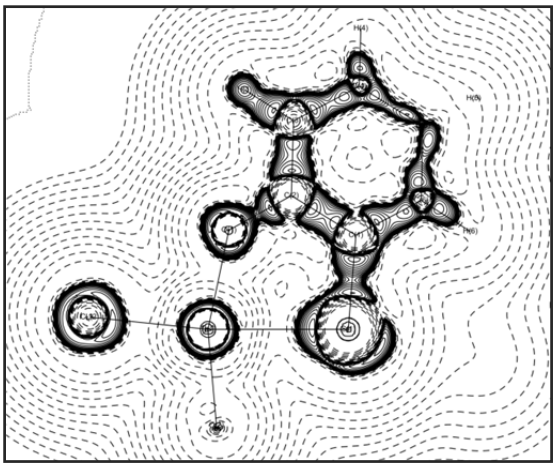

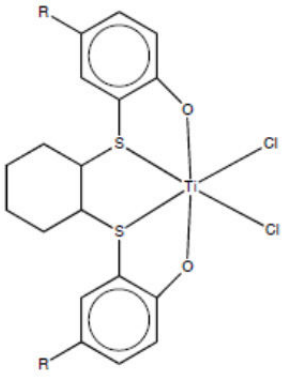

Figure 2: Laplacian of the electron density in the plane subtended by sulfur, titanium and oxygen (left) of the mismatched interaction catalyst shown on the right.

Crystal Engineering (D. Bock): Co-crystals are a specific implementation of supra-molecular chemistry, maximising the use of intermolecular interactions. Liquid assisted ball milling was used to obtain co-crystals composed of chiral carboxylic acids and chiral amides. Combining enantiopure educts in separate experiments it was possible to obtain diastereomeric co-crystals for a number of acid-amide pairs. From clearly distinguishable powder diffraction patterns of the diastereomers it was possible to elucidate not only the crystal structures but also to determine the absolute configuration of one of the two co-crystallised compounds.[2]

Chemical Crystallography Synchrotron Beamline: The extension to the PETRA III synchrotron laboratory at DESY in Hamburg is under construction. Hall East will accommodate the dedicated chemical crystallography beamline P24. A consortium involving the University of Bayreuth (S. van Smaalen), the University of Hamburg (U. Bismayer), the University of Dresden (D. Meyer), the University of Munich (W. Schmahl), and this group has secured bmbf funding for a second period of three years and is responsible for planning, building and commissioning the end-station of this beamline. Specific emphasis is being placed on handling reactive and sensitive samples in a state-of-the-art diffraction set-up. A proof-of-principle experiment has been carried out already at the macromolecular beamline P11. The ChemCryst-beamline, scheduled

for 2015, will permit high resolution single crystal data collections at variable energies up to 40 keV.

Core-shell nano particles (J. von der Heyden): Unambiguous characterization of core-shell particles remains a challenge as the overall diameter of these particles is reduced to about 5 nm. Using synthetic methods developed in the department of heterogeneous catalysis (F. Schüth) core-shell nano particles were synthesized ranging from 5 to 50 nm. At the smaller end of this range a positive identification of the core-shell structure was possible only by using a probe corrected scanning transmission electron microscope equipped with an EDX detector of approx. 1 sr solid angle.

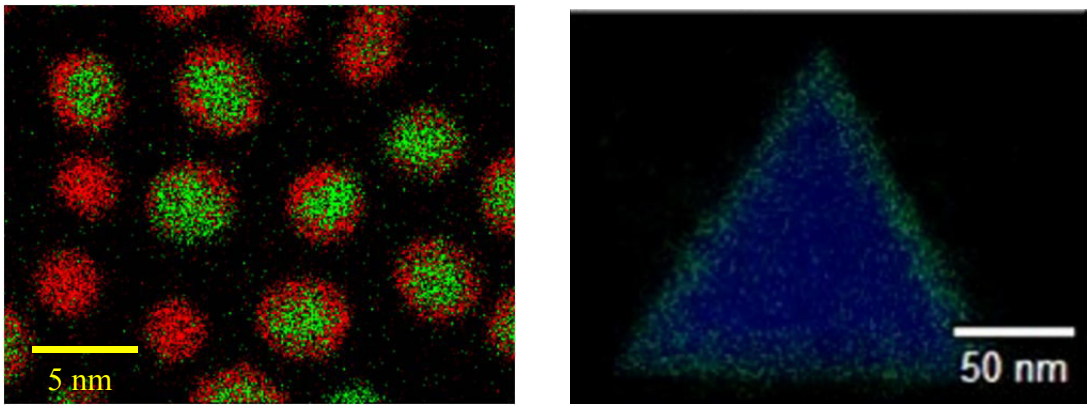

Figure 3: EDX mappings of ruthenium-platinum (core-shell) nanoparticles (left) measured within 10 min. using a C_s corrected STEM and of a Pt@Pd nano-triangle collected using the ultra-high resolution SEM.

Synthetic opals (A.-C. Swertz): A further research project in electron microscopy was directed at preparing cross-sections of synthetic opals (research group of F. Marlow) in order to study lattice defects in these photonic crystals. Using a combination of diamond wire cutting and argon ion milling, cross sections of the as-grown opal films could be obtained for the first time. These were investigated extensively by scanning electron microscopy and revealed unexpected long range domains within the bulk, tilted with respect to the observed {1 1 1} layer formation on the surface.

Publications resulting from this research area:

Lehmann

(1) Wang, R.; Dols, T.S.; Lehmann, C.W.; Englert, U. *Z. Anorg. Allg. Chemie* **2013**, 639, 1933-1939

(2) Bock, D.A..; Lehmann, C.W. *CrystEngComm* 2012, 14, 1534-1537.

(3) Grünert, W.; Gies, H.; Muhler, M.; Polarz, S.; Lehmann, C.W.; Grossmann, D.; van den Berg, M.; Tkachenko, O.P.; de Toni, A.; Sinev, I.; Bandyopadhyay, M.; Narkhede, V.; Dreier, A.; Klementiev, K. V.; Birkner, A.; Löffler, E *Phys. Stat. Solidi B.* **2013**, 250, 1081-1093.

(4) Sternberg, M.; Rust, J.; Lehmann, C.W.; Mohr, F. *Phys. Stat. Solidi B.* **2013**, 96, 280-288.

(5) Deiana, L.; Zhao, G.-L.; Leijonmarck, H.; Sun, J.; Lehmann, C.W.; Córdova, A. *ChemistryOpen* **2012**, 1, 134-139.

(6) Macabeo, A.P.G.; Lehmann, C.W.; Reiser, O. *Synlett* **2012**, 23, 2909-2912.

(7) Molter, A.; Rust, J.; Lehmann, C.W.; Mohr, F. Tetrahedron 2012, 68, 10586-10591.

(8) Mohr, F.; Niesel, J,; Schatzschneider, U.; Lehmann, C.W. *Z. Anorg. Allg. Chemie* **2012**, 638, 543-546.

(9) Wang, R.; Dols, T.; Lehmann, C.W.; Englert, U. *Chem. Commun.* **2012**, 48, 6830-6832.

(10) Molter, A.; Rust, J.; Lehmann, C.W.; Deepa, G.; Chiba, P.; Mohr, F. *Dalton Trans.* **2011**, 40, 9810-9820.

(11) Molter, A.; Rust, J.; Lehmann, C.W.; Mohr, F. *ARKIVOC* **2011**, 6, 10-17.

Goddard

(12) Seidel, R. W.; Dietz, C.; Breidung, J.; Goddard, R.; Oppel, I. M. *Acta Crystallogr., Sect. C: Cryst. Struct. Commun.* **2013**, 69, 1112-1115.

(13) Rose, M.; Weber, D.; Lotsch, B. V.; Kremer, R. K.; Goddard, R.; Palkovits, R. *Microporous Mesoporous Mater.* **2013**, 181, 217-221.

(14) Seidel, R. W.; Goddard, R.; Oppel, Iris M. *Polymers* **2013**, 5, 527-575.

(15) Seidel, R. W.; Dietz, C.; Goddard, R.; Oppel, I. M. *Journal of Chemical Crystallography* **2013**, 43, 229-234.

(16) Seidel, R. W.; Goddard, R.; Breidung, J.; Bamfaste, P.; Neff, D.; Oppel, I. M. *Struct. Chem.* **2013**, 24, 181-189.

(17) Krasnopolski, M.; Seidel, R.W.; Goddard, R.; Breidung, J.; Winter, M. V.; Devi, A.; Fischer, R. A. *J. Mol. Struct.* **2013**, 1031, 239-245.
(18) Spallek, M. J.; Stockinger, S.; Goddard, R.; Trapp, O. *Adv. Synth. Catal.* **2012**, 354, 1466-1480.
(19) Sproules, S.; Weyhermueller, T.; Goddard, R.; Wieghardt, K. *Inorg. Chem.* **2011**, 50, 12623-12631.
(20) Seidel, R. W.; Goddard, R.; Zibrowius, B.; Oppel, I. M. *Polymers* **2011**, 3, 1458-1474.
(21) Seidel, R. W.; Goddard, R.; Hoch, C.; Oppel, I. M. *Z. Anorg. Allg. Chem.* **2011**, 637, 1545-1554.
(22) Spallek, M. J.; Stockinger, S.; Goddard, R.; Rominger, F.; Trapp, O. *Eur. J. Inorg. Chem.* **2011**, 2011, 5014-5024.
(23) Krause, M. R.; Goddard, R.; Kubik, S. *J. Org. Chem.* **2011**, 76, 7084-7095.
(24) Seidel, R. W.; Graf, J.; Goddard, R.; Oppel, Iris M. *Acta Crystallogr., Sect. E: Struct. Rep. Online* **2011**, 67, m236-m237.
(25) Seidel, R. W.; Goddard, R.; Hoch, C.; Breidung, J.; Oppel, Iris M. *J. Mol. Struct.* **2011**, 985, 307-315.

External Funding: DFG priority program 1178 “Experimental Electron Densities”

Cooperation: U. Englert (Aachen), W. Grünert (Bochum), F. Mohr (Wuppertal), O. Reiser (Regensburg), J. J. Schneider (Darmstadt), T. Spaniol (Aachen), J. Sun (Stockholm), O. Terasaki (Stockholm), H. Willner (Wuppertal)

3.6 Library and Information Management (P. Fischer, R. Lohmer)

The general responsibilities of the library group have changed since the previous evaluation. Formerly, our one-person library was responsible for the library-services of our Institute. In 2012, the neighboring Institute changed direction and became the Max-Planck-Institute for Chemical Energy Conversion (MPI CEC). As part of the restructuring, MPI CEC and MPI KOFO decided to eventually merge their libraries to one campus-library. The new library will be installed on the premises of the MPI KOFO.

To prepare this fusion the library of the MPI KOFO was refurbished and additional bookshelves were installed before ca. 10.000 books were moved from the MPI CEC to our library. A physical inventory was performed and a library commission was founded.
Currently, this commission is about to define the services, a new web-portal, the financial aspects, the legal frameworks and questions regarding human resources.

Some general information about the library of MPI KOFO:
Our library, founded in 1912, serves the five chemical departments by buying, collecting and archiving books and journals from the field of chemistry and chemical catalysis in general. It focuses on organometallic, theoretical, polymer and coal chemistry as well as on materials science. 17000+ books and monographs and 630 dissertations reflect various aspects of catalysis; they are electronically searchable by the ALEPH program. The library contains a large collection of recent and many older print-journals. 120+ subscribed journals are electronically catalogued and linked with their digital equivalents.

On the other hand, most journals are now available online. All digital activities of the Max Planck Society are concentrated in the Max Planck Digital Library (MPDL). Since 2008 all needed processes for collaboration between MPDL and local libraries were established, and they all work well now.

As already mentioned in the last report, “MPDL basic service” of the Max Planck Society allows online access to most of the core journals needed by our scientists. A list of all relevant journals is part of the library intranet page of our institute.

The “MPDL basic service” allow us to receive many print journals for a deep discount price – e.g. the products from the American Chemical Society, the Royal Society of Chemistry, and the Wiley-VCH Group. Therefore, we keep selected journals from their journal list until the electronic long term archive problem is solved either by the publishers themselves or by the Max-Planck-Society. Additionally we subscribe to several other print journals, which are not included in the “MPDL basic service”. Overall, about 80 journals are available at MPI KOFO. For scientific articles that are not available in our and other MPG libraries, we rely on loans through the SUBITO, British Library and Chemical Abstracts Service.

Apart from the Web of Knowledge (ISI/Thomson Scientific) which has been licensed through the MPG, the major source of information for our Institute is the Chemical Abstracts Service. In 2004 the Institute acquired 50 personal SciFinder licenses which were increased to a total of 129. SciFinder enables users to run their own structural and bibliographic inquiries; the introduction to updated versions and the more intricate questions are handled by the library. The files from Elsevier are also accessible.

Despite the large effort of publishing companies like Wiley or Elsevier to promote their e-books, neither the license modes nor the leasing offers have convinced us to switch from printed books. This may change in the future, and we are prepared to buy or lease single chapters as we buy review articles now. The problem of long term archival storage seems to be solved only for printed media. A central digital book archive is being discussed within the MPG but without clear perspectives. Printed books still are of major importance for our library, and their number is constantly growing by ~ 260 titles per year. However, due to a strong scientific diversification, many additional books are borrowed from other libraries.

Open Access to the scientific literature is a major theme at MPDL, however, activities in our institute are very limited: There is neither a central chemical open archive like the arXive.org for physicists nor high ranking open access journals in the field of chemistry.

Within 2012 we moved all the data from eDoc-server to the new publication repository (PubMan) of MPDL. With the new interfaces of PubMan we will be able to generate publication lists within our internet portal. Presently we are working on this project.

3.7 Computer Group (P. Fischer)

The general responsibilities of the IT group have changed since the previous evaluation. Formerly, our IT group was responsible for the IT infrastructure of both Max Planck Institutes on the campus. In 2012, the neighbouring Institute changed direction and became the Max Planck Institute for Chemical Energy Conversion (MPI CEC), with an expansion from two to four departments. As part of the restructuring, MPI CEC decided to create an own IT service group and to terminate the agreement on joint IT infrastructure services. This change has now been implemented, and hence the scientific IT tasks at MPI CEC are handled by their own IT service group. Our IT group still takes care of the common administrative IT infrastructure of both Institutes.

Within our Institute, the IT group supports the following areas:

- Electronic Laboratory Notebook with connected Archive (ELNA).
- Operation and enhancement of the common local area network (LAN).
- Acquisition, operation, and system management of central servers and attached devices.
- Selection and installation of new hardware and software in general.
- Computerization of experiments.
- Development of application software and its adaptation to new requirements.
- Administration of web pages and data bases.
- Information and education of computer users.
- Trouble shooting in the case of failures.

Electronic Laboratory Notebook with connected Archive (ELNA):
As already mentioned in the previous report, the institute had decided to introduce an electronic laboratory infrastructure for the experimental and analytical groups, on the basis of the Open Enventory (OE) software developed by Felix Rudolphi at TU Kaiserslautern. The upscaling of the OE software to the needs of our Institute made it necessary to adopt a more flexible architecture and to re-engineer many of the components. Many new features were developed and implemented, for example:

- New role and authorization concepts.
- New workflows for the analytic service groups.
- Improved handling of the chemical database.
- Tailor-made options for optimum use of the electronic lab notebook.
- A new backup process.

- An electronic archive for long-time data storage.

The new system called ELNA (Electronic Lab Notebook with connected Archive) is currently being made available in a stepwise fashion. The chemical database of ELNA has been used productively by all experimentalists since August 2012. The rollout of the electronic lab notebook started in June 2013. ELNA is now in operation in the research department of Prof. Fürstner and all analytic service groups. The daily use of the system has resulted in a number of requests for changes and new features, which will be implemented according to the assigned priorities. Thereafter, the rollout will continue with the research department of Prof. List.
The electronic archive is already in productive use. It is based on an Oracle WebLogic Content Management System combined with an HP ICAS solution. This setup satisfies all legal requirements (e.g., with regard to patents) and is certified as an electronic archive by KPMG.

Local area network:
The common hierarchically structured LAN was described in previous reports. Over the past three years, it has been improved and optimized as needed, mostly in the context of construction projects. In some parts, the physical backbone was upgraded to fiber optic cables. In other parts, the number of LAN connections was increased to enable higher transfer rates.

Computing center:
The Department of Theory is growing. Two new junior groups were created, and new projects in the framework of the ERC Advanced Grant will need more high performance computing capacity in the future. In the central computing facility of the institute, the existing APC cubicle had reached its limits with respect to power supply and cooling. Instead of attempting a complicated and time-consuming upgrade, with inevitable downtimes, it was decided to install a second APC cubicle and to increase the power supply and cooling capacity accordingly (up to 160 kW). This extension of the hardware infrastructure was completed in 2012.

Computer hardware:
The IT group operates the central UNIX and Windows servers of the Institute, and it manages the applications, compute and file servers of the Department of Theory. The jobs from the Department Theory are handled by a “grid engine queue system”.
The UNIX servers that host central services (external and internal logins, email dispatch and receipt, internet and intranet web pages, web cache, DNS, DHCP, RADIUS, etc.)

were replaced with three new ESX servers. The services run as virtual instances on these servers under 64-bit LINUX.
The library of the backup system was updated with LTO5 drives.
Previously, both Institutes on the Mülheim campus shared a common hierarchically structured Windows Server 2008 based Active Directory with one superordinate domain and two subdomains, one for each Institute. As a consequence of the general restructuring (see above), the MPI CEC domain was separated off into an own infrastructure that is now maintained by the IT group of MPI CEC.
Formerly, data was stored centrally on a highly redundant EMC Celerra NS80 network attached storage (NAS) server. This system was replaced by two new highly redundant NetApp systems (FAS3240 and FAS2240) with a capacity of 96 TB. These servers were placed into two separate buildings (i.e., separate fire areas). The new data storage solution offers the following advantages:

- Deduplication detects redundant files and significantly reduces the needed space.
- Snapshot functionality allows for a new backup concept.
- The two redundant systems enable a disaster recovery solution.

For the Department of Theory, the IT group maintains ca. 150 Linux clusters based on Intel XEON and AMD Opteron CPUs, which are equipped with different amounts of memory (small/medium/large) to support different computational applications. Currently there is a total of

- 384 cores for small computations,
- 792 cores for medium-sized computations, and
- 128 cores for large computations.

In addition, one server is presently equipped with 2 NVIDIA Tesla 2090 GPUs for code development and evaluation purposes.
Most systems are attached to the network via 1 Gbit/s ethernet. The NetApp systems have a 10 Gbit/s ethernet connection.

Workstations and PCs:
PCs represent the largest number of work-place computers. There are ca. 700 in our Institute. Most of them run Windows 7. In the Department of Theory as well as in several other service and research groups, there are Linux- or UNIX-based workstations to allow more demanding applications. The workstations and PCs in the Departments of Theory and Homogeneous Catalysis have 1 Gbit/s connections to the network.

Computerization of experiments:

Among the real-time data acquisition systems that had been designed and implemented by the IT group in the past, the systems for gas and liquid chromatography were in use for 29 years. These systems have now been retired and replaced by a new commercial software (Chromeleon of Dionex).

Application software:

Safety data sheets for all chemical compounds used in our laboratories can be retrieved conveniently by a web browser from our in-house data base system. The underlying data is kept up to date according to current legal regulations. Analyses can be ordered electronically for gas chromatography, X-ray crystallography, and mass spectrometry. The IT group maintains an elaborate book-keeping system for gas-chromatography samples that had previously been designed and implemented in-house. Raw data and reports from mass spectrometry and gas chromatography are archived automatically.

The IT group continues to provide support to the libraries of both Institutes through the Aleph 500 integrated library system. It also supports the Beilstein CrossFire database and the SciFinder interface to the Chemical Abstracts Service.

Finally, the IT group provides support for the travel-expenses reporting system, the flexitime logging system, and the new session desk Archimedes.

Development projects:

As already pointed out, the upgrade of features in the electronic laboratory notebook is an ongoing process that is driven by the needs of the scientists.

At present, we are planning a new video-conferencing room with Cisco technology that will become part of the MPG video-conferencing network.

To prepare the necessary renewal of our telecommunication system, the IT group is currently evaluating several commercially available systems, also with regard to Voice-over-IP functionality.

CHAPTER 4

The Training of Young Scientists

4 The Training of Young Scientists

The Institute considers the training of **young scientists** (**diploma** and **doctoral students**, **postdocs**) an important task. Their number amounts to more than 160 (cf. Figure 1 – the ratio of funding by the Institute's standard research budget and third party funds depends upon their relative contributions).

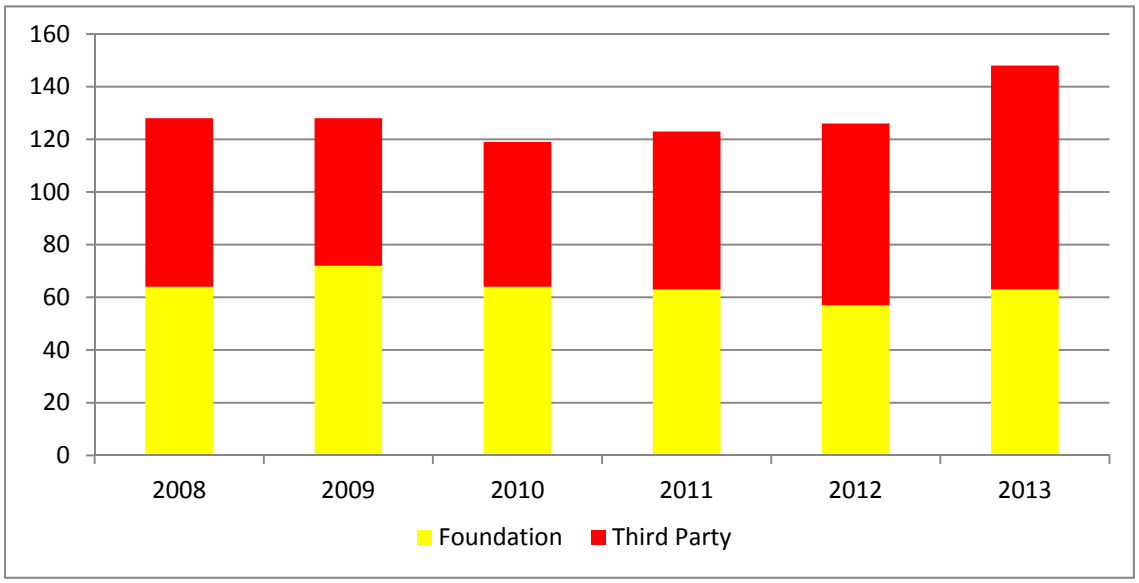

Fig. 1. Support for young scientists

The financial resources of the Institute allow for the support of about 50-60 such positions in the five departments of the scientific members, including the positions of the research groups assigned to them. In addition the independent junior research groups have a separate budget for such positions. Further positions are financed by third-party funds and by support grants awarded to individual scientists. From 2011 to 2013 the latter category included 23 scholarship awardees (1 Heisenberg, 12 Alexander von Humboldt, 2 Deutscher Akademischer Austauschdienst, 7 Kekulé, 1 Liebig) and in addition 27 similar awards from abroad (Austria, Belgium, China, Denmark, Japan, Mexico, Portugal, Spain, Switzerland, Turkey).

Status Dec 31, 2011	Total	MPG and Foundation Funds	Third Party Funds	National (n) Internat. (i)	Female (f) Male (m)
Diploma students	1	-	1	1 n - i	1 f - m
PhD students	69	26	43	29 n 40 i	27 f 42 m
Post-docs	53	37	16	1 n 52 i	13 f 40 m
	123	63	60	31 n 92 i	41 f 82 m
Status Dec 31, 20112					
Diploma students	4	3	1	4 n - i	3 f 1 m
PhD students	72	23	49	34 n 38 i	30 f 42 m
Post-docs	50	31	19	1 n 49 i	10 f 40 m
	126	57	69	39 n 87 i	43 f 83 m
Status Sept 30, 2013					
Diploma students	8	5	3	8 n - i	4 f 4 m
PhD students	84	27	57	38 n 46 i	33 f 51 m
Post-docs	56	31	25	1 n 55 i	13 f 43 m
	148	63	85	47 n 101 i	50 f 98 m

Table 1. Young Scientists

The vast majority of the diploma and doctoral students come from German and European universities, including those at which the Institute's group leaders hold lectures. These are the Universities of Aachen, Bochum, Cologne, Dortmund, Duisburg/Essen, Düsseldorf, Münster and Wuppertal.

The following table specifies, on an annual basis, the number of postdocs as well as their geographical origin.

Postdocs (country of origin)	2008	2009	2010	2011	2012	Sept 30, 2013
Europe	34	32	27	27	29	27
USA / Canada	5	4	3	1	-	4
Latin & South America	3	3	6	5	3	3
Asia	25	24	21	20	18	21
Africa / Australia	2	-	-	-	-	1
Total	69	63	57	53	50	56

Table 2. Postdocs / country of origin

The training of the young scientists is supplemented by regular seminars within their department or group and by interdisciplinary colloquia including poster sessions. The latter are open to the whole Institute and held by the young scientists themselves. Once per year there is a 3-day long workshop for young scientists held by an internationally renowned scientist as part of the duties of the Karl Ziegler Guest Professorship. The daily lectures are supplemented by discussions. Special emphasis is laid on active participation of the young scientists.

Since summer 2004 the Institute has participated in the International Max Planck Research School (IMPRS) for Surface and Interface Engineering in Advanced Materials. The Eisenforschung, Kohlenforschung, Ruhr-Universität Bochum and Institutes in China cooperate in this school.

The Institute also contributes to the training of young scientists in the framework of collaborative large-scale research projects, for example:

- the DFG Collaborative Research Center “Metal-surface Interactions in Heterogeneous Catalysis” (ended in summer 2012, SFB 558)
- the DFG priority programme “Organocatalysis” (ended in summer 2011)
- the Max Planck Research Initiative: “EnerChem” = Nanochemical Concepts for Sustainable Energy Supply with 5 participating MPIs (ended in December 2011)
  four research projects in the Excellence Cluster “Tailor-made Fuels from Biomass” at the RWTH Aachen (ended in October 2012)
- four research projects in the Excellence Cluster “RESOLV” at the University of Bochum (lasting until October 2017)
- five research projects in the Excellence Cluster “Tailor-made Fuels from Biomass” at the RWTH Aachen (lasting until October 2015)

In addition every year selected young scientists from the Institute participate in workshops on catalysis organized by the chemical industry such as the Catalysis Research Laboratories (BASF together with the University of Heidelberg) or the Bayer PhD Student Course.

A survey of the diploma and doctoral theses completed in the reporting period is given at the end of this chapter. Students finished their doctoral studies between 2011 and 2013, on average, within a period of 3.9 years and were awarded their doctorates at the age of 29.1 years. The Rampacher Prize of the MPG, awarded annually since 1985 to the youngest doctoral student in the entire MPG to have completed his or her doctoral work in that year, has been won six times out of a possible twenty-four by students from the MPI für Kohlenforschung.

During the reporting period one PhD candidate won the Otto Hahn Medal by the Max Planck Society for her excellent thesis.

Special emphasis is put on the support of excellent postdocs for building up their independent research group. At present there are six such groups at our Institute (e.g. 5.1.3). During the period 2008-2013 several junior scientists from the Institute have received calls to faculty positions.

Name	**Year**	**University**
Mukherjee	2008	Bangalore, India
Trapp	2008	Heidelberg University
Yang	2009	Sungkyunkwan University, South Korea
Lu	2009	Dalian University, China
Moyeux	2009	Université de Paris, France
Palkovits	2010	RWTH Aachen
Zhang	2010	Dalian University, China
Lan	2011	CAS Institute Qingdao, China
Shao	2011	Kyushu University
Jia	2011	Shandong University
Jiang	2012	Quingdao CAS Institute on Bioenergy
Maulide	2013	University of Vienna, Austria

Table 3. Calls from Universities

Doctoral Theses 2011

Benighaus, T.: Boundary Potentials for Hybrid Quantum Mechanical/Molecular Mechanical Simulations of Solvated Biomolecules. Düsseldorf 2011.

Benson, S.: Totalsynthese von Spirastrellolide F Methylester. Dortmund 2011.

Greven, Raphaela: Nickel(II)-ή^3-allyl---- und Nickel(II)-ή^5-cyclopentadienyl-Komplexe mit N-heterocyclischen Carben-Liganden und Gold(I)-Komplexe mit sterisch anspruchsvollen Phosphan-Liganden. Düsseldorf 2011.

Hickmann, V. A.: Schutzgruppenfreie enantioselektive Totalsynthese von Ecklonialacton A und B sowie biologische Tests aktiver Naturstoffe. Dortmund 2011.

Liao, S.: Asymmetric Counteranion-Directed Transition Metal Catalysis: Enantioselective Epoxidation and Sulfoxidation with Ion-Pair Catalysts. Köln 2011.

Ramos da Silva, M.: Quantum Mechanical/Molecular Mechanics Study of Electronically Excited states and Assessment of Methods for Calculating Vertical Excitation Energies. Düsseldorf 2011.

Yachmenev, A.: Variational calculations of rational-vibrational spectra and properties of small molecules. Düsseldorf 2011.

Yan, Kai M. Sc.: Transformation of Biogenic Carbohydrates into Levulinic Acid and further Hydrogenation using Supported Nanoparticles Catalysts Synthesized by Chemical Fluid Deposition. Aachen 2011.

Doctoral Theses 2012

Čorić, Ilija: Asymmetric Brønsted Acid Catalysis: Acetals & Confined Catalysts. Köln 2012.

Gallenkamp, Daniel: Stereoselektive Synthese von (E;Z)-konfigurierten 1,3-Dienen durch Ringschlußmetathese. Dortmund 2012.

Heppekausen, Johannes: Effiziente Silyloxy-basierte Katalysatoren für die Alkin-Metathese. TU Dortmund 2012.

Lee, Anna: Asymmetric Aminocatalysis. Köln 2012

Lifchits, Olga: Organocatalytic Approaches to Asymmetric Oxidation. Köln 2012.

Lu, You: Studying Excited States: From Small Molecules to Large Biological Systems. Düsseldorf 2012.

Meine, Jan Niklas: Novel Routes for the Catalytic Depolymerisation of Cellulose. Bochum 2012.

Müller, Steffen: The Catalytic Asymmetric Fischer Indolization and Beyond. Köln 2012.

Muldarisnur: Opal Photonic Crystals: Structure, Formation and Optical Properties. Bochum 2012.

Petuskova, Jekaterina: Synthesis of Phosphorus(III)-Centered Cations and their Applications as Ligands. Dortmund 2012.

Ratjen, Lars: Organic Lewis Acid Catalysis. Köln 2012.

Stade, Robert Michael: Entwicklung und Anwendung neuer Katalysatoren für die Alkinmetathese. Dortmund 2012.

Teller, Henrik: Synthese chiraler, einzähniger Phosphoramidit-Liganden und deren Anwendung in der homogenen, enantioselektiven Gold(I)-Katalyse. Dortmund 2012.

Wang, Shanshan: Copper-Colloid-Based Catalysts for Methanol Synthesis. Bochum 2012.

Doctoral Theses 2013

Arlt, Alexander: Totalsynthesen von Spirastrellolide A Methylester und der vermeintlichen Struktur von Gobienine A. Dortmund 2013.

*Galeano Nunez, Diana Carolina***:** Nanostructured Carbon Materials for Applications in Polymer Electrolyte Membrane Fuel Cells. Bochum 2013.

Lababidi, Sami: Effect of Sample Preparation on the Characterization of Crude Oil and its Complex Fractions by High Resolution Mass Spectrometry. Duisburg-Essen 2013.

Lee, Ji-Woong: Unconventional Homogeneous and Heterogeneous Asymmetric Organocatalysis. Köln 2013.

Oliveira, Maria Teresa: diastereodivergent Processes in Allylic alkylation: Catalytic Asymmetric Synthesisof Cyclobutenes. Bochum 2013.

Persich, Peter: Totalsynthesen von Isomigrastatin, Dehydrocurvularin und Kendomycin. TU Dortmund 2013:

Polyak, Iakov: QM/MM Investigations of Enzymatic Reactions. Düsseldorf 2013.

Tajvidi, Kameh: Hydrolytische Hydrierung und Hydrogenolyse von Cellulose-Katalysatoroptimierung und Aufklärung des Reaktionsnetzwerks. RWTH Aachen 2013.

*Valerio, Viviana***:** Cascade Electrophilic Activation of Amides: stereoselective Synthesis of Substituted Lactones. Bochum, 2013.

Wang, Xingyu: Valorization of lignin and bio-oil by catalytic hydrogenation with Ni catalyst. Bochum 2013.

Bachelor Theses

2011

Meister, B.: Bimetallische Katalysatoren zur Hydrogenolyse von Cellulose. Aachen 2011.

2012

Machowski, Thomas: Synthese und Charakterisierung von fluoreszierenden Reaktivfarbstoffen zur Fluoreszenzmarkierung von Aminosäuren und Proteinen. Krefeld 2012.

2013

Schauenburg, Dominik: Goldkatalysierte Cycloisomerisierung und ihre Anwendungen in der Naturstoffsynthese. 2013

Meier, Armin: Synthesis and catalytic transformation of 3-Deoxy-D-erythro-hexos-2-ulose. Aachen 2013.

Master Theses

2011

Heyden von der, J.: Untersuchung von bimetallischen Nanopartikeln mittels Elektronenmikroskopie. Wuppertal 2011.

2013

Deden, Tobias: Application of a decationic ligand in the gold catalyzed cycloisomerization of ortho-alkynnnylated biaryls. Düsseldorf 2013.

Habilitation 2013

Maulide, Dr. Nuno: Catalytic Rearrangements As Tools For C-C Bond Formation. Bochum 2013.

CHAPTER 5

Equal Opportunities

5 Equal Opportunities

In line with the general policy of the Max-Planck-Society, the Institute is committed to increase the number of female employees in all sectors of its work force. Compared to 2010, the total number of female employees was kept stable over the report period at 36%. Also the fraction of female PhD students and women on postdoctoral positions remained stable.

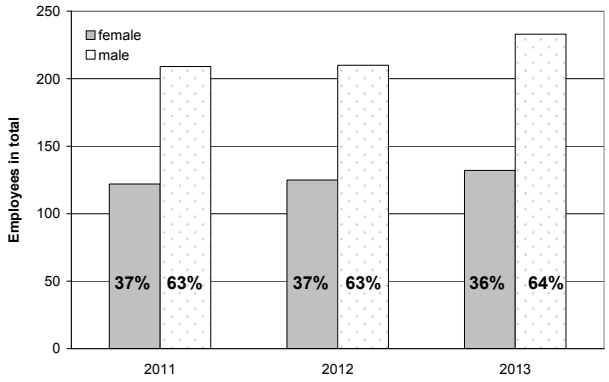

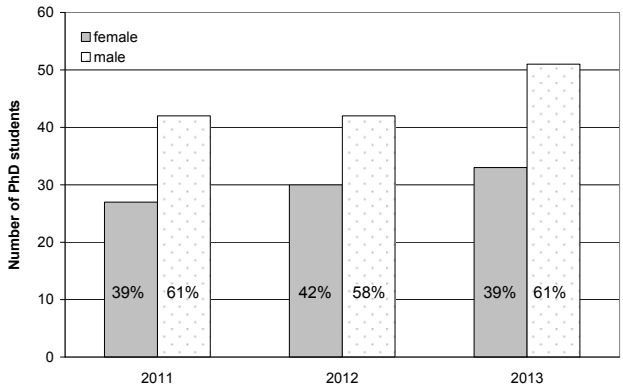

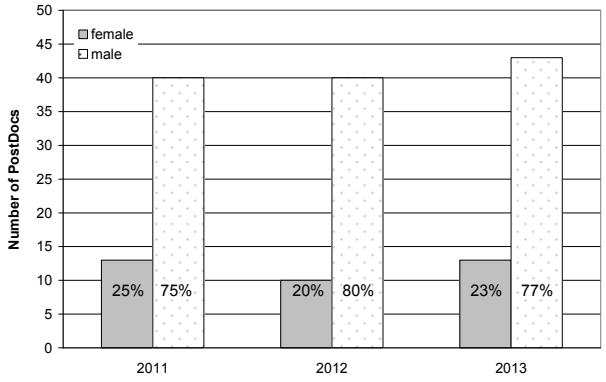

The number of female scientist on positions of the staff allocation plan of the Institute could be slightly improved from 11% to 14% over the last three years. Currently, six female scientists are working at the Max-Planck-Institut für Kohlenforschung, one of

them on a permanent position: Dr. Claudia Weidenthaler (group leader in the Department of Heterogeneous Catalysis). All other female scientists work on temporary positions: Dr. Monika Lindner (Department of Homogeneous Catalysis), Dr. Mariem Meggouh and Dr. Kameh Tajvidi (Department of Heterogeneous Catalysis), Dr. Garazi Talavera Urquijo (Department of Organometallic Chemistry), and Dr. Kakali Sen (Department of Theoretical Chemistry). In 2010, Dr. Elsa Sánchez-García started her own group within the Department of Theoretical Chemistry as junior research group leader on third party money (Liebig Stipendium des Fonds der Chemischen Industrie).
The fraction of female scientists on temporary positions has increased from 13% in 2010 to 19%, whereas the fraction of female scientists (6%) on permanent positions compared to male scientists (94%) needs further improvement.

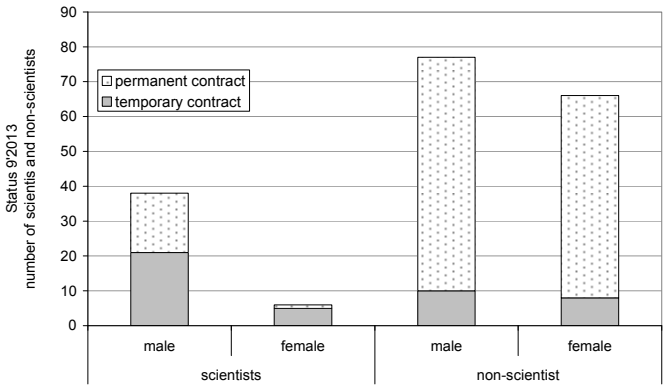

As already in 2010, the Institute has signed an agreement with a local kindergarten. According to this agreement, care is guaranteed for two children under the age of three for a minimum of 30 h per weak each. The Institute subsidizes these positions according to the child care allowances stipulated by the MPG and covers the risk in case these positions remain vacant. Since the Max Planck Institute for Chemical Energy Conversion needed childcare on a short-term, one of the childcare places was transferred to the neighboring institute.

Dr. C. Weidenthaler was re-elected as the “equal opportunities representative” (“Gleichstellungsbeauftragte”) of the Institute in 2012, with S. Holle as her deputy. Her rights and duties correspond to those previously defined by the MPG.